THESE DE DOCTORAT DE L'ETABLISSEMENT UNIVERSITE BOURGOGNE FRANCHE-COMTE

PREPAREE A L'INSTITUT NATIONAL DE LA RECHERCHE AGRONOMIQUE DE DIJON,

UMR AGROECOLOGIE

Ecole doctorale n°554

Ecole doctorale Environnements Santé

Doctorat de Sciences agronomiques

Par

Mme Pointurier Olivia

Modélisation des effets des systèmes de culture sur la dynamique de la plante parasite orobanche rameuse en interaction avec les adventices

Thèse présentée et soutenue à Dijon, le 13 Décembre 2019

Composition du Jury :

M. Debaeke Philippe	Directeur de recherche, INRA Toulouse	Rapporteur
M. Delavault Philippe	Professeur, Université de Nantes	Rapporteur
Mme Leborgne-Castel Nathalie	Professeure, Université de Bourgogne Franche-Comté	Présidente
M. Rodenburg Jonne	Senior lecturer, Université de Greenwich	Examinateur
Mme Leflon Martine	Docteure, responsable du département Génétique et Protection des Cultures, Terres Inovia	Examinatrice
Mme Colbach Nathalie	Directrice de recherche, INRA Dijon	Directrice de thèse
Mme Moreau Delphine	Chargée de recherche, INRA Dijon	Codirectrice de thèse

Remerciements

Tout d'abord, je tiens à remercier chaleureusement mes deux encadrantes, Nathalie et Delphine, pour tout ce qu'elles m'ont appris avec beaucoup de pédagogie, pour leur disponibilité, leurs encouragements et leur bienveillance qui ont été un moteur essentiel pour moi. Je suis ravie et chanceuse d'avoir pu travailler avec elles. Elles ont été l'argument majeur pour me décider à me lancer dans l'aventure de la thèse, que j'avais initialement boudée. Nathalie, merci de m'avoir fait confiance en me recrutant à l'issue de mon stage, de m'avoir laissé beaucoup de libertés dans le travail, et d'avoir toujours cherché à mettre mon travail en valeur et à me préserver des « idiotypes ».

Je remercie également Stéphanie, qui m'a encadrée au cours de mon stage de fin d'études et avec qui j'ai continué à travailler durant cette thèse. Merci pour les échanges scientifiques stimulants et merci pour ta compréhension et ta gentillesse.

Merci à Carole et Florence d'avoir partagé leur expertise sur le terrain et au laboratoire, merci pour votre bonne humeur et votre générosité. Je remercie également Valérie, Loïc, Jacques et Jean avec qui j'ai eu le plaisir de collaborer et qui se sont toujours rendus disponibles pour répondre à mon milliard de questions. Merci à Bruno de m'avoir également recrutée sur différents contrats, dont le tout premier au cours duquel tu m'as présentée à l'ambroisie. Merci à Eric Baraton, Delphine Molenat, Antoine Gardarin et Anne-Sophie Voisin d'avoir eu la gentillesse de me fournir des échantillons d'orobanche et des données.

Je remercie les membres de mon comité de pilotage, Jean-Noël Aubertot, Loïc Pagès, Xavier Pinochet et Philippe Simier pour l'intérêt qu'ils ont porté à ce travail de thèse et pour leurs précieux conseils qui m'ont aidée à prendre du recul, à clarifier mon approche, et à envisager des perspectives nouvelles.

Je remercie également les membres de mon jury, Philippe Debaeke, Philippe Delavault, Nathalie Leborgne-Castel, Martine Leflon et Jonne Rodenburg d'avoir accepté d'évaluer ce travail de thèse.

J'ai fait beaucoup de belles rencontres à et via l'INRA, et je remercie mes collègues de m'avoir accueillie aussi chaleureusement, cette atmosphère va beaucoup me manquer. Merci pour les discussions, les repas de Noël, les sorties, les tournages de films… Merci à vous, Claude, Julie, Mathieu, Wilfried, Rebecca, Chloé, Louis, Marthe, Rémi, Morgane J, Justine, Orla, Benoit, Luc, Dave, Benjamin, Emilien, Auxence, Melinda, Alice, Gwladys, Violaine, Ophélie, Maé, Ingvild, Séverin, Inès, Damien, Thomas, Guillaume, Stéphane, Franck, Kevin, Hugues, Fabrice, Chantal, Annick, Sandrine, Xavier, Nicolas, Clément, Antoine, Fanny, Séverine, Eric, Britta, Sylvie, Jean-Philippe, Thibault, et tous ceux que j'oublie.

Un grand grand merci à Floriane, Laurène, Morgane, Emeline et Sarah avec qui j'ai passé le plus clair de mon temps ici, merci pour la dose de joie et de réconfort quotidienne que vous m'avez offerte avec vos histoires, vos talents d'artistes, vos bonnes idées, vos petites attentions, les litres de thé bus ensemble... Merci aux « anciens », Martin, Florent, Marilou, Annette, Sébastien et Rémi pour les bons week-end passés à voir du pays.

Merci à mes amis de toujours, mes amis d'école, mes amies danseuses, Charline, Fanny, Aurélia, Noémie, Solène, Mélina, pour leur soutien et leur présence.

Je remercie aussi ma famille de me faire grandir (intérieurement) dans un environnement si riche et inspirant, tous artistes, indiens d'Amérique, paysans et milords. Merci à mes parents, Lysiane et Rémy, de m'avoir éveillée à l'école de la nature et de m'avoir offert la vie en rose. Merci à ma sœur et à mon frère, Marie et Charlie, ma Malu et mon gémeau magnifique. Merci à ma chaleureuse belle famille. Merci à mon Colin pour son écoute (hein quoi ?), sa patience, son soutien infaillible, son énergie, et les choses moins sérieuses, tout ce qu'on partage, qui font mon bonheur quotidien.

Table des matières

Liste des tableaux

Liste des figures

Liste des annexes

Glossaire

Adventice	Plante couramment appelée « mauvaise herbe », poussant sur un terrain cultivé sans y avoir été semée l'année donnée (Morlon, 2010). Dans cette thèse, désigne en particulier les plantes non parasites.
Agroécologie	« Application des concepts et principes de l'écologie pour la conception et la gestion d'agroécosystèmes durables » (Altieri, 1995).
Agroécosystème	Ecosystème cultivé pour la production agricole : « ensemble composé du milieu et d'êtres vivants organisés par l'homme » (Chauvel *et al.*, 2018).
Agronomie	« L'agronomie a pour objet d'étude premier le champ cultivé, considéré à la fois comme objet physique et comme objet d'application d'un raisonnement : celui des techniques par un agriculteur. » Elle a des intersections avec d'autres disciplines telles que la physiologie végétale, la science du sol ou l'écologie (Doré, 2006).
Agronomie systémique	« Manière de faire l'agronomie » qui « vise à prendre en charge la question de la gestion des champs cultivés dans leur globalité » (Doré and Meynard, 2006). Voir les définitions de « agronomie » et « système de culture ».
Allélopathie	« Phénomène biologique commun par lequel un organisme produit des substances biochimiques qui influencent la croissance, la survie, le développement et la reproduction d'autres organismes » (Cheng and Cheng, 2015).
Analyse de sensibilité	Etude de l'influence de différentes sources de variabilité dans les entrées d'un modèle sur la variabilité dans les sorties du modèle (Saltelli *et al.*, 2008b).
DECIFLORSYS	Outil d'aide à la décision développé à partir du modèle FLORSYS (Colas, 2018).
Dormance	Incapacité des semences viables à germer dans des conditions favorables d'atmosphère, de température et d'humidité (Murdoch and Kebreab, 2013).
Ecologie	« Science qui étudie les rapports entre les organismes et le milieu où ils vivent » (Encyclopédie Universalis).
Ecophysiologie	« Branche de l'écologie qui a pour objet d'analyser le fonctionnement de l'organisme individuel dans le cadre des contraintes que lui impose son milieu, afin de comprendre son adaptation à ces contraintes et de déterminer sa capacité à survivre lorsqu'elles changent » (Encyclopédie Universalis). Elle est également une sous-discipline de l'agronomie (voir la définition d'« agronomie »).
Faux-hôte	Plantes qui stimulent la germination des semences de plantes parasites mais ne permettent pas le développement consécutif de ces plantes parasite (Goldwasser and Rodenburg, 2013)
FLORSYS	Modèle mécaniste des effets des systèmes de culture sur la dynamique des adventices (Gardarin *et al.*, 2012; Munier-Jolain *et al.*, 2013; Colbach *et al.*, 2014b; Colbach *et al.*, 2014c; Munier-Jolain *et al.*, 2014). « FLORSYS » pour flore adventice dans les systèmes de culture.
Germination suicide	Germination d'une semence de plante parasite obligatoire en l'absence de plante hôte.
GR24	Stimulant synthétique de germination des semences parasites, régulateur de croissance, analogue du strigol (voir la définition de "strigolactones", Mangnus *et al.*, 1992)

Hémiparasite	Plante parasite capable d'effectuer la photosynthèse, ce qui ne lui permet pas nécessairement d'acquérir tout le carbone dont elle a besoin (Heide-Jørgensen, 2013).
Holoparasite	Plante parasite incapable d'effectuer la photosynthèse (Heide-Jørgensen, 2013).
Hôte	Dans le cas des plantes parasites, les hôtes désignent les plantes capables de supporter le développement complet des plantes parasites (Timko and Scholes, 2013).
Idéotype	Plantes idéales théoriques combinant des caractéristiques optimisant leurs performances dans un contexte de production donné (Martre *et al.*, 2015).
Indicateur	Variable mesurée, ou calculée à partir de variables liées aux pratiques agricoles ou des sorties d'un modèle, pour estimer une autre variable difficile d'accès (Bockstaller *et al.*, 2008).
Modèle	« Représentation simplifiée, relativement abstraite, d'un processus, d'un système, en vue de le décrire, de l'expliquer ou de le prévoir » (Dictionnaire de l'environnement).
Modèle empirique	Modèle qui relie directement les observations aux entrées du modèle sans tenter d'expliquer le lien entre ces variables (Colbach, 2006).
Modèle mécaniste	« Modèle fondé sur des sous-modèles qui sont des propositions d'explications de processus biophysiques » (Colbach, 2006).
Non-hôte	Dans le cas des plantes parasites, les non-hôtes désignent les plantes incapables de supporter le développement complet des plantes parasites (Timko and Scholes, 2013).
Orobanche	Plante parasite appartenant aux genres *Orobanche* et *Phelipanche* (et d'autres genres apparentés) de la famille des Orobanchaceae (Schneeweiss, 2013)
Parasite	« Organisme animal ou végétal qui, pendant une partie ou la totalité de son existence, se nourrit de substances produites par un autre être vivant sur lequel ou dans les tissus duquel il vit, lui causant un dommage » (Centre National de Ressources Textuelles et Lexicales)
Parasite facultatif	Parasite capable de survivre en l'absence d'hôte, mais avec une croissance réduite. Les plantes parasites facultatives sont nécessairement hémiparasites (Heide-Jørgensen, 2013).
Parasite obligatoire	Parasite incapable de survivre en l'absence d'hôte. Les plantes parasites obligatoires peuvent être holoparasites ou hémiparasites (Heide-Jørgensen, 2013).
Pathovar	Dans le cas de la plante parasite *Phelipanche ramosa*, les pathovars désignent des populations génétiquement différenciées avec différentes préférences d'hôtes (Benharrat *et al.*, 2005; Brault *et al.*, 2007; Le Corre *et al.*, 2014; Stojanova *et al.*, 2019).
Pédoclimat	Nous désignons par « pédoclimat » les conditions météorologiques et les caractéristiques du sol (ex : texture).
PHERASYS, PHERASYS.2	Modèles mécanistes de dynamique de la plante parasite *Phelipanche ramosa* dans les agroécosystèmes. « PHERASYS » pour *Phe*lipanche *ra*mosa dans les systèmes de culture. PHERASYS est une version préliminaire, et PHERASYS.2 est la version améliorée développée au cours de cette thèse.
Plante piège	Plantes hôtes infectées détruites avant la reproduction de la plante parasite (Goldwasser and Rodenburg, 2013).

Préconditionnement	Période d'imbibition au cours de laquelle les semences de plantes parasites deviennent sensibles aux stimulants de germination (Murdoch and Kebreab, 2013).
RSCone	Modèle de croissance racinaire de plantes cultivées et adventices (Pagès *et al.*, submitted).
Stock semencier du sol	Ensemble des semences viables dans le sol et à la surface du sol (Saatkamp *et al.*, 2014).
Strigolactones	Molécules stimulant la germination des plantes parasites, dont le strigol (Yoneyama *et al.*, 2013).
Système de culture	« Ensemble des modalités techniques mises en œuvre sur des parcelles cultivées de manière identique. Chaque système se définit par : - la nature des cultures et leur ordre de succession, - les itinéraires techniques appliqués à ces différentes cultures, ce qui inclut le choix des variétés. » (Sebillote, 1990)
Temps hydrothermique	Echelle d'expression du temps en fonction de la température et du potentiel hydrique, exprimée en °C·MPa·j. Calculé par analogie avec le temps thermique (voir définition) en cumulant le produit du potentiel hydrique moyen et de la température moyenne de chaque jour auxquels on retire respectivement le potentiel hydrique et la température de base (température et potentiel hydrique minimum en dessous desquels le développement est supposé nul) (Gummerson, 1986).
Temps thermique	Echelle d'expression du temps en fonction de la température, exprimée en °C·j. Calculé en cumulant la température moyenne de chaque jour à laquelle on retire la température de base (température minimum en dessous de laquelle le développement est supposé nul) (Gummerson, 1986; Bonhomme, 2000).
Trait	« Tout caractère morphologique, physiologique ou phénologique mesurable à l'échelle individuelle, de la cellule à l'organisme entier, sans référence à l'environnement ou à un autre niveau d'organisation », donnant une indication de la performance d'un organisme (Violle *et al.*, 2007).
Trophisme	« Processus de nutrition des tissus » (Encyclopédie Universalis).
TTC	2,3,5-triphenyl tetrazolium chloride. Molécule utilisée pour tester la viabilité des semences.

Introduction générale

Les adventices désignent les plantes qui croissent dans une parcelle sans y avoir été semées (Morlon, 2010). En entrant en compétition pour la lumière et les ressources du sol avec les cultures, elles causent la majeure partie des pertes de rendement d'origine biotique (Oerke, 2006). Les herbicides sont massivement utilisés pour contrôler les adventices, constituant la principale catégorie de pesticides appliqués en France (Potier, 2014) et représentant un chiffre d'affaires annuel d'environ 1 milliard d'euros pour l'industrie phytosanitaire (Union des Industries de la Protection des Plantes, 2018). Cependant l'utilisation des pesticides est aujourd'hui contestée du fait de leur toxicité pour l'environnement et la santé (Potier, 2014) et de leur baisse d'efficacité liée à l'apparition de résistances (Réseau de Réflexion et de Recherches sur les Résistances aux Pesticides, 2018). Face à ces constats, des mesures ont été mises en place au niveau européen à partir du début des années 90, et le plan Ecophyto a été lancé en France en 2008 afin de réduire l'utilisation des produits phytosanitaires au profit de méthodes agroécologiques (Potier, 2014). Avec la réduction d'usage d'herbicides, une flore adventice résiduelle plus conséquente devra être tolérée, accompagnée d'un cortège de bioagresseurs associés probablement plus important.

Parmi les bioagresseurs associés aux adventices, l'orobanche rameuse *Phelipanche ramosa* (L.) Pomel est une plante parasite des cultures et des adventices (Parker, 2013). En tant que parasite racinaire obligatoire, elle dépend entièrement de ressources qu'elle détourne de ses hôtes pour survivre (Heide-Jørgensen, 2013). Du fait de ce mode de vie parasitaire, elle est un bioagresseur majeur d'une vingtaine de cultures dans le monde (Parker, 2013). En France elle est particulièrement problématique en culture de colza d'hiver (Terres Inovia, 2018b). La seule méthode curative disponible en grandes cultures en France est l'application d'herbicides en cultures résistantes aux herbicides (Fernández-Aparicio *et al.*, 2016b; Données Ephy - Anses, 2018), mais cette méthode entre en contradiction avec la nécessité de limiter l'usage de pesticides. Différentes techniques prophylactiques à effet partiel doivent être combinées pour parvenir à contrôler l'orobanche efficacement (Grenz *et al.*, 2005a; Rubiales and Fernández-Aparicio, 2012). Elles doivent en outre s'intégrer dans la stratégie de gestion des adventices, parmi lesquelles l'orobanche rameuse compte plusieurs dizaines d'espèces hôtes (Boulet *et al.*, 2001; Gibot-Leclerc *et al.*, 2003; Simier *et al.*, 2013; Gibot-Leclerc *et al.*, 2015). Parvenir à conjuguer la gestion de plusieurs bioagresseurs est complexe mais possible et efficace. Des techniques de push-pull permettent par exemple de lutter à la fois contre une plante parasite et des insectes ravageurs en associant aux cultures hôtes de la plante parasite des plantes aux propriétés allélopathiques[1] inhibant le parasitisme et repoussant les insectes (Samejima and Sugimoto, 2018). De telles stratégies s'intègrent parfaitement dans le cadre de l'agroécologie, reposant sur des principes d'écologie et d'agronomie, mais restent à développer pour lutter contre l'orobanche rameuse. Pour cela, il est fondamental de bien connaître la biologie de la plante parasite et ses interactions avec les autres plantes.

La gestion de l'orobanche rameuse doit être raisonnée à l'échelle du système de culture, échelle définie par les cultures dans la succession culturale et les techniques appliquées à ces cultures[2] (Papy, 2013). Déterminer la performance d'un système de culture implique d'étudier l'effet de multiples

[1] « L'allélopathie est un phénomène biologique commun par lequel un organisme produit des substances biochimiques qui influencent la croissance, la survie, le développement et la reproduction d'autres organismes. » (Cheng and Cheng, 2015)

[2] « Un système de culture est l'ensemble des modalités techniques mises en œuvre sur des parcelles cultivées de manière identique. Chaque système se définit par :

- la nature des cultures et leur ordre de succession,
- les itinéraires techniques appliqués à ces différentes cultures, ce qui inclut le choix des variétés. » (Sebillote, 1990)

facteurs en interaction (par exemple l'efficacité d'une technique dépend des conditions climatiques dans laquelle elle est réalisée et des autres techniques dans le système), ce qui est complexe et requiert des méthodes adaptées. L'expérimentation est indispensable mais reste insuffisante car elle ne permet de tester qu'un nombre limité de techniques sur quelques années et dans un nombre limité de contextes pédoclimatiques[3] et floristiques (Jeuffroy *et al.*, 2014). Les modèles de simulation sont particulièrement utiles pour aider à concevoir des systèmes de culture en les évaluant à long terme et dans différentes conditions pédoclimatiques et floristiques (Colbach *et al.*, 2014a; Colbach *et al.*, 2017b). Ils répondent en outre au besoin de développer des démarches participatives pour favoriser l'adoption des pratiques innovantes par les agriculteurs (Guichard *et al.*, 2017) car ils peuvent être utilisés comme outils d'aide à la décision.

L'objectif de cette thèse est de compléter et synthétiser les connaissances sur la dynamique de l'orobanche rameuse en interaction avec les adventices et les cultures dans les agroécosystèmes, afin de développer un modèle de simulation indispensable pour concevoir des stratégies de gestion durables valorisant la biodiversité et les régulations biologiques.

[3] Pédoclimat : dans cette thèse, désigne les conditions météorologiques et les caractéristiques du sol (ex : texture).

Chapitre 1. Problématique

1.1. L'orobanche rameuse, *Phelipanche ramosa*

1.1.1. Espèces d'orobanches, pathovars et dégâts

Parmi les plantes parasites de la famille des Orobanchaceae, deux clades incluent des espèces nuisibles d'importance économique mondiale, le clade *Orobanche*, regroupant les genres *Phelipanche* et *Orobanche*, et le clade *Striga-Alectra* (Schneeweiss, 2013). L'orobanche rameuse *Phelipanche ramosa*, par exemple, provoque globalement 30 à 50% de pertes de rendement en cultures de tomate et tabac (Parker, 2013) et infeste des cultures dans plus de 10 familles botaniques différentes dont les *Solanaceae*, les *Brassicaceae* et les *Asteraceae* (Parker and Riches, 1993; Molenat *et al.*, 2013). Elle est présente sur tous les continents, en particulier en Europe et au Moyen-Orient (Parker, 2013). En France elle est particulièrement dévastatrice sur colza d'hiver dans l'Ouest et sur chanvre dans le Nord-Est, avec des pertes de rendement pouvant atteindre jusqu'à 100% dans les cas extrêmes (Jestin, 2017). Trois populations génétiques différentes, ou pathovars, ont été identifiées, infestant préférentiellement et plus efficacement le colza (*Brassica napus* L.), le tabac (*Nicotiana tabacum* L.) et le chanvre (*Cannabis sativa* L.) respectivement (Brault *et al.*, 2007; Le Corre *et al.*, 2014; Stojanova *et al.*, 2019). Les symptômes d'une infestation en colza sont un retard de croissance de la culture, du nanisme, de la chlorose et des siliques avortées (Gibot-Leclerc *et al.*, 2012).

Ainsi, l'orobanche rameuse provoque des pertes de rendement conséquentes dans des cultures d'importance économique dans le monde entier, et particulièrement en grandes cultures en France. Afin de comprendre comment lutter contre l'orobanche rameuse, il est nécessaire de bien connaître son cycle de vie et de caractériser les spécificités des différents parthovars. Par la suite, nous désignerons l'orobanche rameuse par son nom latin, *P. ramosa*, et les espèces du clade *Orobanche* en général par « les orobanches » (sauf dans la section 4.2, où l'orobanche rameuse est désignée par le terme « broomrape », car cela permettait de clarifier le texte).

1.1.2. Morphologie et cycle de vie

P. ramosa est un parasite obligatoire, c'est-à-dire qu'elle ne peut survivre en l'absence d'un hôte dont elle dépend pour prélever ses ressources en eau et nutriments (Heide-Jørgensen, 2013). Ses caractéristiques morphologiques reflètent son incapacité à faire la photosynthèse puisqu'elle ne possède que de petites feuilles réduites sous forme d'écailles brunes (Parker, 2013). C'est une plante de 15-25 cm de haut constituée d'une tige ramifiée portant de nombreuses fleurs bilabiées bleues-violettes (Figure 1). Des différences morphologiques sont observées entre pathovars (Benharrat *et al.*, 2005; Brault *et al.*, 2007) mais n'ont jamais été caractérisées précisément. *P. ramosa* ne passe en fait qu'un quart de sa vie sous cette forme émergée, son cycle s'effectuant principalement sous terre (Figure 2)(Gibot-Leclerc *et al.*, 2012). Les principales étapes de son cycle de vie sont présentées dans les sections suivantes et synthétisées dans la Table 1.

Figure 1 : Hampe florale de *Phelipanche ramosa* (Gibot-Leclerc *et al.*, 2012)

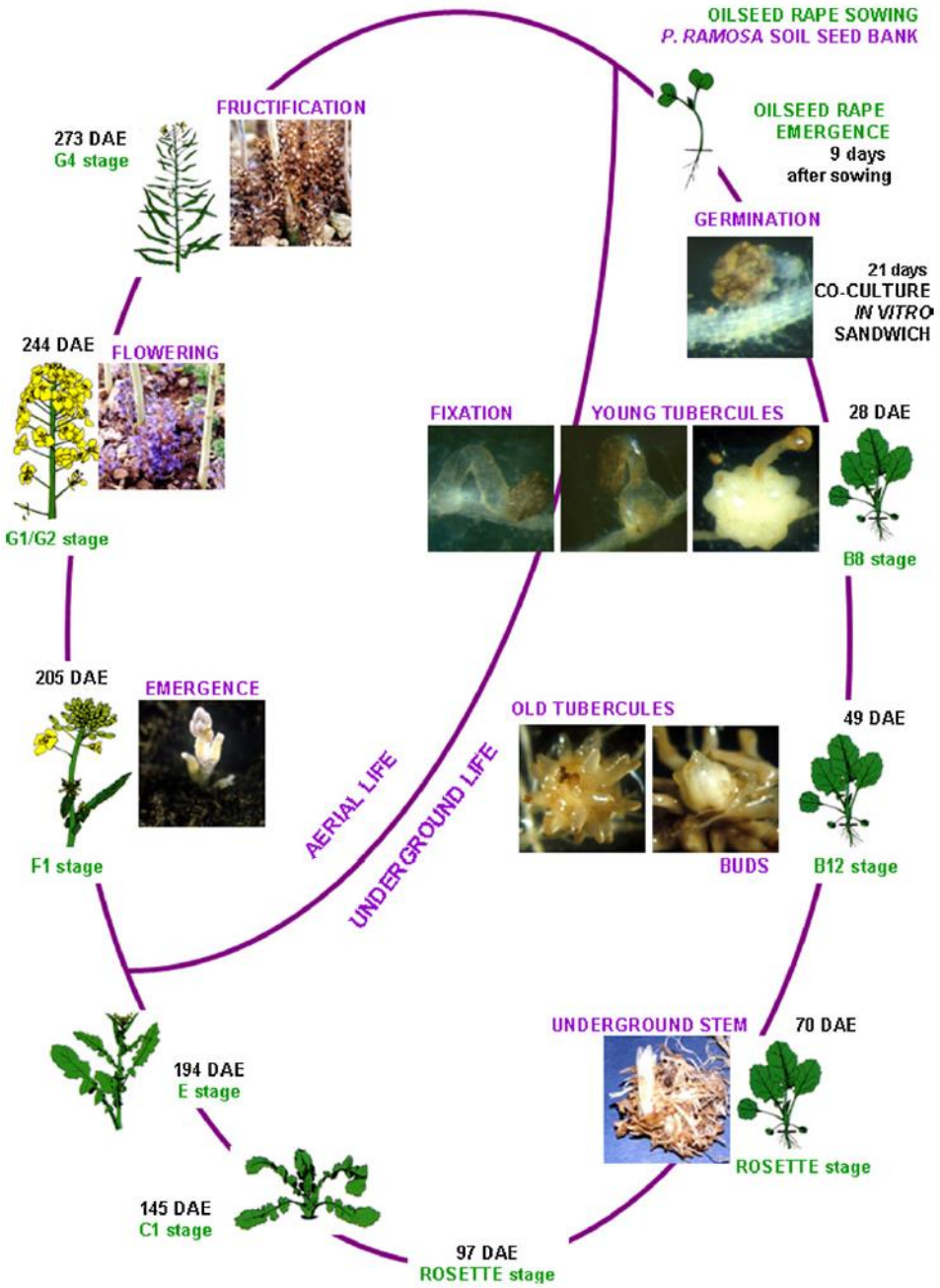

Figure 2 : Cycle de développement de *Phelipanche ramosa* sur culture de colza d'hiver. DAE = jours après émergence du colza. (Gibot-Leclerc *et al.*, 2012)

Table 1 : Recensement des études apportant des connaissances sur les processus clés de la dynamique de *Phelipanche ramosa*. Seuls les principaux facteurs et processus sont considérés (voir section 1.2.1). Par exemple, le processus de dispersion des semences et l'influence du sol ne sont pas détaillés car ils ont été relativement peu étudiés.

Processus	**Facteurs**	**Références pour *P. ramosa***
Mortalité des semences	Saison	Pas d'étude
Dormance	Conditions hydrothermiques	(Gibot-Leclerc *et al.*, 2004)
	Saison	Pas d'étude
Germination	Conditions hydrothermiques	(Gibot-Leclerc *et al.*, 2004)
	Exsudats racinaires des espèces végétales non-parasites	(Westwood, 2000; Goldwasser and Yoder, 2001; Gibot-Leclerc *et al.*, 2003; Denev *et al.*, 2007; Fernández-Aparicio *et al.*, 2009; Fernández-Aparicio *et al.*, 2011; Auger *et al.*, 2012; Gauthier *et al.*, 2012; Arslan and Uygur, 2013; Gibot-Leclerc *et al.*, 2013a; Gibot-Leclerc *et al.*, 2016; Perronne *et al.*, 2017)
Fixation	Sensibilité des espèces végétales non parasites	(Parker and Riches, 1993; Boulet *et al.*, 2001; Gibot-Leclerc *et al.*, 2003; Zehhar *et al.*, 2003; Benharrat *et al.*, 2005; Boulet *et al.*, 2007; Brault *et al.*, 2007; Qasem and Foy, 2007; Gauthier *et al.*, 2012; Gibot-Leclerc *et al.*, 2012; Boulet *et al.*, 2013; Gibot-Leclerc *et al.*, 2013a; Gibot-Leclerc *et al.*, 2013b; Molenat *et al.*, 2013; Simier *et al.*, 2013; Jestin *et al.*, 2014; Gibot-Leclerc *et al.*, 2015; Moreau *et al.*, 2016)
Croissance au dépend de l'hôte	Sensibilité des espèces végétales non parasites	(Díaz *et al.*, 2006; Mauromicale *et al.*, 2008; Moreau *et al.*, 2016)
	Phénologie	(Gibot-Leclerc *et al.*, 2012; Gibot-Leclerc *et al.*, 2013b)
Production de semences	Biomasse de la plante parasite	Pas d'étude

1.1.2.1. Survie dans le sol

Les semences d'orobanches peuvent survivre jusqu'à 20 ans dans le sol (Murdoch and Kebreab, 2013). Cependant la mortalité des semences dans le sol n'a été quantifiée précisément que sur quelques espèces de plantes parasites mais pas pour *P. ramosa* (López-Granados and García-Torres, 1999; Gbèhounou *et al.*, 2003; Van Mourik *et al.*, 2003; Prider *et al.*, 2012). Cette faible mortalité permet aux semences d'orobanches de persister dans le sol, à l'état de dormance, dans l'attente de conditions favorables, c'est-à-dire la présence d'un hôte qui stimulera leur germination.

1.1.2.2. Dormance dans le sol

La dormance désigne l'incapacité des semences viables à germer dans des conditions favorables d'atmosphère, de température et d'humidité (Murdoch and Kebreab, 2013). Les semences acquièrent une dormance primaire au cours de leur développement sur la plante mère. Trois étapes successives sont nécessaires pour lever cette dormance chez les orobanches : une période en conditions sèches, suivie d'une période d'imbibition appelée préconditionnement au cours de laquelle les semences deviennent sensibles aux exsudats racinaires des plantes hôtes qui, lors de la troisième étape, stimulent leur germination. Les semences de *P. ramosa* sont peu exigeantes en termes de conditions hydrothermiques durant le préconditionnement et sortent très rapidement de dormance primaire (Gibot-Leclerc *et al.*, 2004). Si les semences d'orobanches restent imbibées trop longtemps sans être stimulées, elles entrent à nouveau en dormance, appelée dormance secondaire, qui peut être levée selon les trois étapes mentionnées ci-dessus (Murdoch and Kebreab, 2013). Au champ les variations du niveau de dormance en réponse aux fluctuations des conditions climatiques du sol produisent des cycles de dormance saisonnière. De tels cycles n'ont été étudiés que pour quelques espèces d'orobanches (Van Hezewijk *et al.*, 1994; López-Granados and García-Torres, 1999; Prider and Craig, 2013) mais jamais pour *P. ramosa*.

1.1.2.3. Germination

La germination des semences d'orobanches, caractérisée par l'émergence d'une radicule, n'est possible qu'une fois les semences sorties de dormance et stimulées par des exsudats racinaires de plantes voisines. Cette étape assure que les semences germent à proximité d'une racine hôte pour pouvoir la parasiter rapidement (Yoneyama *et al.*, 2013) sans quoi elles meurent en quelques jours (3-4 jours pour *P. ramosa*, Gibot-Leclerc *et al.*, 2012). Bien qu'il existe des conditions optimales, les semences de *P. ramosa* sont capables de germer dans de larges gammes de températures, d'humidité et de tension en oxygène (Gibot-Leclerc *et al.*, 2004). La germination des semences d'orobanches dépend également de la qualité des exsudats racinaires qui varie en fonction des espèces stimulatrices (Fernández-Aparicio *et al.*, 2009; Fernández-Aparicio *et al.*, 2011), car différentes molécules peuvent être impliquées (strigolactones pour la plupart des espèces, isothiocyanates pour le colza d'hiver, Auger *et al.*, 2012; Yoneyama *et al.*, 2013), et des saisons (López-Granados and García-Torres, 1996; Auger *et al.*, 2012). Chez *P. ramosa*, la sensibilité des semences aux exsudats racinaires varie également en fonction des pathovars (Gibot-Leclerc *et al.*, 2016). La flore microbienne (Yoneyama *et al.*, 2013) et les caractéristiques physico-chimiques du sol (P. Simier, communication personnelle) peuvent également influencer la germination des semences d'orobanche, mais ces phénomènes complexes ont été relativement peu étudiés.

1.1.2.4. Fixation

La radicule émise lors de la germination croît en direction de la racine hôte, s'y fixe, et envahit les tissus hôtes pour y établir une connexion vasculaire (Joel, 2013d). A ce stade différents types d'interactions entre les orobanches et les autres plantes peuvent-être identifiées (Table 2). Les hôtes, à l'inverse des non-hôtes, sont capables de supporter le développement complet des plantes parasites (Timko and Scholes, 2013). Les faux-hôtes stimulent la germination des semences de plantes parasites mais ne permettent pas de fixation viable (Goldwasser and Rodenburg, 2013). Les non-hôtes

facilitateurs sont des non-hôtes qui favorisent la stimulation de germinations parasites et l'infection d'hôtes à proximité par des mécanismes encore inconnus (Gibot-Leclerc *et al.*, 2013a).

Table 2 : Synthèse des caractéristiques définissant le statut hôte, non-hôte ou faux-hôte d'une plante vis-à-vis d'une plante parasite.

Statut	**Capacité à stimuler les germinations de la plante parasite**	**Capacité à supporter le développement complet de la plante parasite**	**Capacité à amplifier l'infection des plantes voisines**
Hôte	Oui	Oui	Pas d'information
Non-hôte	Non	Non	Voir non-hôte facilitateur
Faux-hôte	Oui	Non	Pas d'information
Non-hôte facilitateur	Non	Non	Oui

1.1.2.5. Croissance au dépend de l'hôte

A partir de la fixation, la plante parasite commence à croître au dépend de son hôte. Les orobanches agissent comme un organe supplémentaire auquel l'hôte alloue une partie de sa biomasse, au détriment en particulier de ses organes reproducteurs (Manschadi *et al.*, 2001; Grenz *et al.*, 2008; Fernández-Aparicio *et al.*, 2016a), d'où les pertes de rendement. Les feuilles de l'hôte, qui assurent l'approvisionnement en ressources via la photosynthèse, sont en revanche très peu affectées (Moreau *et al.*, 2016). Grâce à ces ressources, *P. ramosa* émet d'abord une tige souterraine en direction de la surface du sol puis émerge pour donner une hampe florale (Gibot-Leclerc *et al.*, 2012). A l'émergence elle a déjà considérablement réduit la biomasse de l'hôte (*P. ramosa* cause 20% à 90% de pertes de biomasse avant émergence selon les espèces hôtes, Moreau *et al.*, 2016). Si l'hôte alloue suffisamment de biomasse à la plante parasite, ce qui est variable en fonction de l'espèce hôte (Moreau *et al.*, 2016), et si son cycle de vie est suffisamment long (Gibot-Leclerc *et al.*, 2013b), *P. ramosa* poursuit son développement jusqu'à fructification et libération de ses semences. La durée du cycle de vie de *P. ramosa* varie entre pathovars, correspondant au cycle de leurs hôtes préférentiels respectifs (Gibot-Leclerc *et al.*, 2013b).

1.1.2.6. Production de semences

Les orobanches produisent 10 000 à 500 000 minuscules semences par plante (longueur : 350-450 µm, largeur : 250 à 300 µm, Parker and Riches, 1993; Joel, 2013a) en fonction de la biomasse de la plante (Grenz *et al.*, 2005a), et un pied de colza peut supporter une vingtaine de hampes florales de *P. ramosa* en cas de forte infection (Gibot-Leclerc *et al.*, 2012). Ces chiffres donnent une idée de la rapidité avec laquelle le stock semencier[4] de *P. ramosa* peut s'accroître mais restent approximatifs car la production de semences de cette espèce n'a jamais été quantifiée précisément.

Du fait de leur petite taille, les semences d'orobanches sont facilement dispersables, notamment via les activités humaines (machines, bétail... Goldwasser and Rodenburg, 2013). Les mécanismes de dispersion des orobanches restent pourtant mal connus car les vecteurs de dispersion anthropiques ont été relativement peu étudiés de manière générale, y compris chez les plantes non parasites (Auffret *et al.*, 2014).

[4] Sock semencier du sol : Ensemble des semences viables dans le sol et à la surface du sol (Saatkamp *et al.*, 2014).

1.1.2.7. Conclusion partielle : *P. ramosa*, un bioagresseur redoutable dont la biologie est mal connue

***P. ramosa* possède les caractéristiques d'un bioagresseur redoutable. Elle possède de nombreux hôtes et est capable de produire des milliers de semences facilement dispersables, dont la dormance et la faible mortalité assurent une grande persistance dans le sol. Ces caractéristiques indiquent les processus clés à viser pour contrôler la plante parasite. Les processus affectant les semences en particulier déterminent sa dynamique à long terme. Pourtant la plupart restent mal connus pour *P. ramosa*, la dormance et la mortalité des semences dans le sol ainsi que la production de semences n'ayant jamais été quantifiées pour cette espèce (Table 1).**

1.1.3. Moyens de lutte contre *P. ramosa*

Les méthodes de lutte employées contre *P. ramosa* exploitent les connaissances sur sa biologie (Figure 3). Nous distinguons les techniques ayant un effet direct sur la plante parasite de celles ayant un effet indirect via la flore adventice.

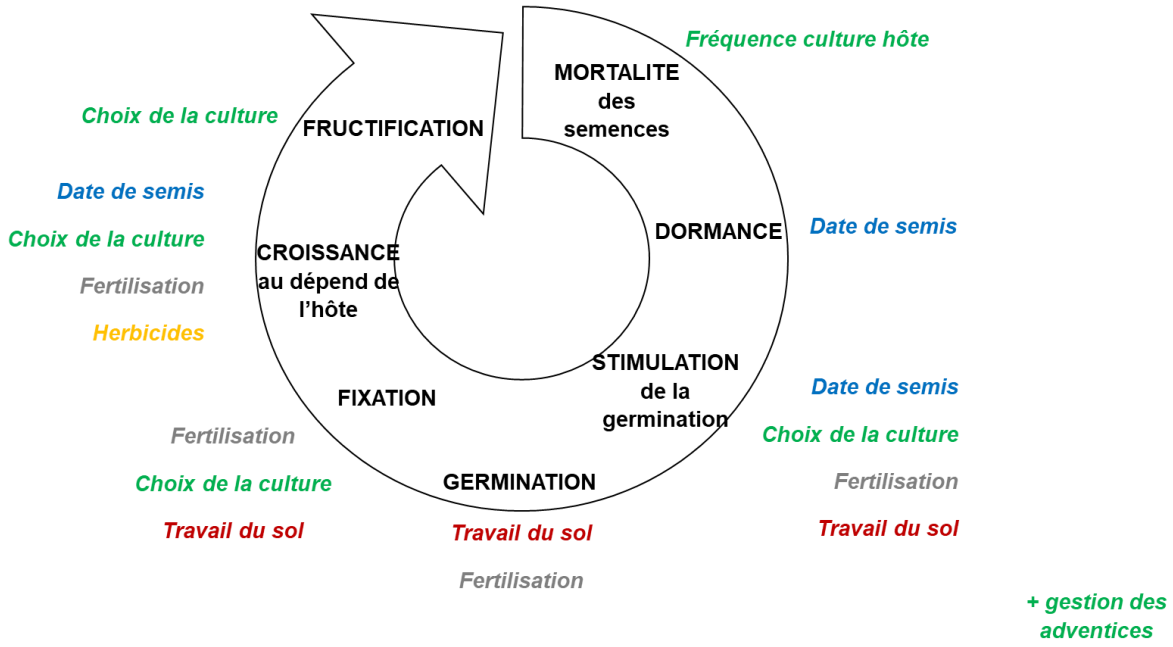

Figure 3 : Effets de techniques de lutte disponibles en grandes cultures (en italiques) pour lutter contre *Phelipanche ramosa* à différents stades de son cycle de vie (en noir). Toutes les techniques représentées sont prophylactiques, à l'exception de l'application d'herbicides, méthode curative représentée en jaune. Inspiré de Fernández-Aparicio *et al.*, (2016b).

1.1.3.1. Effet des techniques culturales

Parmi les techniques de lutte utilisées contre *P. ramosa*, certaines sont curatives, visant à tuer directement la plante parasite, d'autres sont prophylactiques, ayant pour objectif d'éviter ou de limiter son développement.

1.1.3.1.1 Les méthodes curatives

Parmi les herbicides efficaces contre *P. ramosa*, seuls quelques herbicides foliaires (glyphosate, imazamox et certains sulfonylurés) appliqués sur variétés tolérantes aux herbicides sont autorisés en France (Fernández-Aparicio *et al.*, 2016b; Données Ephy - Anses, 2018). Ils sont appliqués sur les feuilles de la culture hôte et transloqués vers la plante parasite fixée, ou directement dans le sol au niveau des semences fixées via l'eau d'irrigation. Les produits de fumigation, injectés dans le sol pour tuer les semences parasites, sont interdits en grandes cultures en France. Le bromure de méthyl par exemple, a été largement utilisé pour éradiquer *P. ramosa* mais a été prohibé au niveau international du fait de sa toxicité (Goldwasser and Rodenburg, 2013). D'autres fumigants (métham sodium et dazomet) sont autorisés uniquement en culture ornementales, fruitières et légumières (Fernández-Aparicio *et al.*, 2016b; Données Ephy - Anses, 2018). Les produits de biocontrôle constituent une alternative a priori moins polluante mais sont encore en cours de développement (Fernández-Aparicio *et al.*, 2016b).

Des méthodes physiques sont également utilisées contre les orobanches. La solarisation par exemple consiste à appliquer des bâches plastiques transparentes sur le sol pour augmenter la température du sol et le désinfecter thermiquement. Elle a montré son efficacité contre *P. ramosa* en culture de tomate (Mauromicale *et al.*, 2005) mais est trop coûteuse pour être appliquée à des cultures à moins forte valeur ajoutée. De même, le désherbage manuel est employé en agriculture de subsistance mais est peu envisageable en grandes cultures. En outre, le désherbage manuel permet de limiter les futures infestations mais intervient relativement tard, après émergence de la plante parasite, alors que celle-ci a déjà causé d'importants dégâts sous terre (Goldwasser and Rodenburg, 2013).

Peu de méthodes curatives sont donc applicables pour lutter contre *P. ramosa* en grandes cultures, et toutes sont sources de pollution pour l'environnement et/ou trop coûteuses. Les méthodes prophylactiques sont plus prometteuses.

1.1.3.1.2 Succession culturale

Etant donnée la persistance des semences d'orobanches dans le sol, il est préférable de concevoir des rotations où les cultures hôtes sont peu fréquentes. La découverte du mécanisme de facilitation (voir section 1.1.2.4) impose cependant d'être vigilant en introduisant des cultures non-hôtes en association avec des cultures hôtes puisque celles-ci peuvent favoriser l'infection des cultures hôtes (Gibot-Leclerc *et al.*, 2013a). Pour les cultures hôtes, des variétés résistantes doivent être privilégiées. Des variétés de colza induisant peu de germinations, limitant le nombre de fixations ou perturbant la croissance post-fixation de *P. ramosa* ont été mises en évidence (Gauthier *et al.*, 2012). Quelques dizaines de variétés de colza parmi plus de 300 inscrites en France présentent une moindre sensibilité à *P. ramosa* mais aucune n'est totalement résistante (Terres Inovia, 2018a).

Les cultures pièges sont des hôtes détruits avant la reproduction de la plante parasite (Goldwasser and Rodenburg, 2013). Les cultures pièges et les faux-hôtes (voir section 1.1.2.4) peuvent être utilisées en interculture pour vider le stock semencier parasite en stimulant des germinations suicides (c'est-à-dire des germinations en absence d'hôte assurant le développement complet de la plante parasite). Le lin (*Linum usitatissimum* L.) et le lotier (*Lotus corniculatus* L.) par exemple sont de bons candidats comme faux-hôtes (Parker and Riches, 1993; Molenat *et al.*, 2013), et la moutarde blanche (*Sinapis alba* L.) ou les repousses de colza comme cultures pièges (Molenat *et al.*, 2013), car ils induisent une proportion élevée de germinations chez *P. ramosa* (Fernández-Aparicio *et al.*, 2009; Perronne *et al.*, 2017).

1.1.3.1.3 Travail du sol

Un travail du sol profond permettrait d'empêcher les semences parasites de germer en profondeur par manque d'oxygène (Rubiales *et al.*, 2009). L'efficacité de la méthode est cependant discutable dans le cas de *P. ramosa* dont les semences sont capables de germer à de très faibles teneurs en oxygène (Gibot-Leclerc *et al.*, 2004). En outre, le travail du sol peut remonter des semences enfouies lors de précédentes opérations et les placer en conditions favorables pour germer. A l'inverse, un travail du sol réduit est préconisé pour limiter l'incorporation des semences parasites dans le sol et ainsi réduire leur probabilité de rencontre avec les racines hôtes (Fernández-Aparicio *et al.*, 2016b).

1.1.3.1.4 Date de semis

Un semis tardif permet de réduire l'infestation de plusieurs plantes parasites dont *P. ramosa* en cultures d'hiver (Gibot-Leclerc *et al.*, 2006; Fernández-Aparicio *et al.*, 2016b) mais pas en cultures d'été (Grenz *et al.*, 2008). Différents mécanismes expliquent l'efficacité de la technique. D'une part, moins de germinations de semences parasites sont induites car le semis est décalé vers le moment où ces semences entrent en dormance (Murdoch and Kebreab, 2013). De plus, les exsudats racinaires des cultures semées tardivement sont moins stimulants (Fernández-Aparicio *et al.*, 2016b). D'autre part, la culture bénéficie d'un avantage compétitif vis-à-vis de la plante parasite car, du fait de son cycle raccourci, la culture atteint le stade floraison plus rapidement alors que la plante parasite reste à un

stade plus précoce (Fernández-Aparicio *et al.*, 2016b). Cependant le raccourcissement du cycle de vie de la culture est également à l'origine d'une diminution du rendement parfois telle qu'elle annule les bénéfices de la technique (Díaz *et al.*, 2006).

1.1.3.1.5 Fertilisation

L'application d'engrais azotés et phosphatés est utilisée pour lutter contre certaines espèces d'orobanches. Leur mode d'action est double, ils ont un effet toxique inhibant la germination des semences parasites et l'élongation de la radicule, et ils réduisent l'exsudation de strigolactones (stimulants de germination, voir section 1.1.2.3) par les plantes hôtes (Fernández-Aparicio *et al.*, 2016b). Bien que cette technique ait permis de réduire l'infestation de *P. ramosa* en cultures de tomate et de pomme de terre (Haidar *et al.*, 2003; Disciglio *et al.*, 2016), son efficacité est controversée (Goldwasser and Rodenburg, 2013), en particulier lorsque d'autres stimulants de germination que les strigolactones sont impliqués comme c'est le cas pour *P. ramosa* en colza (Auger *et al.*, 2012; Fernández-Aparicio *et al.*, 2016b). Dans ce cas, il serait au contraire préférable de ne pas fertiliser les cultures de colza pour limiter l'exsudation de stimulants de germinations, le nombre de fixations et leur biomasse (Gaudin, 2013). Cependant, en favorisant la croissance des cultures hôtes, la fertilisation peut potentiellement accroître leur compétitivité vis-à-vis des orobanches après fixation (Labrousse *et al.*, 2010). Cette méthode est complexe car elle peut également aggraver l'infection en augmentant la quantité de ressources disponibles pour les orobanches (Grenz *et al.*, 2008).

1.1.3.2. Effet indirect des techniques via la flore adventice

Dans cette section et par la suite, nous désignons par « adventices » les adventices non parasites.

1.1.3.2.1 Réduire le risque orobanche dû aux adventices

P. ramosa est capable de parasiter près d'une cinquantaine d'espèces d'adventices (Boulet *et al.*, 2001; Gibot-Leclerc *et al.*, 2003; Simier *et al.*, 2013; Gibot-Leclerc *et al.*, 2015) qui peuvent potentiellement servir de relais en absence de culture hôte. Il est donc recommandé de les désherber soigneusement, y compris en bordure de champs, jachères et intercultures (Gibot-Leclerc *et al.*, 2003). Les non-hôtes facilitateurs, tels que le liseron (*Convolvulus arvensis*), doivent également être éliminés pour éviter qu'ils ne favorisent l'infection des hôtes, bien que ce phénomène n'ait jamais été observé au champ (Gibot-Leclerc *et al.*, 2013a).

1.1.3.2.2 Favoriser les adventices pour contrôler l'orobanche

Les adventices hôtes peuvent être tolérées, notamment en interculture, lorsqu'elles peuvent servir de plantes pièges. *Geranium dissectum* est un bon candidat par exemple car il stimule de nombreuses germinations de *P. ramosa* mais très peu de fixations parviennent à émergence sur cet hôte (Moreau *et al.*, 2016). De même, quelques espèces de faux-hôtes ont été identifiées parmi les adventices (Boulet *et al.*, 2001; Gibot-Leclerc *et al.*, 2003).

1.1.3.3. Les méthodes d'études pour évaluer les effets des techniques de lutte contre les orobanches

Dans les sections précédentes, différentes méthodes ont été employées pour évaluer les effets des techniques de lutte contre les orobanches.

L'expérimentation au champ a été utilisée pour évaluer l'efficacité de techniques individuelles (ex : solarisation, Mauromicale *et al.*, 2005) ou de quelques techniques combinées (ex : irrigation et densité de semis, Manschadi *et al.*, 2001) et pour comprendre leurs effets en analysant les déterminants de la dynamique des orobanches (ex : la fertilisation peut favoriser le parasitisme en stimulant la croissance des plantes hôtes, et en particulier la partie racinaire qui détermine le nombre de fixations parasites,

Grenz *et al.*, 2008). L'expérimentation est indispensable pour tester l'effet des techniques dans un contexte réaliste. Cependant, elle est relativement coûteuse et laborieuse, ce qui limite le nombre de mesures, de répétitions, de facteurs et de contextes qui peuvent être étudiés et la durée de l'expérimentation (Colbach *et al.*, 2014a).

Les enquêtes auprès d'agriculteurs permettent de couvrir une plus large gamme de contextes (ex : enquêtes dans l'Est et l'Ouest de la France pour identifier les techniques favorables et défavorables à *P. ramosa*, Jestin *et al.*, 2014), mais ne donnent généralement qu'une image instantanée des systèmes de culture qui ne permet pas de comprendre les mécanismes impliqués (Colbach *et al.*, 2014a).

Enfin, des modèles[5] de simulation ont été utilisés pour étudier de nombreuses situations avec de nombreuses répétitions et à long terme, en effectuant des expérimentations virtuelles à moindre coût (ex : Grenz *et al.*, 2005a ont testé l'effet de différentes combinaisons de techniques culturales sur la dynamique d'une espèce d'orobanche pendant 10 ans). En outre, les modèles peuvent aider à mieux comprendre les processus sous-tendant l'effet des techniques de lutte en prédisant des variables difficiles à mesurer au champ (Colbach *et al.*, 2014a).

L'approche modélisation est donc particulièrement appropriée pour concevoir des stratégies de gestion complexes des orobanches combinant de multiples techniques sous l'influence de divers facteurs. Elle doit cependant nécessairement être combinée à l'expérimentation et aux enquêtes, indispensables pour construire et paramétrer les modèles, les alimenter (ex : les enquêtes offrent une large gamme de systèmes de culture à simuler) et évaluer leur qualité de prédiction afin de vérifier qu'ils ne sont « pas trop faux » et utiles pour répondre aux objectifs fixés.

1.1.3.4. Conclusion partielle : la modélisation est une approche appropriée pour raisonner la gestion de *P. ramosa* qui repose sur une combinaison de méthodes prophylactiques et doit s'intégrer dans la stratégie de gestion des adventices

La lutte contre *P. ramosa* repose essentiellement sur un ensemble de mesures prophylactiques à effet partiel et à long terme qui doivent être combinées pour parvenir à une gestion efficace. Ces mesures exploitent tous les processus mentionnés dans la section 1.1.2 (Figure 3). Beaucoup d'entre elles imposent de bien connaître les interactions entre *P. ramosa* et les autres plantes (cultivées et adventices), et sont susceptibles d'être influencées par les conditions environnementales qui déterminent le développement et la croissance de la plante parasite. La gestion de *P. ramosa* doit donc être raisonnée à l'échelle du système de culture pour prendre en compte de multiples facteurs en interactions : les techniques culturales, les plantes cultivées et adventices présentes dans la parcelle et le pédoclimat. Les modèles de simulation sont des outils adaptés à ce niveau de complexité et à l'échelle long-terme imposée par la persistance des semences d'orobanches dans le sol.

[5] Modèle : « Représentation simplifiée, relativement abstraite, d'un processus, d'un système, en vue de le décrire, de l'expliquer ou de le prévoir » (Dictionnaire de l'environnement).

1.2. Les modèles utilisables pour raisonner la gestion de *P. ramosa*

1.2.1. Quel type de modèle nous faut-il ?

Différentes approches peuvent être employées pour modéliser l'effet des systèmes de culture sur la dynamique des bioagresseurs des cultures. L'approche mécaniste utilise des sous-modèles qui sont des propositions d'explications de processus biophysiques, tandis l'approche empirique relie directement les observations aux entrées du modèle sans tenter d'expliquer le lien entre ces variables (Colbach, 2006). L'approche mécaniste est capable de prédire l'effet d'interactions complexes, tels que les effets techniques culturales × adventices × pédoclimat, et de mieux comprendre leurs résultats en les décortiquant à l'échelle des processus (Colbach, 2010). En outre, en modélisant des processus universels, le modèle mécaniste est utilisable dans une large gamme de conditions sans qu'un reparamétrage soit systématiquement nécessaire, ce qui est particulièrement intéressant pour la prospection de stratégies de gestion et pour aider à la conception de systèmes de culture innovants.

Le modèle idéal pour raisonner la gestion de *P. ramosa* est donc un modèle **mécaniste**, décrivant les processus déterminant la dynamique de la plante parasite (section 1.1.2). Pour cela, il doit représenter le **système racinaire** des plantes sur lesquelles *P. ramosa* peut potentiellement se fixer, et ce pour toutes les espèces, **cultures et adventices**, rencontrées dans une parcelle. En outre, il doit prendre en compte les effets des **techniques de lutte curatives et prophylactiques** listées précédemment, en interaction avec le **pédoclimat** sur **plusieurs dizaines d'années**, et ce non seulement sur la plante parasite mais aussi sur les adventices et les cultures (voir section 1.1.3). Idéalement, il doit modéliser l'effet du parasitisme sur les hôtes cultivés et adventices pour mieux prédire l'effet rétroactif des cultures et des adventices sur la plante parasite. Cela permettrait en outre de calculer les pertes de rendement dues au parasitisme, critère fondamental pour évaluer la performance des systèmes de culture. Chaque processus devrait être modélisé à un pas de temps journalier, pour optimiser finement la date d'application des techniques (Colbach, 2010). Enfin, parmi la multitude de facteurs et processus ayant une influence sur la dynamique de *P. ramosa*, nous nous concentrerons, dans notre recherche du modèle idéal, sur ceux qui déterminent les effets des systèmes de culture en interaction avec le pédoclimat sur la dynamique de *P. ramosa* à long-terme. Dans ce cadre, un modèle à l'échelle de la parcelle est adapté car l'infestation est surtout déterminée par l'historique cultural de la parcelle du fait de la persistance des semences dans le sol, tandis que la dispersion à une échelle plus large est conséquente mais secondaire (Cohen *et al.*, 2017).

1.2.2. Les modèles de dynamique des orobanches

Différents modèles de dynamiques des orobanches existent dans la littérature (Table 3). Seuls les modèles permettant de tester ou d'optimiser l'effet d'une ou plusieurs techniques culturales ont été pris en compte ici. Deux types principaux peuvent être distingués : les modèles phénologiques, prédisant la durée de stades de développement des orobanches en temps thermique[6], et les modèles démographiques, quantifiant les populations d'orobanches à différents stades. En marge de ces deux types de modèles, (Colbach *et al.*, 2017a) ont développé une approche originale consistant à estimer le risque orobanche résultant de la flore adventice à l'aide d'un indicateur[7], à partir de l'abondance d'adventices hôtes ou faux-hôtes présentes dans une parcelle, sans modéliser les mécanismes du parasitisme. Les modèles démographiques correspondent plus aux critères que nous recherchons car

[6] Temps thermique : Echelle d'expression du temps en fonction de la température, exprimée en °C·j. Calculé en cumulant la température moyenne de chaque jour à laquelle on retire la température de base (température minimum en dessous de laquelle le développement est supposé nul) (Gummerson, 1986; Bonhomme, 2000)

[7] Indicateur : Variable calculée à partir des sorties d'un modèle pour estimer une autre variable difficile d'accès (Bockstaller et al., 2008).

ils permettent de prendre en compte l'effet de plusieurs techniques sur la dynamique des orobanches sur plusieurs années, tandis que les modèles phénologiques permettent surtout d'optimiser la date d'application des herbicides, et que l'indicateur de risque ne modélise pas l'effet direct des techniques sur la plante parasite (seulement l'effet indirect via les adventices). Le modèle de Grenz *et al.* (2005a) en particulier, simule le cycle de vie d'*Orobanche crenata* comme la succession des processus que nous avons identifiés comme déterminants pour raisonner la gestion des orobanches (Table 1). Il est le seul qui intègre le système racinaire de l'hôte, en calculant l'infection par l'orobanche en fonction de la densité de longueur racinaire de l'hôte. Il prédit l'effet de la fréquence d'hôte dans la rotation, du travail du sol, de l'arrachage manuel et de la date de semis sur la dynamique d'*O. crenata*. En outre il prend en compte l'effet du pédoclimat. Colbach *et al.* (2011) s'en sont inspirés pour développer PHERASYS (pour ***Phe**lipanche **ra**mosa* dans les sys**t**èmes de culture), un modèle de dynamique de la plante parasite, qu'ils ont couplé à un modèle simplifié de dynamique des adventices dans les systèmes de cultures. Ils ont pu ainsi simuler la culture hôte colza en rotation avec plusieurs espèces cultivées non-hôtes et une adventice hôte type interagissant avec l'orobanche. Cependant, le modèle de Colbach *et al.* (2011) doit être amélioré car la représentation des plantes cultivées et adventices est fortement simplifiée, et la plupart des formalismes et paramètres proviennent du modèle d'*O. crenata,* tandis qu'il visaient à modéliser la dynamique de *P. ramosa*. Dans PHERASYS, le système racinaire des plantes hôtes n'est pas simulé mais est une variable d'entrée, et la partie post-émergence du cycle de l'orobanche a été fortement simplifiée. Contrairement au modèle de Grenz *et al.* (2005a), les relations trophiques entre l'orobanche et son hôte ne sont pas modélisées, ce qui est pourtant déterminant pour prédire la biomasse de l'orobanche et donc sa production de semences (section 1.1.2.6), et les pertes de rendement dues au parasitisme. De manière générale, les interactions entre l'orobanche et les autres plantes ne sont pas modélisées assez précisément pour prendre en compte tous les leviers de gestion disponibles (ex : efficacité des faux-hôtes et plantes piège en fonction de leur capacité à stimuler les germinations d'orobanche, différents niveaux de sensibilité des cultures hôtes…), et trop peu d'espèces cultivées et adventices ont été considérées.

Table 3 : Caractéristiques des modèles de dynamique des orobanches disponibles dans la littérature. En vert, les critères idéaux remplis par le modèle, et en orange les critères non remplis.

Espèce parasite	**Mécaniste**	**Nombre d'espèces hôtes ou faux-hôtes**	**Pluriannuel**	**Variables climatiques**	**Techniques culturale**	**Système racinaire**	**Source**
P. aegyptiaca	non	1 culture	non	oui	non	non	(Hosseini *et al.*, 2017)
O. minor	non	1 culture	non	oui	non	non	(Eizenberg *et al.*, 2005)
O. cumana	non	1 culture	non	oui	non	non	(Eizenberg *et al.*, 2012b)
P. aegyptiaca, *O. cumana*	non	1 culture	non	oui	non	non	(Ephrath and Eizenberg, 2010)
O. crenata	non	3 cultures	non	oui	non	non	(Pérez-de-Luque *et al.*, 2016)
O. cernua, *O. cumana*	non	1 culture	non	non	Herbicide	non	(Castro-Tendero and García-Torres, 1995; García-Torres *et al.*, 1996)
P. aegyptiaca	non	1 culture	non	oui	Herbicide	non	(Eizenberg *et al.*, 2009; Eizenberg *et al.*, 2012a; Cohen *et al.*, 2017; Eizenberg and Goldwasser, 2018)
P. ramosa	non	7 cultures et 9 adventices	oui	oui	Gestion des adventices	non	(Colbach *et al.*, 2017a)
P. mutelii	oui	0	oui	non	Rotation et gestion des adventices, fumigation	non	(Regan *et al.*, 2011)
O. crenata	oui	1 culture	oui	non	Date de semis, rotation	non	(López-Granados and García-Torres, 1997)
O. crenata	oui	4 cultures	oui	non	Rotation	non	(Schnell *et al.*, 1996)
O. crenata	oui	1 culture	oui	oui	Rotation, travail du sol, arrachage manuel, date de semis	oui	(Manschadi *et al.*, 2001; Manschadi *et al.*, 2003; Manschadi *et al.*, 2004; Grenz *et al.*, 2005a)
Plante parasite (orobanche)	oui	1 culture et 1 adventice générique	oui	oui	Rotation et gestion des adventices, travail du sol, date et densité de semis, herbicide, fauche	non	(Colbach *et al.*, 2011)

1.2.2.1. Conclusion partielle : les interactions entre les orobanches et les autres plantes, cultivées et adventices, doivent être mieux modélisées

Parmi les modèles de dynamiques d'orobanches trouvés dans la littérature, aucun n'est paramétré spécifiquement pour *P. ramosa* et aucun ne remplit tous les critères du modèle idéal permettant d'en raisonner la gestion. Certains cependant s'approchent de cet idéal. Les modèles de Grenz *et al.* (2005a) et de Colbach *et al.* (2011) en particulier sont mécanistes, et simulent l'effet de plusieurs techniques et du pédoclimat. Le modèle de Colbach *et al.* (2011) est en outre le seul à intégrer des espèces cultivées et adventices. En revanche, il doit être amélioré pour mieux caractériser les interactions entre l'orobanche et les autres plantes, en s'inspirant par exemple du modèle de compétition entre hôte et plante parasite de Grenz *et al.* (2005a), et en intégrant plus d'espèces. Un couplage avec un modèle de dynamique des adventices dans les systèmes de culture serait judicieux pour intégrer les multiples espèces, notamment adventices, présentes dans une parcelle et leurs potentielles interactions avec le parasite, et l'effet des techniques culturales en interaction avec le pédoclimat à long terme. Ce modèle devrait être mécaniste pour être compatible avec le modèle idéal de dynamique de *P. ramosa*.

1.2.3. Les modèles de dynamiques des adventices non parasites

Parmi les modèles de dynamique des adventices existant dans la littérature, seuls quelques-uns simulent l'effet de multiples techniques sur plusieurs années (Table 4). Un seul, FLORSYS (Gardarin *et al.*, 2012; Munier-Jolain *et al.*, 2013; Colbach *et al.*, 2014b; Colbach *et al.*, 2014c; Munier-Jolain *et al.*, 2014), est mécaniste, prend en compte l'effet du climat, et est paramétré pour plusieurs espèces de cultures et d'adventices. Il est donc le plus adapté pour le couplage que nous souhaitons réaliser avec un modèle de dynamique de l'orobanche (section 1.2.2.1).

Table 4 : Synthèse des modèles de dynamique pluriannuelle des adventices possédant tout ou partie des critères requis (en vert, les critères non remplis sont en orange) pour un couplage avec un modèle de dynamique de *Phelipanche ramosa*. Parmi les nombreux modèles existant dans la littérature (voir synthèse de Holst et al., 2007; Freckelton and Stephens, 2009; Colbach, 2010), seuls les modèles prédisant l'effet des systèmes de culture sur la dynamique pluriannuelle des adventices et l'effet des adventices sur la production agricole, critère fondamental pour évaluer la performance des systèmes de culture, ont été retenus.

Modèle	**Techniques culturales**	**Climat**	**Mécaniste**	**Cultures**	**Adventices**	**Système racinaire**	**Référence**
RIM	Principales opérations et options	non	non	Grandes cultures	Une espèce (*Lolium rigidum*)	non	(Pannell *et al.*, 2004; Lacoste and Powles, 2017)
Weed Manager	Principales opérations et options	oui	oui	Blé	Flore adventice plurispécifique	non	(Parsons *et al.*, 2009; Benjamin *et al.*, 2010)
FLORSYS	Liste détaillée d'opérations	oui	oui	Grandes cultures (incluant des poacées pérennes et des légumineuses)	Flore adventice plurispécifique	non	(Gardarin *et al.*, 2012; Munier-Jolain *et al.*, 2013; Colbach *et al.*, 2014b; Colbach *et al.*, 2014c; Munier-Jolain *et al.*, 2014)

FLORSYS modélise les mécanismes de mortalité, dormance, germination des semences et de croissance de la plantule dans le sol en fonction du pédoclimat en 1D (les semences sont réparties en fonction de la profondeur dans des couches de sol horizontales homogènes). A l'émergence, chaque plante, culture ou adventice, est positionnée et représentée en 3D dans la parcelle (approche individu-centrée), afin de prendre en compte la compétition entre plantes pour la lumière. Les plantes croissent en fonction la biomasse qu'elles produisent par photosynthèse jusqu'à fructification. La phénologie est déterminée par la température et la saison de levée. Dans le cas des adventices, les semences libérées rejoignent le stock semencier. Les semences des cultures sont récoltées, ce qui permet à FLORSYS de prédire le rendement. Le travail du sol et le désherbage mécanique déplacent les semences dans le sol et tuent une partie des semences germées et des plantes. L'application d'herbicides et le gel détruisent aussi une partie des plantes. La date, la densité et le motif de semis ainsi que le choix des espèces semées chaque année (en pur ou en mélange) influencent les relations de compétition entre plantes. Les techniques culturales à implémenter sont données en entrée par l'utilisateur, ainsi que les caractéristiques de la parcelle (texture du sol, latitude...), les données météorologiques et le stock semencier initial d'adventices.

En sortie, FLORSYS prédit le stock semencier adventice, et la densité et la biomasse d'adventices quotidiennement. Il permet d'évaluer les performances des systèmes de culture en calculant, à partir des sorties, des indicateurs d'impact de la flore adventice en terme de nuisibilité (ex : pertes de rendement dues aux adventices), de contribution à la biodiversité (ex : source de nourriture pour les pollinisateurs) et à la préservation de l'environnement (ex : limitation de l'érosion) (Mézière *et al.*, 2015). Grâce à ces indicateurs, il peut être utilisé pour concevoir des stratégies de gestion de la flore adventice répondant à plusieurs objectifs (Colbach *et al.*, 2017b). Il a été utilisé, avec d'autres outils plus simples, en atelier de co-conception avec des agriculteurs (Colas, 2018).

Malgré ses atouts, FLORSYS ne remplit pas tous les critères requis pour un couplage avec un modèle de parasitisme par *P. ramosa* car il ne représente pas la partie racinaire des plantes.

1.2.3.1. Conclusion partielle : le système racinaire des plantes sur lequel se développe *P. ramosa* doit être modélisé

Parmi les modèles de dynamique des adventices, FLORSYS est le meilleur candidat pour un couplage avec un modèle de dynamique de *P. ramosa* car il simule la dynamique d'un couvert plurispécifique en fonction de l'effet des techniques culturales et du pédoclimat sur plusieurs années. Sa structure mécaniste est suffisamment générique pour pouvoir intégrer un module de dynamique de *P. ramosa* et l'effet de techniques spécifiques à la gestion des plantes parasites. En outre, FLORSYS est un outil pratique pouvant faciliter l'accompagnement au changement de pratiques en étant utilisé comme outil d'aide à la décision. En revanche, FLORSYS ne simule que la partie aérienne des plantes tandis que *P. ramosa* est une plante parasite racinaire. Il doit donc être couplé à un modèle de croissance racinaire.

1.2.4. Les modèles de croissance racinaire

Afin de pouvoir être couplé à FLORSYS, le modèle de croissance racinaire retenu doit remplir les critères suivants, il doit être 1) individu-centré, 2) paramétré pour plusieurs espèces de cultures et d'adventices, 3) comporter peu de variables pour pouvoir simuler les nombreuses plantes présentes sur la parcelle chaque jour en un temps de simulation raisonnable, et 4) prédire la densité de longueur racinaire qui détermine le nombre de semences parasites germées et fixées par couche de sol (Grenz *et al.*, 2005a). Parmi les modèles de croissance racinaire trouvés dans la littérature, seulement quelques-uns sont paramétrés pour des cultures et des adventices (Berger *et al.*, 2013) (Table 5). De manière générale, deux types de modèles de croissance racinaires existent, les modèles de densité racinaire (ex : APSIM) et les modèles d'architecture racinaire (ex : ArchiSimple ou OpenSimRoot) (Dupuy *et al.*, 2010; Dunbabin *et al.*, 2013). Les premiers ont l'avantage de représenter la croissance racinaire simplement, en répartissant la densité de racines dans l'espace. Mais la plupart ne sont pas adaptés pour l'approche individu centrée car ils modélisent un couvert homogène, en répartissant la densité racinaire en 1D en fonction de la profondeur (répartition homogène des racines dans des couches horizontales de sol). Au contraire, les modèles d'architecture racinaire simulent la croissance racinaire de chaque plante mais sont trop détaillés (représentation 3D de chaque segment racinaire) pour nos besoins de simulation. Quelques modèles adoptent une représentation plus appropriée, à la fois simple et adaptée à l'approche individu-centrée, en modélisant la densité de racines en fonction de la profondeur et de l'extension latérale du système racinaire. Parmi ceux-ci, le modèle COMPETE (Pedersen *et al.*, 2010) présente l'inconvénient d'être très empirique avec des paramètres souvent difficiles à mesurer et variables avec l'environnement (ex : paramètres de forme sans unité gouvernant la répartition des racines). RSCone (Pagès *et al.*, submitted) a un statut hybride entre un modèle de densité individu-centré empirique et une approche mécaniste qui lui permet d'être paramétré pour de nombreuses espèces de culture et d'adventices (35). Il correspond donc à notre modèle idéal.

En effet, RSCone a été construit par simplification (métamodélisation) du modèle ArchiSimple qui représente chaque segment racinaire en 3D produit quotidiennement via les processus d'émission, de croissance, de ramification et de décomposition des racines (Pagès *et al.*, 2014). RSCone représente le système racinaire via seulement quatre variables, sous la forme d'une enveloppe géométrique (volume de révolution) dans laquelle est répartie la densité de racines en fonction de la profondeur. Etant dérivé d'ArchiSimple, il intègre l'effet des facteurs environnementaux (température et structure du sol, données en entrée) sur la croissance racinaire, et bénéficie des nombreux travaux de paramétrage d'ArchiSimple entrepris pour une centaine d'espèces cultivées et adventices (Drouet *et al.*, 2005; Pagès *et al.*, 2014; Pagès and Picon-Cochard, 2014; Bui *et al.*, 2015; Moreau *et al.*, 2017; Pagès and Kervella, 2018; Faverjon *et al.*, 2019). RSCone peut être couplé à un modèle de morphogénèse aérienne via la biomasse allouée aux racines qui lui est donnée en entrée.

Table 5 : Principaux modèles potentiellement adaptés pour simuler la croissance racinaire des cultures et adventices. En vert, les critères idéaux remplis par le modèle, et en orange les critères non remplis.

Modèle	**Individu-centré**	**Espèces paramétrées**	**Représentation du système racinaire**	**Calcul de la densité de longueur racinaire**	**Référence**
APSIM	Non	Grandes cultures et adventices	Densité racinaire par couche horizontale de sol	Oui	(Keating *et al.*, 2003)
OpenSimRoot	Oui	Grandes cultures et 1 adventice	Architecture racinaire en 3D	Oui	(Lynch *et al.*, 1997; Postma *et al.*, 2017)
ArchiSimple	Oui	Grandes cultures et adventices	Architecture racinaire en 3D	Oui	(Pagès *et al.*, 2014)
COMPETE	Oui	1 culture (maïs) et 1 adventice	Volume de sol exploré par les racines par couche horizontale de sol	Non	(Berger *et al.*, 2013)
Modèle de densité racinaire 2D	Non (mais adaptable en passant en 3D par symétrie axiale)	Cultures légumières	Densité racinaire par unité de sol en 2D (profondeur × distance au milieu du rang de culture)	Oui	(Pedersen *et al.*, 2010)
RSCone	Oui	Grandes cultures et adventices	Densité racinaire par couche horizontale de sol au sein d'une enveloppe racinaire	Oui	(Pagès *et al.*, submitted)

1.2.4.1. Conclusion partielle : trois modèles doivent être couplés pour simuler la dynamique de *P. ramosa* dans les agroécosystèmes

Le modèle RSCone, avec sa représentation simplifiée du système racinaire et son paramétrage pour de nombreuses espèces cultivées et adventices, est adapté pour un couplage avec FLORSYS. Outre sa simplicité, il intègre des connaissances fines, issues du modèle mécaniste à partir duquel il a été construit, sur les processus affectant le développement et la croissance des racines. Ce niveau de détail offre la possibilité d'explorer et d'intégrer l'effet des facteurs environnementaux sur le système racinaire. Le couplage entre RSCone et FLORSYS peut être effectué via la biomasse allouée aux racines, ce qui implique de pouvoir la prédire en fonction de la biomasse aérienne des plantes. Finalement le couplage de RSCone, de FLORSYS et d'un modèle de dynamique de *P. ramosa* permettra de tester l'effet de combinaisons de techniques culturales sur la plante parasite, en interaction avec la flore adventice, et d'en déduire des stratégies de gestion efficaces à long terme.

1.3. Objectifs

Dans les sections précédentes, nous avons montré que pour comprendre comment gérer *P. ramosa*, il est nécessaire de décortiquer les éléments d'un système complexe comprenant de multiples interactions biotiques et abiotiques. Il s'agit en effet d'étudier les effets des systèmes de culture en interaction avec le pédoclimat sur les plantes cultivées, adventices et parasites interagissant entre elles via des relations de parasitisme et de compétition pour les ressources (lumière, eau, nutriments). Nous avons déterminé que la modélisation mécaniste est une méthodologie adaptée pour synthétiser les connaissances disponibles sur ce système complexe et quantifier l'effet des multiples interactions qu'il comprend par simulations. Nous avons identifié des modèles ou des approches de modélisation pour représenter certaines parties du système complexe "système de culture x pédoclimat x cultures x adventices x parasite", et mis en évidence les connaissances manquantes à acquérir au préalable par expérimentation pour modéliser l'ensemble de ce système. Le modèle résultant de ce couplage permettra de tester virtuellement l'effet de multiples techniques culturales dans divers contextes pédoclimatiques et floristiques, afin de déduire des stratégies de gestion agroécologiques de *P. ramosa* et des adventices.

L'objectif de cette thèse est de compléter et de synthétiser les connaissances sur la dynamique de *P. ramosa* en interaction avec les adventices et les cultures dans les agroécosystèmes, afin de développer un modèle de simulation indispensable pour concevoir des stratégies de gestion durables valorisant la biodiversité et les régulations biologiques. Pour parvenir à cet objectif, nous tenterons de répondre aux sous-objectifs suivants au cours d'étapes successives (Figure 4) :

(1) **Quels sont les déterminants de la persistance des semences de *P. ramosa* dans le sol ?**
Dans cette étape, nous mettrons en place des expérimentations pour acquérir des connaissances sur les processus cruciaux et pourtant mal connus de dormance et de mortalité des semences d'orobanche dans le sol (Chapitre 2). Pour quantifier et modéliser ces processus, nous adapterons une méthodologie d'expérimentation et d'analyse de données employée sur des adventices non-parasites.

(2) **Quels sont les déterminants, en termes de développement et de croissance des plantes non-parasites, de la dynamique d'infection des racines par *P. ramosa* ?**
Cette étape consiste à intégrer le système racinaire des plantes dans un modèle de dynamique des adventices et des cultures dans les agroécosystèmes, en couplant FLORSYS et RSCone, en vue de modéliser le parasitisme racinaire par *P. ramosa* (Chapitre 3). Des simulations seront réalisées d'une part pour évaluer la qualité de prédiction des modèles couplés, et d'autre part pour identifier les caractéristiques des communautés végétales (en termes de développemement et de croissance) susceptibles d'être parasitées par *P. ramosa* et/ou favorisant le prélèvement de ressources du sol par les racines.

(3) **Peut-on développer une gestion agroécologique de *P. ramosa* sans herbicides ?**
Nous tenterons de répondre à cette question en développant un nouveau modèle de dynamique de *P. ramosa*, PHERASYS.2, à partir des résultats de l'étape (1), en adaptant les formalismes de FLORSYS et des modèles de dynamique des orobanches existants (voir section 1.2) pour les processus de pré-infection, et en développant de nouveaux formalismes pour les relations trophiques hôte-parasite. Puis PHERASYS.2 sera couplé au complexe FLORSYS-RSCone issu de l'étape (2) pour simuler différentes stratégies de gestion de la plante parasite et évaluer leurs efficacités (Chapitre 4). Ces simulations permettront d'estimer dans quelle mesure il est possible d'utiliser les adventices pour réguler la plante parasite, ou d'identifier des techniques culturales efficaces pour lutter à la fois contre *P. ramosa* et les adventices.

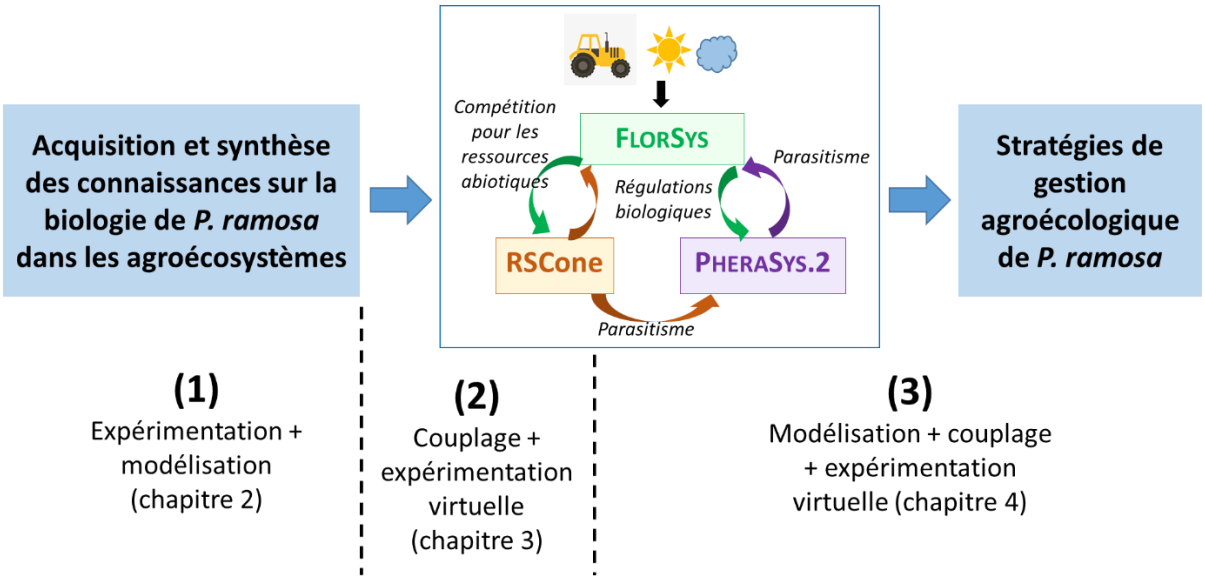

Figure 4 : Objectifs (cadres bleus) et étapes de la thèse (numérotées), détaillés dans la section 1.3. Pour parvenir à ces objectifs, différents types d'interactions entre plantes (en italiques) doivent être modélisés via le couplage de trois modèles (couplages indiqués par les flèches courbes) : FLORSYS (Gardarin *et al.*, 2012; Munier-Jolain *et al.*, 2013; Colbach *et al.*, 2014b; Colbach *et al.*, 2014c; Munier-Jolain *et al.*, 2014), modèle des effets des systèmes de culture (techniques culturales et pédoclimat, représentés par les pictogrammes) sur la dynamique des adventices, RSCone (Pagès *et al.*, submitted), modèle de croissance racinaire, et PHERASYS.2, modèle de dynamique de *Phelipanche ramosa* développé au cours de la thèse.

Chapitre 2. Combler les lacunes dans les connaissances sur *P. ramosa* : mortalité et dormance des semences dans le sol

2.1. Objectifs et démarche

Pour développer le modèle PHERASYS.2 de la dynamique de *P. ramosa* dans les agroécosystèmes (Chapitre 4), il est tout d'abord nécessaire de quantifier les processus mal connus de la biologie de la plante parasite (Figure 5).

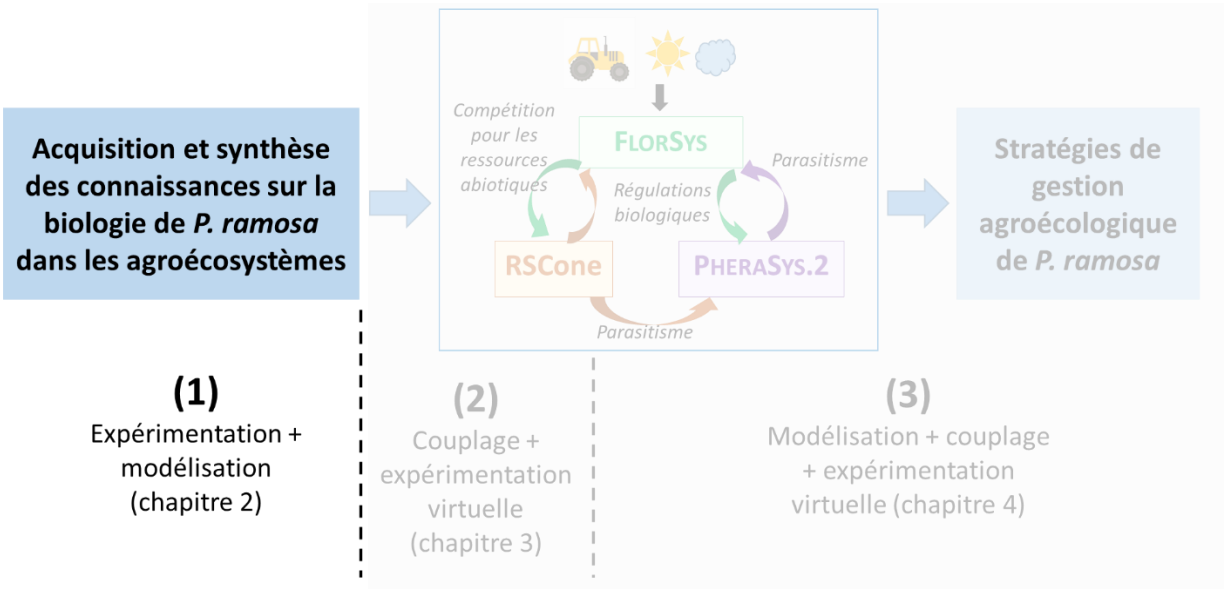

Figure 5 : Objectifs et démarche du Chapitre 2 dans le cadre de la thèse. Pour la légende, voir Figure 4.

Le Chapitre 1 a permis d'identifier trois processus-clés jamais quantifiés pour cette espèce : la production de semences par la plante parasite à maturité ainsi que la mortalité et la dormance des semences dans le sol. Caractériser ces processus est fondamental car ils déterminent le succès des mesures de contrôle à long-terme. Par exemple, la survie des semences dans le sol, combinée à leur capacité à rester dormantes dans l'attente de conditions favorables, imposent la durée minimum requise avant de pouvoir semer une culture hôte sans risquer d'accroître l'infestation.

Nous avons caractérisé la production de semences de *P. ramosa* sur des échantillons prélevés dans différentes parcelles. Ces résultats sont présentés en même temps que la formalisation des résultats dans le Chapitre 4.

L'objectif du présent chapitre est d'acquérir les connaissances manquantes en vue de modéliser les processus de mortalité et de dormance des semences de *P. ramosa* dans le sol. Pour cela, nous avons mis en place une expérimentation au champ de deux ans. Le protocole a été adapté d'une méthode utilisée pour modéliser la persistance dans le sol des semences d'adventices non-parasites. L'existence de différentes préférences d'hôtes et comportements entre pathovars de *P. ramosa* nous a incitée à

étudier plusieurs populations au sein de cette espèce. Nous avons choisi deux populations issues des cultures hôtes les plus infestées en France, c'est-à-dire le colza et le chanvre.

Les résultats présentés dans ce chapitre ont fait l'objet d'un article publié dans la revue *Weed Research* et ont été présentés lors de trois conférences internationales et trois séminaires.

Article scientifique

Pointurier, O., Gibot-Leclerc, S., Le Corre, V., Reibel, C., Strbik, F. & Colbach, N. (2019). Intraspecific seasonal variation of dormancy and mortality of branched broomrape seeds. *Weed Research*. https://onlinelibrary.wiley.com/doi/full/10.1111/wre.12378

Communications

Pointurier, O., Gibot-Leclerc, S., Le Corre, V., Reibel, C., Strbik, F. & Colbach, N. (2019). Les semences de la plante parasite orobanche rameuse ont une dormance saisonnière qui varie au niveau intrespécifique et une faible mortalité au champ. In *Séminaire du Projet de Recherche ANR CoSAC*, Paris, France. Poster.

Pointurier, O., Gibot-Leclerc, S., Moreau, D., Le Corre, V., Reibel, C., Strbik, F. & Colbach, N. (2019). Modélisation des effets des systèmes de culture sur la dynamique de la plante parasite orobanche rameuse en interaction avec les adventices. In *Journée des doctorants de l'UMR Agroécologie*, Dijon, France. Oral.

Pointurier, O., Gibot-Leclerc, S., Moreau, D., Reibel, C., Strbik, F. & Colbach, N. (2018). Modelling Cropping System Effects on Branched Broomrape Dynamics in Interaction with Weeds. In *XVe European Society for Agronomy Congress*, Geneva, Switzerland. Poster (premier prix poster étudiant).

Pointurier, O., Gibot-Leclerc, S., Moreau, D. & Colbach, N. (2017). Modélisation des effets des systèmes de culture sur la dynamique de l'orobanche rameuse en interaction avec les adventices. In *Séminaire de Restitution à mi-parcours du Projet de Recherche ANR CoSAC Paris*, France. Poster.

Pointurier, O., Gibot-Leclerc, S., Moreau, D. & Colbach, N. (2016a). Modelling cropping system effects on branched broomrape dynamics in interaction with weeds. In *23e Conférence du COLUMA: Journées internationales sur la lutte contre les mauvaises herbes*, Dijon, France: AFPP. Poster.

Pointurier, O., Gibot-Leclerc, S., Moreau, D., Darmency, H. & Colbach, N. (2016b). Modelling cropping system effects on branched broomrape dynamics in interaction with weeds. In *7th International Weed Science Congress*, Prague, Czech Republic. Poster.

2.2. Intraspecific seasonal variation of dormancy and mortality of *Phelipanche ramosa* seeds.

O POINTURIER, S GIBOT-LECLERC, V LE CORRE, C REIBEL, F STRBIK, N COLBACH*

* Agroécologie, AgroSup Dijon, INRA, Univ. Bourgogne, Univ. Bourgogne Franche-Comté, F-21000 Dijon, France

Received 6 February 2019

Revised version accepted 12 July 2019

Subject Editor: Harald Albrecht, TUM, Freising, Germany

Running head: Seed mortality and dormancy of P. ramosa

https://onlinelibrary.wiley.com/doi/full/10.1111/wre.12378

Correspondence: Dr Nathalie Colbach, INRA, UMR1347 Agroécologie, BP 86510, 17 rue Sully, F-21065 Dijon Cedex, France. Tel: +33-380693033; Fax: +33-380693262; E-mail: nathalie.colbach@inra.fr

WEED RESEARCH An International Journal of Weed Biology, Ecology and Vegetation Management

DOI: 10.1111/wre.12378

Intraspecific seasonal variation of dormancy and mortality of *Phelipanche ramosa* seeds

O POINTURIER, S GIBOT-LECLERC, V LE CORRE, C REIBEL, F STRBIK & N COLBACH

Agroécologie, AgroSup Dijon, INRA, Univ. Bourgogne Franche-Comté, Dijon, France

Received 6 February 2019
Revised version accepted 12 July 2019
Subject Editor: Harald Albrecht, TUM, Freising, Germany

Summary

Phelipanche ramosa (Branched broomrape) is an obligate root parasitic plant that is a major pest of oilseed rape in France. Knowledge on seed viability and dormancy under field conditions is crucial to understand how to control *P. ramosa,* but is as yet unknown. Our study aimed to quantify these processes with a 2-year seed burial experiment. Two genetically distinct populations of *P. ramosa* were studied, collected on winter oilseed rape (population O) and hemp (population H). Seed mortality was very low in both populations (4–7% per year). Although obligate parasitic seeds are assumed to germinate only after exposure to germination stimulants from host root exudates, a high proportion of population H seeds germinated spontaneously (up to 90%). Seeds of both populations displayed seasonal dormancy, with timing and magnitude depending on the population. Dormancy was low at the time each native host crop is usually sown. Populations differed in germination dynamics, with seeds of population H germinating faster. The difference in behaviour that we observed between populations is consistent with reported adaptations of pathovars to their preferred hosts. The results indicate that the parasitic plant management requires targeting at the populations concerned. For example, delayed sowing is more promising against population O than against population H.

Keywords: branched broomrape, seed longevity, germinability, spontaneous germination.

POINTURIER O, GIBOT-LECLERC S, LE CORRE V, REIBEL C, STRBIK F & COLBACH N (2019). Intraspecific seasonal variation of dormancy and mortality of *Phelipanche ramosa* seeds. *Weed Research*. https://doi.org/10.1111/wre.12378

Introduction

Broomrape species in the *Phelipanche* and *Orobanche* genera are holoparasites and derive resources from their hosts, due to their lack of chlorophyll and associated inability to photosynthesise (Heide-Jørgensen, 2013); some species are noxious weeds of key agricultural crops (Schneeweiss, 2013). Broomrape seed germination is necessarily triggered by host root exudates (Murdoch & Kebreab, 2013). This ensures that they germinate close to a host root where they attach and establish a vascular connection to take up water and nutrients (Heide-Jørgensen, 2013). *Phelipanche ramosa* (L.) Pomel (Branched broomrape), for example, is a major pest which globally infects diverse families such as *Solanaceae*, *Brassicaceae* or *Asteraceae* (Parker, 2013). In France, *P. ramosa* infests particularly winter oilseed rape (*Brassica napus* L.; www.terresinovia.fr/orobanche/carte.php), where it may decrease the yield by up to 90% in extreme cases (Gibot-Leclerc *et al.*, 2012). The species comprises several pathovars, that is genetically distinct populations with different host

Correspondence: N Colbach, INRA, UMR1347 Agroécologie, BP 86510, 17 rue Sully, F-21065 Dijon Cedex, France. Tel: +33 380693033; Fax: +33 380693262; E-mail: nathalie.colbach@inra.fr

2.2.1. Summary

Phelipanche ramosa (branched broomrape) is an obligate root parasitic plant that is a major pest of oilseed rape in France. Knowledge on seed viability and dormancy under field conditions is crucial to understand how to control *P. ramosa*, but is as yet unknown. Our study aimed to quantify these processes with a 2-year seed burial experiment. Two genetically distinct populations of *P. ramosa* were studied, collected on winter oilseed rape (population O) and hemp (population H). Seed mortality was very low in both populations (4-7% per year). Although obligate parasitic seeds are assumed to germinate only after exposure to germination stimulants from host root exudates, a high proportion of population-H seeds germinated spontaneously (up to 90%). Seeds of both populations displayed seasonal dormancy, with timing and magnitude depending on the population. Dormancy was low at the time each native host crop is usually sown. Populations differed in germination dynamics, with seeds of population H germinating faster. The difference in behaviour that we observed between populations are consistent with reported adaptations of pathovars to their preferred hosts. The results indicate that the parasitic plant management requires targeting at the populations concerned. For example, delayed sowing is more promising against population O than against population H.

Keywords: Branched broomrape, seed longevity, germinability, spontaneous germination

2.2.2. Introduction

Broomrape species in the *Phelipanche* and *Orobanche* genera are holoparasites and derive resources from their hosts, due to their lack of chlorophyll and associated inability to photosynthesize (Heide-Jørgensen, 2013); some species are noxious weeds of key agricultural crops (Schneeweiss, 2013). Broomrape seed germination is necessarily triggered by host root exudates (Murdoch & Kebreab, 2013). This ensures that they germinate close to a host root where they attach and establish a vascular connection to take up water and nutrients (Heide-Jørgensen, 2013). *Phelipanche ramosa* (L.) Pomel (branched broomrape), for example, is a major pest which globally infects diverse families such as *Solanaceae*, *Brassicaceae* or *Asteraceae* (Parker, 2013). In France, *P. ramosa* infests particularly winter oilseed rape (*Brassica napus* L.) (www.terresinovia.fr/orobanche/carte.php), where it may decrease the yield by up to 90% in extreme cases (Gibot-Leclerc et al., 2012). The species comprises several pathovars, i.e. genetically distinct populations with different host preferences. Three pathovars have been identified so far, preferentially infesting oilseed rape, tobacco (*Nicotiana tabacum* L.) and hemp (*Cannabis sativa* L.), respectively (Brault et al., 2007, Le Corre et al., 2014). Pathovars differ in their aggressiveness toward hosts (Brault et al., 2007), life cycle durations (Gibot-Leclerc et al., 2013b), susceptibility to host root exudates (Gibot-Leclerc et al., 2016) and morphology (Brault et al., 2007). These intraspecific variations should be considered when implementing cultural techniques to manage *P. ramosa*.

Broomrape control is based on a combination of techniques, each of which is individually of low efficiency (Rubiales et al., 2009). Knowledge of seed viability and dormancy (i.e. the failure of a viable seed to germinate under favourable air, moisture and temperature conditions, Murdoch & Kebreab, 2013) is crucial to optimize many cultural techniques, such as the frequency of host crops in the rotation (the faster seed viability decreases, the more often host crops can be grown) or crop type and sowing dates (choosing crops and dates coinciding with parasitic seed dormancy), for example. While studies investigated the hydrothermal conditions needed for germination (Gibot-Leclerc et al., 2004) and the ability of potential host species to trigger germination in the laboratory (Gibot-Leclerc et al., 2016), seed viability and susceptibility to root exudates over time in field conditions remains unknown in *P. ramosa*. Broomrape species seeds are generally assumed to persist up to 20 years in the soil and to display seasonal dormancy (Murdoch & Kebreab, 2013), but few experiments precisely quantify seed mortality and dormancy in the soil (eg. *Orobanche crenata*, Van Hezewijk et al., 1994, López-Granados & García-Torres, 1999, or *Phelipanche mutelii*, Prider et al., 2012, Prider et al.,

2013). Although it could significantly contribute to the difference in behaviour of *P. ramosa* pathovars, intraspecific variation in seed mortality and dormancy has never been investigated in the broomrapes.

Consequently, the objectives of the present study were to quantify (1) the decrease in seed viability over time, (2) the variation in susceptibility to root exudates (germinability) and (3) the germination dynamics of *P. ramosa* seeds across seasons in order to model *P. ramosa* seed bank dynamics and ultimately deduce long term management strategies from simulations (Pointurier et al., 2016). To achieve this, we adapted experimental protocols developed for non-parasitic weed seeds (Gardarin et al., 2010), buried parasitic seeds in a field, excavated them at regular intervals over two years, and measured seed viability and germinability *in vitro*. In order to understand how to adapt management strategies to different pathovars, we investigated intraspecific variations by studying two populations collected from the most frequently infested crops in France, i.e. oilseed rape and hemp (www.terresinovia.fr/orobanche/carte.php).

2.2.3. Materials and Methods

2.2.3.1. Seed material

P. ramosa seeds were harvested from arable fields of oilseed rape in Fontenay-Le-Comte (46°28’00″N, 00°49’00″W, 33m; Vendée, France) on 26 June 2014 (population O), and of hemp in Fresnay (48°18’52″N, 04°45’04″E, 233m; Aube, France) on 26 September 2014 (population H).

Seeds were disinfected under a laminar flow hood by a 5-minute immersion in 70% ethanol, followed by a 5-minute immersion in a solution of $Ca(OCl)_2$ at 3 % (p/v) and Tween 20 (0,1%) to limit fungal spread (Gibot-Leclerc et al., 2012). They were then rinsed five times with twice distilled water, and placed onto Whatman® paper squares of 1 cm x 1 cm (Glass microfiber filters GF/A) with a pipette. Pipetting resulted in a variable number of seeds (i.e. 19-183 seeds per paper square). Depositing a constant number of seeds onto the paper squares would have required using a stereoscopic microscope to transfer the seeds one by one because of their small size (350 × 250µm, Gibot-Leclerc et al., 2012). This was not possible under sterile conditions in the laminar flow hood. The paper squares were put into Petri dishes (9 cm diameter), and 3 mL of distilled water was added. In total, two dishes with eight paper squares each were prepared. Seeds were conditioned (14 days at 20°C in the dark) to make them susceptible to germination stimulants, and then germination and viability tests were carried out, following the procedure in the section 2.2.3.5.

2.2.3.2. Genetic analyses

Genetic analyses were conducted to confirm that the two *P. ramosa* populations used, O and H, were genetically distinct pathovars. Twelve individuals from each seed population were genotyped at 10 microsatellite markers, as described in Le Corre et al. (2014). These genotyping data were collated with some formerly acquired genotyping data on 973 individuals of *P. ramosa* sampled across France from 32 agricultural fields cultivated with oilseed rape, hemp or tobacco (Le Corre et al., 2014 and unpubl. data). A principal component analysis was performed to compare the genotypes of our populations to those of pathovars previously identified by Le Corre et al. (2014). The dataset used for this analysis describes the occurrences of each allele found over all markers for each individual tested. Plotting individuals on the plane defined by the first two principal components of the PCA allowed the visualisation of genetic similarities and genetic clusters among individuals.

2.2.3.3. Seed burial

The remaining *P. ramosa* seeds were buried in garden plots at INRA Dijon (47°19’2.624”N, 5°4’26.883”E, 257m asl) on 17 July 2014 and 14 October 2014 for populations O and H, respectively. Soil texture was 0.33 g/g clay, 0.49 g/g silt and 0.17 g/g sand. The protocol was adapted from Gardarin et al. (2010) who investigated non-parasitic weeds. Seeds were placed in nylon bags (10 x

5 cm, mesh size 100 µm) with 40 g sand (BIOT B4, 0.8-1.6 mm) and 100 seeds per bag. Usually, bags are filled with soil to limit seed-seed contact and reduce microbial transmission but seed recovery was found to be better with sand (annex A.1.1.1). Seed bags were placed in baskets, with three bags per species and basket, which were buried at a depth of approximately 30 cm. In total, 16 and 17 baskets, i.e. 5100 and 4800 seeds, were buried for populations O and H respectively. The garden was regularly hand-weeded and seeds were buried at 30 cm depth to mimic burial after mouldboard ploughing and put them far from potential residual host roots to prevent triggering *P. ramosa* germination in the soil. No oilseed-rape crop was cultivated in the garden before the experiment.

2.2.3.4. Seed excavation

Every six weeks over the following two years, one basket per *P. ramosa* population was randomly excavated. The seed bags were sieved in the laboratory with three successive sieves (800µm/425µm/125µm). The content of the 125-µm sieve was put into an erlenmeyer with 500 mL of K_2CO_3 2,9M, to separate the seeds in the supernatant from the sand that deposited at the bottom. The supernatant and centrifugate were transferred separately to Whatman® paper disks imbibed by 2-3 mL of distilled water (which soaked the paper without letting seeds float in water surplus) and placed into a Petri dish (9 cm diameter). Germination and viability tests were carried out after conditioning, following the procedure of section 2.2.3.5. Additional measurements were carried out to check that conditioning did not affect seed viability and mortality (see annex A.1.1.2). In population H, many seeds were found to germinate during conditioning before a germination stimulant was added. Two additional baskets were therefore excavated on 19 October 2015 to compare viability and germination with and without adding the germination stimulant (see sections 2.2.3.5).

2.2.3.5. Seed viability and germination tests

The Petri dishes were sealed with parafilm strip, wrapped in aluminium foil and placed in a dark growth chamber, at 20°C, over 14 days to condition the seeds (Gibot-Leclerc et al., 2004). The germination stimulant strigol analogue growth regulator GR24 (2 mL at 1 $mg \cdot L^{-1}$, optimal concentration, Gibot-Leclerc et al., 2004) was then added to each Petri dish and, over the next 40 days, the number of germinated seeds was counted every two days using a stereoscopic microscope (1.95x – 250x). A seed was considered to have germinated when the radicle length exceeded the seed width. The synthetic stimulant GR24 was chosen over host root exudates because it was more stable, whereas the stimulatory activity of root exudates varies between species and may be affected by environmental conditions (such as light for example, Yoneyama et al., 2013). This allowed us to quantify the potential ability of *P. ramosa* seeds to germinate over the season, irrespective of the host plant, and to compare populations that have potentially different preferred hosts. GR24 was added to all seed lots, except for those from one basket excavated on 19 October 2015 that were used to assess the effect of the germination stimulant (section 2.2.3.6.7) by comparing the germination of seeds stimulated with GR24 to that of unstimulated seeds. Seeds used to test the effect of the germination stimulant were not conditioned so the counting of germinated seeds started on the day the seeds were excavated and put into the Petri dishes.

Finally, the viability of the seeds that did not germinate was assessed by adding 2,3,5-triphenyl tetrazolium chloride (TTC, 1.5 mL TTC at 1%) to each Petri dish. The dishes were sealed with parafilm, wrapped in aluminium foil and placed into a drying oven at 40°C for 48 h. The seeds were then placed onto a new Whatman® disk imbibed with a saline solution (1% NaOCl). Viability was assessed after 10 minutes as viable seeds being stained a reddish pink colour (Gibot-Leclerc et al., 2004).

2.2.3.6. Analysis

2.2.3.6.1 Seed discrimination

For each excavation date (d), each excavated seed bag (r) and each *P. ramosa* population (O and H), the excavated seeds were classified as follows:

- The number of seeds retrieved from the bag that were not germinated (NT_{dr}),
- The number of seeds that germinated spontaneously during conditioning before GR24 was added ($NG0_{dr}$),
- The number of seeds that germinated at time x after GR24 addition (NG_{drx}),
- The number of seeds that germinated 40 days after GR24 addition ($NGmax_{dr}$),
- The number of seeds that did not germinate after exposure to GR24 and reacted to TTC (NNG_{dr}).

The same classification was used for the fresh seeds that were tested before seed burial, with NT_{0r} being the number of seeds tested in each Petri dish (r).

2.2.3.6.2 Measured seed viability

Seeds were considered viable if they germinated or reacted to TTC, resulting in the number of viable seeds NV_{dr}:

[a] $NV_{dr} = NG0_{dr} + NGmax_{dr} + NNG_{dr}$

At each excavation date, d, the proportion of viable seeds relative to the initial viability rate pV_{dr} was calculated for each seed bag r:

[b] $pV_{dr} = NV_{dr}/(pV_0 \cdot NS_0)$

where $NS_0 = 100$ is the number of seeds buried in each seed bag, and pV_0 the average viability of the seeds before burial measured on R=2 seed samples:

[c] $$pV_0 = \frac{\sum_{r=1}^{R}\left(\frac{NV_{0r}}{NT_{0r}}\right)}{R}$$

The proportion of viable seeds pV_{dr} was corrected for some seed bags due to measurement errors (see section 2.2.3.6.3). It was then analysed vs. time over the two years with a broken-stick regression inspired by Gardarin et al. (2010) with slopes depending on seed age (details in annex A.1.2.2.1) using the function lm in R (R Core Team, 2015). The annual seed mortality rates, given by the slopes, were compared between the two *P. ramosa* populations using a linear model in the function lm of R (details in annex A.1.3.2).

2.2.3.6.3 Reestimated seed viability

The combination of germination and tetrazolium tests was insufficient to detect all viable seeds in population O. Indeed, the proportion of viable seeds was found to decrease and increase again periodically over time, to reach about 0.9 at the end of the experiment. Rates of viability lower than this final rate were not reliable because they would suggest that seeds were resurrected. These unexpected drops in viability occurred from November to June, where viability measurements relied mostly on tetrazolium tests because few seeds germinated (annex A.1.3.3). Thus, we suspect that tetrazolium tests failed to discriminate all viable seeds. Given the high spontaneous germination of population-H seeds, their viability measurement relied less on the tetrazolium test and did not show this inconsistency. Inconsistent rates of viability in population O (i.e. data at excavations where viability was on average lower than the final rate, shown by open dots in Figure 6.A) were removed from the data before fitting the model of viability vs. time (Figure 6.A). The latter model was used to

estimate seed viability when measures were inconsistent for subsequent calculations of proportions of germinated seeds among viable seeds (sections 2.2.3.6.4 to 2.2.3.6.6).

2.2.3.6.4 Seed dormancy

The proportion of non-dormant seeds at each excavation date, d, and for each seed bag, r (or Petri dish, r, for pre-burial tests), was calculated from the number of viable seeds that germinated during the 40 days of monitoring, $NGmax_{dr}$, following exposure to GR24, relative to the number of viable seeds in the seed bag that had not yet germinated when GR24 was added:

$$[d]\quad pND_{dr} = \frac{NGmax_{dr}}{pV_{dr} \cdot NT_{dr} - NG0_{dr}}$$

The proportion of non-dormant seeds pND_{dr} was analysed over time since burial t_d (in days since burial) for each *P. ramosa* population with a broken-stick regression, using the generic seed dormancy model proposed by Gardarin & Colbach (2015) with slopes depending on season (annex A.1.2.2.2). This regression was fitted using PROC NLIN of SAS (version 9.4, SAS Institute, Cary NC) with the fit calculated as a pseudo-R^2, as 1 - $\frac{SSE}{SST}$, with SSE sum of squared errors and SST total sum of squares (UCLA: Statistical Consulting Group, 2015). 95% confidence intervals were calculated for each proportion pND_{dr} with the modified Wilson method, as recommended for binomial proportions, using the function BinomCI from the package DescTools of R (R Core Team, 2015).

2.2.3.6.5 Spontaneous germination

For each excavation date d and seed bag r (or Petri dish r for pre-burial tests), the proportion of seeds pSG_{dr} that germinated spontaneously during conditioning (before GR24 was added) was:

$$[e]\quad pSG_{dr} = \frac{NG0_{dr}}{pV_{dr} \cdot NT_{dr}}$$

2.2.3.6.6 Germination dynamics after GR24 addition

For each excavation date d and seed bag r (or Petri dish r for pre-burial tests), the proportion of seeds pG_{drx} that germinated at time x (°C·days) after adding GR24 was:

$$[f]\quad pG_{drx} = \frac{NG_{drx}}{pV_{dr} \cdot NT_{dr} - NG0_{dr}}$$

Modified Weibull equations (Colbach et al., 2002) were fitted to pG_{drx} vs. thermal time x since GR24 addition (°C·days) using PROC NLIN of SAS**:**

[g] if $x > x0_{dr}$

then $pG_{drx} = pND_{dr} \cdot \left(1 - e^{-\ln 2 \left(\frac{x - x0_{dr}}{x50_{dr} - x0_{dr}}\right)^{b_{dr}}}\right)$

else $pG_{drx} = 0$

where $x0_{dr}$ and $x50_{dr}$ are the time to the first germinated seed and until half the non-dormant seeds have germinated, respectively (in °C·days from GR24 addition), and b_{dr} is a unitless shape parameter. This approach has been used successfully in multispecific weed-germination studies (Colbach et al., 2002, Gardarin et al., 2011) and was preferred here to the recently developed method of Ritz et al. (2013) that disregards the germination lag $x0_{dr}$. Thermal time x (°C·days) was calculated from daily mean

temperature (20°C) and base temperature for *P. ramosa* germination (5°C, Gibot-Leclerc et al., 2004) under optimal moisture conditions as in Gardarin et al. (2011).

The germination parameters $x0_{dr}$, $x50_{dr}$ and b_{dr} were then analysed against the time since burial, proportion of non-dormant seeds and seed age (younger or older than 1 year), using linear regression in the lm function of R. The difference in germination parameters between population O and H was tested with the function lm of R. Data were log-transformed where necessary to achieve normality of residuals.

2.2.3.6.7 Effect of germination stimulant

The effect of the synthetic germination stimulant GR24 was evaluated on 19 October 2015 for population H by comparing the proportion of viable seeds pV_{dr} or the proportion of non-dormant seeds pND_{dr} of seed lots with vs. without adding GR24. A generalized linear model with a binomial distribution and a logit transformation was used to analyse the effect of the germination stimulant such that for the example for seed viability:

[h] $f(pV_{dr})$ = constant + GR24 effect + error with $f(y) = \ln(\frac{y}{1-y})$

The model was fitted with the glm function of R (R Core Team, 2015), weighting the proportion of viable seeds by the initial number of viable seeds ($pV_0 \cdot NS_0$) and the proportion of non-dormant seeds by the number of viable seeds that did not germinate before adding GR24 if any ($pV_{dr} \cdot NT_{dr}$-$NG0_{dr}$).

The effect of adding GR24 on the three germination parameters $x0_{dr}$, $x50_{dr}$ and b_{dr} was also tested with a linear model using the lm function of R.

2.2.4. Results

2.2.4.1. Characterizing *P. ramosa* populations

Genetic data obtained from the genotyping of microsatellite markers showed that the two populations used in this study are genetically well differentiated. The principal component projection (annex A.1.3.1) of seeds harvested on oilseed rape (population O) was clearly identified as the "oilseed rape" pathovar, while seeds harvested on hemp (population H) belong to a distinct genetic group comprising populations able to infest hemp or tobacco.

2.2.4.2. Seed viability over time

Almost all buried seeds were retrieved from the seed bags (100 ± 6 on average per seed bag). The proportion of germinated or tetrazolium-sensitive seeds of population O decreased rapidly after two months but then increased, before the same pattern was repeated (Figure 6.A). Conversely, the viability of population H did not present any increase in viability over time (Figure 6.B).

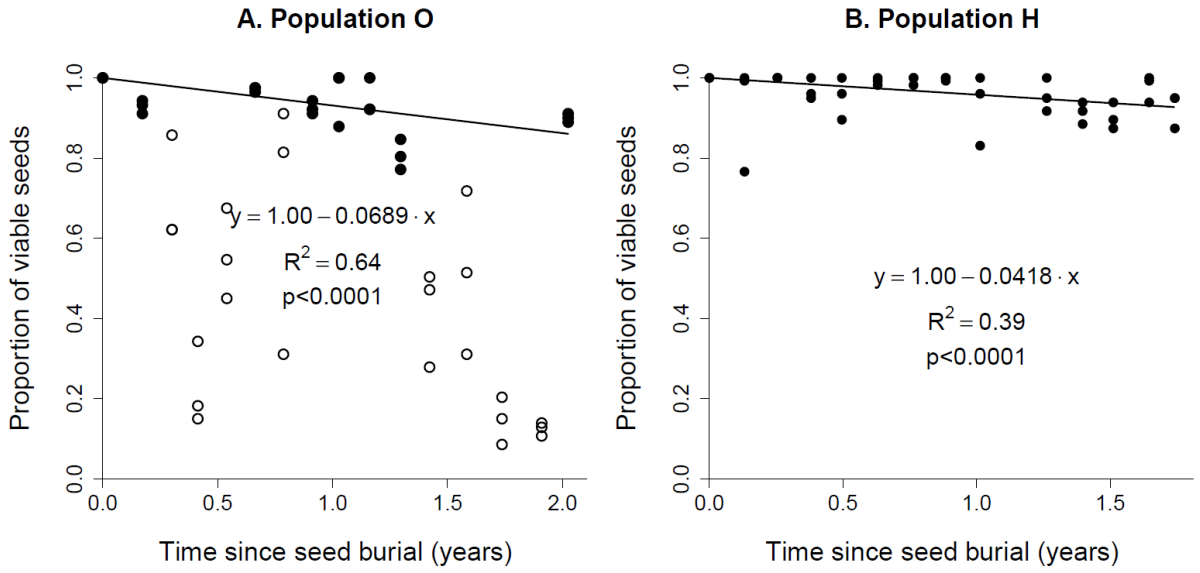

Figure 6: Viability of buried *Phelipanche ramosa* seeds over two years for populations O (collected on oilseed rape, A) and H (collected on hemp, B). Each point is the proportion of recovered seeds that germinated or reacted to tetrazolium from a bag of initially 100 buried seeds. Lines show broken-stick regressions fitted to bold dots. Open dots were not used in the regressions because they were deemed unreliable (see section 2.2.3.6.3).

After removing unreliable data in population O (see section 2.2.3.6.3 and open dots in Figure 6.A), seed viability steadily decreased over time in both *P. ramosa* populations, with no significant difference in the rate of seed loss between the two years of the experiment. The average annual seed decay was 6.9 and 4.2% per year for populations O and H, respectively. The viability rates did not significantly differ between populations (p-value = 0.44, details in annex A.1.3.2).

2.2.4.3. Spontaneous germination

Seed germination in the soil was rare as almost all buried seeds were recovered and only one germinated or empty (i.e. having germinated) seed was found per bag on average in both populations. In population O, only very few seeds germinated spontaneously in the lab (i.e. before GR24 was added to the seeds, Figure 7.A). Conversely, seeds of population H germinated spontaneously after excavation from January onwards (Figure 7.B). Seeds buried for less than 250 days showed a lower proportion of spontaneous germination (15-50%) than seeds buried for more than 250 days (50-90%). Although many seeds germinated spontaneously without GR24, adding GR24 increased the proportion of non-dormant seeds even further (an additional 17% in autumn, i.e. when the proportion of non-dormant seeds was the highest, see annex A.1.1.3).

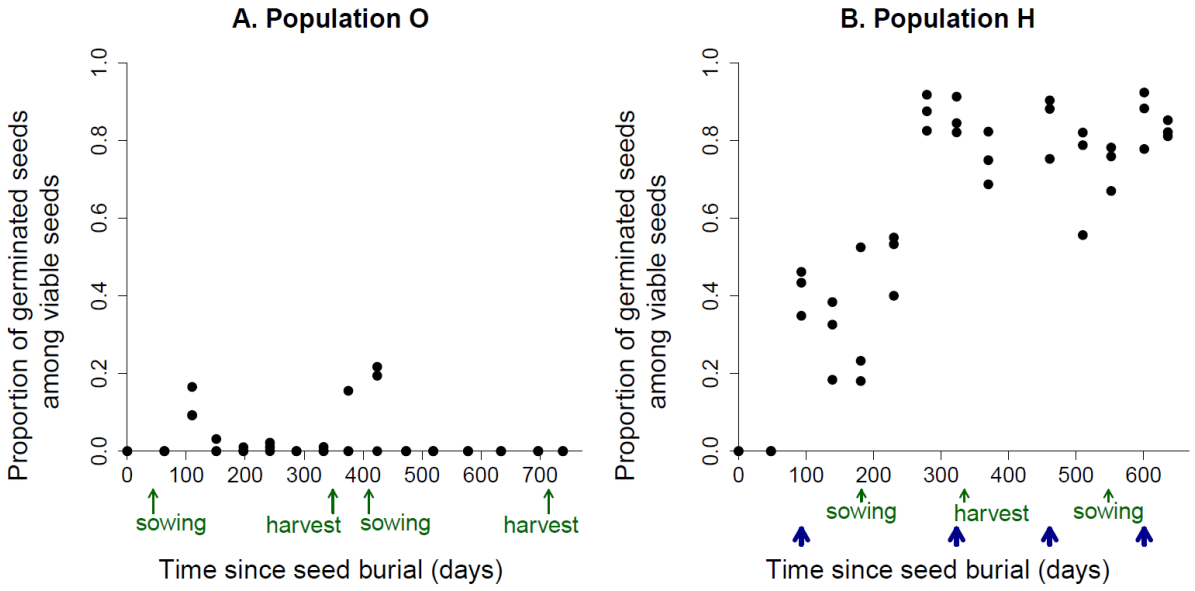

Figure 7: Spontaneous germination of *Phelipanche ramosa* seeds of population O (A) and H (B). Each point is the proportion of viable seeds germinating during conditioning following seed-bag recovery, and prior to the addition of GR24. Day 0 = date of burial (17 July 2014 and 14 October 2014 for figures A and B respectively). Usual sowing and harvesting dates of the native host of each population (i.e. oilseed rape and hemp respectively) were added to the x-axis.

2.2.4.4. Seasonal seed dormancy

Fresh seeds of population O were non-dormant until September, with an average germination of 91% after the addition of GR24 (Figure 8.A, Table 6). From September onwards (i.e. soon after oilseed rape crops are sown), the proportion of non-dormant seeds fell progressively to approximately 16% in early January. The non-dormant proportion then increased from the end of April onwards, up to 91% in May. Seeds remained non-dormant during summer. The same pattern was repeated during the second year of the experiment, but with a two-month delay compared to the first year, i.e. dormancy onset started only in November (i.e. a date considerably later than oilseed rape sowing).

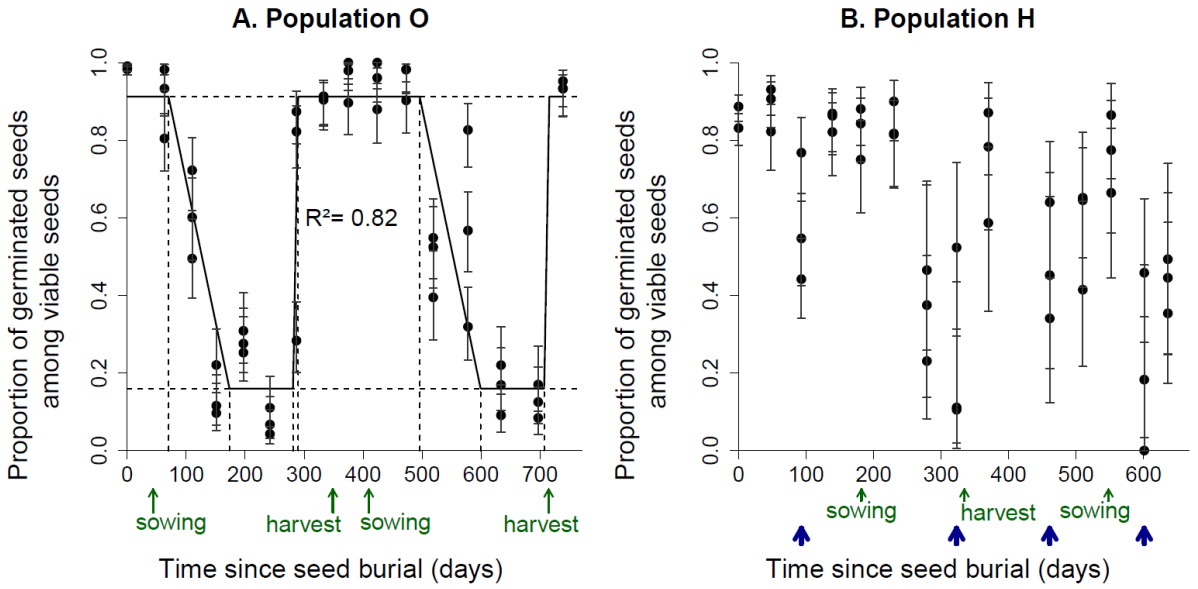

Figure 8: Seasonal non-dormancy of buried *Phelipanche ramosa* seeds over two years for populations O (A) and H (B). Each point is the proportion of viable seeds germinating after seed-bag recovery, conditioning and addition of GR24. Day 0 = date of burial (17 July 2014 and 14 October 2014 for figures A and B respectively). The line on fig. A shows the broken-stick regression fitted to the data, with regression parameters in Table 6. Thick arrows on fig. B show dormancy peaks. Usual sowing and harvesting dates of the native host of each population (i.e. oilseed rape and hemp respectively) were added to the x-axis. Vertical lines show 95% confidence intervals.

Table 6: Parameter estimates of the broken-stick regression fitted to the proportion of non-dormant *Phelipanche ramosa* seeds of population O (collected on oilseed rape) with time (R^2 = 0.82).

Dormancy parameters	**Parameter**		**Corresponding date**
	Estimate	**Standard-error**	
Timing in young seeds (days since burial on July 17)			
Onset of dormancy induction	70.0	0.00	September 25
End of dormancy induction	173	14.4	January 6
Onset of dormancy break-up	281	3.23	April 24
End of dormancy break-up	290	NA	May 3
Timing in old seeds			
Delay vs. young seeds (days)	426	11.1	+ 61 days
Proportion of non-dormant seeds			
Maximum (summer)	0.912	0.0337	
Minimum (winter)	0.160	0.0452	

The seasonal dormancy pattern was confused for seeds collected on hemp (Figure 8.B). This was partially due to the increase in data uncertainty over time since more and more seeds germinated spontaneously (see section 2.2.4.3 and Figure 7.B) leaving fewer seeds to study germinability (only 20% remained for the last year of the experiment). There seemed to be two dormancy peaks per year, one in January and one in early September the first year, and then 3 months earlier in the second year of the study. Dormancy was low during spring when hemp is usually sown.

2.2.4.5. Germination parameters

There was a short delay before seeds started to germinate following the addition of GR24 (Figure 9). In population O, this lag lasted on average 57.9 °C·days (4 days), ranging from 0 to 174 °C·days (details in annex A.1.3.4). Seeds then germinated quickly over the next 2-3 days, and half of the non-dormant seeds had germinated after 98.3 °C·days on average, ranging from 12.0 to 290 °C·days. The maximum proportion of germinated seeds in the germination flush corresponds to the proportion of non-dormant seeds of Figure 8.A. This proportion varied with season, and the germination flush was very limited during winter (Figure 9.B). Germination occurred one day earlier (germination lag of 39.4 °C·days on average, ranging from 0 to 86.7 °C·days, p-value = 0.0048) and 1.6 times faster (time to mid-germination of 61.9 °C·days on average, ranging from 28.2 to 102 °C·days, p-value < 0.0001) for population H (details in annex A.1.3.4).

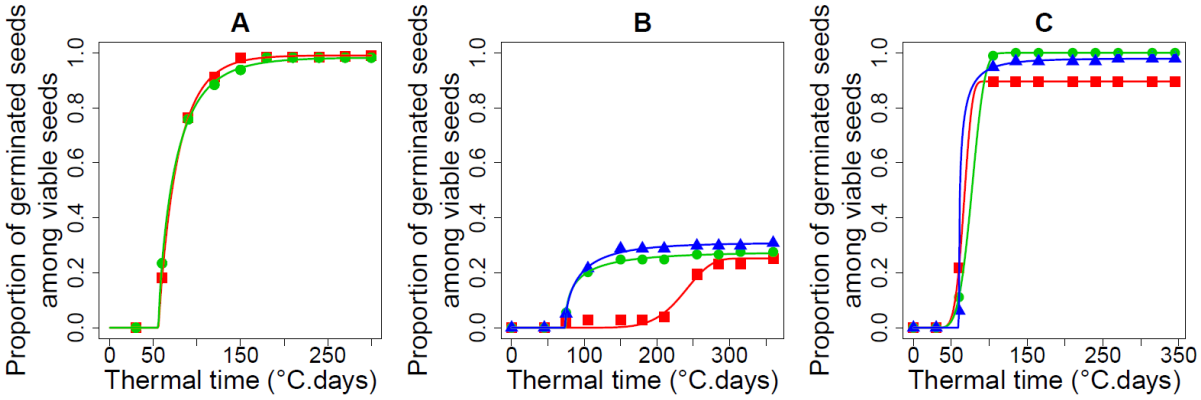

Figure 9: Germination progress with thermal time (base 5°C) for fresh seeds (A) and seeds buried for six (B), and 12 months (C) in *Phelipanche ramosa* seeds of population O (collected on oilseed rape). Each point is the proportion of seeds that germinated since the addition of GR24 to conditioned seeds from one excavated seed bag (each seed bag is represented by a symbol). Lines are fitted Weibull (with a lag) equations (equation [g]).

Germination parameters did not depend on dormancy levels, burial duration (details in annex A.1.3.4) or the use of the germination stimulant GR24 (details in annex A.1.1.3).

2.2.5. Discussion

2.2.5.1. Assessment of seed viability and dormancy

We adapted protocols developed for non-parasitic plants to quantify parasitic seed decay over time, seasonal variation in seed dormancy and parameters driving seed germination for two distinct *P. ramosa* populations. The methodology was modified for both the minute size of parasitic seeds and their need for chemical germination stimuli (Murdoch & Kebreab, 2013). We could not dissect the seeds of *P. ramosa* to assess seed viability, as done by Gardarin et al. (2010), because they were too small. We used the tetrazolium viability test but we found, as for other parasitic species (López-Granados & García-Torres, 1996, Van Mourik et al., 2003) this failed to discriminate well viable seeds of *P. ramosa*. We therefore estimated, statistically, seed viability over time from data for the number of seeds germinating during periods of low dormancy, rather than relying on the tetrazolium test. Moreover, our experiment was limited to two years of study and may have underestimated the long-term mortality rates given that seed decay may increase with seed age. However, such 2-year experiments were carried out on non-parasitic weeds and results were included into a weed dynamics

model which gave satisfying predictions compared to field observations of plant and seed bank densities over 13 years (Colbach et al., 2016).

Despite these methodological obstacles, the annual mortality rates measured for seeds of *P. ramosa* over two years (4 to 7 %) were similar to those measured for *P. mutelii* on a 9-year experiment with tetrazolium tests (<10% on average, Prider et al., 2012). They were however much lower than for two parasitic species from other genera of the Orobanchaceae family, i.e. *O. crenata* (approximately 25% per year for 2 years after burial, López-Granados & García-Torres, 1999) and *Striga hermonthica* (all seeds die in less than 2 years, Gbèhounou et al., 2003). Seed mortality may have been overestimated in *O. crenata* since it was estimated from germinated seeds, ungerminated seeds being considered as dead (López-Granados & García-Torres, 1999). The difference between our results and those on *S. hermonthica* cannot be attributed to methodological problems since the authors checked for the presence of an embryo by squeezing the seeds, which is a more reliable method than the tetrazolium test we used (Gbèhounou et al., 2003, Van Mourik et al., 2003). The difference between both species is perhaps not surprising considering that *S. hermonthica* belongs to a clade different from *P. ramosa* and might have different biology (Schneeweiss, 2013). Given that seeds of both species have similar sizes (Van Mourik et al., 2003, Gibot-Leclerc et al., 2012), the "squeezing test" should be applied in the future to determine more precisely *P. ramosa* seed viability.

The methodological problems in estimating seed viability mentioned above did not affect the results on seed dormancy (annex A.1.3.3). We found seasonal dormancy in *P. ramosa*, possibly in response to seasonal climate variations, since seeds buried in the field displayed annual patterns of dormancy, whereas seeds stored for a year in the laboratory under constant moisture and temperature conditions germinated consistently (Gibot-Leclerc, 2004). In the laboratory, induction and loss of dormancy of broomrape seeds were shown to depend on temperature (Kebreab & Murdoch, 1999), suggesting that soil conditions are a major factor explaining seasonal dormancy. However, we did not attempt to correlate seasonal seed dormancy to soil conditions because, based on our experience on non-parasitic weeds, simpler models are more robust for modelling the seasonal dormancy of weed species (Gardarin & Colbach, 2015) and the prediction of seed bank dynamics (Colbach et al., 2016).

In contrast to population O, we could not show a clear dormancy pattern in population H because of data uncertainty due to massive spontaneous germination (up to 90%). Such frequent spontaneous germination has to date only been reported in artificial hybrids of *O. cernua* and *O. cumana* (up to 65%), indicating that prevention of spontaneous germination may have been selected by evolution (Plakhine et al., 2012).

The "spontaneous" germination observed here might have been triggered by environmental factors in the soil, such as microbial metabolites (Evidente et al., 2006) or residual weed flora. The latter is unlikely though, as only root fragments of *Convolvulus arvensis* (field bindweed), which does not stimulate *P. ramosa* germination (Gibot-Leclerc et al., 2013a), were found in some population-O baskets. A seasonal pattern in spontaneous germination might be expected as the germination stimulant activity of plants varies over seasons (López-Granados & García-Torres, 1996). We observed, however, a continuous increase in spontaneous germination over two years. Moreover, as the seeds only germinated once in the laboratory, this would suggest that the environmental triggers of germination would need to have been muted when the seeds were still in the field. Possibly, the seeds lacked sufficient oxygen for germination at 30 cm depth (Rubiales et al., 2009).

Temperature and moisture are two other factors that are known to influence germination (Yoneyama et al., 2013) and might explain spontaneous germination because the temperature and moisture conditions of our experiment did not reflect natural conditions. We buried broomrape seeds 30 cm deep where hydrothermal conditions are more stable than in the top 10 cm of soil where seeds are typically found in arable fields (Prider et al., 2013). Temperature fluctuations, which could have occurred when excavating the seeds in our experiment, have been reported to cause spontaneous germination in *O. cumana* (P. Simier, pers. comm.) though never for *P. ramosa*. Seeds are also more

likely to be exposed to light closer to the soil surface than at the 30 cm depth of our experiment, but light is not known to affect germination in holoparasitic plants such as *P. ramosa* (Yoneyama et al., 2013).

Finally, spontaneous germination resulting from experimental artefacts in the laboratory are unlikely because preliminary tests showed that our retrieval protocol did not affect germination (details in annex A.1.1.1). Further experiments are required to understand whether spontaneous germination is a unique behaviour in population H or are due to our experimental set up.

2.2.5.2. A dormancy cycle adapted to the host life cycle

Both *P. ramosa* populations studied here displayed little dormancy during the sowing season of their native host crops and high dormancy during the intersowing period. This may allow them to parasitize the host early in its development and to benefit from its resources throughout its entire life cycle. This ability to remain dormant combined with a very low mortality in the soil enables *P. ramosa* seeds to await the sowing of a host crop. This is crucial in French cropping systems where monocultures are rare (Agreste, 2014) and several years may elapse between two successive host crops being sown.

It is noteworthy that fresh seeds of population O became dormant earlier than older ones. In France, oilseed rape is usually grown in rotation with winter cereals (Agreste, 2014), so it is likely that *P. ramosa* seeds produced from oilseed rape hosts spend the first year of their life in a cereal field. As cereals are non-hosts (Parker, 2013), becoming quickly dormant from September onwards would help to avoid fatal germination in the following cereal crop, usually sown in October.

The germination ecology of the Orobanchaceae is generally considered to mirror that of winter annuals (Baskin & Baskin, 1998), with high dormancy during winter-spring and low-dormancy in summer-autumn, which is consistent with our results on population O and previous reports on *O. crenata* (Van Hezewijk et al., 1994, López-Granados & García-Torres, 1999) and *P. mutelii* (Prider et al., 2013). However, seeds collected on hemp seemed to display two peaks of dormancy per year, in winter and summer, which could point to a shorter life-cycle, as for the tobacco pathovar that is genetically close to population H (14 and vs. 40 weeks for the oilseed rape pathovar Gibot-Leclerc et al., 2013b). The differences observed in dormancy cycles between populations O and H might therefore reflect adaptations to their host life-cycle duration. Theoretically, population H with its short life cycle and two periods of low dormancy in autumn and spring could parasitize both winter and summer crops. Consistently, the tobacco pathovar was reported to be able to reproduce on both oilseed rape and tomato, whereas the tomato lifespan was too short for the oilseed rape pathovar (Gibot-Leclerc et al., 2013b).

The benefits of dormancy for precise timing of germination are questionable in the case of population H given that seeds germinated spontaneously in our experiment. Spontaneous germination is considered lethal in obligate parasites (Plakhine et al., 2012) as seeds could germinate in the absence of hosts (suicidal germination). Such a behaviour might better be hypothesized opportunistic, potentially allowing parasitism of hosts that are not able to stimulate *P. ramosa* germination (e.g. *C. arvensis*, Gibot-Leclerc et al., 2013a), or to germinate quickly to attach to hosts as soon as they are available. Interestingly, seeds of population H germinated earlier and faster than population O in our experiment.

The difference in *P. ramosa* populations observed here suggests further distinct behaviours at the intraspecific scale, in addition to the distinct aggressiveness (Brault et al., 2007, Gibot-Leclerc et al., 2013b) and life-cycle durations (Gibot-Leclerc et al., 2013b) already reported among pathovars. The seasonal dormancy pattern of population O allows it to parasitize winter crops on which it completes its long life cycle. Conversely, population H could be more opportunistic, parasitizing both winter and summer crops with its shorter dormancy cycle, quicker germination progress and massive spontaneous germination. Further studies with populations from various locations are needed to confirm our results and generalize them at the pathovar scale, though our populations were genetically close to

populations from other locations in France used to define the pathovars. Moreover, both populations should be tested in other locations, particularly in the native region of population O where climatic conditions and soil properties are different from our experimental site, with milder and moister winters and siltier soils. Indeed, seed longevity may greatly vary between two experimental sites, as argued by Prider et al. (2012), although part of this variation could be due to the inaccuracy of the tetrazolium test they used. Dormancy patterns were however reported to be unaffected by location in *O. crenata* (Van Hezewijk et al., 1994).

2.2.5.3. Agronomic implications

Our results also allow recommendations for practical management. Crop rotations including consecutive host crops should be avoided as decay of *P. ramosa* seeds in the soil is very low for at least the first two years. Promoting fatal germination during fallows, when *P. ramosa* dormancy is low, by adopting catch crops (host species that are destroyed before parasite reproduction) and trap crops (stimulating germination without supporting further parasitic development) is a promising practice (Rubiales et al., 2009).

The efficiency of delaying oilseed rape sowing to reduce *P. ramosa* infestation in the field (Gibot-Leclerc et al., 2006) is consistent with our results. As fresh seeds enter dormancy at the end of summer, few are available to infect the crop once it emerges. Accordingly, Gibot-Leclerc et al. (2012) found no new parasitic seeds attaching to winter oilseed rape under field conditions after mid-November. The efficiency of the technique is probably limited in France, because oilseed rape sowing cannot be delayed beyond the end of September (www.terresinovia.fr/-/date-de-semis-colza-periodes-de-semis-conseillees-selon-les-regions) when a large proportion of *P. ramosa* seeds can still germinate.

Deep tillage buries seeds and prevents them from germinating via a lack of oxygen at depth (Rubiales et al., 2009). However, deep tillage should not be used more frequently than every two years because returning the soil would unearth persistent *P. ramosa* seeds at a time when they are still viable and able to germinate.

Ultimately, we would recommend a combination of several cultural techniques and to consider their long-term effects to develop more efficient strategies for managing *P. ramosa*. We are currently including the results of this paper in a simulation model that quantifies and predicts the effect of cropping systems on *P. ramosa* dynamics (Pointurier et al., 2016).

2.2.6. Acknowledgements

The present work was supported by INRA and, the research program “Assessing and reducing environmental risks from plant protection products” funded by the French Ministries in charge of Ecology and Agriculture, and by AgroSup Dijon (ARS O129). We thank Charles Poncet and his team from the platform Gentyane at INRA Clermont-Ferrand for performing microsatellite genotyping. We thank Hugues Busset and François Dugué who prepared the field for seed burial. We are grateful to David Bohan for improving the syntax and wording of the paper.

2.3. Conclusion du chapitre

Dans ce chapitre, nous avons réussi à modéliser les processus de mortalité et de dormance des semences de *P. ramosa* dans le sol, une des deux connaissances lacunaires identifiées au Chapitre 1 en termes de processus du cycle de vie de cette plante parasite. L'autre processus restant à étudier pour construire notre modèle de dynamique de la plante parasite, la production de semences, sera étudié au Chapitre 4.

Ici, nous avons modélisé la mortalité et la cinétique de germination des semences des deux populations étudiées et la dormance saisonnière de la population apparentée au colza uniquement, les résultats étant trop variables pour l'autre population du fait d'un taux de germinations spontanées exceptionnel. Dans ce travail de thèse, nous nous concentrerons donc sur la modélisation de la dynamique du pathovar colza. Les mêmes formalismes ont été utilisés pour modéliser la mortalité et la cinétique de germination des deux populations testées. Ils pourront donc être facilement adaptés à d'autres populations de *P. ramosa* en modifiant les valeurs de paramètres. Cependant des expérimentations complémentaires et possiblement de nouveaux formalismes seront nécessaires pour modéliser leur dormance saisonnière.

Outre les apports pour notre objectif de modélisation, ce chapitre contribue à mieux connaître la biologie des orobanches de manière générale pour lesquelles les processus de mortalité et de dormance des semences ont été relativement peu étudiés et jamais au niveau intraspécifique. Les différences que nous avons observées entre populations semblent renforcer les préférences d'hôtes reportées chez les pathovars. La population prélevée sur chanvre montre un comportement original, avec des germinations spontanées massives et plusieurs pics de dormance par an, alors qu'il est généralement admis que les orobanches sont incapables de germer sans stimulation préalable par des exsudats racinaires et ont un cycle de dormance annuel.

Chapitre 3. Modéliser le système racinaire des hôtes de *P. ramosa*

3.1. Objectifs et démarche

Au Chapitre 1, nous avons identifié FLORSYS comme étant le modèle le plus adéquat pour simuler la dynamique des plantes non-parasites interagissant avec *P. ramosa* en fonction des systèmes de culture et du pédoclimat, à condition de compléter FLORSYS par un modèle de croissance racinaire. Le Chapitre 1 a permis d'identifier les critères requis pour ce modèle de croissance racinaire : individu-centré, ayant une représentation suffisamment simple du système racinaire pour que toutes les plantes d'une parcelle puissent être simulées en un temps de calcul raisonnable, suffisamment générique pour pouvoir être appliqué à une grande diversité d'espèces, paramétré pour de nombreuses espèces de cultures et d'adventices (et facilement paramétrable pour pouvoir rajouter des nouvelles espèces dans le futur), et prédisant la densité de racines dans le sol afin de pouvoir simuler le parasitisme par *P. ramosa* et le prélèvement de ressources du sol. Nous avons donc tout d'abord mis en place une collaboration avec un modélisateur d'architecture racinaire (Loïc Pagès, INRA PSH Avignon) pour développer le modèle RSCone précisément adapté à nos besoins. Le développement de ce modèle racinaire a fait l'objet d'un article auquel j'ai participé et qui a été soumis à la revue *Plant and Soil* (Pagès *et al.*, submitted) (annexe A.2.1).

L'objectif de ce chapitre est de coupler le modèle RSCone au modèle FLORSYS et d'évaluer l'adéquation de ce complexe FLORSYS-RSCone pour répondre à nos objectifs de modélisation (Figure 10). Tout d'abord, les points de couplage ont été identifiés, puis les formalismes permettant de connecter les deux modèles ont été établis sur la base d'analyses de données collectées dans l'équipe, dans la littérature et à dire d'experts. Ensuite, des simulations de systèmes de culture ont été réalisées avec le modèle FLORSYS-RSCone, avec un double objectif. (1) Evaluer la qualité prédictive de FLORSYS-RSCone en comparant les résultats de simulations à des observations de terrain acquises précédemment dans l'équipe. (2) Déterminer les paramètres-clés dans le parasitisme par *P. ramosa* et dans le prélèvement de ressources du sol par les racines. Cette dernière étape avait pour objectif d'identifier les paramètres à mesurer précisément en priorité sur les futures espèces à paramétrer. Elle visait également à évaluer l'influence des paramètres intervenant dans les approximations que nous avons dû faire dans les formalismes de couplage. Cela nous a permis d'estimer s'il était nécessaire d'améliorer ces formalismes. Enfin, elle a préparé le couplage avec d'autres modèles de fonction racinaire, en évaluant l'effet des paramètres sur des variables proxys de deux grandes fonctions racinaires : le parasitisme par *P. ramosa* et le prélèvement de ressources du sol. Ces travaux ont fait l'objet d'un article qui sera soumis prochainement dans la revue *Ecological Modelling* et d'une présentation en séminaire.

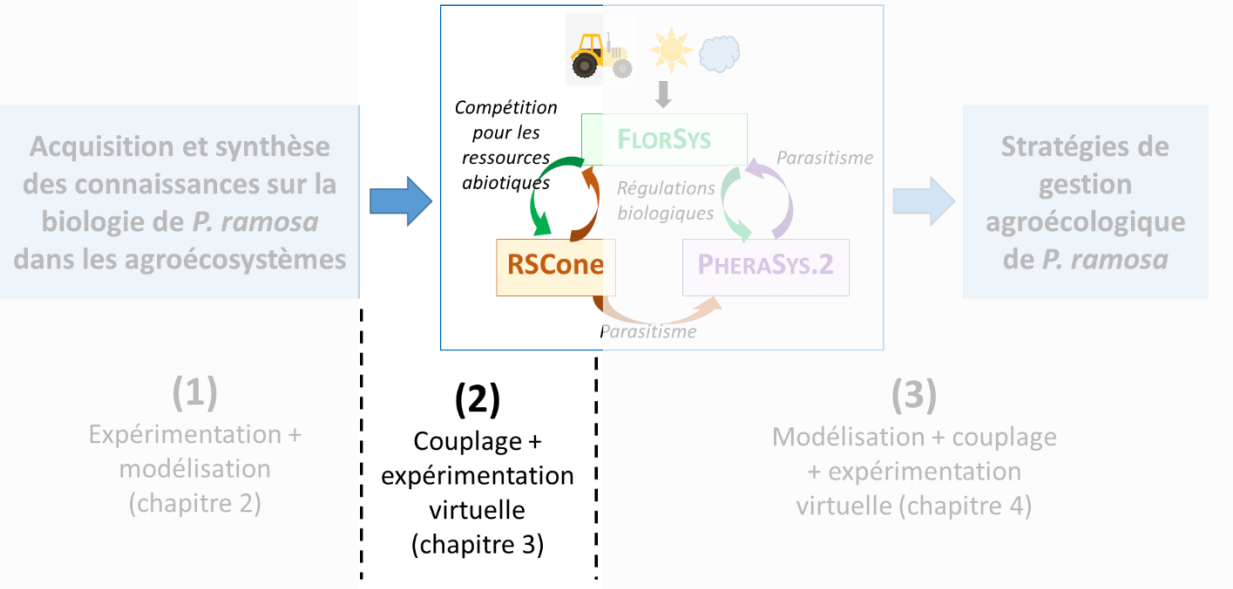

Figure 10 : Objectif et démarche du Chapitre 3 dans le cadre de la thèse. Pour la légende, voir Figure 4.

Articles scientifiques

Pointurier, O., Moreau, D. & Colbach, N. (en cours de soumission). Individual-based 3D modelling of root systems in heterogeneous plant canopies at the multiannual scale. Case study with a weed dynamics model. *Ecological Modelling.*

Pagès, L., Pointurier, O., Moreau, D., Voisin, A. S. & Colbach, N. (soumis). Simplifying an individual-based 3D root architecture model with virtual experiments. *Plant and Soil*.

Communication

Pointurier, O., Moreau, D., Pagès, L. & Colbach, N. Modélisation de l'architecture racinaire dans FLORSYS et perspectives : Application à la modélisation du parasitisme par l'orobanche rameuse (2018). In *2ème Journée de présentation de modèles de l'atelier thématique modélisation de l'UMR Agroécologie*, Dijon, France. Oral.

3.2. Individual-based 3D modelling of root systems in heterogeneous plant canopies at the multiannual scale. Case study with a weed dynamics model

Olivia Pointurier, Delphine Moreau, Loïc Pagès, Jacques Caneill, Nathalie Colbach

3.2.1. Abstract

Reducing pesticide use in agriculture is essential but involves shifting towards more complex agroecosystems. Plant canopies are expected to be more heterogeneous because a more abundant weed flora is likely to remain in low-herbicide fields, and because intercropping (i.e. mixing various crops species or varieties) is a promising option to reduce chemical inputs. Simulation models are useful to understand and design complex agroecological cropping systems, but they rarely represent the root systems of plants. However, belowground processes, such as competition for soil resource or infection by root-parasitic plants, are key determinants of the structure of plant communities. The aim of our study was to develop a model that simulates heterogeneous 3D individual-based crop-weed canopies from cropping system and pedoclimate and that will ultimately be used to design agroecological cropping systems. Therefore, we 1) connected a root system model (RSCone) to a weed dynamics model (FLORSYS) in order to include both above and belowground processes, 2) evaluated the prediction quality of our model, and 3) analysed the influence of species parameters on potential soil-resource uptake and root infection by parasitic plants. We used the well-known allometric relationship between root and total plant biomass to connect RSCone and FLORSYS, and we created new formalisms to model the effect of soil compaction on root growth. Our model was shown to correctly predict long-term weed dynamics in various cropping systems. From step 3), we characterized crops and weed communities that are potentially competitive for soil resource and most likely to be infected by parasitic plants, and we deduced agronomic recommendations. For example, species emerging and occupying the soil quickly were the most likely to relay broomrape infestation and control of such species should take precedence. Although we focussed on crop-weed competition, our approach can be applied to other heterogeneous canopies, for designing crop mixtures for example.

Keywords: soil resource, competition, parasitic plants, heterogeneous stands, weed management

3.2.2. Introduction

Weeds can greatly reduce yields and harvest quality, both directly, by competing with the crop for light, nutrients and water (Oerke, 2006), and indirectly, serving as alternative hosts for pests (Norris, 2005) or increasing workload for the farmer for example (Mézière *et al.*, 2015). They are mostly controlled by application of herbicides, but this practice must be drastically reduced because it was shown to have detrimental side-effects on environment and human health (Novotny, 1999). Alternative non-chemical techniques, such as diversifying crop rotation or soil tillage, are efficient to control weeds but must be combined because their effects are partial (Liebman and Gallandt, 1997). This is complex given the multiple techniques to implement, whose efficiencies depend moreover on pedoclimatic conditions and floristic contexts. This is why models are increasingly used to redesign cropping systems (Bergez *et al.*, 2010).

Mechanistic models are useful to synthesize existing knowledge, identify knowledge gaps, explore prospective scenarios in different contexts in the long term, represent and rank hypotheses on the processes implicated in a complex system, and design new cropping systems (Colbach, 2010).

FLORSYS (Gardarin *et al.*, 2012; Munier-Jolain *et al.*, 2013; Colbach *et al.*, 2014c; Munier-Jolain *et al.*, 2014) is among the many existing weed dynamics models (Holst *et al.*, 2007). To our knowledge, it is to date the only model quantifying the effects of cropping systems on the dynamics of multispecies weed floras with a daily time-step, in interaction with pedoclimatic conditions. This model is useful to design sustainable weed management strategies (Colbach *et al.*, 2017b). In addition to many other processes, FLORSYS simulates the competition between crops and weeds for light by representing each individual crop and weed plant in 3D in a virtual field and their shading effect on each other's growth and morphological plasticity (Munier-Jolain *et al.*, 2013; Colbach *et al.*, 2014c; Munier-Jolain *et al.*, 2014).

However, FLORSYS ignores plant roots and thus does not account for belowground processes such as uptake of soil resource or root infection by soil-borne pests. But, optimising the use of soil resource by crops is essential today to reduce mineral fertilization and environmental pollution (Raun and Johnson, 1999) and to improve resilience to droughts which become more frequent due to climate change (Turral *et al.*, 2011). Among soil-borne pests, root-infecting parasitic plants are very damaging to crops and difficult to control (Goldwasser and Rodenburg, 2013). Branched broomrape (*Phelipanche ramosa*) is one of the most harmful ones worldwide and is continuously extending its distribution area (Parker, 2013). It can also infect weeds which may spread the infection in the absence of crops (Gibot-Leclerc *et al.*, 2003).

Potentially, two kinds of root-system models are found in literature that could complement models such as FLORSYS, i.e. root density and root system architecture models (Dupuy *et al.*, 2010). The first type describes root density distribution generally in one dimension with depth empirically. It is based on simple mathematical formalisms and usually provides good predictions. However, it disregards the lateral extent of root systems, considering an average root profile below a plant cover without overlapping or spacing between root systems. This is satisfactory for crops in pure stands but not for either intercropping or crop-weed canopies where contrasting root systems coexist, shaped by species characteristics and competition with neighbouring plants. Root system architecture models represent root systems explicitly in three dimensions, in which the individual roots are segmented into pieces and have precise locations in space (Dunbabin *et al.*, 2013). But, they are too detailed and require too much computer time and memory to be compatible with simulations of all plants in a field for decades, as is necessary when considering weed dynamics (Mortensen *et al.*, 2000).

The recently developed RSCone model (Pagès *et al.*, submitted) is a compromise between the two approaches, reconciling a 3D representation of the root system with simplicity and speed, without neglecting the effects of environmental conditions and species diversity. RSCone is a metamodel (i.e. a simplified model derived from a pre-existing model) whose structure and parameter values were derived from a root system architecture model (ArchiSimple, Pagès *et al.*, 2014). It can be connected to models such as FLORSYS because, 1) its 3D individual-based representation of root systems is compatible with the individual-based representation of plants in FLORSYS, 2) but sufficiently simple for multiannual simulations of thousands of plants in a field, 3) it is already parameterized for 35 crop and weed species, has a relatively low number of parameters (22) with a biological meaning that can be estimated from ArchiSimple simulations, thus benefitting from experience on root system architecture models (Drouet and Pagès, 2003; Dunbabin *et al.*, 2013) and specific parameterization work of the ArchiSimple community (Drouet *et al.*, 2005; Pagès *et al.*, 2014; Pagès and Picon-Cochard, 2014; Bui *et al.*, 2015; Moreau *et al.*, 2017; Pagès and Kervella, 2018; Faverjon *et al.*, 2019), and 4) it predicts the key variables that drive water and nutrient uptake and infection by parasitic plants, i.e. root biomass and length density in the soil (Grenz *et al.*, 2005a; Malagoli and Le Deunff, 2014).

The objectives of this study were to 1) model root systems in FLORSYS by integrating RSCone as a submodel, 2) evaluate the predictive power of the new FLORSYS-RSCone model by comparing simulation results to field observations, 3) identify the key parameters for soil-resource uptake and

root infection by parasitic plants from simulation results and 4) deduce from the latter step which parameters must be measured precisely when parameterizing new species and which processes the most influence soil resource competition and parasitism. Step 3) also allowed us to deduce agronomic recommendations.

Ultimately, this study aims at developing a tool for weed management, which takes into account both above and belowground competition between plants for light and soil resource, as well as interactions with parasitic plants.

3.2.3. Material and methods

3.2.3.1. Model structures

3.2.3.1.1 The weed dynamics model FLORSYS

FLORSYS is a mechanistic model, i.e. it models processes of the life cycle of annual crops and weeds that determine their multiannual dynamics. It has been described in detail in other studies (Gardarin *et al.*, 2012; Munier-Jolain *et al.*, 2013; Colbach *et al.*, 2014c; Munier-Jolain *et al.*, 2014). We present here a quick summary of the model. The user inputs data describing the virtual field to be simulated (e.g. soil texture, latitude), weather (temperature, rainfall and radiation), cropping techniques (including crop sequence) and initial weed flora at the beginning of the simulation. From this information, FLORSYS predicts the weed seed bank and the density and biomass of weed and crop plants daily in the virtual field.

FLORSYS represents each individual, whether crop or weed plant, the same way and affected by the same processes. Processes relevant for seeds in the soil are mortality, dormancy and germination which are driven respectively by seed age, season, and soil climate. Seedlings emerge provided that the seeds are sufficiently close to the soil surface and that the soil is sufficiently moist and warm, without compact soil clods blocking shoot growth. These belowground processes are represented vertically over horizontally homogeneous 1-cm-thick soil layers, down to a depth of 30 cm. Soil temperature and water potential are predicted by the STICS soil submodel (Brisson *et al.*, 2003) included in FLORSYS. Soil structure, in terms of clod proportion and type, is predicted by the DéciBlé soil submodel (Chatelin *et al.*, 2005) included in FLORSYS.

From emergence onwards, plant phenology is driven by temperature, with time to flowering depending on emergence season. Plant growth results from the accumulation of biomass by photosynthesis after removing losses due to respiration. Biomass accumulated daily is shared among aboveground organs, i.e. leaves, stems and seeds. Photosynthesis depends on the amount of photosynthetically active radiation (PAR) intercepted by plants depending on plant morphology and shading due to neighbouring plants. To model this plant-plant interaction, each plant, whether crop or weed, is represented in three dimensions aboveground and located inside the field. Each plant is modelled as a cylinder, the dimensions of which are defined by the height and width of the plant, with leaf area distributed along plant height. Tillage and mechanical weeding operations move seeds in the soil, and kill part of germinated seeds and plants. Plants may also die from frost, herbicide applications, or ageing.

In total, 41 crop species or varieties (including both cash and cover crops) as well as 26 weed species are parameterized in FLORSYS.

3.2.3.1.2 The root-system model RSCone

The RSCone model has been described by Pagès et al (submitted). From daily inputs detailing allocation of biomass to roots, soil constraint on root growth and soil temperature in each soil layer, RSCone predicts the root-system dimensions of a plant daily, together with the distribution of root biomass and root lengths (shaded lines in Table S 16). The root system is depicted in three

dimensions, as a cylinder on top of a spilled cone, inside which root density is distributed. The dimensions of the root-system envelop grow over time and are limited by soil compaction and low temperatures. Root biomass is calculated by confronting the biomass demand from roots, which is determined by the root-system dimensions, to the biomass supply given as input. Root biomass is then distributed into each soil layer within the root-system envelop, assuming a homogeneous distribution within each layer and a linear decrease from a maximal value down to 0 with depth. Root-length density is determined by multiplying root-biomass density by the specific root length (SRL).

Twenty-one weed species and 23 crop species or varieties are parameterized in RSCone.

3.2.3.2. Integrating RSCone as a root distribution submodel into FLORSYS

Integrating RSCone as a submodel of FLORSYS required connecting both models at the ports (i.e. connecting functions) described below and in Figure 11. For now, most of the connection is one-way, i.e. FLORSYS variables are used as inputs of RSCone. Root functions such as nutrient uptake will be implemented in another paper (Moreau *et al.*, in prep.). Here, only biomass remobilization from below to above-ground after disturbances such as mowing or frost are considered.

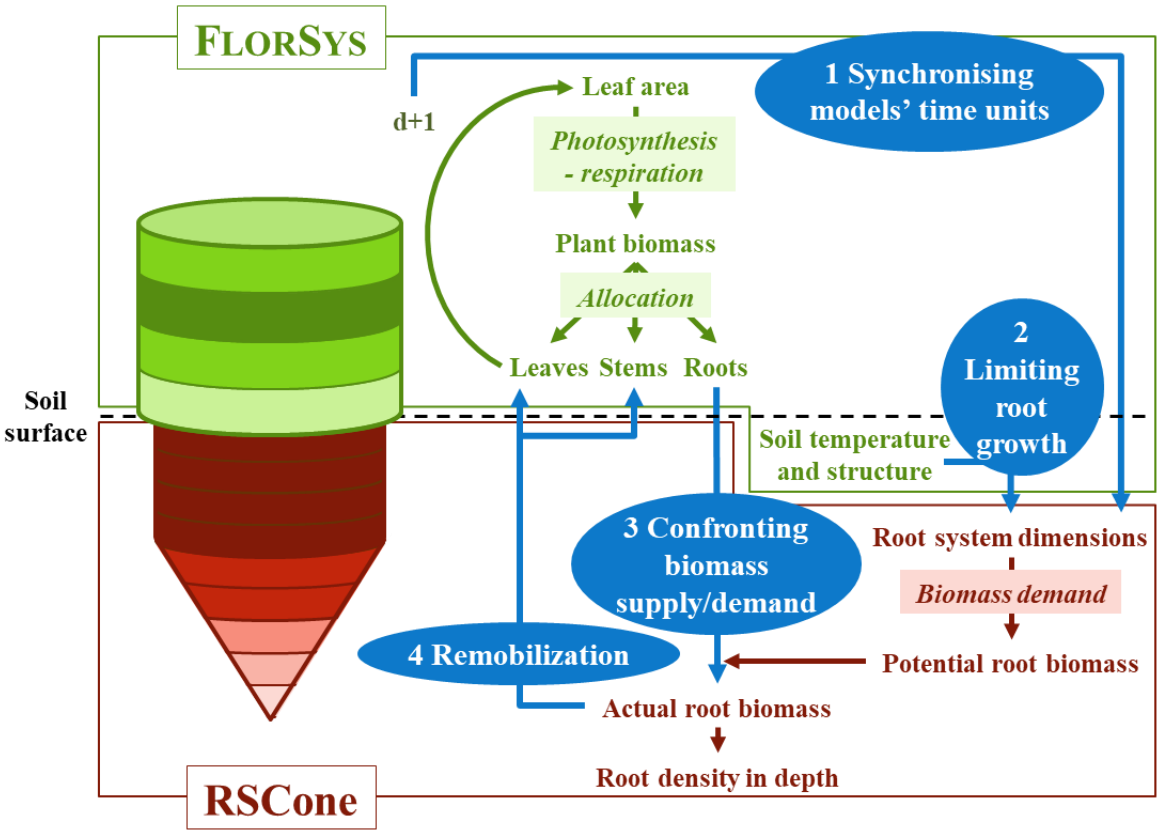

Figure 11: Overview of the variables linking FLORSYS (Gardarin *et al.*, 2012; Munier-Jolain *et al.*, 2013; Colbach *et al.*, 2014c; Munier-Jolain *et al.*, 2014), which predicts aboveground plant growth, soil structure and climate, to RSCone (Pagès *et al.*, submitted), which predicts root growth. Variables (in bold) and processes (in italics in boxes) from FLORSYS are in green and those from RSCone in brown. Blue arrows show variables used to connect both models, with connecting functions ("ports") added in the present paper in blue ellipses. Cylinder and cone shapes show how FLORSYS and RSCone represent the aboveground and root parts of plants in three dimensions, with vertical distributions of leaf area and roots respectively within homogeneous horizontal layers.

3.2.3.2.1 Phenology

RSCone and FLORSYS use different time units for plant age. In RSCone, plant age is given in days since germination under optimal temperature ("optimal days"). FLORSYS uses two scales, thermal time (in °C·days, with base temperature depending on species) since plant emergence, and plant stage (cotyledon, plantlet, vegetative, flowering onset, maturity onset, death) with the duration of the vegetative stage depending on the plant's emergence season. Conversions had to be done to make optimal days of RSCone compatible with thermal time in FLORSYS (see port 1 in Figure 11).

3.2.3.2.2 Soil constraint on root growth

In RSCone, soil conditions can limit root-system extension in width and depth if the soil is too cold or too compacted (Pagès *et al.*, submitted). RSCone uses soil temperature as an input, which will now be provided by FLORSYS for connecting both models.

Conversely, RSCone does not directly use soil structure variables as input, but an abstract coefficient of root-growth limitation by the soil ranging from 0 (no root growth) to 1 (no soil constraint) in each soil layer. Here, we added a function to quantify this soil constraint from soil-structure variables (see port 2 in Figure 11) predicted by FLORSYS from soil texture, tillage, soil moisture and frost.

3.2.3.2.3 Allocation of biomass to roots

Allocation of biomass to roots is an input of the RSCone model and must be provided by FLORSYS. Root biomass is known to be correlated to total plant biomass (Wilson, 1988a; Weiner, 2004). Therefore, we aimed at finding a relationship to calculate biomass allocated to roots from the aboveground biomass of plants predicted by FLORSYS in order to connect both models (see port 3 in Figure 11). We collected data from different experiments described in Table 7 to investigate this relationship. We used data collected on a large range of crop and weed species, including experiments testing the effect of nitrogen and light on root growth.

The relationship between root and total plant biomass of plants was analysed as a function of the effects of species, nitrogen and light treatments with the following model using the function lm of R (R Core Team, 2019):

(1) log10(root biomass) = constant + log10(total plant biomass) + species + nitrogen stress index + light + two-way interactions + residuals.

The nitrogen stress index was calculated as explained in Perthame *et al.* (submitted). When plant nitrogen nutrition is optimal, the nitrogen stress index is close to zero, and nitrogen stress increases with the index value. Equation (1) was applied to the data from experiment E1 in Table 7.

In other experiments listed in Table 7, the nitrogen stress index was not calculated, and the effect of light was not tested. Only the nitrogen treatments (listed in Table 7) that we knew from experience from previous experiments that gave near optimal plant nitrogen nutrition were kept for the analysis. The following model was fitted to the data:

(2) log10(root biomass) = constant + log10(total plant biomass) + species + two-way interaction + residuals.

As data came from various experiments, the effect of the experimental set-up was also tested:

(3) log10(root biomass) = constant + log10(total plant biomass) + species + experiment + two-way interaction (except species×experiment) + residuals.

The interaction between species and experimental set-up could not be tested because the experiments did not have enough species in common. Models were fitted by backward selection. Note that in legume species, root biomass did not include nodule biomass since nodules only constituted a small part of belowground plant biomass under optimal nitrogen nutrition (<4%) and are not modelled in FLORSYS.

Table 7: Data used for parameterizing the relationship between root and total plant biomass for several crop and weed species at vegetative stage.

Exp.	Species tested (crops in bold, weeds in plain font)	Light treatment	Nitrogen treatment (mM of nitrates in the nutrient solution)	Growth medium (in greenhouse)	Sampling stages (time since sowing)	Reference
E1	**Wheat (*Triticum aestivum*) cv Caphorn, fescue (*Schedonorus arundinaceus*) cv Soni** (without light limitation)**, Lucerne (*Medicago sativa*) cv Agathe NF[1]**, *Alopecurus myosuroides*, **oilseed rape (*Brassica napus*) cv Kadore**, *Geranium molle*	100% (no shading) and -90%[3]	0.2 to 14 mM	Expanded clay and attapulgite	Vegetative (37-125 DAS[2])	(Perthame *et al.*, submitted)
E2	**Wheat (*Triticum aestivum*) cv Caphorn**, *Galium aparine*, *Polygonum aviculare*	100% (no shading)	10 and 14 mM	Expanded clay and attapulgite	Vegetative (55-151 DAS[2])	(Perthame *et al.*, submitted)
		-60%	5 and 10 mM			
E3	*Abutilon theophrasti*, *Alopecurus myosuroides*, *Amaranthus hybridus*	100% (no shading)	10.5 mM	Expanded clay and attapulgite	Vegetative (25-94 DAS[2])	(Moreau *et al.*, 2018)
E4	**Chickpea (*Cicer arietinum*) cv Twist, common bean (*Phaseolus vulgaris*) cv Flavert, common vetch (*Vicia sativa*) cv Candy, faba bean (*Vicia faba*) cv Espresso, fenugreek (*Trigonella foenum-graecum*) cv Fenu-fix, lentil (*Lens culinaris*) cv Anicia, lupine (*Lupinus albus*) cv Feodora, Narbonne vetch (*Vicia narbonensis*) cv Clara, pea (*Pisum sativum*) cv Kayanne, soybean (*Glycine max*) cv Sultana**	100% (no shading)	2.5 mM	Hydroponics	Vegetative (6-24 DAS[2])	(Seneze J., 2018; Guinet, 2019)
E5		100% (no shading)	14 mM	Rhizotrons (=transparent tubes inner coated with a membrane and filled with expanded clay and attapulgite, where roots grew between the tube wall and the membrane)	Vegetative (27 DAS[2])	
E6	**Pea (*Pisum sativum*) genotypes Amino, Austin, Cameor, Cuzco 1, Isard, Kayanne, L1073, Livioletta, Nepal A and Pi186093**	100% (no shading)	14 mM	Hydroponics	Vegetative (7-28 DAS[2])	
E7	**Pea (*Pisum sativum*) genotypes Kayanne and Pi186093**	100% (no shading)		Expanded clay and attapulgite	Vegetative (14-28 DAS[2])	
E8	*Alopecurus myosuroides*, **wheat (*Triticum aestivum*) cv Caphorn,** *Bromus hordeaceus*,	100% (no shading)	10.5 mM	Expanded clay and attapulgite	Vegetative (14-56 DAS[2])	(Moreau *et al.*, 2017)

Exp.	Species tested (crops in bold, weeds in plain font)	Light treatment	Nitrogen treatment (mM of nitrates in the nutrient solution)	Growth medium (in greenhouse)	Sampling stages (time since sowing)	Reference
	Cyanus segetum, **oilseed rape (*Brassica napus*) cv Kadore,** *Echinochloa crus-galli*, *Geranium molle*, *Tripleurospermum inodorum*, **pea (*Pisum sativum*) cv Kayanne,** *Teucrium botrys*, *Microthlaspi perfoliatum*, *Vulpia myuros*					
E9	*Alopecurus myosuroides*, *Brachypodium distachyon*, *Bromus hordeaceus*, **oilseed rape (*Brassica napus*) cv Kadore**, *Cyanus segetum*, *Echinochloa crus-galli*, *Geranium molle*, *Tripleurospermum inodorum*, **strong-spined medick (*Medicago truncatula*)**, *Teucrium botrys*, *Microthlaspi perfoliatum*, **wheat (*Triticum aestivum*) cv Caphorn**, *Vulpia myuros*	100% (no shading)	14 mM	Silty clay loam soil	Vegetative (56 and 77 DAS[2])	(Moreau *et al.*, 2015)
E10	*Vulpia myuros*, *Teucrium botrys*, *Microthlaspi perfoliatum*, *Bromus hordeaceus*, *Geranium molle*, *Alopecurus myosuroides*, *Cyanus segetum*, *Echinochloa crus-galli*, *Tripleurospermum inodorum*, *Persicaria lapathifolia*, **oilseed rape (*Brassica napus*) cv Kadore, wheat (*Triticum aestivum*) cv Caphorn**	100% (no shading)	10.5 mM	Expanded clay and attapulgite	Vegetative (34-64 DAS[2])	(Moreau *et al.*, 2013; Moreau *et al.*, 2014)

[1]NF for 'Non-Fixing', [2]DAS for days after sowing, [3]no data for fescue under 90% shading

3.2.3.2.4 Remobilization from roots to aboveground biomass

When part of the aboveground plant biomass is destroyed by events such as frost or mowing, plants change their source-sink relationships, and remobilize resource from the root compartment toward the aboveground compartments (see port 4 in Figure 11). Here, this was approximated by changing the biomass allocation and respiration rates (see section 3.2.4.1.3). According to preliminary simulation results (not shown), damages due to frost were overestimated. We improved the model predictions by including a snow submodel to simulate the insulating effect of snow cover that protects plants from frost damages (Trnka *et al.*, 2010; Jégo *et al.*, 2014) (annex A.2.3.1).

3.2.3.3. Simulations

3.2.3.3.1 Principle

Simulations of cropping systems were performed with FLORSYS-RSCone to 1) evaluate the model by comparing simulation results to independent field observations (section 3.2.3.3.2), and 2) identify key species parameters for potential soil-resource uptake and infection by root parasitic plants (section 3.2.3.3.3). Data of ten cropping systems from the INRA experimental station of Dijon-Époisses from 1999 to 2012 were simulated as described in Colbach *et al.* (2016) (annex A.2.4). They vary from herbicide-intensive to herbicide-free, with various rotations, tillage strategies and use of mechanical weeding. Initial weed seedbank and soil characteristics given as inputs in the model were measured on soil samples taken in the fields. Weather data were obtained from the INRA weather station (INRA platform CLIMATIK). Each cropping system was repeated 10 times with the same inputs to take into account the stochastic effects of FLORSYS. The simulated field sample was 6x4m². As the evaluation of the first FLORSYS version showed the phenology submodel to badly predict flowering dates of weeds in the South of France and of some crop varieties (Colbach *et al.*, 2016), a corrective patch was added to keep weeds from flowering too early and to force crops to mature at harvest date.

Not all FLORSYS species have yet been parameterized in RSCone. In that case, default parameter values were calculated by averaging parameters of species from the same clade (i.e. monocotyledon or dicotyledon), as clade was shown to discriminate RSCone parameters (Pagès *et al.*, submitted), and from the same seasonal type (i.e., winter annuals, summer annuals or perennials).

3.2.3.3.2 Model evaluation

Aboveground plant biomass, weed plant density, weed seed bank and crop yield were measured in all ten fields during the 13 years of the trial and compared to variables predicted by FLORSYS-RSCone as explained in Colbach *et al.* (2016). Density and aboveground biomass were measured in several quadrats per field several times a year, and weed seed bank was measured on ten soil samples every two years. As root biomass was not measured, we could not directly evaluate the prediction quality of roots in our model. Instead, we checked whether including roots improved the prediction quality of aboveground variables by FLORSYS.

Variables were either analysed 1) at the species scale or 2) at the community scale, i.e. they were summed over all species. The prediction quality of the model was estimated with various complementary criteria described in Colbach *et al.* (2016):

The prediction bias is the mean of residuals (simulated – observed values) and determines whether the model systematically under- or overestimated variables. It was calculated relatively to the range of variation of observations (i.e. divided by ½[max-min observed values]).

The relative root square of the mean square error (RRMSEP) evaluates the relative prediction error of the model. It was calculated relatively to the standard deviation of observed values, and corrected for variability in observations (i.e. variability due to measurement errors) and in simulations (i.e. variability due to model stochasticity).

The ability of the model to rank cropping systems and weed species correctly was calculated as the maximum between the modelling efficiency, the Pearson and the Spearman correlation coefficients between observations and predictions. Coefficients close to 1 indicate that the variables are well predicted by the model in terms of absolute values, relative values (i.e. differences between values) and ranks respectively.

The three criteria (relative bias, RRMSEP and proportion of correctly predicted observation) were calculated from data averaged over the rotation (i.e. over all simulated values or measurements per cropping system) to check the model's ability to compare cropping systems. To assess how well the model predicts outputs on a given day, the criteria were calculated from data averaged per day (i.e. averaged over quadrats, samples and repetition), except for daily weed density and biomass. For these

two outputs, the proportion of correctly predicted observations was the proportion of observations inside the simulated 90%-confidence interval obtained over the 10 repetitions. This criterion was preferred over the three first evaluation criteria, because the latter are considerably deteriorated by a delay of a few days in the simulations vs the observations (or vice-versa), whereas such delays do not affect the prediction quality of the weed dynamics over the years (Colbach *et al.*, 2016).

All the evaluation criteria were also calculated from simulations with FLORSYS before the RSCone model was connected in order to study whether the connection improved FLORSYS predictions.

3.2.3.3.3 Indicators of potential soil-resource uptake and risk of parasitism

In order to study which species parameters determine potential soil-resource uptake and risk of infection by *P. ramosa*, we analysed proxy variables because these processes are not yet modelled in FLORSYS. We did not considered characteristics relative to root functioning when calculating our proxies (e.g. host status or uptake efficiency), which are included in further studies (Pointurier *et al.*, 2018; Moreau *et al.*, in prep.), focussing on the influence of the morphology and the photosynthetic functioning of plants on root exploration.

Root biomass summed over respectively all crop and weed plants was used as a proxy for potential soil-resource uptake by crops and weeds (Malagoli and Le Deunff, 2014). It was taken at the beginning of crop flowering, when crop root biomass is near maximal (Gregory *et al.*, 1995) in order to get a global overview of root growth over the crop cycle. The percentage of crop root volume overlapped by root systems of weeds was also calculated at crop flowering and averaged over the field, in order to estimate crop-weed competition for soil resource.

Risk of infection by root parasitic plants was approximated by the cumulated root length of crops and weeds (Grenz *et al.*, 2005a) because parasitic seeds only germinate close to host roots (< 4 mm) in order to infect them quickly otherwise they die in a few days (Joel, 2013c). Only crops and weeds roots in the first 30 cm of soil were considered because parasitic seeds are unlikely to be buried deeper by tillage. This proxy was calculated in autumn (end of November) and summer (end of June), when seeds are most likely to germinate (before and after dormancy respectively, Pointurier *et al.*, 2019).

In order to analyse the relationships between species parameters and proxy variables for soil-resource uptake and parasitism, an RLQ analysis combined with a fourth-corner analysis was performed for weeds and Pearson correlations were calculated for crops as in Colbach *et al.* (2019). The RLQ analysis was performed with the library ade4 of R (Dray and Dufour, 2007). It consisted in relating three tables ("R", "L" and "Q") in order to study the relationships between our proxy variables (described in table "R", e.g. total weed root biomass for soil-resource uptake by weeds) and the species parameters (in table "Q") while taking into account the relative contribution of each species within the weed community (given by maximum annual weed species densities in table "L"). The latter consisted of the maximum densities of weed species over the growing cycle (i.e. from sowing to harvest) for each simulated year, each cropping system and each repetition. Table Q consisted of the root parameters described in Table S 17, and the aboveground parameters described in Colbach *et al.* (2019) were added to investigate the relative influence of the two types of parameters. Parameters relative to resource uptake and use (e.g. nitrogen uptake strength) or sensitivity to parasite infection (e.g., ability to trigger parasite infection or attachment) were disregarded. The significance of the correlations obtained in the RLQ analysis was tested with a fourth-corner analysis with 999 permutations of rows and columns in table L. The latter procedure allowed to check that the correlations observed did show a relationship between proxy variables and parameters and that they were not affected by preferential distributions of weed species depending on cropping systems or on their parameters. Results of the RLQ analysis were displayed with the package adegraphics of R (Siberchicot *et al.*, 2017).

Pearson correlations between crop proxy variables and parameters were calculated with the function rcorr from the package Hmisc of R. A Principal Component Analysis (PCA) was performed on proxy

variables with the function PCA from the library FactoMineR (Lê *et al.*, 2008) and displayed using the function fviz_pca_var from the library factoextra of R. Parameters were projected as supplementary variables on the correlation circle (i.e. they were not used for calculations in the PCA) to illustrate their relationship with the proxy variables.

Proxy variables for both crops and weeds were log-transformed prior to analysis because they were skewed.

3.2.4. Results

3.2.4.1. Integration of RSCone as a root distribution submodel in FLORSYS

3.2.4.1.1 Phenology

Radicle growth and water uptake prior to seedling emergence was already included in FLORSYS in a previous work (Gardarin *et al.*, 2012). Before emergence nitrogen uptake is negligible (Fayaud *et al.*, 2014) and no germination stimulants for parasitic plants are exudated (Gibot-Leclerc *et al.*, 2012). Therefore, we focused on post-emergent root-system development. We considered that the post-emergent root system starts to grow from the moment the plant emerges in FLORSYS and we readjusted the relevant RSCone timing parameters accordingly (eq. [2] in Table S 16).

In FLORSYS, the duration of the plant life cycle, calculated in °C·days, depends on the time of the year the plant emerges (Colbach *et al.*, 2014c). Conversely, in RSCone, the durations of root development stages are constants for a given species or cultivar and calculated in days, assuming a constant temperature optimal for the species. We recalibrated these durations to account for the season of emergence of the plant [3], considering that the shortest life-cycle duration in FLORSYS reflects plant development under optimal temperature and thus correspond to the RSCone durations. A plant emerging at a different season has a longer life cycle in FLORSYS and the ratio of this longer duration to the minimum duration was used to lengthen the RSCone root-stage durations. The effect of soil temperature on root-system expansion was included in the $rSoil_{dls}$ variables reflecting structural and thermal constraints in the soil (see section 3.2.4.1.2).

The timing of root-system stages influences both the root-system expansion and its root density. The cylinder-shaped part of the root system only starts to grow in depth once the plant age exceeds $t0cyl_{sc}$ days (eq. [11] taken from Pagès *et al.*, submitted), which is recalibrated in eq. [3]. The root system stops to grow when its maximum extent $Emax_s$ is reached (eq. [10] taken from Pagès *et al.*, submitted) though this timing did not need to be recalibrated. SRL stops to increase when plant age exceeds $tSRLmaxe_{sc}$ days (eq. [31] taken from Pagès *et al.*, submitted), which is also recalibrated in eq. [3]. SRL is then used to convert root-biomass density in each layer into root-length density (eq. [32] taken from Pagès *et al.*, submitted).

3.2.4.1.2 Effect of soil limiting factors on root growth

Root-growth limitation by soil compaction was calculated from soil structure. In FLORSYS, soil structure is predicted for the top three 10-cm soil layers, as the proportion of soil clods distinguished by their degree of compaction and the process they were formed (Roger-Estrade *et al.*, 2004). Types bΔ and cΔ are the most compact and block root growth. Contrary to cΔ clods, bΔ clods are partially fragmented so they do not completely block root growth. Stones (whose proportion in the soil is given as an input in FLORSYS) are assumed to have the same effect as cΔ clods on root growth in the top soil layers (up to 30 cm depth).

Equation [4] (Table S 16) was based on these assumptions. Root growth is reduced proportionally to the percentage of stones, bΔ and cΔ soil clods in the soil. Only half the proportion of bΔ soil clods was considered in this equation to roughly take into account that they do not completely block root growth. This sum was divided by 100+stone percentage to fit into [0,1], and multiplied by a 50% factor

(rSmax) borrowed from the STICS crop model (CONTRDAMAX, Brisson *et al.*, 1998; Brisson *et al.*, 2002; Brisson *et al.*, 2003) which correspond to the maximal reduction the soil can exert on root growth. The result (or rather 1-this result to get a corrective factor for root growth) was multiplied by a species parameter pen_s reflecting the species ability to penetrate the soil.

As soil structure and temperature are not predicted below 30 cm in FLORSYS, soil constraint in deeper soil layers was predicted from soil variables at 30 cm depth (eq. [5] and [7]).

The effects of soil compaction and temperature were then combined to get the total soil constraint on root growth in each layer (eq. [8] taken from Pagès *et al.*, submitted). Potential dimensions of the root-system envelop under non-limiting conditions (i.e. no soil constraint, eq. [9], [10] and [11] taken from Pagès *et al.*, submitted) were then reduced proportionally to the soil constraint averaged over relevant soil layers (eq. [12] taken from Pagès *et al.*, submitted) to deduce the actual root-system dimensions (eq. [13], [14] and [15] taken from Pagès *et al.*, submitted).

As soil constraint was applied to the entire root system every day in RSCone (and not only to new roots), it could happen that a sudden high soil constraint (for example compaction due to tractor wheels on a wet soil or a drop in temperature) could dramatically shrink the root system from one day to another. We added a condition to prevent such root system shrinkage (eq. [13], [14] and [15]) because it was unrealistic, apart in case of frost.

3.2.4.1.3 Biomass allocation to roots

Data analysis

In experiment E1 (Table 7), root biomass was strongly correlated to total plant biomass, irrespective of species, light condition or nitrogen stress index (partial R^2 = 62% of total R^2, $p \leq 0.02$, annex A.2.5.1, Figure 12). The latter three factors, i.e. species, light and nitrogen stress index, as well as two-way interactions, had a significant effect ($p<0.001$), except for the interaction between total plant biomass and nitrogen stress index. However, the effect of light was negligible (partial R^2= 10% of total R^2, annex A.2.5.1) given the huge difference between shading levels (i.e., 0 vs 90%) and was removed from the model. Then, data on fescue, which had been removed from the analysis because it did not allow to test the effect of light (see Table 7), was included in the analysis. The effect of the interaction between nitrogen stress index and species was also removed because it was negligible (partial R^2 = 0.061% of total R^2), particularly compared to the primary effects of these variables and mainly due to one species (i.e. fescue, annex A.2.5.2). Finally, the following linear model was obtained (annex A.2.5.3):

(4) $\log10(\text{root biomass}) = a1_s + a2_s \cdot \log10(\text{total plant biomass}) + a3 \cdot (\text{nitrogen stress index}) + \text{residuals}$,

where $a1_s$, $a2_s$ and a3 are parameters described in Table S 17, with $a1_s$ and $a2_s$ depending on the species.

In other experiments, where the nitrogen stress index was not calculated, parameters $a1_s$ and $a2_s$ were determined by fitting equation (2) from section 3.2.3.2.3. A strong linear relationship was also found with this model and data (R^2=0.98, Figure 13) even though experiments with very different protocols were included in the analysis. The effect of the experiment was found significant but negligible compared to the species effect (partial R^2 = 10 and 50% of total R^2 respectively, $p<0.001$, see annex A.2.5.4). As parameter a3 did not depend on the species, the value determined with equation (4) on the E1 experiment was used for all species, even if parameters $a1_s$ and $a2_s$ were estimated on different experiments.

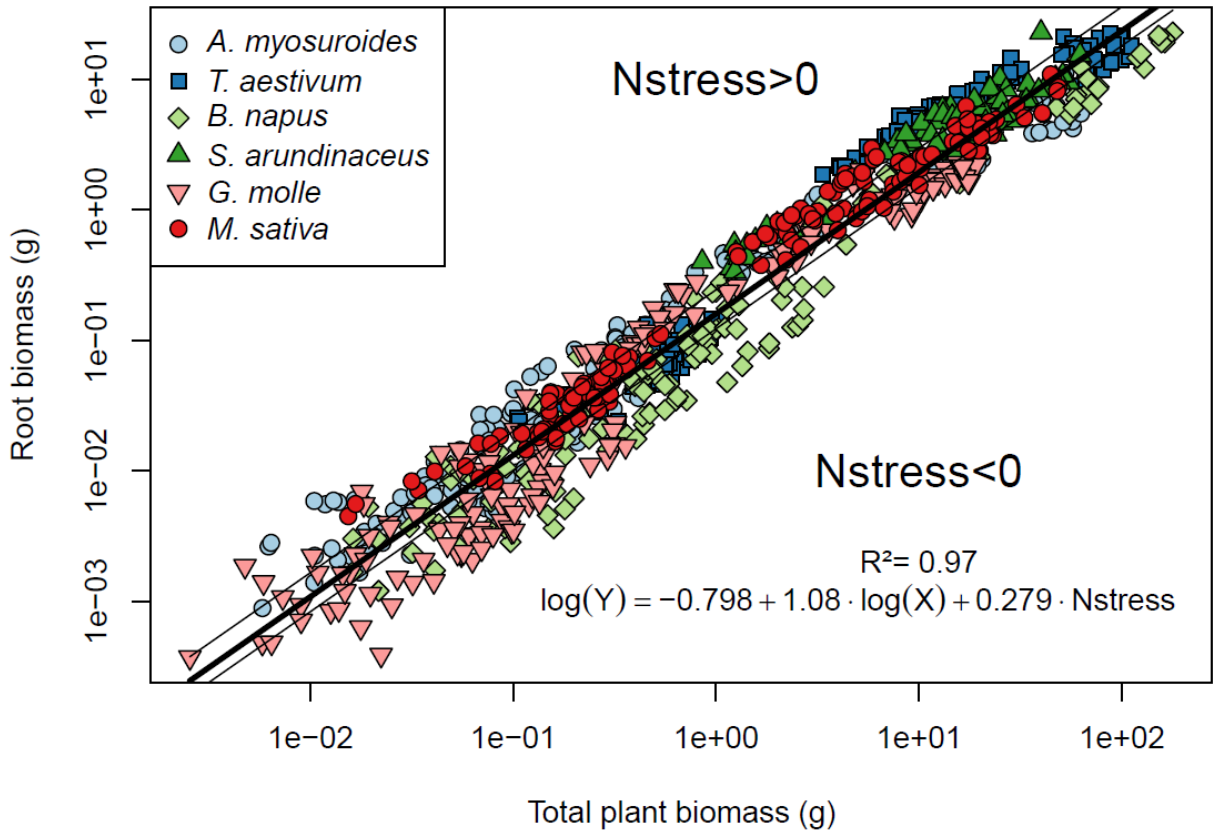

Figure 12: Root biomass as a function of total plant biomass and nitrogen stress index for six species of crops and weeds under different shading and nitrogen stress conditions during the vegetative stage (data from experiment E1 in Table 7). Each data point represents a plant, each coloured symbol a species. Lines represent model (4) fitted to the data for an average species (i.e. disregarding the species effect) for optimal nitrogen nutrition (no nitrogen stress, thick line), supra-optimal (nitrogen stress <0) and sub-optimal (nitrogen stress >0) nitrogen nutrition (thin lines, with supra and sub-optimal conditions corresponding to 5 and 95% quantiles of nitrogen stress values respectively).

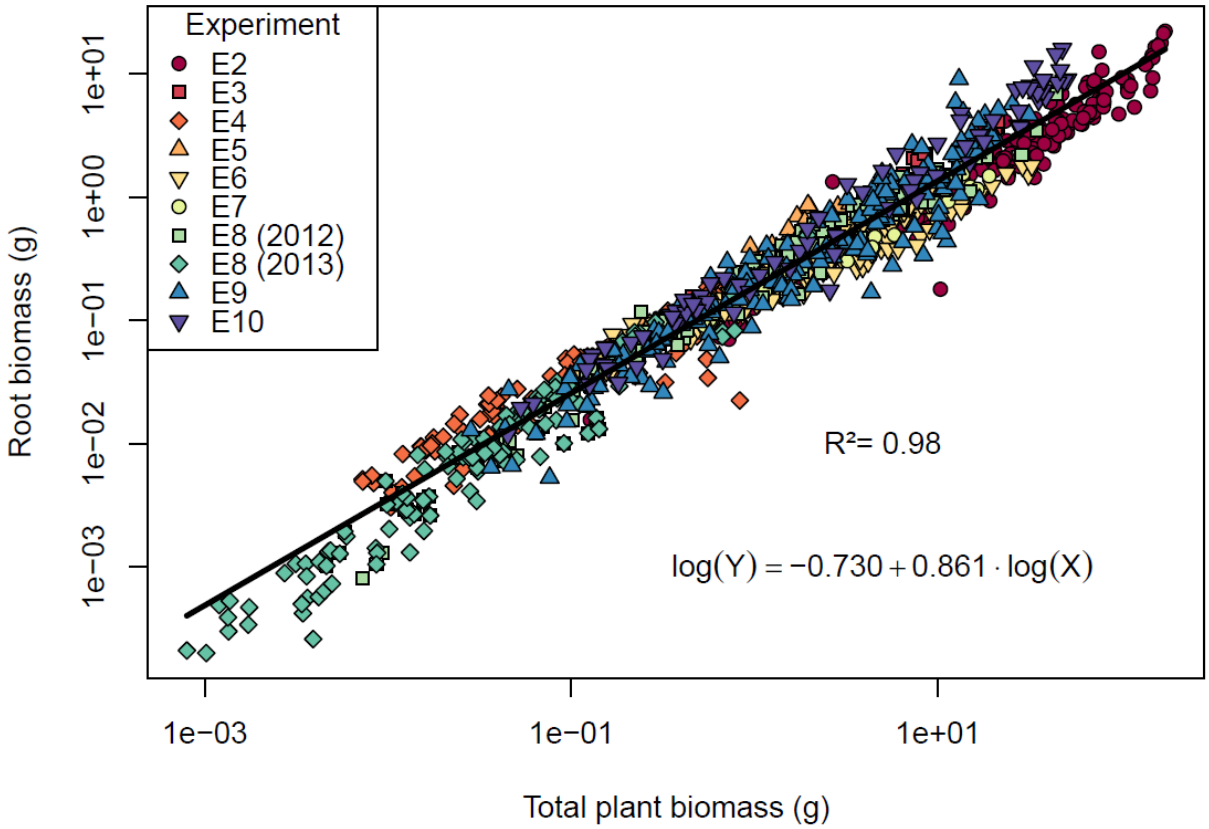

Figure 13: Root biomass as a function of total plant biomass for 28 species of crops (with 10 varieties of pea) and weeds. Data from several experiments were used (details in Table 7), each coloured symbol representing an experiment. Each data point represents a plant. Thick line represents model (2) fitted to the data for an average species (i.e. disregarding the species effect).

Although we only used data obtained during vegetative stages, data from other experiments showed that the relationship we found between root and total plant biomass remained valid at earlier and later stages (see annex A.2.5.5).

Formalism used to connect FLORSYS and RSCone

Model (4) was used to calculate the root biomass ratio, i.e. the ratio of the plant root biomass to its total biomass (RBR_{dsi}), depending on species and nitrogen stress index. This ratio was used to connect FLORSYS and RSCone (eq. [20] and [23] in Table S 16).

In FLORSYS, plant growth is modelled differently depending on whether the plant is surrounded by shading neighbouring plants or not. Before plants start to compete for light, i.e. at early stages (generally less than 15 days after emergence, Munier-Jolain *et al.*, 2014), aboveground biomass accumulation is driven solely by thermal time since emergence (Colbach *et al.*, 2014c). We added an equation to calculate the amount of biomass allocated to roots in RSCone from the aboveground biomass predicted by FLORSYS and the root biomass ratio RBR_{dsi} (eq. [21]). We assumed that nitrogen stress was negligible (i.e. a3 set to 0 in eq. [20]) because it was not observed in such young plants (Perthame *et al.*, submitted).

When plants start to compete for light in FLORSYS, they grow by accumulating biomass from photosynthesis daily, losing some through respiration (eq. [22]). We used the resulting total plant biomass of the day to calculate the root biomass ratio RBR_{dsi} (eq. [23]) and deduced the daily amount

of photosynthesized biomass to be allocated to roots (eq. [24]). We calculated the part of root biomass that was lost through respiration. The remaining amount of photosynthesized biomass was allocated to aboveground organs that also lost some due to their respiration. From the beginning of flowering onward, when plants stop to allocate new biomass to roots (Gregory *et al.*, 1995), root biomass was assumed to be remobilized for aboveground organs. The same occurred after plants lost aboveground biomass due to mowing [17] or frost damage [18], as long as the biomass level from before that event was not reached again [19]. This remobilization was modelled by charging respiration losses from both roots and aboveground organs to roots and by allocating all biomass gained by photosynthesis to aboveground organs only (eq. [25]).

For very small plants, because of the log-log relationship, root biomass could mathematically exceed total plant biomass (i.e. RBR_{dsi} >1). To avoid this biological non-sense, we added a condition to limit RBR_{dsi} to the maximum root to total biomass ratio observed in our data (eq. [20] and [23]).

3.2.4.2. Simulation results

3.2.4.2.1 Crop production and multiannual species weed dynamics are well predicted by FLORSYS-RSCone

Crop variables were satisfactorily predicted by FLORSYS-RSCone (Table 8), with crop biomass in particular well ranked with no bias. Crop yield was less well predicted with a slight underestimation and a high prediction error. Although the model was bad at predicting absolute values, it correctly ranked cropping systems and years (i.e. it could predict correctly that yield in cropping system “x” on year “a” was better than in cropping system “y” on year “b” for example).

Weed variables were generally well predicted at the species scale, with a small bias (7-17%), more than 50% (up to 67%) of well-ranked observations and very good predictions of daily dynamics (more than 80% of observations within the simulated confidence interval). However, predictions were less good at the community scale, particularly for seed bank and aboveground biomass (Spearman coefficients of -0.08 and 0.13, respectively), because they were generally largely overestimated (relative bias ranging from 15 to 206%). Aboveground biomass and density of the weed community were also overestimated at the daily time-scale (more than 50% of observations lower than the simulated confidence interval). Only multiannual weed density was as well ranked at the community scale as at the species scale (Pearson coefficient of 0.65 and 0.67 respectively).

Table 8: RSCone-FLORSYS ability to rank cropping systems and weed species (in case variables were analysed at the species scale). Crop and weed variables are given per species or at the community scale (summed over all simulated species) in bold. Values in italics shows variations compared to simulations without RSCone.

A. Daily weed dynamics

Variable	Species scale	Daily dynamics [x]					
		Correct		Over-estimated		Under-estimated	
Weed biomass (aboveground) (g/m²)	Sum	**0.24**	*0.01*	**0.68**	*-0.01*	**0.08**	*0.00*
	Per species	**0.79**	*-0.01*	**0.14**	*0.01*	**0.07**	*0.00*
Weed plant density (plants/m²)	Sum	**0.34**	*-0.01*	**0.55**	*0.02*	**0.11**	*-0.02*
	Per species	**0.86**	*0.00*	**0.10**	*0.00*	**0.04**	*0.00*

B. Annual and multiannual crop and weed variables

Variable	Species scale	Relative bias (%) [§]		Relative prediction error (%)[$]		Proportion of correctly predicted observations		
						Prop [&]		In terms of
Crop yield (t/ha)	Per species	**-8%**	*4%*	**110%**	*4%*	**0.42**	*-0.09*	**Absolute values**
Crop biomass (g/m²)	Per species	**-2%**	*0%*	**~0**	*0%*	**0.59**	*0.03*	**Rank**
Weed seed bank (seeds /m²)	Sum	**15%**	*6%*	**~0**	*0%*	**-0.08**	*0.01*	**Rank**
	Per species	**7%**	*0%*	**74%**	*-3%*	**0.51**	*0.02*	**Rank**
Multiannual weed biomass (aboveground) (g/m²)	Sum	**206%**	*-70%*	**~0**	*0%*	**0.13**	*0.11*	**Rank**
	Per species	**17%**	*-5%*	**~0**	*-347%*	**0.55**	*-0.04*	**Rank**
Multiannual weed plant density (plants/m²)	Sum	**154%**	*1%*	**228%**	*-6%*	**0.65**	*0.11*	**Relative values**
	Per species	**17%**	*-1%*	**148%**	*-3%*	**0.67**	*0.01*	**Rank**

§ Relatively to the range of variation of observations ½[max-min observed values]. Colours: from green (0%) to red (|50%|), grey (too much variability in observations to conclude). $ Corrected for variability in observations and in simulations, relatively to the standard deviation of observations. Colours: red (bad, > 120%), yellow (satisfactory, 60-90%), light green (good, 30-60%), green (very good, < 30%) and grey (too much variability in observations to conclude). & Maximum of the modelling efficiency, the Pearson and the Spearman correlation coefficients. Colours: from red (0) to green (1). x Proportion of observations inside the simulated confidence interval. Colours: from red (0) to green (1) for the first column, from green (0) to red (1) for the two other columns. Colours for values in italics: from green (improvement in prediction quality when connecting RSCone to FLORSYS) to red (deterioration in prediction quality).

3.2.4.2.2 Modelling roots improves the predictions of FLORSYS

Integrating RSCone allowed partly to correct FLORSYS deficiency because it greatly improved the predictions of weed aboveground biomass (prediction error largely decreased per species by 347%) which is now better ranked (bias decreased by 70% and Spearman coefficients increased by 0.11, Table 8). The predictions of weed densities and crop production did not improve nor deteriorate overall. Weed seed bank and crop yield were slightly less well predicted (relative bias decreased by 6 and 4% respectively, and modelling efficiency by 0.09), but this was negligible compared to variations due to model stochasticity observed between two simulations (3%, 1% and 0.04 respectively, all other things being equal).

3.2.4.2.3 Crop parameters determining potential competition for soil resource, uptake and parasitism

Strong correlations were found between crop parameters and proxy variables for potential soil-resource uptake and parasitism risk (absolute values of Pearson correlation coefficients of 0.3 on average, up to 0.7, see Table 9 and annex A.2.6.1). Both proxies were strongly correlated at crop flowering (Pearson correlation coefficient = 0.85 in Table 9 and close arrows on the Principal Component Analysis in annex A.2.6.1) and associated to similar species parameters (annex A.2.6.1). In terms of plant structure, crops potentially able of large uptakes of soil resource and most likely to be

infected by *P. ramosa* were mainly winter monocotyledons (associated to "winter_annual" and opposite to dicot species in Table 9) whose plants are little sensitive to frost (low tFrostEarly3, tFrostMid3, tFrostLate3) and whose photosynthesis does not support high temperatures (low tPhoto3). Their root systems presented a large cylinder-shaped top (rCD) and their roots reached their maximal SRL late (tSRLmax). Their plant height depended little on plant biomass (low b_HMMid and b_HMLate), resulting on homogeneously tall canopies. Crops likely to suffer competition for soil resource from weeds tended to have the same characteristics, but correlations were very weak (absolute values of Pearson correlation coefficients ≤0.3, annex A.2.6.1).

Different parameters drove risk of parasitism at different dates, with opposite effects possible (arrows perpendicular or in opposite directions on the PCA in annex A.2.6.1). The strongest correlations with species parameters were found at dormancy induction of *P. ramosa* seeds in autumn (significant coefficients of 0.4 on average compared to 0.3 at the other dates, annex A.2.6.1). The crops most likely to be infected then were dicotyledons (Table 9). They had large, quickly growing root systems (high Emax, rD and a2), although they allocated a low proportion of biomass to their roots (low aa1). Their plants were wide per unit biomass (WMMid and WMLate) and, from flowering onwards, allocated a larger proportion of their biomass to leaves (LBRLate), which were located lower on the plant (low RLHLate). The crops most likely to be infected were also those that etiolated most when shaded by neighbour plants: they increased their plant height per unit biomass (mu_HMEarly), allocated more biomass to stems (low mu_LBREarly, mu_LBRMid and mu_LBRLate), compensating with thinner larger leaves (mu_SLAEarly and mu_SLAMid) which were shifted toward the plant top (mu_RLHEarly and mu_RLHLate). They had an epigeal germination requiring relatively wet conditions (high baseWaterPotential) and their photosynthesis was sensitive to high temperatures (low tPhoto4). They grew quickly after emergence (high RGR).

At dormancy release of *P. ramosa* seeds in summer, no strong correlations between proxy for parasitism and parameters could be identified (Table 9).

Table 9: Pearson correlations between parameters and proxy variables for soil-resource uptake, competition for soil resource and *Phelipanche ramosa* infection in crops. Correlations between proxy variables are in blue. Correlations between parameters and a high potential uptake, competitiveness for soil resource and a low risk of parasitism are in green, opposite correlations are in red. The darker the colour, the stronger the correlation. Only significant correlations ≥ |0.50| are presented. The complete table can be found in annex A.2.6.1. Some parameters were calculated at different stages: after emergence in young seedlings ("Early"), during vegetative stage ("Mid") and from flowering onwards ("Late").

Parameter/proxy \ Proxy		Parasitim at dormancy induction (autumn)	Parasitim at dormancy release (summer)	Parasitim at crop flowering	Soil-resource uptake at crop flowering	Competition for soil resource at crop flowering
Proxies						
Parasitism at dormancy induction						
Parasitism at dormancy release						
Parasitism at crop flowering					0.851	
Soil-resource uptake at crop flowering				0.851		
Competition for soil resource at crop flowering						
Root parameters						
Timing of maximum SRL (tSRLmax, days under optimal temperature)					0.520	
Maximum root-system extent (Emax, cm)		0.550				
Speed at which root-system depth increases (rD, cm per day under optimal temperature)		0.504				
Ratio of speed at which depth of cylinder-shaped part of root system increase vs speed of total root-system depth increase (rCD, cm per day under optimal temperature)					0.635	
Root biomass when total plant biomass is near zero (aa1, $g \cdot g^{-1}$)		-0.610				
Slope of allometric relationship of root vs total plant biomass (a2, no unit)		0.647				
Parameters for early growth						
Relative growth rate (RGR, $cm^2 \cdot cm^{-2} \circ C day^{-1}$)		0.563				
Epigeal preemergent growth (1=epigeal, 0= hypogeal)		0.622				
Base water potential for germination (Mpa)		0.661				
Parameters for potential aboveground morphology in unshaded conditions						
Leaf biomass ratio (leaf biomass vs. aboveground biomass, LBR, $g \cdot g^{-1}$)	Late	0.696				
Impact of biomass on plant height (the larger the parameter, the more height increases with biomass, b_HM, no unit)	Mid				-0.530	
	Late				-0.590	
Specific plant width (width per unit of aboveground biomass, WM, $cm \cdot g^{-1}$)	Mid	0.686				
	Late	0.665				
Median relative leaf height (relative plant height below which 50% leaf	Late	-0.688				

Parameter/proxy	Proxy	Parasitim at dormancy induction (autumn)	Parasitim at dormancy release (summer)	Parasitim at crop flowering	Soil-resource uptake at crop flowering	Competition for soil resource at crop flowering
area are located, RLH, cm·cm^{-1})						
Parameters for response to shading						
Increase of specific leaf area under shading (mu_SLA, no unit)	Early	0.600				
	Mid	0.535				
Increase of leaf biomass ratio under shading (mu_LBR, no unit)	Early	-0.635				
	Mid	-0.556				
	Late	-0.597				
Increase of specific plant height under shading (mu_HM, no unit)	Early	0.575				
Distribution of leaf area towards the top of the plant under shading (mu_RLH, no unit)	Early	0.636				
	Late	0.541				
Taxonomy						
Dicot species		0.520			-0.516	
Life-cycle parameters						
Seasonal type: winter annual				0.514	0.516	
Parameters for sensitivity to temperatures						
Temperature above which photosynthesis starts to decrease (tPhoto3, °C)				-0.554		
Maximum temperature for photosynthesis (tPhoto4, °C)		-0.532				
Temperature below which all plants die due to frost (tFrost3, °C)	Early			-0.532		
	Mid			-0.533		
	Late			-0.509	-0.504	

3.2.4.2.4 Weed parameters determining potential competition for soil resource, uptake and parasitism

Correlations between proxy variables and parameters were weaker for weeds than for crops (absolute values of correlation coefficients <0.2, Table 10, compared to up to 0.7 in Table 9). Although proxies for potential soil-resource uptake and parasitism risk at crop flowering were highly correlated (Pearson correlation coefficients = 0.85), they were not associated to the same species parameters (Table 10). Only a predominantly low shade response after emergence within the weed community (low mu_SLAEarly) increased both proxies. Risk of weed infection by *P. ramosa* at crop flowering was moreover associated with weed species with more leaf area at their top (RLHEarly) and a low relative growth rate after emergence (low RGR).

In contrast to crops, no opposite effects were observed between parameters driving proxies for parasitism at different dates (arrows in the same direction on the RLQ axes in annex A.2.6.2). Most key parameters were the same at crop flowering and at dormancy release of *P. ramosa* seeds (low RGR and high mu_SLAEarly at both dates). The proxy at the latter date was moreover associated with weed species with a low base temperature for germination and growth.

The proxy for early weed infection (in autumn at dormancy induction) was correlated to several other weed species parameters (Table 10). It was linked to weed species that allocated more biomass aboveground than to roots (low root biomass ratio a2), which placed their large initial leaf area (LA0,

SLAearly) above other weeds thanks to a large allocation of biomass to stems (low leaf biomass ratio LBREarly) and a top distribution of the leaf area on the plant (RLHEarly). Their plants responded less to shade in terms of plant width and leaf area after emergence (low mu_WMEarly and mu_SLAEarly). For these species, having fine roots (large srlmax) increased more the risk to encounter parasitic seeds than exploring a large volume of soil (as illustrated by low Emax and rE). All these parameters were found to have a similar but much lower influence on the proxies for soil-resource uptake and parasitism in summer (correlation coefficients twice lower or not significant, annex A.2.6.2).

The proxy for competition exerted by weeds over crops for soil resource was the best correlated to two parameters of aboveground morphology (Table 10). As for the proxy for soil-resource uptake, weed species with a high relative growth rate (RGR) after emergence reduced competition. Competition was also increased by weeds that increased biomass allocation to leaves when shaded after emergence (large mu_LBREarly).

Table 10: Correlations between parameters and proxy variables for soil-resource uptake, competition for soil resource and *Phelipanche ramosa* infection in weeds. Correlations between proxies are Pearson correlations (in blue), and correlations between proxies and parameters are results from the fourth-corner analysis (in red and green). Correlations between parameters and a high potential uptake, competitiveness for soil resource and risk of parasitism are in red, opposite correlations are in green. The darker the colour, the stronger the correlation. Only significant correlations >|0.10| are presented. The complete table can be found in annex A.2.6.2. Some parameters were calculated at different stages: after emergence in young seedlings ("Early"), during vegetative stage ("Mid") and from flowering onwards ("Late").

Proxy / **Parameter/proxy**		**Parasitim at** dormancy induction (autumn)	**Parasitim at** dormancy release (summer)	**Parasitim at** crop flowering	**Soil-resource uptake at** crop flowering	**Competition for soil resource at** crop flowering
Proxies						
Parasitism at dormancy induction			0.355	0.343	0.370	0.284
Parasitism at dormancy release		0.355		0.865	0.783	0.518
Parasitism at crop flowering		0.343	0.865		0.847	0.471
Soil-resource uptake at crop flowering		0.370	0.783	0.847		0.480
Competition for soil resource at crop flowering		0.284	0.518	0.471	0.480	
Root parameters						
Maximum root-system extent (Emax, cm)		-0.116				
Speed at which root-system extent increases (rE, cm per day under optimal temperature)		-0.121				
Maximum SRL (srlmax, $cm \cdot g^{-1}$)		0.112				
Slope of allometric relationship of root vs total plant biomass (a2, no unit)		-0.106				
Parameters for early growth						
Relative growth rate (RGR, $cm^2 \cdot cm^{-2} \cdot °Cday^{-1}$)			-0.139	-0.105		-0.129
Leaf area at emergence (LA0, cm^2)		0.101				
Base temperature for germination (°C)			-0.115			
Parameters for potential aboveground morphology in unshaded conditions						
Specific leaf area (total leaf area vs. total leaf biomass, SLA, $cm^2 \cdot g^{-1}$)	Early	0.104				
Leaf biomass ratio (leaf biomass vs. aboveground biomass, LBR, $g \cdot g^{-1}$)	Early	-0.118				
Median relative leaf height (relative plant height below which 50% leaf area are located, RLH, $cm \cdot cm^{-1}$)	Early	0.116		0.118		
Parameters for response to shading						
Increase of specific leaf area under shading (mu_SLA, no unit)	Early	-0.124	-0.160	-0.149	-0.118	
Increase of leaf biomass ratio under shading (mu_LBR, no unit)	Early					0.120
Increase of specific plant width under shading (mu_WM, no unit)	Early	-0.103				

3.2.5. Discussion

3.2.5.1. What is new in our modelling approach?

We developed the first plant dynamics model for heterogeneous multispecies canopies that 1) takes into account both aboveground and root compartments, so that it could ultimately integrate competition between plants for all resources (light, water and nutrients), 2) for as many as 56 species of crops and weeds interacting in a field 3) for several years 4) under the influence of cropping techniques and pedoclimate (Gaudio *et al.*, 2019). To achieve this, we linked two existing models, RSCone and FLORSYS, predicting root system growth and aboveground weed dynamics in agroecosystems.

Connecting both models required to develop additional formalisms. The allometric relationship we used to calculate the proportion of plant biomass allocated to roots is well known (Wilson, 1988b; Weiner, 2004). We improved it in order to take into account that plants allocate more biomass to roots under nitrogen deficiency. Other additional formalisms were more original because they had to link different approaches chosen by the respective teams that developed FLORSYS and RSCone. For example, we combined agronomical knowledge on soil structure synthetized in FLORSYS to knowledge on the developmental biology of roots from RSCone, in order to predict the effect of soil compaction on root growth. Generally, this effect is estimated empirically from measures of penetrometer resistance (Bengough *et al.*, 2011; Colombi *et al.*, 2018) or bulk density (Brisson *et al.*, 2003). We used a more mechanistic approach that allowed, for example, to simulate that roots grow more easily in a compact soil that has been fragmented by tillage than in a continuously compact soil (Tardieu, 1994). However, this approach did not allow us to model shrinkage cracks, whereas they allow roots to attain resources below compact soil layers (Hasegawa and Sato, 1987). Modelling shrinkage cracks would require a very fine-scale representation of the soil (Sánchez *et al.*, 2014) which is not compatible with our modelling purposes at the field scale.

Our work shows that simulation models are useful to synthetize current knowledge from different approaches and disciplines. However, linking such different approaches required to make some assumptions for which no quantitative measurements were available (e.g. only half the proportion of $b\Delta$ contributed to block root growth in FLORSYS). Fortunately, our simulations showed that, in the context we tested (i.e. a few cropping systems and a local pedoclimate and weed flora of Burgundy), parameters from our additional formalisms had only a limited influence on the model outputs, except for parameters from the allometric relationship, so our assumptions seem acceptable. Moreover, the model was shown to correctly predict the daily and multiannual weed dynamics as well as crop production. The evaluation step comparing simulations to independent observations constitutes another original aspect of our work because it is rarely done for models, particularly for weed dynamics models (Holst *et al.*, 2007). Including the root sub-model improved the overall prediction quality of FLORSYS, and this even without detailed root system architecture or functions simulating soil-resource uptake and use, because there was less overestimation in terms of biomass as suspected by Colbach *et al.* (2016).

Therefore, when parameterizing new species, only parameters of the allometric relationship need to be measured precisely in priority. Given the genericity of the allometric relationship and the low influence of other formalisms we developed, our approach could easily be adapted for connecting other models, benefitting from parameters already acquired in our study for 30 species of crops and weeds for the allometric relationship. However, further simulations with a large diversity of cropping systems and pedoclimatic and floristic contexts must be run first to define in which conditions our formalisms and conclusions apply.

3.2.5.2. What are the parameters involved in potential uptake of soil resource and root parasitism risk?

Species parameters were more correlated to proxies for uptake of soil resource and root parasitism for crops than for weeds. For the latter, proxy variables were the result of a community of interacting species and parameters rather than of individual species or parameters. Therefore, links between proxy variables and parameters were less obvious for weeds and could even seem counter intuitive. For example, weed communities most likely to be infected by *P. ramosa* in autumn, i.e. communities with the largest cumulated root length, consisted mostly of species that did not invest much in roots and that explored the soil only at short distance (when considering only morphological features and photosynthetic functioning). Instead, they invested in strategically placed leaf area after emergence (above neighbours) to occupy space as fast as possible and shade their neighbours rather than be shaded (as illustrated by their low shading response). Indeed, occupying the field area as quickly as possible is crucial for a plant to survive and grow within a community (Liebman and Gallandt, 1997; Colbach *et al.*, 2019), particularly if soil resource are assumed to be mostly non-limiting as in the present case. In terms of belowground exploration, the fine scale seemed most important for parasitism of weeds because root length density was the key parameter (as demonstrated by the specific root length parameter) rather than root-system volume (depending on root-system lateral extension). This is consistent with literature reporting that large specific root length is a crucial trait for belowground exploration because it allows to explore greater soil volumes per unit of biomass invested in roots (Ma *et al.*, 2018).

In contrast to weeds, in terms of morphology and photosynthetic functioning, the crops most likely to be infected in autumn were large both above and belowground and very plastic in response to shade all along their life-cycle. Therefore, it is likely that for crops, which are deliberately sown and promoted by farming practices to the detriment of weeds, exerting a strong competition once established is as at least as important as being able to establish quickly.

In summer, key parameters for parasitism risk and potential soil-resource uptake were different and more difficult to interpret. For example, for crops, they were characteristics of winter cereals. It is difficult to tell whether these characteristics did promote parasitism risk and potential uptake or whether this reflected the way we estimated missing parameters, i.e. by averaging parameters by clade and seasonal type.

Generally, root parameters were less influent than aboveground parameters in our simulations. This is not surprising considering that root functions, except remobilization, are not modelled yet. Uptake of soil resource and *P. ramosa* infection have a retroactive effect on plant growth (respectively beneficial and detrimental) (Barker *et al.*, 1996; Weiner, 2004; Lins *et al.*, 2007), which could amplify the influence of root parameters. However, even after implementing root functions in the model, aboveground parameters could still be more influential than root parameters because soil-resource uptake (Berger *et al.*, 2013) and the number of broomrapes supported by their hosts (Grenz *et al.*, 2008) are driven by the aboveground parts of plants.

It is noteworthy that our proxies quantify potential parasitism and soil-resource uptake, but disregard major aspects involved such as nitrogen uptake efficiency of plants (Aziz *et al.*, 2017) or host status (Qasem and Foy, 2007), which we are currently implementing in the model (Pointurier *et al.*, 2018; Moreau *et al.*, in prep.).

3.2.5.3. Agronomic implications

As potential soil-resource uptake was strongly correlated to the risk of parasitism in the simulations, it will often be difficult to both improve crop nutrition and reduce *P. ramosa* infection in situations where the latter is an issue. However, it is possible, because the crops with the highest potential uptake

were cereals, which generally do not host *P. ramosa* (Parker, 2013). Some species of cereals could even contribute to control *P. ramosa* by depleting the parasite seed bank because they are false-hosts (e.g. oat, *Avena sativa*, Fernández-Aparicio *et al.*, 2009), i.e. they stimulate *P. ramosa* germination but do not support its development (Goldwasser and Rodenburg, 2013). In the case of cover crops, the correlation between increased soil-resource uptake and increased *P. ramosa* infection is actually an opportunity to reduce both nitrate leaching and *P. ramosa* seed banks. Indeed, the principle of "*P. ramosa* catch crops" is to promote *P. ramosa* infection on host crops to reduce the parasite seed bank and destroy the infected crops before *P. ramosa* reproduction (Goldwasser and Rodenburg, 2013).

Our approach allows identifying ideotypes of crops, i.e. theoretical ideal crop plants that combine all the characteristics required to reach one or several goals in a production situation (Martre *et al.*, 2015), here greater soil exploration abilities. For example, breeding less vigorous varieties which would be less likely to encounter *P. ramosa* seeds would be a solution for host crops such as oilseed rape for which no parasite resistance has yet been found (Fernández-Aparicio *et al.*, 2016b). However, such varieties would be less competitive for soil resource against non-parasitic weeds, and their benefits would depend on whether parasitic or non-parasitic weeds were the main limiting factor.

Identifying ideotypes is also interesting for designing crop mixtures. For example, we showed that mixing winter cereals with dicotyledons, which take up potentially fewer soil resources according to our simulations, is relevant under limited water and nutrient supply. Another option is to mix species that explore complementary niches (for example one taking up superficially and the other one more in depth) (Postma and Lynch, 2012). Our approach could be adapted to identify such mixtures.

The trade-off between soil-resource uptake and *P. ramosa* control is interesting for weed management. It means that strategies targeting resource-hungry weed species (e.g. deep banding fertilization that limits nutrient uptake by weeds to the advantage of crops, Blackshaw *et al.*, 2004) also control weeds that favour *P. ramosa* infection. The latter could though be achieved by different management strategies as we showed that interactions between different species with different parameters are very important within the weed community. For example, limiting broomrape infestation via weeds could be achieved either by directly controlling massively infected weed species, as generally advised (www.terresinovia.fr/-/en-savoir-plus-sur-l-orobanche-rameuse), or by tolerating non-host weeds that compete with the latter (Colbach *et al.*, 2017a). Simulating a large number of cropping systems with our model could help to better understand the link between cropping techniques and proxies, and to identify different efficient strategies, including complex ones relying on interactions between weed species.

3.2.6. Conclusion

By connecting a root model to a weed dynamics model, we developed one of the rare plant dynamics model adapted to take into account competition for all resources (light, water and nutrients) in multispecies heterogeneous stands. We focused on weed dynamics in agroecosystems, but our approach is sufficiently generic to be adapted to crop models aiming at designing crop mixtures for example. We also propose a method to identify major plant characteristics involved in competition between crops and weeds for soil resources, which could be adapted for designing crops mixtures.

We used proxies for competition for soil resource and for parasitism of crops and weeds, and the results will help to implement the actual processes in FLORSYS (Pointurier *et al.*, 2018; Moreau *et al.*, in prep.). This will ultimately make FLORSYS a powerful tool for designing agroecological cropping systems. It will allow testing complex strategies that modulate competitive relationships between crops, weeds and broomrape, via, e.g., sowing dates and patterns or fertilization.

3.2.7. Acknowledgements

This project is supported by INRA, the French project CoSAC (ANR-14-CE18-0007) and the research programme “Assessing and reducing environmental risks from plant protection products” funded by the French Ministries in charge of Ecology and Agriculture. We are very grateful to Antoine Gardarin, Maé Guinet, Laurène Perthame and Anne-Sophie Voisin for providing data for our analysis.

3.3. Conclusion du chapitre

Dans ce chapitre, nous sommes parvenues à coupler RSCone et FLORSYS pour prédire la densité de longueur racinaire des hôtes de l'orobanche en vue de modéliser la dynamique d'infection de la plante parasite dans les agroécosystèmes. Les résultats positifs de l'évaluation du modèle, ainsi que la faible influence des approximations nécessaires pour les formalismes de couplage, montrent que le modèle peut être utilisé pour simuler le parasitisme et le prélèvement des ressources du sol dans le contexte pédoclimatique et floristique testé (Bourgogne). L'évaluation dans d'autres contextes est actuellement réalisée par l'équipe mais ne fait pas partie de ce travail de thèse. Il en est de même pour l'intégration du prélèvement de nutriments dans FLORSYS-RSCone (Moreau *et al.*, in prep.).

Nous avons paramétré une trentaine d'espèces cultivées et d'adventices et nous proposons une méthode d'approximation des paramètres pour les nouvelles espèces. Le modèle permet donc de simuler le parasitisme dans une grande diversité de rotations, incluant des mélanges de cultures et de variétés, et de flores adventices. Dans le cas où de nouvelles espèces végétales devraient être paramétrées, quelques mesures devront être effectuées, principalement sur la partie aérienne des plantes (plus facile à étudier que la partie racinaire). Une grande partie des paramètres racinaires indispensables sont bien connus et donc potentiellement disponibles dans la littérature.

Au-delà de l'intérêt du couplage FLORSYS-RSCone pour ce travail de thèse, nous proposons un outil original et utile pour mieux comprendre l'assemblage des communautés végétales (voir section 5.2.2). En effet, FLORSYS-RSCone constitue le premier modèle individu-centré représentant à la fois la partie aérienne et racinaire des plantes, dans des couverts plurispécifiques hétérogènes, sous l'influence des techniques culturales et du pédoclimat pendant plusieurs années.

En outre, nous présentons une méthodologie pour coupler des modèles construits selon des approches différentes. Cette méthodologie est suffisamment générique pour être utilisée pour le couplage d'autres modèles de morphogénèse aérienne et racinaire, avec par exemple des modèles de culture pour créer des outils pour la sélection variétale et la conception de mélanges de cultures (voir section 5.3.2).

Chapitre 4. Modéliser le cycle de vie complet de *P. ramosa* pour concevoir des stratégies de gestion

4.1. Objectifs et démarche

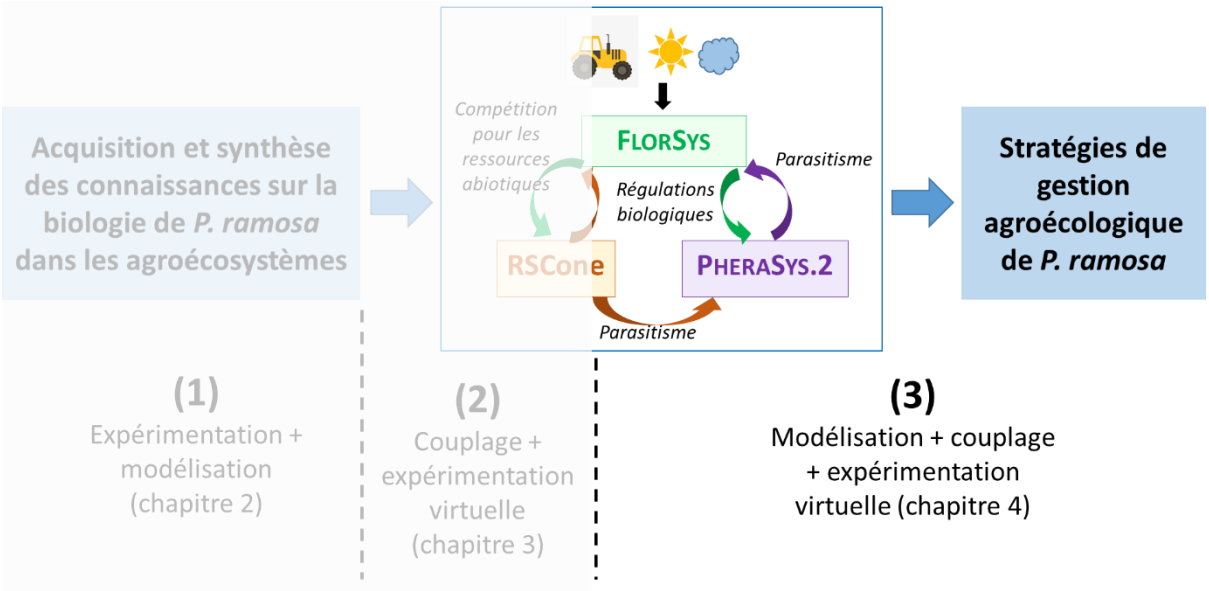

Figure 14 : Objectif et démarche du Chapitre 4 dans le cadre de la thèse. Pour la légende, voir Figure 4.

Dans le Chapitre 1, nous avons mis en évidence que le modèle idéal pour aider à développer une gestion agroécologique de *P. ramosa* serait le résultat d'un couplage entre trois modèles : deux existants, FLORSYS et RSCone, pour modéliser les plantes interagissant avec la plante parasite dans les parcelles et l'effet des techniques et du pédoclimat ; et un modèle mécaniste de dynamique de *P. ramosa* à développer, PHERASYS.2. Les principales connaissances manquantes nécessaires pour modéliser le cycle de vie complet de la plante parasite dans PHERASYS.2 ont été acquises dans le Chapitre 2. Dans le Chapitre 3, le modèle FLORSYS a été couplé à RSCone afin de pouvoir intégrer un module de parasitisme racinaire.

Le présent chapitre a deux objectifs :

(I) S'inspirer des modèles de dynamique des orobanches existants (section 1.2.2) pour proposer, formaliser et paramétrer le modèle PHERASYS.2, et l'utiliser pour évaluer l'efficacité de divers systèmes de culture pour gérer *P. ramosa* et les adventices.

(II) Illustrer l'intérêt d'utiliser un modèle complexe tel que PHERASYS.2 pour évaluer l'efficacité des régulations biotiques de *P. ramosa* par les adventices.

Pour répondre à l'objectif (I), nous avons :

(1) proposé une structure pour le modèle PHERASYS.2,
(2) transcrit nos résultats d'expérimentation en équations représentant des processus biologiques, avec un paramétrage spécifique pour *P. ramosa*,
(3) complété le paramétrage et les formalismes manquants grâce aux données de la littérature,
(4) effectué des simulations après avoir couplé PHERASYS.2 au complexe FLORSYS-RSCone.

Une courte expérimentation a été mise en place avant l'étape (2) pour quantifier la production de semences de *P. ramosa*.

Pour répondre à l'objectif (II), les prédictions de PHERASYS.2 ont été comparées aux prédictions d'un indicateur de risque orobanche développé précédemment dans l'équipe (Colbach *et al.*, 2017a), plus simple que notre approche mécaniste (voir section 1.2.2).

L'objectif (I), traité dans la section 4.2 de ce chapitre, a fait l'objet d'un article qui sera soumis prochainement dans la revue *European Journal of Agronomy* et a été partiellement présenté lors de trois conférences internationales et deux séminaires. L'objectif (II), ainsi que l'indicateur de risque orobanche, sont présentés dans la section 4.3. L'indicateur de risque orobanche a fait l'objet d'un article publié dans la revue *Ecological Indicators* auquel j'ai participé. Il a également été utilisé pour illustrer une méthode de conception de stratégies de gestion répondant à de multiples objectifs dans un article auquel j'ai été associée et qui a été publié dans la revue *European Journal of Agronomy*.

Articles scientifiques

Pointurier, O., Gibot-Leclerc, S., Moreau, D., Reibel, C., Vieren, E. & Colbach, N. (en préparation). Designing a model to investigate the regulation of parasitic plants by weeds. *European Journal of Agronomy*.

Colbach, N., Bockstaller, C., Colas, F., Gibot-Leclerc, S., Moreau, D., Pointurier, O. & Villerd, J. (2017a). Assessing broomrape risk due to weeds in cropping systems with an indicator linked to a simulation model. *Ecological Indicators* 82: 280-292.

Colbach, N., Colas, F., Pointurier, O., Queyrel, W. & Villerd, J. (2017b). A methodology for multi-objective cropping system design based on simulations. Application to weed management. *European Journal Of Agronomy* 87: 59-73.

Communications

Pointurier, O., Gibot-Leclerc, S., Moreau, D., Reibel, C., Strbik, F. & Colbach, N. (2018). Modelling Cropping System Effects on Branched Broomrape Dynamics in Interaction with Weeds. In *XVe European Society for Agronomy Congress*, Geneva, Switzerland. Poster (premier prix poster étudiant).

Pointurier, O., Gibot-Leclerc, S., Moreau, D. & Colbach, N. (2017). Modélisation des effets des systèmes de culture sur la dynamique de l'orobanche rameuse en interaction avec les adventices. In *Séminaire de Restitution à mi-parcours du Projet de Recherche ANR CoSAC Paris*, France. Poster.

Pointurier, O., Gibot-Leclerc, S., Moreau, D. & Colbach, N. (2016). Modelling cropping system effects on branched broomrape dynamics in interaction with weeds. In *23e Conférence du COLUMA: Journées internationales sur la lutte contre les mauvaises herbes*, Dijon, France: AFPP. Poster.

Pointurier, O., Gibot-Leclerc, S., Moreau, D., Darmency, H. & Colbach, N. (2016). Modelling cropping system effects on branched broomrape dynamics in interaction with weeds. In *7th International Weed Science Congress*, Prague, Czech Republic. Poster.

Pointurier, O., Gibot-Leclerc, S., Moreau, D., Le Corre, V., Reibel, C., Strbik, F. & Colbach, N. (2016). Modélisation des effets des systèmes de culture sur la dynamique de la plante parasite orobanche rameuse en interaction avec la flore adventice. In *Séminaire des doctorants du Laboratoire de Mathématiques de Besançon*, Besançon, France. Oral.

4.2. Modélisation de la dynamique de *P. ramosa* dans les agroécosystèmes pour concevoir des stratégies de gestion

Designing a model to investigate the regulation of parasitic plants by weeds

Olivia Pointurier, Stéphanie Gibot-Leclerc, Delphine Moreau, Carole Reibel, Eric Vieren, Nathalie Colbach

Agroécologie, AgroSup Dijon, INRA, Univ. Bourgogne Franche-Comté, F-21000 Dijon, France

Nathalie.colbach@inra.fr

4.2.1. Abstract

Branched broomrape is a parasitic plant, which causes severe yield losses on major crops worldwide. Because of its broad host range, including numerous non-parasitic weed species, the persistency of its seeds in the soil, and the poor efficiency of management techniques available, broomrape management is complex. The objective of the present paper was to develop a broomrape-dynamics model to support the design of management strategies combining multiple techniques aiming at long-term control of broomrape. Towards this goal, we developed a simulation model with formalisms and parameters based on data from our own experiments and the literature. This model called PHERASYS.2 combines 1) a demographic submodel to predict broomrape seed bank dynamics, 2) a trophic-relationships submodel to predict the effect of parasitism on crops and weeds, and 3) a submodel of weed dynamics in agroecosystems to predict the growth of crops and weeds from cropping techniques and pedoclimate. Thanks to an individual representation of each host plant, PHERASYS.2 is able to simulate complex heterogeneous canopies. This model can be used as a tool to test management strategies including crop mixtures and relying on biological regulations by weeds. Simulations with this model showed that delayed sowing in combination with the use of trap and catch crops are promising for reducing broomrape infestation and yield losses in the long term. Tolerating a residual weed flora in such cropping systems could even improve broomrape management.

Keywords: branched broomrape, weed, agroecology, modelling, cropping systems, *Phelipanche ramosa*, PHERASYS, biological regulation

4.2.2. Introduction

Broomrapes are parasitic plants that threaten major crops worldwide (Parker, 2013). As holoparasites, they are not able to photosynthesize and entirely rely on host resources to survive (Heide-Jørgensen, 2013). They must germinate close to a host root, after being stimulated by its exudates (Yoneyama et al., 2013), to connect to its vascular system and derive all resources they need (Heide-Jørgensen, 2013). Among broomrapes, branched broomrape, *Phelipanche ramosa* (L.) Pomel, is particularly devastating since it is found on every continent and is able to infect crops in more than 10 botanical

families including *Solanaceae*, *Brassicaceae* and *Asteraceae* (Parker and Riches, 1993; Molenat et al., 2013). In France, it is a major pest of winter oilseed rape, where it can cause up to 90% yield losses (Gibot-Leclerc et al., 2012), and it also infects hemp, sunflower and tobacco (Terres Inovia, 2018b).

The only curative method available in arable crops is the application of herbicides on herbicide-resistant crops (Fernández-Aparicio *et al.*, 2016b; Données Ephy - Anses, 2018), but this technique clashes with current policies aiming at reducing the use of pesticides because of their impacts on human health and environment (Potier, 2014). Several preventive techniques with partial effects must be combined to control broomrapes (Grenz *et al.*, 2005a; Rubiales and Fernández-Aparicio, 2012). They must provide long-term control because broomrape seeds are assumed to persist up to 20 years in the soil, although this assumption is based on a few studies on species other than branched broomrape (Murdoch and Kebreab, 2013). Moreover, branched-broomrape management must be thought along with non-parasitic weed management (hereafter, the word "weeds" refers to non-parasitic weeds) because several dozens of weed species are hosts (Boulet *et al.*, 2001; Gibot-Leclerc *et al.*, 2003; Simier *et al.*, 2013; Gibot-Leclerc *et al.*, 2015). Weeds might increase broomrape infestation, as they serve as alternative hosts in the absence of host crops. However, they can also be used to deplete the broomrape seed bank, as some species stimulate broomrape germination without supporting further parasite development (Gibot-Leclerc *et al.*, 2003). Therefore, the latter weed species can potentially provide biological regulation of branched broomrape. Finally, branched-broomrape management must be thought at the cropping system scale, defined by the crop sequence and the techniques implemented in a field (Sebillote, 1990), using multiple techniques and exploiting biological regulations by weeds. Such strategies are in line with the current need to develop agroecological farming, but are complex and require specific tools for decision support.

To define such strategies, the field experimental approach for example, is useful but insufficient, since it allows to test only a limited number of techniques, in a few pedoclimatic and floristic contexts for a few years (Jeuffroy *et al.*, 2014). Simulation models are complementary tools to help designing cropping systems because they allow to evaluate cropping systems performances in the long term in various pedoclimatic and floristic contexts (Bergez *et al.*, 2010; Colbach *et al.*, 2014a; Colbach *et al.*, 2017b). Among the many models of broomrape dynamics (Castro-Tendero and García-Torres, 1995; García-Torres *et al.*, 1996; Schnell *et al.*, 1996; López-Granados and García-Torres, 1997; Eizenberg *et al.*, 2009; Regan *et al.*, 2011; Eizenberg *et al.*, 2012a), only one gets close to the required criteria for designing management strategies, simulating the effects of several cropping techniques and pedoclimate on broomrape dynamics for several years (Grenz *et al.*, 2005a). However, it was parameterized for another broomrape species, *Orobanche crenata*, and does not take into account interactions with weeds. A first attempt to adapt it to *P. ramosa* was made with the PHERASYS model (for *Phelipanche ramosa* in cropping systems) (Colbach *et al.*, 2011). It integrated the interactions with weeds thanks to a connection with FLORSYS, a model simulating the dynamics of multispecies weed floras in agroecosystems (Colbach *et al.*, 2014c). However PHERASYS remains largely based on the model developed by Grenz *et al.* (2005a), with most parameter values borrowed from *O. crenata*, and processes determining interactions with crops and weeds only partially modelled. In particular, PHERASYS does not simulate the effect of parasitism on host growth, and so it cannot predict yield losses due to parasitism, though the latter is a major criterion when designing cropping systems. Consequently, the objective of the present study was to develop a model called PHERASYS.2 to simulate branched broomrape dynamics in agroecosystems. PHERASYS.2 is an improved version of PHERASYS where parameters are specifically measured for branched broomrape and where formalisms that describe the broomrape life cycle and the interactions with other plants in the field are improved. We 1) proposed a structure for PHERASYS.2, 2) translated the results of experiments set up purposely into equations to represent biological processes, 3) completed missing data from the literature, and 4) simulated cropping systems with the model. The later step aimed at evaluating the potential of cropping systems to manage branched broomrape (hereafter simply called "broomrape") and weeds in

interaction. In particular, we investigated whether weeds can contribute to biologically regulate parasitic plants in agroecosystems.

4.2.3. Materials and methods

4.2.3.1. Model structure

From inputs given by the user to characterize the field (daily weather, latitude and soil characteristics), the cropping techniques (with their dates, tools used and options) and the initial weed seed bank (including broomrape and non-parasitic weed species), PHERASYS.2 predicts the number of broomrape individuals at different stages and the biomass of broomrape shoots every day (Figure 15). PHERASYS.2 structure was based on the FLORSYS structure (Colbach *et al.*, 2006a; Colbach *et al.*, 2006b; Colbach *et al.*, 2007; Colbach *et al.*, 2010; Gardarin *et al.*, 2012; Munier-Jolain *et al.*, 2013; Colbach *et al.*, 2014c; Munier-Jolain *et al.*, 2014), i.e. the multiannual dynamics of plants were modelled daily as a succession of life stages depending on biophysical processes (Figure 15). Each day, a part of the seeds dies; non-dormant seeds can germinate only if stimulated by neighbouring plant root exudates; the germinated seeds must attach to nearby susceptible plant roots before emerging, flowering and producing new seeds. Attached broomrapes die either when they have finished their life cycle or when their host dies of old age or destroyed by cultural operations. PHERASYS.2 also simulates the effect of parasitism on host plant growth. As FLORSYS, PHERASYS.2 is spatially explicit, for belowground processes in 1D vertical dimension, with 30 successive 1-cm-thick soil layers, and for aboveground processes in 2D horizontal dimensions at the field surface. The 1D representation belowground assumes that seeds are homogeneously distributed and affected by processes within each soil layer. From emergence onwards, each crop or weed plant is individually located on the field surface (2D). Non-parasitic plants are represented in 3D, with their height, width and leaf area explicitly located to simulate competition with neighbouring plants for light. Broomrape plants are not explicitly represented, only the number and biomass of shoots infecting each host plant is computed.

4.2.3.2. Connection with FLORSYS to model interactions with crops and weeds

PHERASYS.2 was connected to FLORSYS to predict the growth of crops and non-parasitic weeds interacting with broomrape, and soil conditions (Figure 15). PHERASYS.2 and FLORSYS connect two ways, with variables from FLORSYS influencing broomrape dynamics in PHERASYS.2, and variables from PHERASYS.2 driving the effect of parasitism on host growth in FLORSYS. Soil temperature and moisture (which are predicted from weather, soil characteristics and management techniques by FLORSYS) determine dormancy relief of broomrape seeds and germination progress. The root volume of host plants determines the probability that parasitic seeds encounter roots that stimulate them and support their subsequent attachment. Host biomass determines the amount of resources available for broomrapes and thus the number of broomrapes it can potentially support (each host can support several broomrape attachments). Host phenology determines when root exudates that trigger broomrape germination are released and when attached broomrapes start to grow from host resources. Host growth, resulting from photosynthesis and respiration processes in FLORSYS, is reduced by parasitism. Biomass allocation between roots and above-ground organs is also modified due to parasitism. Effect of tillage on broomrape-seed movements in the soil is simulated by FLORSYS. Any effect of cropping technique on host plants in FLORSYS indirectly affects broomrape dynamics in PHERASYS.2 since it results in host mortality or host biomass reduction (ex : effect of herbicides on weed) or host biomass increase (ex : weed management reduces competition with crops).

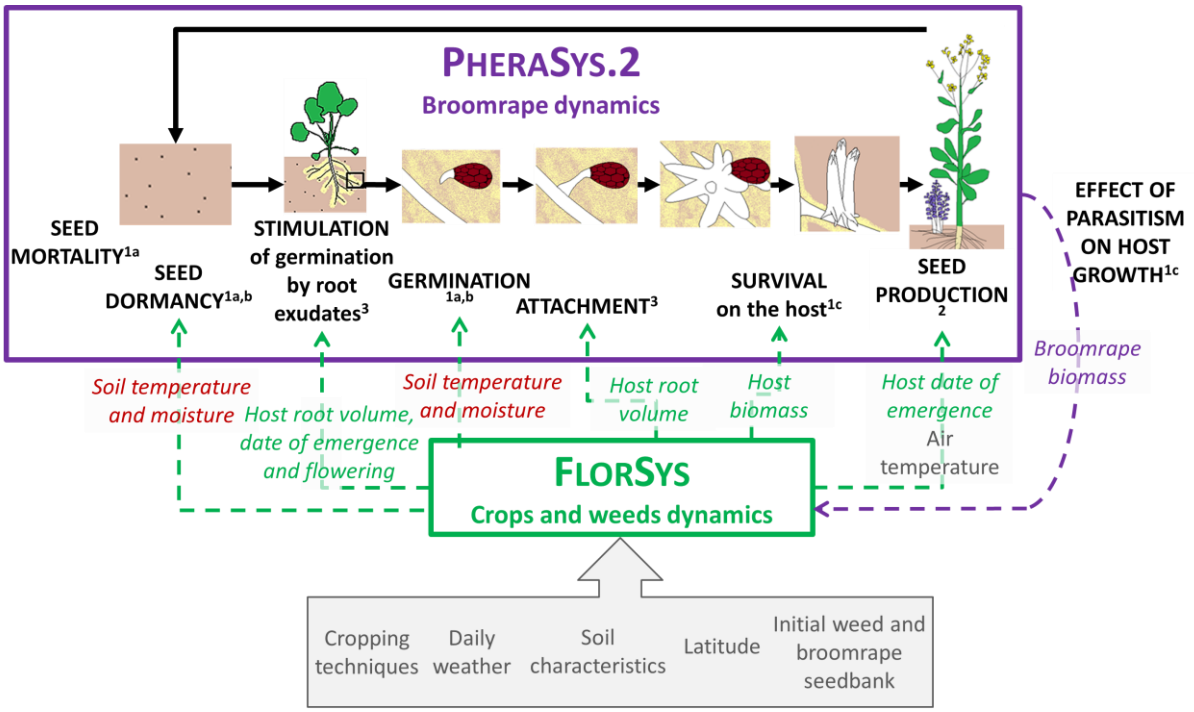

Figure 15: Processes of branched-broomrape life cycle modelled in PHERASYS.2 (in bold, section 4.2.3.1) and connection with FLORSYS. Inputs given by the user are in grey. Variables used to connect both models are in italics (section 4.2.3.2; green and purple: biotic variables from FLORSYS and PHERASYS.2 respectively, brown: abiotic variables). Numbers indicate the origin of the data used with [1]own data published ([1a]Pointurier et al. (2019), [1b]Gibot-Leclerc et al. (2004), and [1c]Moreau et al. (2016), Table 11), [2]experiment described in the present article (section 4.2.3.3.2) and [3]other literature.

4.2.3.3. Data origin

4.2.3.3.1 Published data

The first simplistic PHERASYS model pointed out gaps in knowledge of broomrape biology (Colbach *et al.*, 2011). Experiments were set up to study and quantify insufficiently known processes i.e. seed mortality, and dormancy, as well as production of broomrape seeds, and host-parasite trophic relationships. Most results were published (see [1] in Figure 15) and are summarized in Table 11. The experiment quantifying broomrape seed production was described in the present article (see [2] in Figure 15 and section 4.2.3.3.2). PHERASYS.2 was parameterized from these experiments and from literature (see [3] in Figure 15). Branched broomrape consists of several pathovars i.e. genetically distinct populations with different host preferences (Brault *et al.*, 2007). Our study focussed on the pathovar predominant in oilseed rape which causes the main damages in France (Terres Inovia, 2018b). When no data on this pathovar were available, data on other pathovars were used instead (Table S 40).

Table 11: Summary of own published data used to build and parameterize PHERASYS.2

Data	**Experimental conditions**	**Treatment**	**Measures**	**Branched broomrape pathovar**
Gibot-Leclerc *et al.* (2004)	Germination on glass microfibre paper *in vitro*	Different durations of conditioning at different temperatures and water potentials	Proportion of germinated seed after stimulation with GR24 (synthetic growth regulator used to stimulate broomrape germination)	Oilseed rape pathovar (Brault *et al.*, 2007; Le Corre *et al.*, 2014)
Moreau *et al.* (2016)	Co-cultivation of branched broomrape with hosts in pots in greenhouse	3 hosts species (*Brassica napus, Capsella bursa-pastoris, Geranium dissectum*) grown under 3 light conditions in substrate heavily infested with broomrape seeds or uninfested and harvested at 4 phenological stages	Biomass of broomrape and host organs and number of attached broomrapes.	Oilseed rape pathovar
Pointurier *et al.* (2019)	Seeds buried in the field and put to germination on glass microfibre paper in vitro	Germination after different durations of burial in the soil up to 2 years	Proportion of viable and germinated seeds after different durations of burial and stimulation with GR24	Oilseed rape pathovar

4.2.3.3.2 Measuring broomrape seed production

Broomrape at fructification stage were collected in July 2017 in two oilseed rape fields infested with broomrape in Fontenay-le-Comte (46°26'44" N, 00°46'09" W; Vendée, France) and Saint-Ouenne (46°25'44" N, 00°28'04" W; Deux-Sèvres, France) at crop harvest. Each broomrape consisted of a stem possibly bearing several branches. In total, 36 broomrapes were collected. They were split into two samples to estimate 1) the mean number of seeds produced per seed capsule (structure containing seeds in broomrapes) on six broomrapes (three from each field), and 2) the number of capsules produced per broomrape on the 33 remaining broomrapes. In the first sample, closed capsules (still comprising their seeds) of each broomrape were counted and dried for 48 hours at 80°C. Then, they were opened to collect the seeds, and seeds and empty capsules were weighted separately. The number of seeds was counted under a stereoscopic microscope (1.95x – 250x). Some capsules could not be opened because they were atrophied, contained immature seeds (black seeds that stayed attached in the capsule) or seeds had been eaten by insects (with insect or larvae still inside the capsule). They were counted and weighed separately. In the second sample, the number of capsules was counted on each broomrape, discriminating closed, empty (having already released their seeds) and missing capsules (leaving an abscission mark on the stem). Closed capsules and broomrape stems from which capsules had been removed were dried for 48 hours at 80°C and weighted separately. In broomrapes collected in Fontenay-le-Comte, broomrapes were counted on each host to analyse the trade-off between number of broomrapes attached on a host and the biomass of each broomrape. Biomass per broomrape was calculated as the total biomass of broomrapes (including stems, open and closed capsules) collected on a given host, divided by the number of broomrapes attached on this host. Since the open capsules had not been weighed in the second sample, the mean open capsule weight measured in the first sample was used instead and multiplied by the number of opened capsules counted.

4.2.3.4. Simulation plan

Five cropping systems practiced by farmers in western France (Colbach *et al.*, 2017a), where branched broomrape is the most problematic on oilseed rape (Terres Inovia, 2018b), were simulated. They included a typical local system, i.e. crop rotation including wheat, sunflower and oilseed rape, with mouldboard ploughing and pesticide treatments (Agreste, 2012); and four alternative systems implementing techniques known to control broomrape, namely diversified crop rotations, delayed sowing and reduced tillage (Fernández-Aparicio *et al.*, 2016b) (Table 12). Crops used to diversify the rotations, flax and mustard, are known as a "trap crops" (or "false hosts") and "catch crops" respectively. Both deplete the broomrape seed bank by inducing germination without allowing further development of the parasitic plant because they are resistant (trap crop) or because they are destroyed before broomrape reproduction (catch crop).

Each system was simulated over 30 years with the typical soil, weather and weed flora of the region given as inputs in FLORSYS (Colbach *et al.*, 2017a). Simulations were repeated ten times with ten weather repetitions, each repetition consisting of a series of 30 years randomly chosen in the regional weather database. A moderate broomrape seed density was included in the initial weed seed bank, corresponding to 2000 seeds/m^2 per centimetre of soil layer (Jestin *et al.*, 2014) in the top 10 cm of soil (Prider *et al.*, 2013). Four sets of simulations were run: a) with weeds but no broomrape, b) without weeds but with broomrape, c) with weeds and broomrape and d) without weeds nor broomrape. They allowed to deduce the yield losses due to weeds only, due to broomrape only and due to both weeds and broomrape by comparing a), b) and c) to d) respectively.

Table 12: Characteristics of simulated cropping systems

Cropping system	Rotation*	Oilseed rape sowing date	Tillage	Chemical/ mechanical weeding
1. Reference	O-W-S-W	July 21	25-cm-deep mouldboard ploughing once a year + superficial tillage (≤ 7 cm depth)	2-3 herbicide treatments per year** + mechanical weeding in sunflower
2. Diversified rotation	S-W-F-W-O-W	Aug. 21	25-cm-deep mouldboard ploughing 4 years out of 6 + other tillage operations (5-10 cm depth)	1-3 herbicide treatments per year** + mechanical weeding in sunflower
3. Delayed sowing	same as reference, with mustard as cover crop before sunflower	Sept. 6	25-cm-deep mouldboard ploughing once every 4 years + other tillage operations (5-12 cm depth)	1-2 herbicide treatments per year** + mechanical weeding in sunflower
4. No plough	same as reference	same as reference	No mouldboard ploughing, superficial tillage (≤ 7cm depth)	Same as reference
5. No till	same as reference	same as reference	No tillage	Same as reference + glyphosate before sowing

*O = winter oilseed rape, W = winter wheat, S = sunflower, F = flax; ** herbicide treatments at sowing or on crop.

4.2.3.5. Statistical analysis

Data were analysed using R (R Core Team, 2019). During model development, linear models were fitted with the R package "lm" and non-linear models with "nls" and "nls2" of R. The algorithm "brute-force" was used to solve cases of failed convergence with function "nls2". A pseudo-R^2 was calculated to estimate the predictive quality of non-linear models (UCLA: Statistical Consulting Group, 2015).

In simulation results, the effects of the type of infestation (i.e. with weeds and/or broomrape) and of cropping systems on annual crop yield losses due to pests (i.e. weeds and/or broomrape) were analysed with a linear model with the function "lm" of R:

Annual yield $loss_{tscyr}$ = constant + type of $infestation_t$ + cropping $system_s$ + $crop_c$ + $year_y$ + weather $repetition_r$ + type of $infestation_t$ × cropping $system_s$ + type of $infestation_t$ × $crop_c$ + $error_{tscyr}$ (with "×" standing for two-ways interactions).

Yield loss, i.e. the difference in yield (MJ/ha) in simulations with and without pests, was calculated relatively to yield obtained in simulations without pests. When analysing broomrape-caused yield loss, only host crop species were included in the analysis. Data were squared-root-transformed before analysis to achieve normality of residuals. Least significant difference tests were performed to compare yield losses due to broomrape between cropping systems for each crop species with the function LSD.test from the package agricolae of R.

4.2.4. Results

4.2.4.1. Modelling broomrape dynamics

The following subsections describe how PHERASYS.2 models broomrape dynamics and which data and hypotheses were used. The detailed equations can be found in Table S 37, Table S 38 and Table S 39.

4.2.4.1.1 Seed mortality in the soil

Broomrape life cycle starts in the soil as a seed. Some seeds die due to aging, diseases or predation resulting in annual seed bank decline of 7% (eq. [1] in Table S 37) (Pointurier *et al.*, 2019). This annual mortality rate was converted into a daily rate using the same equation as in FLORSYS for non-parasitic weeds (Gardarin *et al.*, 2012).

4.2.4.1.2 Seed dormancy

Fresh broomrape seeds are dormant. They require 1) a period of dry storage, followed by 2) a period of moist storage ("conditioning"), and finally 3) a stimulation by root exudates of potential host plants to relieve dormancy. In field conditions, seed dormancy varies moreover with seasons (Murdoch and Kebreab, 2013). Dormancy was modelled as two successive phases in PHERASYS.2: 1) dormancy relief of new seeds, as a function of soil temperature and moisture; and 2) seasonal dormancy, as a function of time since seed shed.

According to data from Gibot-Leclerc et al. (2004), once moisture requirements are met (≥ -2MPa), dormancy relief of fresh seeds depends solely on temperature during the conditioning period (annex A.3.2). No seed germinates if temperature during conditioning is too cold or too hot (< 0°C or > 37°C, even if temperature during exposure to root exudates are adequate). In-between these temperature thresholds, the closer the temperature is to the optimum, the faster the seeds lose dormancy (annex A.3.2). Thus, the proportion of non-dormant seeds among viable seeds was modelled as a function of thermal time accumulated during conditioning using a Weibull equation (eq. [3] in Table S 37, Figure 16). Thermal time was calculated in each soil layer as a function of soil temperature and cardinal temperatures of conditioning [2] (equation adapted from Bradford, 2002). The latter were calculated with the method for calculating cardinal temperatures for germination (Bradford, 2002) (annex A.3.2).

Older seeds follow a seasonal pattern of dormancy, with high dormancy in winter-spring and low dormancy in summer-autumn, and seeds older than a year entering dormancy two months later. The dormancy pattern is pronounced, alternating periods of low dormancy where more than 90% of the seeds are responsive to germination stimulants, with periods of high dormancy where more than 80% are dormant (Pointurier *et al.*, 2019). Seasonal dormancy was modelled accordingly as a function of seed age [4], using the same equation as for non-parasitic weeds (Gardarin and Colbach, 2015).

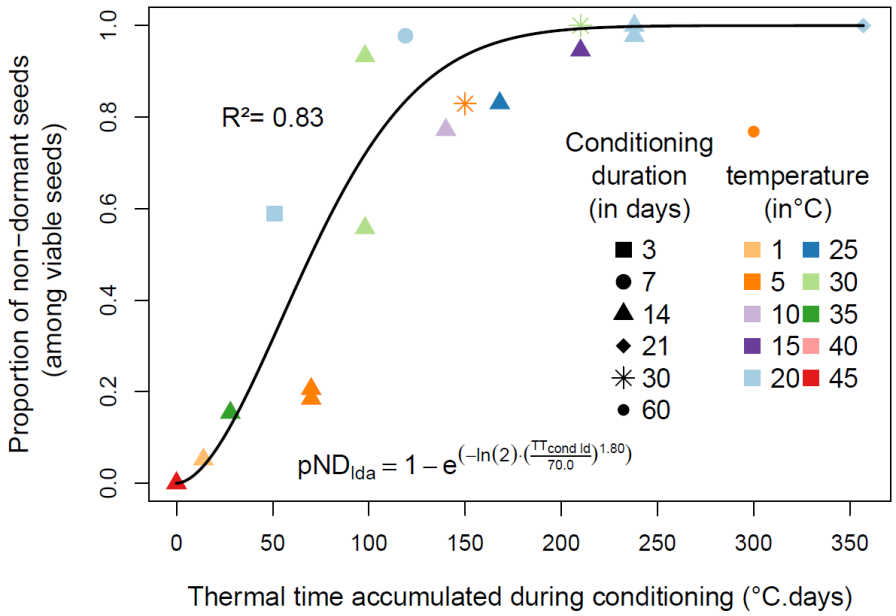

Figure 16: Dormancy relief of branched-broomrape seeds as a function of thermal time accumulated during conditioning ($TT_{cond\ ld}$, base 0°C). Each dot represents the proportion of seeds (pND_{lda}) germinating after being stimulated with a synthetic stimulant (GR24 at 1 $mg.L^{-1}$ at 20°C, i.e. optimal GR24 concentration and temperature for broomrape germination) after being stored in moist conditions ("conditioning") for different durations and temperatures of conditioning respectively (see legend on the figure). The line represents the model fitted to the data. Based on data from Gibot-Leclerc et al. (2004).

4.2.4.1.3 Stimulation of germination

Dormancy relief ends with germination triggering by root exudates of plants. The stimulatory activity of root exudates depends on the species emitting them (Fernández-Aparicio *et al.*, 2009; Gibot-Leclerc *et al.*, 2016; Perronne *et al.*, 2017). Data from germination tests from the literature were compiled to calculate the ability of crop and weed species to stimulate broomrape relatively to GR24, a synthetic stimulant commonly used as a synthetic control (Mangnus *et al.*, 1992)(Table S 40). This method allowed us to compare data from different experiments. When experiments did not include GR24 but oilseed rape as a positive control, the ability of the species to stimulate broomrape was first calculated relatively to oilseed rape, and then multiplied by the ability of oilseed rape to induce germination relatively to GR24. When no data were available for a species, its ability to stimulate broomrape germination was estimated from a close species (e.g., the data of *Medicago lupulina* were used for *Medicago sativa*). When data on germination were not available, the number of broomrapes attached per plant relative to a sensitive species (e.g. oilseed rape, tomato or *Geranium dissectum*) was used instead. If no data could be found in the literature, the species was considered to be unable to stimulate broomrape germination.

Broomrape seeds must be close to the stimulating root to be able to perceive germination stimulants (≤ 36 mm, Goldwasser and Yoder, 2001). So, every day in PHERASYS.2, a part of the non-dormant seeds are stimulated (eq. [6] in Table S 37), corresponding to the proportion of soil volume comprised in the "stimulating zone" [5], i.e. close enough to the roots (annex A.3.3). As root exudates are mainly released at root tips (Brown and Edwards, 1944; Dennis *et al.*, 2010), broomrape seeds are only stimulated by the "new" stimulating zone predicted each day, i.e. the stimulating zone on the present day minus the one from the day before [6]. Plants are considered to be able to induce germination from emergence to the end of flowering (Auger *et al.*, 2012), which is also approximately the time when plants stop emitting new roots (Gregory *et al.*, 1995).

4.2.4.1.4 Germination progress

Once stimulated, seeds start to germinate and the wetter and the warmer the soil layer is (i.e. the higher above base temperature and base water potential, Bradford, 2002), the faster the seeds germinate (Pointurier *et al.*, 2019). Germination dynamics of broomrape seeds were modelled using the same principle as Gardarin *et al.* (2011), i.e. as a function of hydrothermal time accumulated since germination triggering by root exudates (eq. [7] in Table S 37). Too cold temperatures (below base temperature) halt germination temporarily. When the soil is too dry (i.e. below base water potential), or after a tillage operation which dilutes root exudates in the soil, germination stops and new root exudates are necessary to trigger germination again [8]. Base temperature and base water potential of germination were taken from Gibot-Leclerc *et al.* (2004) (annex A.3.2), and germination dynamics parameters from Pointurier et al. (2019).

Every day, germination flushes are triggered by new stimulating roots in the model. Consecutive flushes are merged to avoid storing data from several simultaneous germination flushes in the computer memory. To avoid large under or overestimation (see details in annex A.3.4), only close enough flushes (i.e. the new flush occurs before the ongoing flush has run 2.5 times its time to mid-germination) are merged. Otherwise, only the most recent flush is kept [7].

Germinated seeds are removed from the seed bank daily [9].

4.2.4.1.5 Attachment

Germinated seeds produce a radicle which grows towards the host root to attach and establish vascular connections to take up water and nutrients from the host (Joel, 2013b). Yet not all species that stimulate broomrape germination also support broomrape attachment. The ability of species to allow broomrape attachment after stimulation and consecutive development was compiled from the literature (Table S 40). Radicle elongation is limited, so only germinated seeds within a 4 mm “attachment zone” around host roots and younger than three days can attach, otherwise they die (Gibot-Leclerc *et al.*, 2012). First, the volume of the attachment zone was calculated for each host plant (eq. [10] in Table S 37) and cumulated over all host plants to determine the proportion of soil volume where broomrape seeds are close enough to host roots to attach, and to deduce the total number of broomrape attachments [11]. Then, attachments were distributed over the hosts proportionally to their contribution to the total attachment zone [12]. A host plant with all broomrapes attached on it constitutes a pathosystem.

4.2.4.1.6 Survival on the host

Only a few attached broomrapes survive on the host until flowering (Moreau *et al.*, 2016), depending on the biomass the host allocates to them (Figure 17) (Grenz *et al.*, 2005b; Lins *et al.*, 2007; Grenz *et al.*, 2008). Host biomass at rosette stage represents a potential biomass to be used by broomrapes since at this stage parasitism has not yet an effect on host biomass (Moreau *et al.*, 2016). Above a minimum host biomass threshold, the total number of emerged broomrapes per host plant increases linearly with increasing host biomass at rosette stage. Hosts whose biomass is below the threshold do not have enough biomass to support the growth of emerged broomrapes.

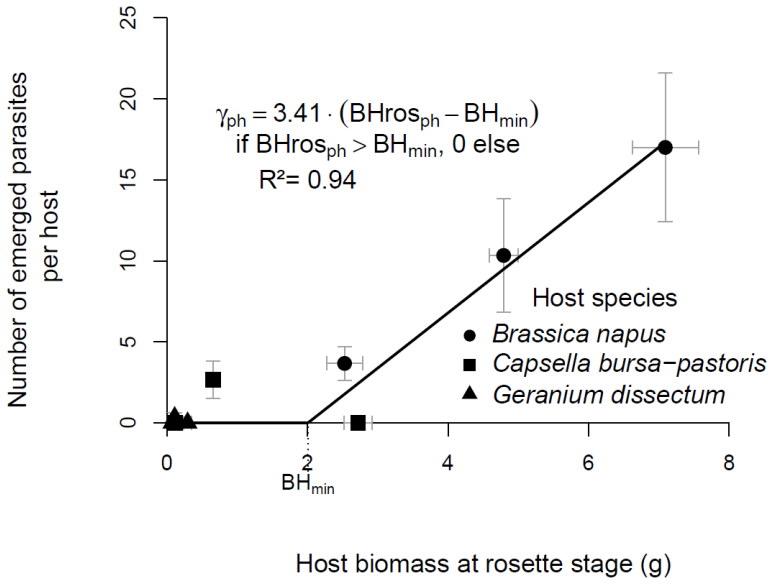

Figure 17: Number of emerged branched broomrapes (γ_{ph}) per host plant surviving until flowering as a function of host biomass at rosette stage ($BHros_{ph}$). Each dot represents the mean value (with bars showing standard deviation) over three independent replicates for a species in a given light condition at rosette stage. The line represents the non-linear model fitted to the data. BH_{min} is the minimum biomass of a host plant at rosette stage to allow the development of broomrapes. Based on data from Moreau et al. (2016).

The relationship of Figure 17 was used to calculate host carrying capacity in PHERASYS.2 (eq. [13] in Table S 37). Moreover, this capacity was limited to a maximum of 20 broomrapes per host plant in our model, which corresponds to the maximum number of broomrapes observed per oilseed rape plant in heavily infested fields (Gibot-Leclerc *et al.*, 2012). The host carrying capacity allows to introduce density-dependence into the model, i.e. the more broomrapes compete on a host, the less likely each of them is to survive. To represent this, we adapted a relationship used to simulate intra-specific competition between oilseed rape seedlings for emergence (Colbach *et al.*, 2001). This relationship [15] was used to calculate number of emerged broomrapes from the number of (unemerged) broomrapes attached at host rosette stage [14], when host carrying capacity was determined [13]. Since broomrape can still attach after host rosette stage, the competition relationship [15] was derivated to calculate the survival probability for broomrapes attached daily after rosette stage [16]. The surviving emerged broomrapes were summed up to broomrape reproduction [17]. They may though die before reaching seed production if the host dies earlier due to old age, frost or management operations (harvest, herbicide, tillage etc) [18].

4.2.4.1.7 Broomrape biomass

Broomrape phenology was predicted solely from temperature, since it does not depend on host phenology (Gibot-Leclerc *et al.*, 2013b), year or experimental conditions (fields or greenhouse) (Gibot-Leclerc, 2004). So, once attached, broomrape biomass accumulation was modelled from thermal time since host emergence (eq. [20] in Table S 37). Broomrape biomass becomes noticeable at about 700°C·days (base 5°C) after host emergence (Figure 18). The maximum biomass that the broomrapes can derive from the host is reached approximately at double this time (50% of this maximum biomass is reached after about 1100 °C·days) [21]. This maximum biomass is determined by the number of emerged broomrapes competing with each other for resources on the same host at the end of their life cycle (see section 4.2.4.1.6). The more emerged broomrapes survive on a host, the less biomass is available for each of them [19] (Hibberd *et al.*, 1998; Grenz *et al.*, 2005b; Mauromicale *et al.*, 2008; Fernández-Aparicio *et al.*, 2016a; Moreau *et al.*, 2016) (Figure 19). The later intraspecific-

competition relationship was parameterized from data from the greenhouse experiment of Moreau et al. (2016) and not from our field measurements (section 4.2.3.3.2) because data from Moreau et al. (2016) presented a larger range of values (on the x-axis, Figure 19). However, our field measurements are consistent with data from Moreau et al. (2016) (Figure 19).

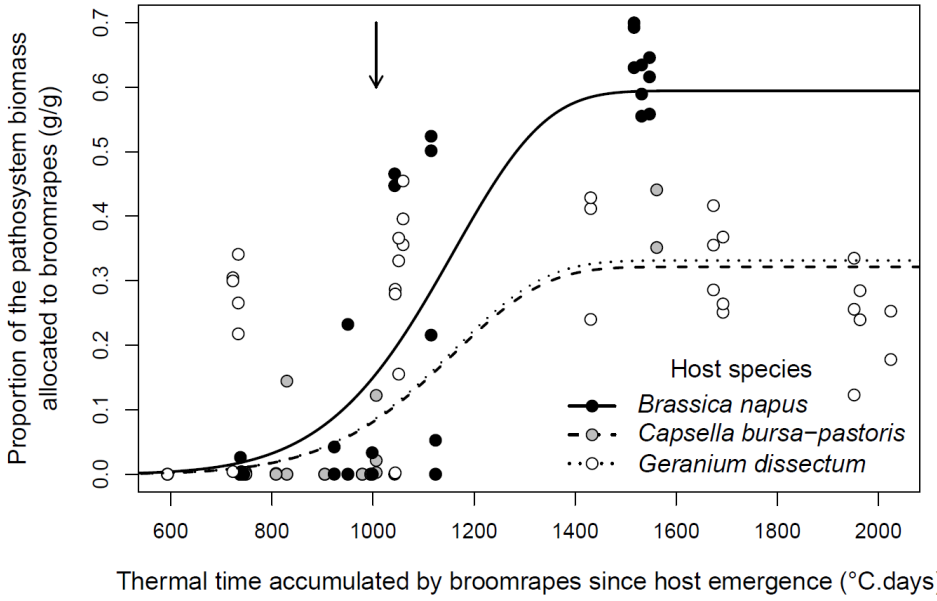

Figure 18: Proportion of the pathosystem biomass (i.e. host + branched-broomrape biomass) allocated to broomrapes over time (thermal time, base 5°C) in three host species. Each dot represents an infected host replicate for a species for one stage and light condition. Lines represent non-linear models fitted for each species. The vertical arrow shows when broomrapes started to emerge. Data from Moreau *et al.* (2016).

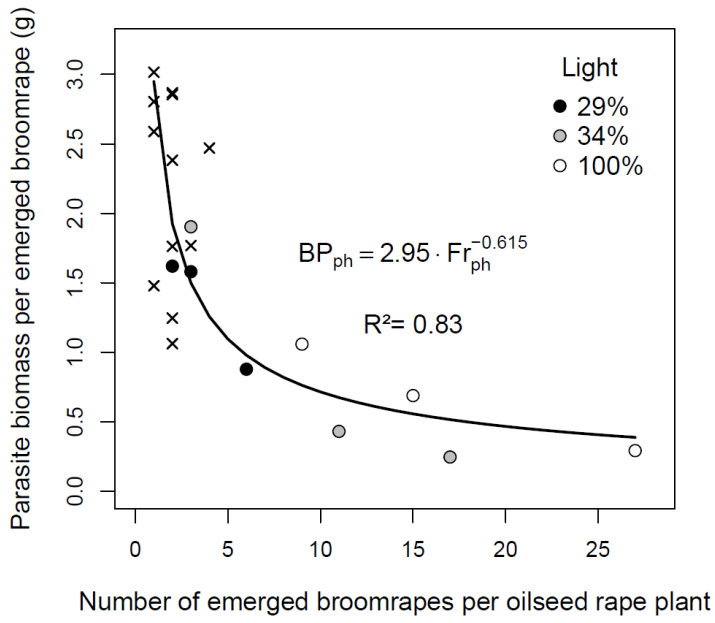

Figure 19: Parasite biomass per emerged branched broomrape (BP_{ph}) as a function of the number of emerged branched broomrapes per oilseed rape plant at host fructification (Fr_{ph}) under greenhouse conditions (dots, Moreau *et al.*, 2016) and in the field (crosses, see section 4.2.3.3.2). Each dot represents a replicate of the total biomass of all broomrapes attached on a host divided by the number of flowering broomrapes in one light condition. Each cross is the mean biomass per fructifying broomrape on a host measured in the experimentation described in section 4.2.3.3.2. The line represents the non-linear model fitted to the data from Moreau et al. (2016) (dots).

4.2.4.1.8 Seed production

Assuming that broomrape phenology was mainly driven by temperature (see section 4.2.4.1.7), broomrape seed production occurs at 1709°C·days (base 5°C, annex A.3.5) after host emergence in the model, whatever the host, the location or the cropping system (eq. [20] in Table S 37).

Our measurements (section 4.2.3.3.2) on broomrape reproduction demonstrated that the number of capsules containing seeds increased linearly with broomrape biomass (Figure 20), while seed biomass per capsule (0.55 ± 0.082 mg) and individual seed biomass (2.1 ± 0.26 µg) were relatively constant. A small proportion (8%) of the analysed capsules did not produce mature seeds as they were either eaten by insects, atrophied or did not have the time to reach maturity. As a result, the model calculates broomrape seed production by (1) calculating the number of capsules from broomrape biomass and the proportion of unproductive capsules, (2) multiplies the capsules by their average seed weight to get seed biomass, (3) divides it by average seed weight to obtain the number of broomrape seeds per host plant, and (4) multiplies it by seed viability in fresh seeds to produce the number of viable broomrape seeds [22]. The seed viability (0.93 seeds·seeds^{-1}) was measured in a previous experiment (Pointurier *et al.*, 2019).

Finally, seeds are released and added to the surface layer of the broomrape seed bank [23].

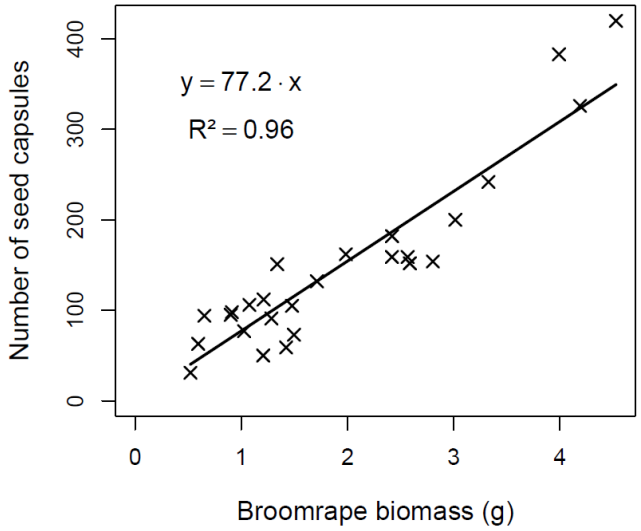

Figure 20: Number of seed capsules produced per branched broomrape as a function of branched broomrape biomass at fructification stage. Each dot represents a measurement on a broomrape collected at maturity from naturally infested fields of winter oilseed rape (see section 4.2.3.3.2). The number of capsules includes closed, open and missing capsules. Broomrape biomass was calculated as explained in section 4.2.3.3.2.

4.2.4.2. Modelling the effect of parasitism on host growth

The following subsections describe the effect of parasitism on host growth and reproduction as well as the data used to justify and fit the equations. As host phenology is not affected by parasitism (Gibot-Leclerc *et al.*, 2013b; Moreau *et al.*, 2016), the relevant equations used by FLORSYS (Colbach *et al.*, 2014c) remain unchanged.

4.2.4.2.1 Pathosystem biomass loss

We considered broomrape as a supplementary sink for the host (Manschadi *et al.*, 2001; Grenz *et al.*, 2008; Fernández-Aparicio *et al.*, 2016a). Consequently, we simulated the total pathosystem biomass,

consisting of both the host and the attached broomrapes. The amount of biomass lost by infected hosts is not fully invested in broomrapes, resulting in a reduction of the pathosystem biomass compared to the biomass of healthy plants (Barker *et al.*, 1996; Eizenberg *et al.*, 2005; Lins *et al.*, 2007; Grenz *et al.*, 2008; Moreau *et al.*, 2016). Up to host flowering, parasitism has little or no effect on the pathosystem biomass (Moreau *et al.*, 2016). Then, broomrape starts to emerge and reduces the pathosystem biomass by 27 % (Figure 21). This loss rate is applied in our model to the daily net biomass produced after photosynthesis and respiration predicted in FLORSYS (eq. [24] in Table S 37).

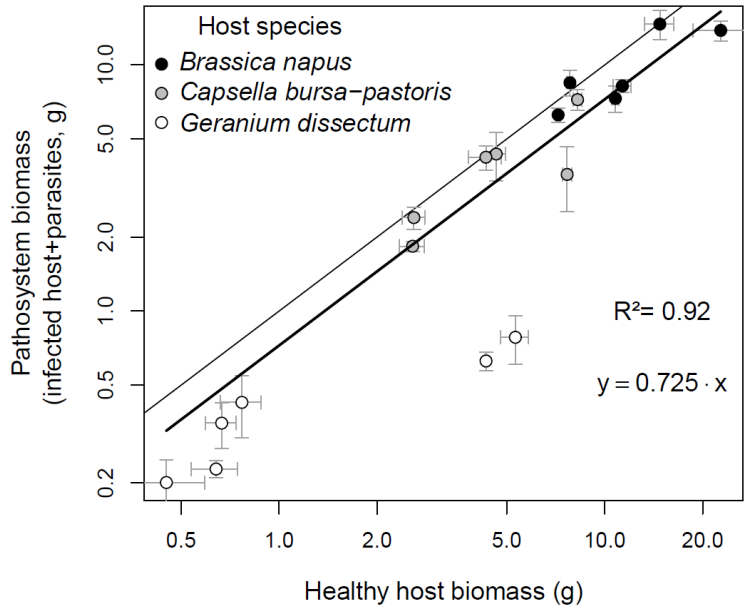

Figure 21: Relationship between the pathosystem biomass (host + branched broomrapes) of infected and healthy plants for three host species from host flowering onwards. Each dot represents the mean value over three independent replicates for a species at a given stage in a given light condition. Bars represent standard deviations. The thick line represents the linear model fitted to the data, thin line shows y=x. Note the log-log scale. Data from Moreau *et al.* (2016).

4.2.4.2.2 Reallocation among vegetative organs

Before rosette stage, parasitism has no effect on the proportion of the pathosystem biomass allocated to roots (p=0.67). After that key stage, it reduces the root to pathosystem biomass ratio by 21% (Figure 22). Biomass allocation to roots is reduced accordingly in PHERASYS.2 (eq. [25] in Table S 37). Biomass allocation to leaves in the pathosystem is not affected by parasitism (Moreau *et al.*, 2016), so the FLORSYS equations determining the leaf biomass ratio remain unchanged (Colbach *et al.*, 2014c) [26].

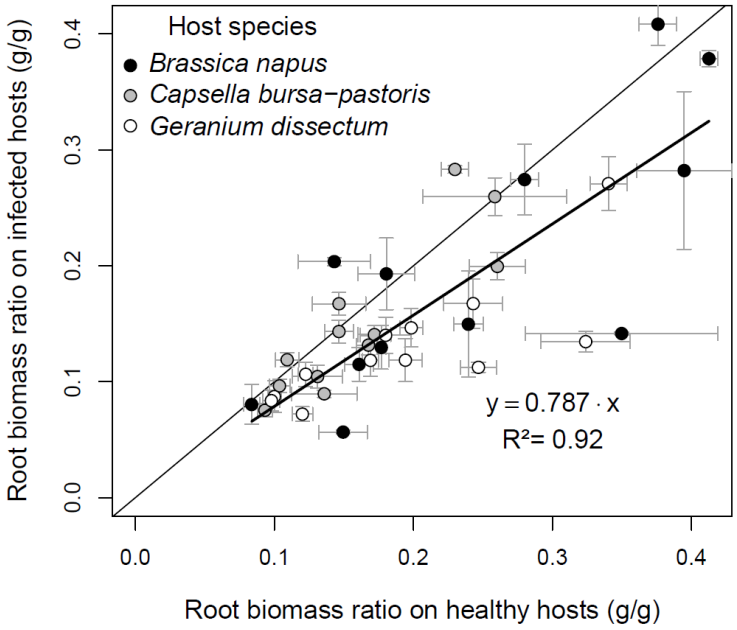

Figure 22: Relationship between the proportions of the pathosystem (host + branched broomrapes) biomass allocated to roots in infected and healthy plants for three host species from host rosette stage onwards. Root biomass ratio is the host root biomass divided by the total pathosystem biomass. Each dot represents the mean value over three independent replicates for a species at a given stage in a given light condition. Bars represent standard deviations. The thick line represents the linear model fitted to the data, thin line shows y=x. Data from Moreau *et al.* (2016).

4.2.4.2.3 Host seed production

Since broomrape competes mostly with the reproductive compartment of the host (Manschadi *et al.*, 2001; Grenz *et al.*, 2008; Fernández-Aparicio *et al.*, 2016a; Moreau *et al.*, 2016), the combined biomass of broomrapes and host reproductive organs (flowers and fruits) was compared to the biomass allocated to reproduction in healthy host plants (Figure 23). In healthy host plants, a part of the above-ground biomass is allocated to seeds (Colbach *et al.*, 2014c) (eq. [27] in Table S 37). In infected hosts, this part, including broomrape biomass, is 1.7 times higher [28]. In the model, the biomass allocated to host seeds in infected hosts is computed by subtracting the broomrape biomass (calculated in section 4.2.4.1.7) from the biomass allocated to host reproduction and broomrapes [29]. Although host plants did not go beyond maturity onset in the data we used from Moreau et al. (2016), we considered that our formalisms were still valid at later stages because the proportion of above-ground biomass allocated to the reproductive compartment varies only little then (Weiner, 2004).

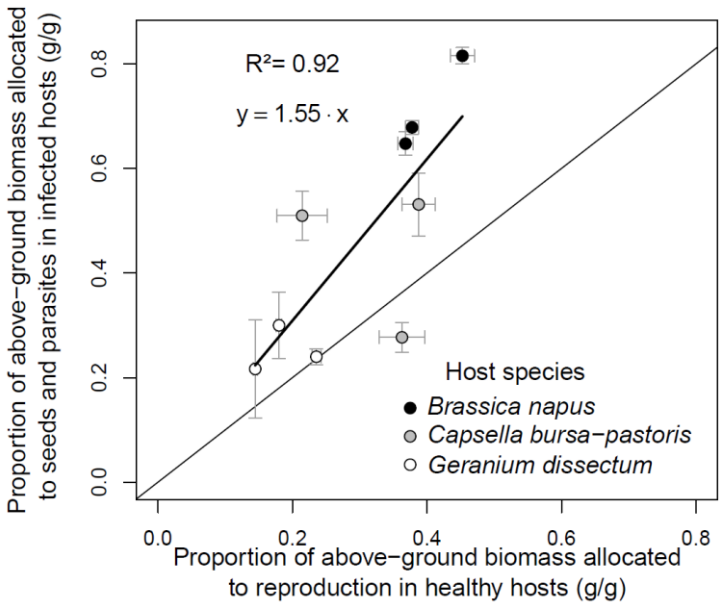

Figure 23: Relationship between the proportions of the above-ground pathosystem (host + branched broomrapes) biomass allocated to reproduction and branched broomrapes in infected and healthy plants for three host species at host fructification. Each dot represents the mean value over three independent replicates for a species in a given light condition. Bars represent standard deviations. The thick line represents the linear model fitted to the data, thin line shows y=x. Data from (Moreau *et al.*, 2016).

This formalism takes into account that hosts reproducing early benefit from a competitive advantage compared to broomrapes (Manschadi *et al.*, 2001; Grenz *et al.*, 2005b). Accordingly, we observed in data from Moreau et al. (2016) that the proportion of biomass allocated to reproduction in infected hosts was not altered, or even increased, compared to the one in healthy hosts if they reproduced before broomrapes started to accumulate significant amounts of biomass (Figure 24).

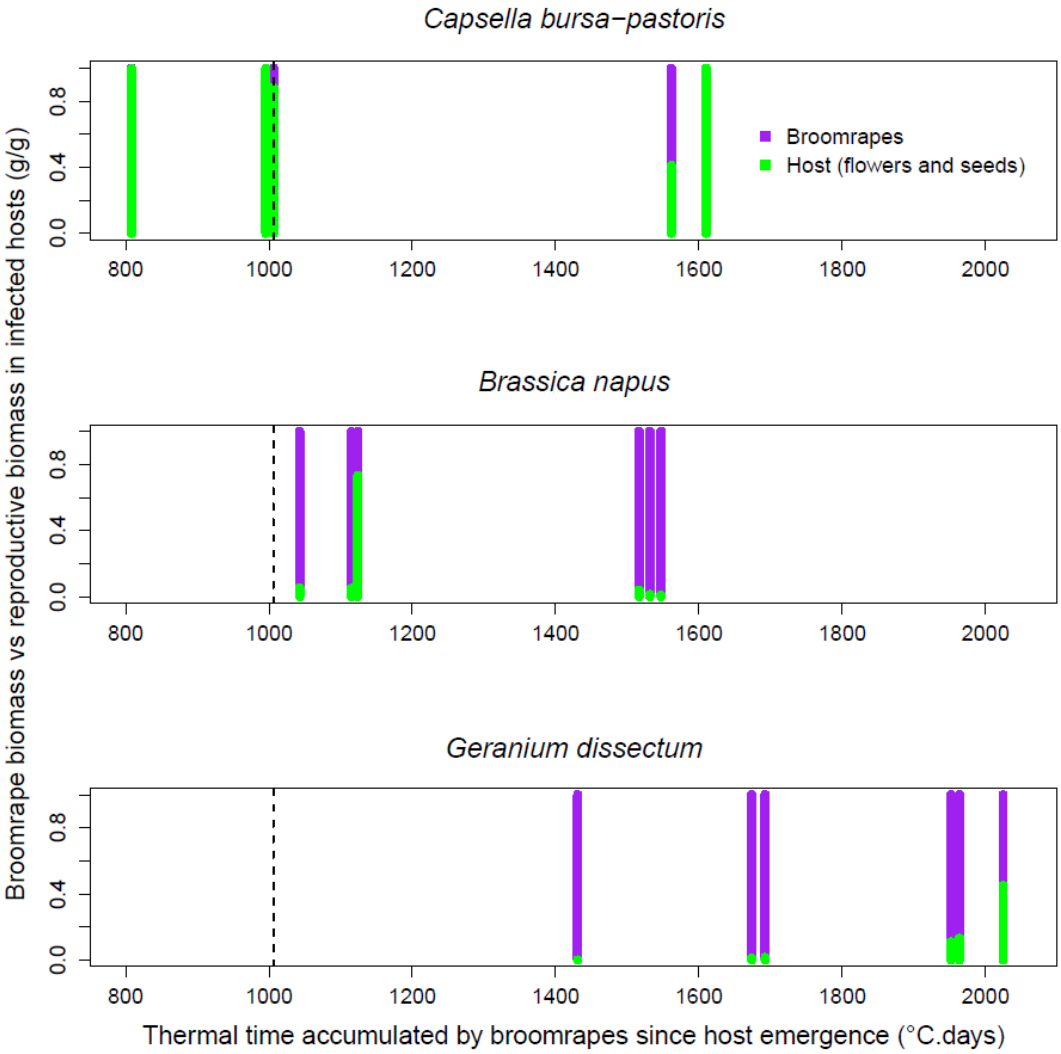

Figure 24: Proportion of biomass allocated to branched broomrapes within the host reproductive + parasite compartment over time (thermal time with base 5°C) measured in three host species from host flowering onwards in greenhouse. Each bar represents the mean value over three independent replicates for a species at a given stage in a given light condition. Dotted lines show when broomrapes start to emerge. Data from Moreau *et al.* (2016).

4.2.4.3. Modelling the effects of copping systems on broomrape dynamics

The different processes modelled in PHERASYS.2 allowed to integrate the effects of several cropping techniques (Table 13). For example, soil tillage move seeds in the soil, which makes them more or less close to stimulating root exudates and to host roots and thus determines the number of stimulated broomrape seeds and attachments.

Table 13: Effects of cropping techniques on branched-broomrape dynamics in PHERASYS.2

Cropping technique	Effect	Consequences on broomrape dynamics
Soil tillage	Buries and excavates seeds	Determines the proximity of broomrape seeds to stimulating/attaching roots, and thus the number of germinated seeds/attachments
Crop species and variety	Crop root distribution	Same as soil tillage
	Broomrape seed stimulation ability	Determines the number of stimulated broomrape seeds
	Broomrape seed attachment ability; host plant biomass	Determines the number of attached broomrape seeds that will survive up to maturity
	Plant life duration	Broomrapes die before reproducing if the host dies. Hosts reproducing early benefit from a competitive advantage compared to broomrape.
	Sowing season	Determines broomrape seed dormancy level when crops stimulate broomrape germination.
	Sowing date	The later broomrape emergence is, the less time there is for broomrapes to damage the crop and to reproduce
Weed management	Indirect effects via the non-parasitic weed flora (see crop species and variety).	
Crop sowing density	Number of crop seeds in the soil	Same as soil tillage

4.2.4.4. Simulation results

4.2.4.4.1 Broomrape dynamics

In simulations with broomrape only, all cropping systems led to a continuous increase of the broomrape seed bank over 30 years, with regular sharp increases of the seed bank after host crops and slow decreases in-between (Figure 25). This dynamic was slower in cropping systems with delayed sowing and diversified crop rotation (scenarios 3 and 2 in Figure 25), where the initial seed bank was multiplied by only 4 and 8 respectively over 30 years, compared to 20 in other systems (annex A.3.6.1.A). Seed bank increased mostly after oilseed rape, except in the cropping system with delayed sowing where broomrape did not have time to reproduce on oilseed rape (Figure 25). Indeed, the more oilseed rape sowing was delayed (i.e. from system 1 to 2 to 3), the later broomrapes matured (from mid-April, mid-June and the end of June respectively, annex A.3.6.3.A). Sunflower increased the broomrape seed bank in cropping systems with delayed sowing and diversified rotation, but depleted it in other systems (1, 4 and 5). In the latter cases, where broomrape seed banks were 3 to 5 times bigger, the number of germinated seeds exceeded broomrape seed production, resulting in a net decrease of the broomrape seed bank (e.g. reference system in Figure 25). Flax and mustard, set up as trap and catch crops, did induce broomrape germination (annex A.3.6.2.A) but did not allow its reproduction (annex A.3.6.3.A). However, those induced by mustard were largely cancelled out by broomrape seed production on the following sunflower (Figure 25). Overall, most broomrape germination occurred in spring, after a smaller germination peak in autumn in winter crops (annex A.3.6.2.A). Broomrapes phenology was consistent with field observation (Gibot-Leclerc *et al.*, 2012) since they started to reach maturity in June in oilseed rape crops sown at the end of August (annex A.3.6.3.A).

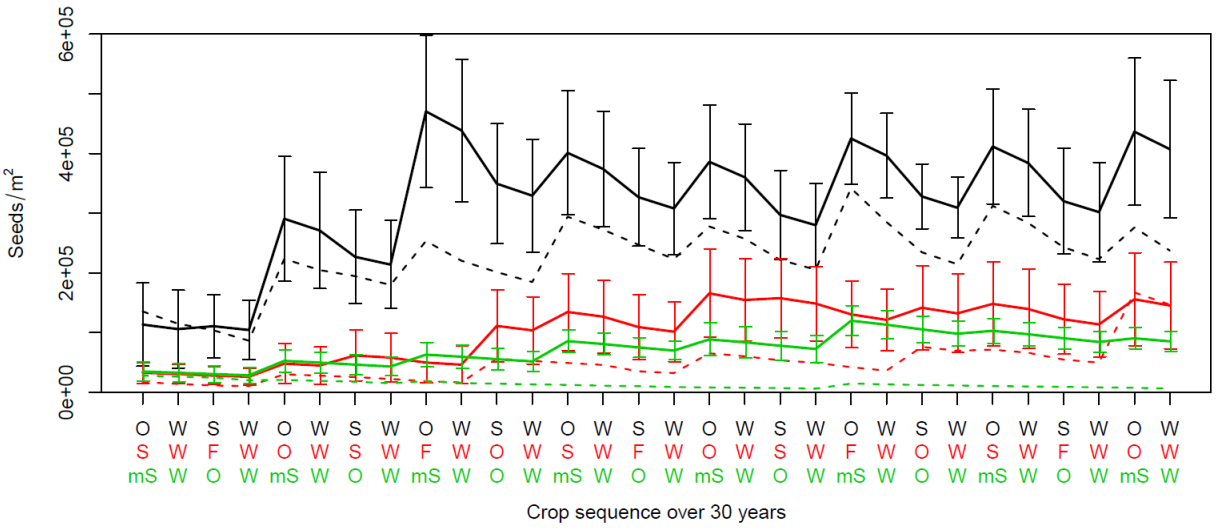

Figure 25: Dynamics of the branched-broomrape seed bank in three cropping systems predicted by PHERASYS.2 over 30 years. Each line shows the mean number of broomrape seeds in the soil after crop harvest averaged over 10 weather repetitions in a given cropping system. Thick lines show data from simulations of infestation with broomrape only, and dashed lines from simulations with both weeds and broomrape. Bars represent standard deviations. Each colour shows a cropping system: reference (1) in black, diversified rotation (2) in red and delayed sowing (3) in green. For details on the cropping systems, see Table 12. Letters indicate the harvested crop: O = winter oilseed rape, W = winter wheat, S = sunflower (mS when sunflower was sown after a mustard cover crop) and F = flax.

4.2.4.4.2 The main drivers of crop yield loss

All tested factors had a significant effect on annual yield losses due to broomrape and/or weeds predicted by PHERASYS.2 ($p < 0.05$, annex A.3.6.4). Crop yield losses were 38% on average and depended mostly on the crop species (partial $R^2 = 0.24$) and on the cropping system (partial $R^2 = 0.15$), and to a lesser extent on the type infestation (i.e. with weeds, broomrape, or both, partial $R^2 = 0.067$). In other words, cropping techniques, including crop choice, were more important than the pest community composition (i.e., including weeds and/or broomrape). Although weeds contributed to deplete the broomrape seedbank (section 4.2.4.4.1), this did not affect much yield loss on average compared to cropping techniques.

4.2.4.4.3 Which management techniques drive broomrape-caused yield loss?

Broomrape caused on average 16 % yield losses in oilseed rape and 45% yield losses in sunflower in the reference cropping system (n° 1, Figure 26.C and D), with a high variability in oilseed rape depending on the year and weather repetition (size of boxes in Figure 26, and annex A.3.6.5). Only the cropping system with delayed oilseed rape sowing and mustard catch crop significantly reduced yield losses due to broomrape to almost zero in oilseed rape (n° 3, Figure 26.C). Systems 2 (diversified rotation) and 4 (no plough) also tended to reduce yield loss compared to the reference system, particularly its variability, but this was not significant. In sunflower, the management of which differed little between cropping systems, broomrape-caused yield loss was similar in all systems, though it was lower in system 3 where sunflower was sown after a mustard catch crop (Figure 26.D). The variations in yield loss observed in wheat (Figure 26.B) are entirely due to stochasticity in the simulations as this crop cannot be infected by broomrape.

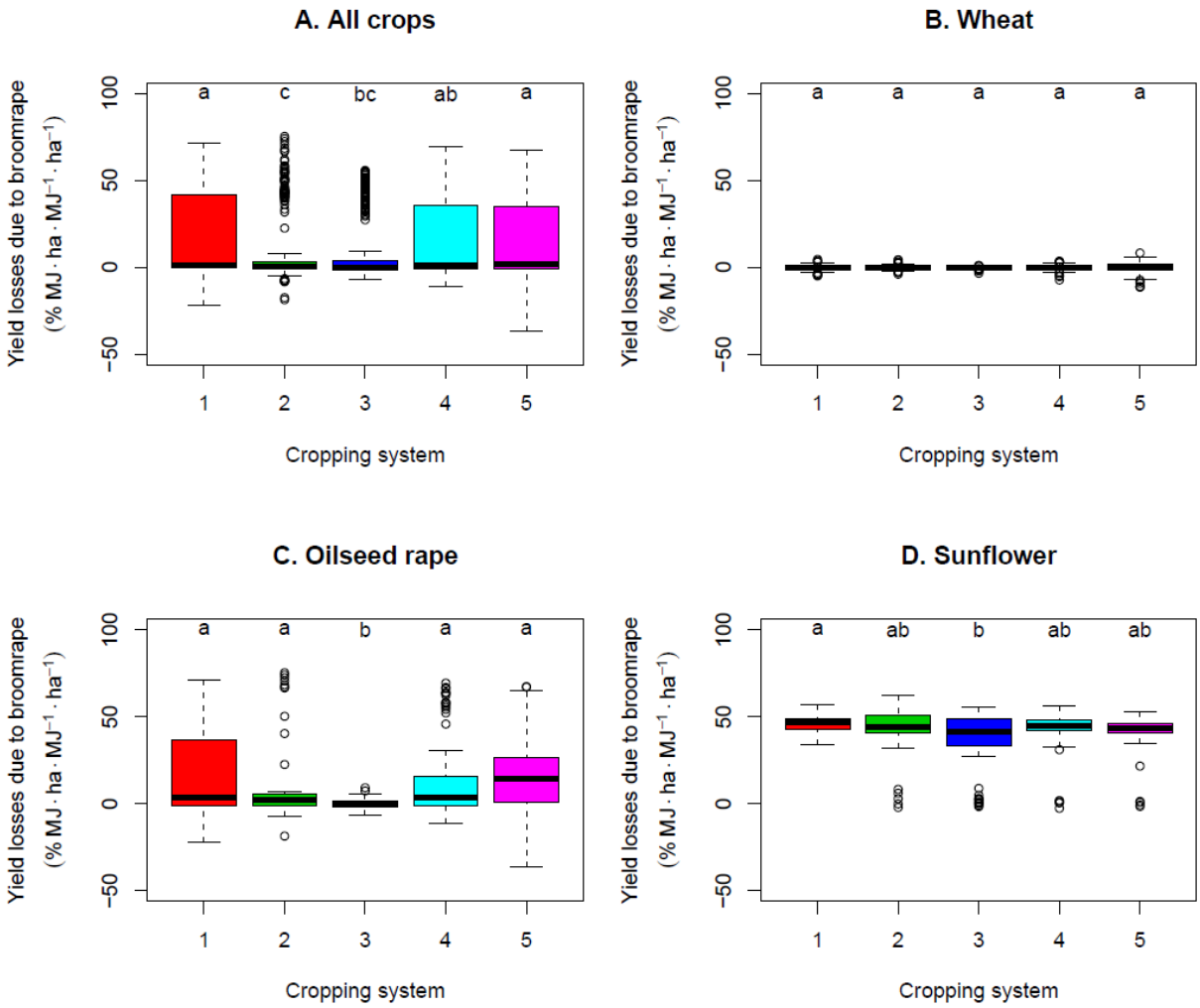

Figure 26: Annual yield losses due to branched broomrape predicted by PHERASYS.2 in each cropping system and crop (simulations without weeds). Cropping systems are 1: reference system, 2: diversified rotation, 3: delayed sowing, 4: no plough and 5: no-till. For details on the cropping systems, see Table 12. Different letters above bars show significant differences in yield losses between cropping systems.

4.2.4.4.4 In which conditions do weeds increase broomrape impacts?

Overall, the combination of weeds and broomrape caused more yield losses than weeds alone (i.e. symbols are significantly above the y=x line in Figure 27.A). Adding broomrape did not change the ranking of the cropping systems in terms of yield loss (i.e. the symbols are placed along a straight line in Figure 27.A). The increase in yield loss caused by adding broomrape was the most important in those cropping systems where weeds already caused large yield losses (i.e. symbols were increasingly above y=x when moving to the right of Figure 27.A).

When doing the opposite, i.e. when adding weeds to broomrape, the cropping system ranking did not change either (i.e. the symbols were again on an approximate straight line in Figure 27.B). However, adding weeds in system 3 with its delayed sowing decreased yield loss compared to a field infested with broomrape only (i.e. blue diamond below the y=x line in Figure 27.B). This was due to weeds inducing broomrape germination year-round (annex A.3.6.2.B) which reduced the final broomrape seed bank by 90% compared to the final seed bank in weed-free simulations (Figure 25 and annex A.3.6.1.B). Conversely, in simplified (system 4) or no till (system 5), adding weeds increased yield

loss tremendously (i.e. triangles above the y=x line), because yield losses due to weeds cancelled out the benefits of broomrape seedbank depletion by weeds (Figure 25 and section A.3.6.1.B).

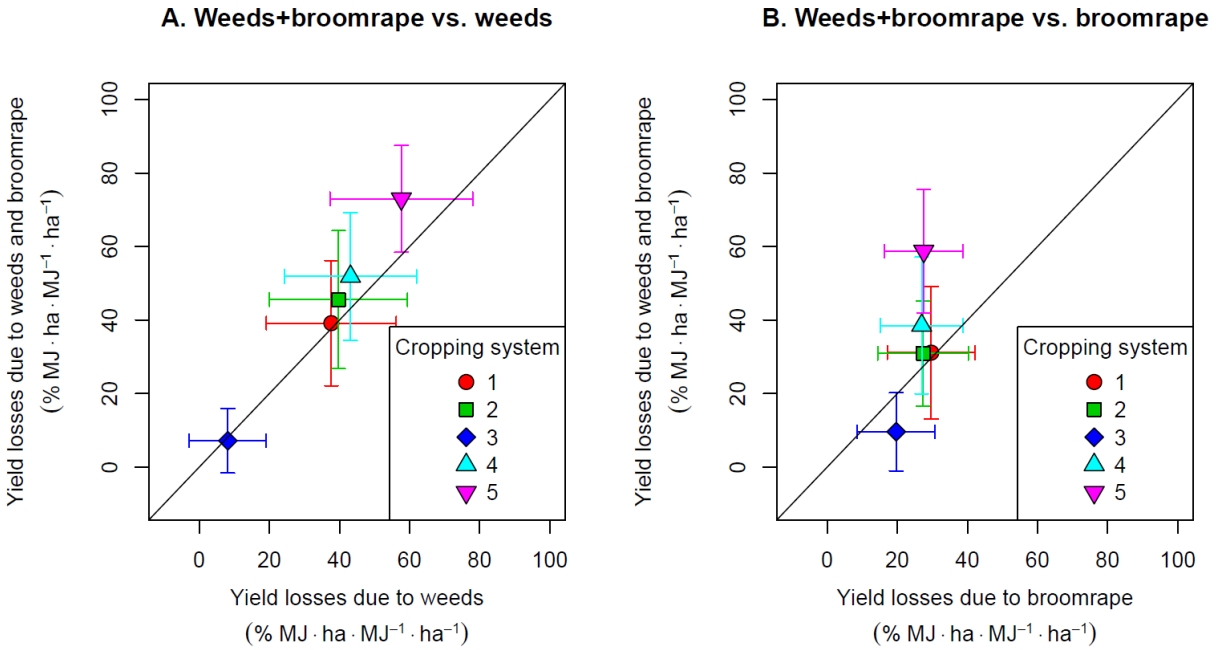

Figure 27: Annual yield losses due to weeds and branched broomrape compared to annual yield losses due to weeds only (A) and broomrape only (B). Each dot represents the mean yield loss averaged over crops, years and weather repetitions for a given cropping system. Cropping systems 1 to 5 refer to 1: reference system, 2: diversified rotation, 3: delayed sowing, 4: no plough and 5: no-till. For details on the cropping systems, see Table 12. Bars show standard deviation.

4.2.5. Discussion

4.2.5.1. Innovations and consistency of PHERASYS.2 with the literature

4.2.5.1.1 The first model of broomrape dynamics specific to branched broomrape…

PHERASYS.2 is the first model of broomrape dynamics in agroecosystems specifically designed and parameterized for branched broomrape. Several formalisms were inspired from other models of broomrape dynamics found in the literature and were adapted to fit the specific nature of branched broomrape. The life-stages chosen as key steps to model broomrape dynamics are basically the same as those included in other models (Schnell *et al.*, 1996; López-Granados and García-Torres, 1997; Eizenberg *et al.*, 2005; Grenz *et al.*, 2005a; Ephrath and Eizenberg, 2010; Pérez-de-Luque *et al.*, 2016). However, dormancy was rarely included in previous models and when it was, this was done very simplistically (i.e., a constant proportion of the seed population was considered to be dormant, López-Granados and García-Torres, 1997; Grenz *et al.*, 2005a), whereas this process is essential for quantifying seed bank dynamics and depends on the season. We modelled dormancy more precisely as two successive phases. First, dormancy relief in fresh seeds depended on temperature, moisture and duration of conditioning. Kebreab and Murdoch (1999) used a similar approach to model both dormancy release and induction of seeds in other broomrape species under laboratory conditions. We preferred using a seasonal model for older seeds, built from a field experiment, more realistic than the latter. This approach was shown to produce satisfactory predictions in non-parasitic weeds (Colbach *et al.*, 2016).

Some PHERASYS.2 formalisms were inspired from the model developed for *O. crenata* (Grenz *et al.*, 2005a), e.g. the calculation of the "stimulating zone" around roots and the estimation of broomrape seed production. Here, we not only estimated parameter values for branched broomrape, we also improved the initial concepts. For instance, we added a dynamic and more realistic approach to the stimulating zone by restricting it to root tips. As Grenz *et al.* (2005a), we found that the number of capsules containing seeds was related to broomrape biomass. From this relationship, we estimated that each broomrape produces 10000 to 55000 seeds, which is at the lower end of the range of 10000 to 500000 seeds found for other broomrape species in the literature across different continents (Grenz *et al.*, 2005a, Turkey; Joel, 2013a; Prider, 2015, Australia). Accordingly, the mean number of seeds per capsule we estimated, 200-300, was lower than the 500-700 seeds generally found in broomrapes, including branched broomrape (Gibot-Leclerc *et al.*, 2012; Joel, 2013a; Prider, 2015). Indeed, because of experimental constraints, our measurements of seeds per capsule only included the closed capsules from the top of the inflorescence, which contain less seeds (Miegel *et al.*, 2013). If future sensitivity analyses demonstrate that this parameter is essential for predicting branched-broomrape dynamics and the resulting yield loss, we will carry out additional measurements with an improved protocol.

We used the well-known concept of thermal time (Bonhomme, 2000) to predict broomrape phenology, which also successfully applied in several other broomrape species (Eizenberg *et al.*, 2005; Eizenberg *et al.*, 2009; Ephrath and Eizenberg, 2010; Eizenberg *et al.*, 2012a; Eizenberg *et al.*, 2012b; Pérez-de-Luque *et al.*, 2016; Hosseini *et al.*, 2017). Using this concept involved assuming that broomrape phenology depends mostly on temperature and not on host phenology. This assumption was supported by observations on *O. crenata* (Manschadi *et al.*, 2001; Grenz *et al.*, 2005b) as well as field observations on branched broomrape (see section 4.2.4.4.1).

4.2.5.1.2 … in interaction with several species of crops and weeds …

The major originality of PHERASYS.2 is that it includes interactions between broomrape and several species of crops and weeds. At present, 70 species are included in the model and its generic structure makes it easy to add new species in the future. Broomrape dynamics models in the literature include generally only one host crop, three to four in a rotation at most (Schnell *et al.*, 1996; Pérez-de-Luque *et al.*, 2016), and no weed species.

We characterized parasite interactions with crops and weeds at the individual host plant level by predicting the number of broomrape germinated seeds, attachments and mature broomrapes as a function of host biomass and root volume. These interactions also depended on the ability of host species to stimulate broomrape germination and to allow attachment. The individual representation of each host plant allowed to model, for the first time, the effects of heterogeneous multispecies stands on broomrape dynamics. For example, our model takes into account the fact that a host plant is infected by more broomrape attachments if it is close to a plant that stimulates numerous broomrape germinations. Conversely, the infection is reduced when host growth is limited by shading neighbouring plants. This is crucial for designing management strategies using biological regulations by either weeds or crop mixtures associating species with complementary functions.

However, our species parameters need to be improved. First, the stimulatory activity of species was estimated from germination tests *in vitro*. It is likely to be different in the fields since seasons (López-Granados and García-Torres, 1996; Fernandez-Aparicio *et al.*, 2014), nutrient availability (Gaudin, 2013) or interactions with microorganisms (Fernández-Aparicio *et al.*, 2010) may influence the specific stimulatory activity of plants. Moreover, data from a close species or from another broomrape pathovar were used to parameterize the stimulatory activity of a species. This assumption is acceptable for *Fabaceae* species (Perronne *et al.*, 2017), but not in the *Brassicaceae* family where similar species induce different responses in branched-broomrape germination which also depend on the broomrape pathovar (Gibot-Leclerc *et al.*, 2016). Even with such proxys, some species known to stimulate branched broomrape could not be parameterized for stimulatory activity (e.g., *Fallopia convolvulus*, Boulet *et al.*, 2007, which was very abundant in our simulations) so they had to be considered as non-

host. Misestimating the stimulatory activity of a species can have very different effects on broomrape dynamics in our model, depending on whether it results in misestimating seed bank depletion due to germination losses rather than broomrape reproduction due to successful germination and attachments. Future sensitivity analyses will be necessary to identify which model parameters should be measured as a priority.

4.2.5.1.3 … and including a submodel for host-parasite trophic relationships

Another innovative aspect of PHERASYS.2 is that interactions between broomrape and host plants are two-ways, i.e. host plants have an effect on broomrape dynamics while parasitism influences host growth. This allows to estimate yield losses due to parasitism and improves the prediction of plant-plant competition for light and other resources in FLORSYS. Broomrape dynamics are also better predicted, via a feedback loop, as host growth and biomass determine broomrape infestation in PHERASYS.2.

Grenz *et al.* (2005a) also combined a demographic submodel and a submodel for host-broomrape trophic relationships as we did here, but on a different broomrape species and with a single host species in homogeneous stands. Grenz's model focused more on within-plant variability on an average host plant ; for instance, parasitism caused abortion of young fruit whereas older more competitive fruit survived. We included little within-plant variability of broomrape effects, only considering that late broomrape attachments rarely survived, in order to focus on between-plant variability, working with a 3D individual-based representation of each host plant. This approach was better adapted to the multispecies nature of FLORSYS and still allows to model the competitive advantage of hosts reproducing early.

Although most formalisms that we proposed to model host-broomrape trophic relationships are new, the concepts involved are supported by the literature (see references in the result section). Some less well-known properties emerged from our work and also found support in the literature. For example, broomrape affects the allocation of resources within host vegetative organs before deriving biomass (Barker *et al.*, 1996), reducing the allocation to roots in the pathosystem (Lins *et al.*, 2007).

However, our formalisms were based on data from only three host species and need to be checked on more species since they may vary between hosts (Fernández-Aparicio *et al.*, 2016a).

4.2.5.2. Agronomic implications

4.2.5.2.1 Promising combinations of cropping techniques for controlling broomrape

The effects of the cropping techniques that we tested by simulation were generally consistent with the literature (Table 14), demonstrating that despite the many simplifications, the model produces realistic predictions. Our simulations showed that cropping techniques must be combined (ex : trap and catch crops aiming to deplete the soil seed bank, with delayed sowing or reduced host crops frequency in the rotation aiming to limit broomrape reproduction) for an efficient control of broomrape in various weather scenarios. These conclusions are only relevant for the context we tested, i.e. typical cropping systems, pedoclimate and weed flora from Western France, and may not be valid in other contexts or cropping systems. This may explain why, contrary to the literature (Fernández-Aparicio et al., 2016), we did not observe any effect of soil tillage on broomrape dynamics. Also, we only partially modelled the mechanisms involved (Table 14).

Table 14: Effects of cropping techniques on branched-broomrape dynamics and crop yield losses in simulations with PHERASYS.2 and consistency with the literature (green cells indicate consistent results, yellow limited consistency)

Cropping technique	**Effects on broomrape and crop yield losses in simulations**	**Consistency of the effects with the literature**	**Consistency of the mechanisms involved with the literature**
Delayed sowing	Fewer broomrape attachments on host crops and less yield loss	Fewer attachments in obligate parasitic plants (Grenz *et al.*, 2005b; Díaz *et al.*, 2006; Gibot-Leclerc *et al.*, 2006; Tippe *et al.*, 2017), but benefits in terms of yield loss can be cancelled out by reduced yield potential (Díaz *et al.*, 2006; Gibot-Leclerc *et al.*, 2006).	Crops grown later grow faster so they are more competitive than broomrapes (Fernández-Aparicio *et al.*, 2016b). Fewer broomrape seeds germinate at crop sowing as they are more dormant later in the season (Tippe *et al.*, 2017).
Trap and catch crops	Seed bank depletion by flax, sunflower (only in case of high infestation) and, to a lesser degree, mustard	Flax and mustard are trap and catch crops (Goldwasser and Rodenburg, 2013); sunflower depletes the broomrape seed bank (Jestin *et al.*, 2014); summer crops and flax deplete more than autumn cover crops (Jestin *et al.*, 2014).	The ability of a plant to stimulate broomrape germination depends on the species emitting them (Fernández-Aparicio *et al.*, 2009; Gibot-Leclerc *et al.*, 2016; Perronne *et al.*, 2017). The longer the crops grow, the bigger their root systems are, the more germination they induce (Grenz *et al.*, 2005a).
			The spring germination flush we predicted in oilseed rape is not systematically observed in the field (Gibot-Leclerc *et al.*, 2012; Gaudin, 2013). The quantity and quality of germination stimulants exudated by plants varies over season (López-Granados and García-Torres, 1996; Auger *et al.*, 2012), not modelled.
	Sunflower slightly infected by broomrape	Sunflower only incidentally allows broomrape to reproduce in the field (Jestin *et al.*, 2014).	Unknown mechanisms
Soil tillage	No effect	Deep tillage reduces the number of broomrape germinated seeds (Fernández-Aparicio *et al.*, 2016b).	Lack of oxygen in deep soil layers prevents broomrape germination (Rubiales *et al.*, 2009), not modelled.
		Reduced tillage can reduce the number of broomrape germinated seeds and attachments (Fernández-Aparicio *et al.*, 2016b).	Prevents seeds from being buried close to host roots where they could be stimulated and attach (Fernández-Aparicio *et al.*, 2016b).
			Volume of host roots in superficial soil layers overestimated by our simplistic representation of root systems, which grow directly from the soil surface instead of from the seed.

4.2.5.2.2 Exploiting interactions between broomrape and weeds

Our simulations showed that weeds helped depleting the broomrape seed bank by inducing germination. Although they sometimes allowed broomrape to reproduce, they mostly played the role of catch plants, as they generally had a shorter life cycle than broomrape so they died before it could reproduce. This effect is highly dependent on the quality of the weed phenology predictions in FLORSYS, which was shown to be deficient at some latitudes (Colbach *et al.*, 2016). This could explain why, in contrast to our simulations, recommendations usually advise to control host weed species as they might relay broomrape infestation in the absence of crop (Gibot-Leclerc *et al.*, 2003; Jestin *et al.*, 2014). Moreover, PHERASYS.2 is still missing some common host species, such as *Aphanes arvensis* (Gibot-Leclerc *et al.*, 2003).

Finally, the catch-crop effect of weeds was only beneficial in terms of crop yield loss when weeds did not compete for light with the crop. Using biological regulations by weeds to control broomrape involves finding the right equilibrium between tolerating a residual weed flora to stimulate broomrape germination, and controlling it to avoid competition with the crop. Dealing with such complex questions shows the utility of simulation models such as PHERASYS.2.

4.2.5.3. Perspectives

The present simulation results are encouraging insofar as they are mostly consistent with literature reports. However, they must still be interpreted carefully since the model has not yet been evaluated with independent field data. A sensitivity analysis will also be run to identify most influential parameters in the model and deduce the ones that need to be measured more precisely and the formalisms that need to be improved. Once the model has been evaluated, a larger set of cropping systems should be simulated in order to track innovative broomrape-management strategies that benefit from biological regulations by weeds. The model could even be used as a decision support system to help designing cropping systems by testing prospective systems and improving them based on simulation results (Colbach *et al.*, 2014a; Colbach *et al.*, 2017b).

More management techniques could be included in the model, such as parasite-tolerant crop varieties, fertilization or biological control with fungi and insects for example. The structure of PHERASYS.2 allows to implement most of their effects quite easily, providing that data for parameterization are available. For example, techniques having a direct toxic effect on broomrape, such as herbicides, could be modelled by eliminating a part of the broomrape population when applied. Indirect effects influencing root exudation, such as fertilization (Fernández-Aparicio *et al.*, 2016b), could be modelled by modulating the stimulatory activity of plants. Other techniques will even be implemented without having to modify PHERASYS.2, benefiting from FLORSYS improvements. For example, as soon as the current implementation of fertilization is finished in FLORSYS (Moreau *et al.*, in prep.), we will be able to simulate complex strategies using fertilization to promote host growth and make it more competitive towards broomrape.

Finally, as suggested above, processes modelled in PHERASYS.2 are quite generic. The same model structure could be used for other pathovars of branched broomrape or other broomrape species, albeit with different parameter values. We started to collect parameter values for the hemp pathovar (Table S 40), which is the second most frequent in France (Terres Inovia, 2018b).

4.2.6. Conclusion

We developed PHERASYS.2, a model of broomrape dynamics in agroecosystems, specifically designed and parameterized for branched broomrape. It allowed, for the first time, to simulate interactions between broomrape and heterogeneous multispecies stands of crops and weeds. It integrates the effects of multiple cropping techniques, including complex ones playing on the competition between broomrapes and hosts for resources. Although the model needs to be evaluated, simulation results point to efficient management strategies consistent with the literature. Combining delayed sowing, which prevents broomrape from reproducing, to the use of trap and catch crops, to deplete the broomrape seed bank, allows to achieve a long-term control of the parasitic plant. Tolerating a residual weed flora, could also help to accelerate the seed bank depletion by stimulating broomrape germination.

4.2.7. Acknowledgements

This project was supported by INRA, the research program APR 2011- Ecophyto 2018 “Assessing and reducing environmental risks from plant protection products” funded by the French Ministries in charge of Ecology and Agriculture, the CoSAC project for designing sustainable weed management strategies in a context of change (climate, cropping practices, biodiversity) funded by the National Agency for Research (ANR-14-CE18-0007), and the IWMPRAISE (“Integrated Weed Management: PRActical Implementation and Solutions for Europe”) project funded by the European Union’s Horizon 2020 research and innovation program (n° 727321). We thank Delphine Molenat and Eric Baraton from Chamber of Agriculture of Vendée and Deux-Sèvres for kindly providing broomrape samples. We gratefully acknowledge Anne-Sophie Voisin, Mae Guinet and Loïc Pagès for transmitting data on species root parameters.

4.3. Quel est l'apport d'un modèle mécaniste par rapport à un simple indicateur de risque pour évaluer l'efficacité des régulations biologiques de *P. ramosa* ?

4.3.1. Objectif

Deux approches différentes ont été développées dans l'équipe pour évaluer l'efficacité des régulations biologiques par les adventices pour lutter contre *P. ramosa* : un modèle mécaniste, PHERASYS.2 (section 4.2), et un indicateur de risque orobanche dû à la flore adventice (Colbach *et al.*, 2017a).

Contrairement à PHERASYS.2, l'indicateur ne simule pas les mécanismes du parasitisme, il traduit la dynamique des adventices prédite par FLORSYS en impact potentiel sur le parasitisme selon le principe développé par Mézière *et al.* (2015). Il approxime la contribution de la flore adventice à relayer ou à réduire l'infestation par *P. ramosa* simplement en fonction de l'abondance d'adventices hôtes et faux-hôtes dans les parcelles, sans prendre en compte la taille du stock de semences parasites.

Afin d'étudier l'intérêt d'utiliser notre modèle complexe PHERASYS.2 par rapport à l'indicateur de risque, plus simple, nous avons comparé les pertes de rendement prédites par PHERASYS.2 aux scores de risque estimés par l'indicateur.

4.3.2. Matériel et méthodes

L'indicateur de risque orobanche est construit selon le principe de (Mézière *et al.*, 2015), c'est-à-dire à partir d'une variable d'état décrivant les adventices pendant une période d'intérêt et en fonction d'un trait d'espèce. Ici, les adventices hôtes et faux-hôtes (trait d'espèce) augmentent ou diminuent le risque d'infection par *P. ramosa* proportionnellement à leur biomasse aérienne (variable d'état) en fonction de la période pendant laquelle elles sont présentes par rapport au cycle de cultures hôtes (période d'intérêt). Trois cas sont distingués sous la forme de trois composantes de l'indicateur (Table 15.A) : 1) les adventices capables de stimuler les germinations de *P. ramosa* diminuent le risque pour les futures cultures en vidant le stock de semences parasites du sol, 2) sauf en culture hôte où elles augmentent le risque d'infection immédiat de la culture, et 3) les adventices hôtes augmentent le risque pour les futures cultures lorsqu'elles arrivent à maturité car elles permettent à la plante parasite de se reproduire. Chaque composante est calculée lors de chaque cycle cultural en sommant les biomasses aériennes quotidiennes des adventices concernées sur la période d'intérêt, puis les trois composantes sont sommées avec des pondérations pour obtenir l'indicateur de risque orobanche final (Table 15.B).

Les différents jeux de simulations avec adventices et/ou *P. ramosa* lancés dans la première partie de ce chapitre (section 4.2, Table 16) ont été utilisés pour comparer les prédictions de PHERASYS.2 aux prédictions de l'indicateur de risque orobanche. L'indicateur a été calculé à partir des simulations avec adventices uniquement (sans *P. ramosa*, Table 16). Etant donné que l'indicateur ne prend pas en compte l'effet direct du parasitisme sur la production agricole, mais uniquement le risque d'infection via les adventices, il n'était pas pertinent de le comparer aux pertes de rendements causées par *P. ramosa*. Nous avons calculé les pertes de rendement supplémentaires induites par les adventices en cas d'infestation par *P. ramosa* (voir explications dans la Table 16), qui reflètent l'effet des adventices sur le parasitisme, afin de les comparer aux prédictions de l'indicateur.

Table 15 : Conceptualisation et équations de l'indicateur de risque orobanche via les adventices traduisant des variables de dynamique des adventices prédites par FLORSYS en scores illustrant le risque d'infestation de la parcelle par *Phelipanche ramosa* via les adventices (Colbach *et al.*, 2017a).

A. Composantes de l'indicateur

	Composante	Variable d'état des adventices W_{spd}	Période d'intérêt	Trait d'espèce T_s
[1]	Stimulation totale de germinations parasites $I_{depletion}$	Biomasse aérienne de la plante p de l'espèce s le jour d, la plante p étant à un stade < début de floraison	d ∈ [$Récolte_{année\ y-1}$, $récolte_{année\ y}$]	Capacité à stimuler les germinations de l'orobanche (oui, non)
[2]	Stimulation de germinations parasites en culture hôte $I_{in\_crop\_germ}$	Biomasse aérienne de la plante p de l'espèce s le jour d, la plante p étant à un stade < début de floraison	d ∈ [$Semis_{année\ y}$, $récolte_{année\ y}$], si la culture est une espèce hôte	Capacité à stimuler les germinations de l'orobanche (oui, non)
[3]	Reproduction de l'orobanche I_{repro}	Biomasse aérienne de la plante p de l'espèce s le jour d à la mort de la plante si la plante est à un stade , la plante p étant à un stade > début de maturité	d ∈ [$Récolte_{année\ y-1}$, $récolte_{année\ y}$]	Hôte (oui, non)

B. Equations

	Echelle temporelle	Echelle de risque		Equation
[4]	Jour	Composante	I_d =	$\sum_s \left(T_s \cdot \sum_p (log_{10}(W_{sp} + 0.0001) + 4)\right)$
[5]	Cycle cultural	Composante	$I_{depletion}$ =	$(\sum_{d=récolte_{y-1}}^{récolte_y} I_{d\ total\ stim})$ / $(\sum_{d=récolte_{y-1}}^{récolte_y} 1)$
[6]	Cycle cultural	Composante	$I_{in\_crop\_germ}$ =	$(\sum_{d=semis_y}^{récolte_y} I_{d\ crop\ stim})$ / $(\sum_{d=semis_y}^{récolte_y} 1)$
[7]	Cycle cultural	Composante	I_{repro} =	$\sum_{d=récolte_{y-1}}^{récolte_y} I_{d\ repro}$
[8]	Cycle cultural	Totale	$I_{parasite}$ =	$\alpha \cdot I_{depletion} + \beta \cdot I_{in\_crop\_germ} + \gamma \cdot I_{depletion} \cdot I_{repro}$, avec α = -0.25, β = 0.50 et γ = 0.75

Table 16 : Jeux de simulations (voir détails dans la section 4.2) utilisés pour comparer l'indicateur de risque orobanche et aux pertes de rendement dues à *Phelipanche ramosa* et aux adventices prédites par PHERASYS.2.

Jeu de simulations	Avec *P. ramosa*	Avec adventices
a)		✓
b)	✓	
c)	✓	✓
d)		

← Indicateur de risque orobanche dû aux adventices

Pertes de rendement dues à *P. ramosa* (PR1)

Pertes de rendement dues à *P. ramosa* et aux adventices (PR2)

Pertes de rendement supplémentaires induites par les adventices en cas d'infestation par *P. ramosa* : PR3 = PR2-PR1

Des corrélations de Pearson ont été calculées avec la fonction cor.test de R (R Core Team, 2019) entre les prédictions de l'indicateur et celles de PHERASYS.2 à deux échelles : 1) à l'échelle de la culture, en utilisant les prédictions en cultures hôtes uniquement (pour l'indicateur, seule la composante $I_{in\_crop\_germ}$ a été analysée car elle estime le risque immédiat pour la culture), et 2) à l'échelle de la rotation, en moyennant les prédictions sur les 30 ans de simulations, toutes cultures confondues, pour chaque système de culture simulé et chaque répétition climatique.

4.3.3. Résultats

L'indicateur de risque orobanche est positivement corrélé aux prédictions de PHERASYS.2, à la fois à l'échelle de la culture (coefficient de corrélation de Pearson = 0.25, $p<0.0001$) et en particulier à l'échelle de la rotation où la corrélation est plus forte (coefficient de corrélation de Pearson = 0.60, $p<0.0001$), mais ne dépasse toutefois pas 60%. L'indicateur et PHERASYS.2 classent les systèmes de culture dans le même ordre, ce qui signifie que l'un comme l'autre peuvent être utilisés pour comparer les systèmes entre eux (ex : c'est dans le système 5 que les adventices contribuent le plus à accroître les dégâts causés par *P. ramosa*, à l'inverse du système 3 où elles réduisent même les dégâts, Figure 28). Cependant, l'indicateur semble surestimer le risque orobanche dans le système sans travail du sol par rapport aux dégâts réels calculés d'après PHERASYS.2, en particulier à l'échelle de la culture (le point correspondant au système 5 semble décalé par rapport aux autres points, plus alignés, sur la Figure 28).

Les simulations permettant de calculer l'indicateur étaient 15 fois plus rapides en moyenne que les simulations avec PHERASYS.2.

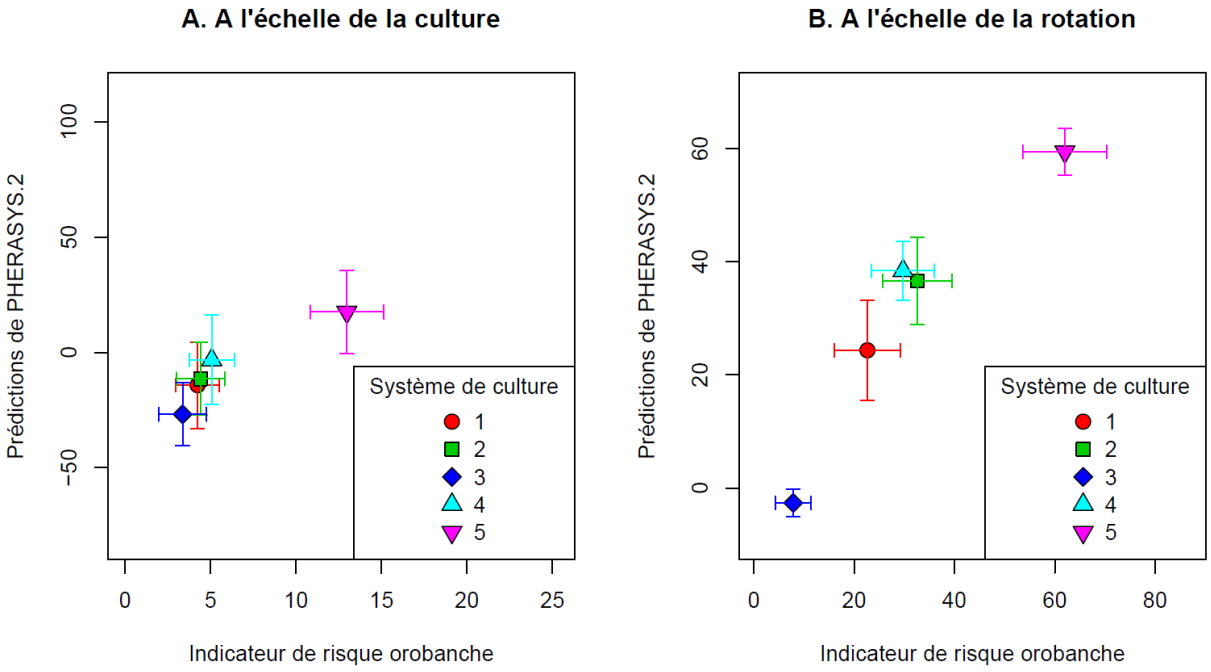

Figure 28 : Comparaison des prédictions de PHERASYS.2 (pertes de rendement supplémentaires induites par les adventices en cas d'infestation par *Phelipanche ramosa*, en % MJ·ha·MJ^{-1}·ha^{-1}) et de l'indicateur de risque orobanche dû aux adventices, à l'échelle de la culture (A, prédictions annuelles à la récolte des cultures hôtes) et de la rotation (B, prédictions moyennées sur 30 ans de simulation). Chaque point représente la moyenne des données par système de culture (moyenne sur les répétitions climatiques, et, pour la figure A, sur les cultures et les années simulées). Les systèmes de culture 1 à 5 correspondent à 1 : système de référence, 2 : rotation diversifiée, 3 : semis tardif, 4 : non labour et 5 : sans travail du sol. Ces systèmes sont détaillés dans la Table 12. Les barres représentent les écart-types.

4.3.4. Discussion

Les prédictions de l'indicateur de risque orobanche et de PHERASYS.2 sont cohérentes, ce qui donne une certaine crédibilité à l'indicateur, alors que ce dernier n'a pas pu être évalué par rapport à des observations de terrain. En effet, l'indicateur donne des résultats similaires à ceux obtenus avec un modèle mécaniste plus complexe et plus proche des processus.

Cependant, les prédictions de l'indicateur et de PHERASYS.2 ne convergent pas totalement, en particulier à l'échelle de la culture en cas de forte infestation par les adventices (c'est-à-dire dans le système sans travail du sol, voir section 4.2.4.4.4). Cela est probablement dû au fait que l'indicateur sous-estime le rôle de plantes pièges des adventices, ressorti comme un effet majeur dans les simulations avec PHERASYS.2 où il a pu être modélisé plus précisément (voir section 4.2.4.4.4). L'indicateur considère que les adventices infectées permettent systématiquement à *P. ramosa* de se reproduire lorsqu'elles arrivent à maturité, tandis que dans PHERASYS.2, les adventices à cycle-court ne laissent pas le temps à la plante parasite de se reproduire. En outre, à l'échelle de la culture, l'indicateur considère que toutes les germinations de *P. ramosa* stimulées par les adventices risquent de se fixer sur la culture, sans tenir compte des distances entre adventices et cultures et des fixations sur les adventices potentiellement plantes pièges (d'où les divergences avec PHERASYS.2 à l'échelle de la culture). Enfin, l'indicateur calcule un risque chaque année sans tenir compte du niveau d'infestation de la parcelle par *P. ramosa* l'année précédente, contrairement à PHERASYS.2 qui simule la dynamique du stock semencier parasite. Cela pourrait expliquer pourquoi l'indicateur surestime le risque orobanche dans le système de culture où les adventices sont très abondantes, car les erreurs d'estimation de l'indicateur s'accumulent d'autant plus au fil des années que l'infestation par les adventices s'accroît.

Malgré cela, l'indicateur de risque orobanche peut être utilisé pour comparer les systèmes de cultures entre eux et présente l'avantage de donner des prédictions plus rapidement que PHERASYS.2. En revanche, l'indicateur ne peut se substituer à PHERASYS.2 car il ne prédit pas les effets directs des techniques culturales sur *P. ramosa*, ce qui est indispensable pour développer une stratégie de gestion globale de *P. ramosa* et des adventices. En outre, à l'inverse de PHERASYS.2, l'indicateur n'intègre pas l'effet du parasitisme sur les cultures et sur les adventices. Il est donc incapable de prédire les pertes de rendement réelles dues au parasitisme, qui constituent un critère plus parlant et concret pour évaluer la performance des systèmes de culture que les scores donnés par l'indicateur. Par ailleurs, grâce à PHERASYS.2, nous avons pu étudier l'influence du parasitisme sur la communauté adventice, ce qui a rarement été étudié. Contrairement à ce qui est observé avec d'autres plantes parasites en milieux naturels (Press and Phoenix, 2005), le parasitisme par *P. ramosa* ne favorise pas les espèces non-hôtes, en tuant ou réduisant la biomasse des espèces hôtes (résultats non montrés). PHERASYS.2 apporte donc une plus-value par rapport à l'indicateur d'un point de vue agronomique, pour évaluer l'efficacité des techniques culturales contre à la fois l'orobanche et les adventices, et d'un point de vue écologique, pour étudier l'influence du parasitisme sur les communautés végétales.

4.3.5. Conclusion

Les deux approches comparées ici peuvent toutes deux être utilisées pour estimer la contribution des adventices à l'infestation par *P. ramosa* et leur potentiel de régulation biologique. Cependant, elles ne visent pas tout-à-fait les mêmes utilisations.

L'indicateur est plus simple et plus rapide d'utilisation que le modèle mécaniste PHERASYS.2, mais donne des prédictions moins précises, il ne prédit qu'un risque potentiel et ne tient pas compte des effets cumulatifs des adventices sur le parasitisme au fil des années. Il est adapté dans les cas où le niveau d'infestation de la parcelle est inconnu, par exemple dans les zones où *P. ramosa* n'est pas encore présente mais pourrait potentiellement se développer, à proximité de zones infestées, pour savoir s'il vaut mieux désherber rigoureusement pour ne pas risquer de relayer l'infestation.

En revanche, si *P. ramosa* est un problème majeur et connu dans une parcelle et que l'utilisateur cherche précisément à lutter contre la plante parasite, le modèle PHERASYS.2 devrait être utilisé pour explorer tous les leviers de gestions possibles, à la fois les techniques culturales et les régulations biologiques par les adventices, et évaluer l'échelle de temps nécessaire pour y parvenir.

4.4. Conclusion du chapitre et perspectives

Dans ce chapitre, les objectifs de la thèse ont été atteints puisque nous avons pu modéliser le cycle de vie complet de *P. ramosa* dans PHERASYS.2 et sa dynamique à long-terme dans les agroécosystèmes grâce à un couplage avec les modèles FLORSYS et RSCone. Cela nous a permis de tester diverses stratégies de gestion de *P. ramosa* par simulations et d'évaluer leurs efficacités.

La cohérence des résultats de simulation avec les effets des techniques reportés dans la littérature indique que le modèle est relativement fiable et peut être utilisé dans le contexte testé (Poitou-Charentes). Cependant, il doit être évalué, en confrontant ses prédictions à des observations de terrain, et peut-être amélioré car il est le reflet des connaissances actuelles sur *P. ramosa* et sur les agroécosystèmes de manière générale. Les conditions d'utilisation du modèle ainsi que ses limites et perspectives d'amélioration sont discutées dans le chapitre suivant (Chapitre 5, discussion générale de la thèse). Nous y abordons également les perspectives d'utilisation de notre modèle dans un cadre plus large que cette thèse, pour étudier la dynamique des communautés végétales, aussi bien dans les agroécosystèmes que dans les milieux naturels.

Chapitre 5. Discussion générale

Ce travail de thèse a permis de modéliser la dynamique de *Phelipanche ramosa* dans les agroécosystèmes en vue de mieux comprendre comment la gérer. Nous avons pour cela synthétisé les connaissances de la littérature, mis en place des expérimentations et couplé trois modèles, deux existants simulant les effets des systèmes de cultures sur la dynamique des adventices et la croissance racinaire, et un entièrement développé au cours de cette thèse simulant la dynamique de *P. ramosa*. Les apports méthodologiques et de connaissances de ce travail, ainsi que ses limites, sont discutés dans les sections suivantes, afin de comprendre à quelles fins et sous quelles conditions le modèle peut être utilisé.

5.1. Apports et originalité de la méthodologie employée

5.1.1. La modélisation au centre d'une approche pluridisciplinaire

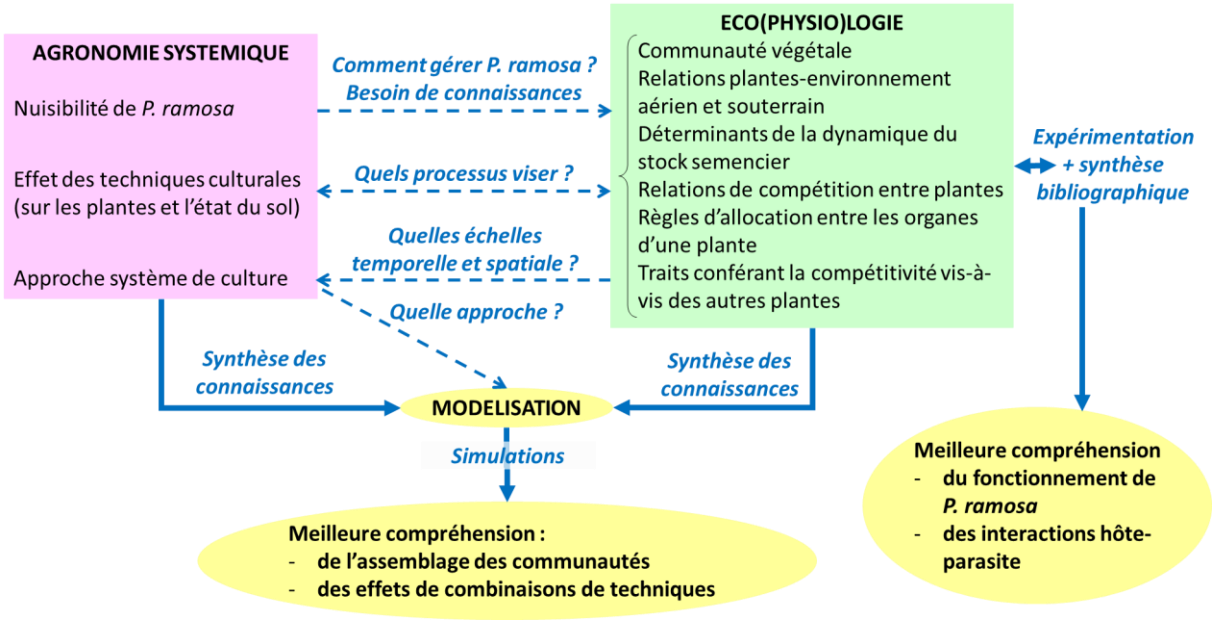

Figure 29 : Liens entre les disciplines mobilisées au cours de la thèse via le développement d'un modèle, pour comprendre comment concevoir une gestion agroécologique de *Phelipanche ramosa*. Les cadres montrent les concepts et connaissances mobilisés dans les différentes disciplines. L'approche suivie est indiquée par les flèches et mots en italiques bleus, avec la problématique illustrée par les flèches en pointillé et les méthodes employées par les flèches épaisses. Les cadres jaunes montrent les objectifs et connaissances nouvelles acquises à l'issue de la thèse, développés dans les sections 5.2 et 5.3.

Afin de répondre à une problématique agronomique, « comment gérer *P. ramosa* ? », ce travail de thèse illustre comment combiner différentes disciplines et approches grâce à la modélisation (Figure 29). Nous avons construit un modèle mobilisant des connaissances de l'agronomie systémique[8] et de

[8]Agronomie systémique : « Manière de faire l'agronomie » qui « vise à prendre en charge la question de la gestion des champs cultivés dans leur globalité » (Doré and Meynard, 2006). Voir les définitions de « agronomie » et « système de culture ».

l'écophysiologie[9] des plantes cultivées, adventices et parasites. Grâce à cette approche pluridisciplinaire, nous avons rassemblé pour la première fois les connaissances sur l'ensemble du cycle de vie de *P. ramosa* et caractérisé ses interactions avec la communauté végétale complexe des parcelles agricoles, ce qui n'avait jamais été fait auparavant, pour aucune espèce d'orobanche (section 1.2.2, Chapitre 1).

Tout d'abord, le questionnement à l'origine de ce travail de thèse est le résultat d'allers-retours entre les deux disciplines (voir Chapitre 1). Etudier la nuisibilité de *P. ramosa* pour la production agricole afin de mieux comprendre comment la gérer (de l'agronomie vers l'écophysiologie, section 1.1.1) nous a amenées à chercher les connaissances disponibles sur l'écophysiologie de la plante parasite. Ces connaissances ont mis en évidence les lacunes à combler et les processus clés à viser par les méthodes de luttes (de l'écophysiologie vers l'agronomie, section 1.1.2.7). Suite à cela, les techniques de lutte disponibles pour lutter contre *P. ramosa* ont été recensées, indiquant les processus écophysiologiques à étudier en priorité (section 1.1.3). Ces processus ont défini les échelles temporelle et spatiale à considérer pour raisonner la gestion de *P. ramosa*, c'est-à-dire l'échelle du système de culture (agronomie systémique, section 1.1.3.4).

Cette échelle nous a conduit à choisir l'approche de la modélisation pour répondre à la problématique et a imposé la structure du modèle à développer (mécaniste, échelle parcelle, échelle pluriannuelle et plante-centré) (section 1.2.1). Le modèle a été construit en synthétisant des connaissances de l'agronomie systémique (sur l'effet des techniques) et de l'écophysiologie végétale (sur les interactions plante-environnement, plante-plante, hôte-parasite, etc.), à partir de la littérature, de modèles existants et d'expérimentations. Nous avons modélisé l'effet des techniques culturales sur les processus écophysiologiques impliqués dans les relations plantes-environnement aussi bien au niveau aérien que souterrain (ex : effet du travail du sol sur la croissance racinaire via la structure du sol, Chapitre 3), dans les relations de compétition entre plantes (ex : effet de la date de semis sur la précocité de l'hôte par rapport à *P. ramosa*, Chapitre 4), dans les règles d'allocation de ressources entre les organes d'une plante (ex : calcul des pertes de rendement dues au parasitisme, Chapitre 4), et dans la dynamique du stock semencier des adventices et de *P. ramosa* (ex : effet des cultures en fonction de leur fréquence dans la rotation par rapport à la mortalité des semences de *P. ramosa*, Chapitre 2).

A l'issue de ce travail de modélisation, nous avons dû reprendre un point de vue agronomique pour choisir les variables à analyser en sortie de notre modèle afin de répondre à notre problématique de départ. Nous avons analysé des variables quantifiant les dégâts causés par *P. ramosa* selon deux approches, en calculant les dégâts potentiels (densité de longueur racinaire comme proxy du risque d'infection par *P. ramosa*, Chapitre 3, indicateur de risque orobanche, Chapitre 4) et effectifs (pertes de rendement dues au parasitisme, Chapitre 4). Dans la première approche, nous avons mobilisé le concept de trait, emprunté à l'écologie, pour approximer les dégâts causés par *P. ramosa* (ex : densité de longueur racinaire dans le Chapitre 3).

Finalement, ce travail de thèse a produit des connaissances nouvelles dans chaque discipline lors de la construction du modèle et à l'issue de simulations. Nous avons construit un outil permettant de mieux comprendre l'assemblage des communautés végétales et l'écophysiologie de *P. ramosa* (section 5.2). Au niveau agronomique, cet outil est utile pour comprendre et prédire l'effet de multiples techniques culturales en interaction sur une flore complexe composée d'adventices et de plantes parasites, et d'estimer les pertes de rendement dues à cette flore grâce à des simulations (section 5.3).

[9]Ecophysiologie : « Branche de l'écologie qui a pour objet d'analyser le fonctionnement de l'organisme individuel dans le cadre des contraintes que lui impose son milieu, afin de comprendre son adaptation à ces contraintes et de déterminer sa capacité à survivre lorsqu'elles changent » (Encyclopédie Universalis). Elle est également une sous-discipline de l'agronomie (voir la définition d'« agronomie »).

5.1.2. Des formalismes génériques extrapolables

Le caractère mécaniste de notre modèle FLORSYS-RSCone-PHERASYS.2, basé sur une représentation de processus biophysiques, lui confère une grande généricité. Certains de nos formalismes peuvent donc être adaptés pour d'autres études.

Notre modèle est l'un des rares permettant d'étudier la dynamique de couverts hétérogènes, en prenant en compte de multiples espèces et leurs relations de compétition pour les ressources (ex : pour la lumière) et des pressions biotiques (ex : parasitisme) (Gaudio *et al.*, 2019) (section 1.2.3, Chapitre 1). Bien que nous nous soyons focalisées sur les relations entre cultures et adventices annuelles, notre modèle est valable pour tout type de couverts végétaux hétérogènes composés de plantes annuelles, tels que les mélanges de variétés ou d'espèces de cultures par exemple (voir section 5.3.2) et, dans une moindre mesure, les communautés végétales en milieux peu anthropisés (section 5.2.2).

Le modèle a été construit et paramétré pour un pathovar particulier de *P. ramosa* mais sa structure est suffisamment générique pour l'adapter à d'autres pathovars de *P. ramosa* et même d'autres plantes parasites racinaires obligatoires de la famille des Orobanchaceae, après avoir ajusté le paramétrage et éventuellement quelques formalismes (voir la conclusion, section 2.2, du Chapitre 2). En effet, ceux-ci partagent les mêmes stades de développement clés (germination, fixation, croissance au dépend de l'hôte jusqu'à production de semences) (Joel, 2013b). D'ailleurs, nous avons déjà commencé à collecter les paramètres pour une population apparentée au pathovar du chanvre de *P. ramosa* (voir Chapitre 4). L'ajustement serait plus facile pour les espèces dont la gamme d'hôte est restreinte, puisque peu de plantes hôtes sont à paramétrer. C'est le cas par exemple de l'espèce *O. cumana*, orobanche spécifique du tournesol (Parker, 2013), pour laquelle aucun modèle de dynamique complet n'a été développé (section 1.2.2, Chapitre 1). L'adaptation du modèle PHERASYS.2 aux plantes hémiparasites (ex : espèces du genre *Striga*, dont certaines sont des bioagresseur majeurs des céréales en Afrique, Parker, 2013) est plus complexe car, contrairement aux holoparasites telles que *P. ramos*a, elles sont capables d'effectuer la photosynthèse. Par conséquent, notre modèle de relations trophiques avec les hôtes n'est pas adapté (Heide-Jørgensen, 2013; Joel, 2013b). Cela est d'autant plus vrai pour les hémiparasites facultatives qui n'ont pas besoin de stimulation par des exsudats racinaires pour germer (Yoneyama *et al.*, 2013) et qui peuvent croître jusqu'à émergence en absence d'hôte (ex : *Ramphicarpa fistulosa*, une autre espèce causant des dégâts en cultures de céréales en Afrique, Parker, 2013).

Certains de nos formalismes peuvent être utilisés pour étudier d'autres composantes biotiques des agroécosystèmes que les plantes. Par exemple, il existe des similitudes entre la biologie de *P. ramosa* et certains champignons pathogènes du sol tels que le piétin échaudage (*Gaeumannomyces graminis* (Sacc.) Arx and Olivier var. *tritici* Walker.), une maladie des céréales (Cook, 2003) qui affecte et peut être transmise par des adventices (Dulout *et al.*, 1997; Gutteridge *et al.*, 2006). En l'absence d'hôte, le champignon survit dans le sol sur les résidus de cultures pendant un an ou deux, et attaque les racines de ses hôtes à condition qu'elles soient suffisamment proches (<1 cm, Gilligan, 1980), ce qui rappelle la persistance des semences d'orobanches dans le stock semencier du sol et leur germination à proximité des racines hôtes. Les formalismes que nous avons utilisés pour calculer le volume de fixation de *P. ramosa* autour des racines (Chapitre 4) peuvent donc servir à étudier la dynamique d'infection du piétin échaudage, pour évaluer le rôle des adventices dans la transmission du champignon par exemple. De la même façon, ces formalismes peuvent contribuer à l'étude de la dynamique de colonisation des racines par des champignons bénéfiques, tels que les mycorhizes arbusculaires, dont les spores germent à proximité des racines de leurs hôtes, stimulés par leurs exsudats racinaires (Gadkar *et al.*, 2001).

Dans ce dernier cas, nos valeurs de paramètres quantifiant la capacité des espèces à stimuler les germinations de *P. ramosa* peuvent même être directement utilisées puisque les orobanches exploitent

les mêmes signaux que les mycorhizes pour reconnaître leurs hôtes (Yoneyama *et al.*, 2013). Ces paramètres peuvent également servir à estimer l'efficacité de différentes cultures pour la pratique de la biofumigation, qui consiste à contrôler les bioagresseurs du sol en cultivant ou en incorporant dans le sol des cultures produisant des composés biocides (Kirkegaard and Sarwar, 1998), car ces composés induisent aussi la germination de *P. ramosa* (Auger *et al.*, 2012). Comme différentes molécules sont impliquées dans la communication avec les mycorhizes et dans la biofumigation (strigolactones et isothiocyanates respectivement), il est d'abord nécessaire de caractériser pour chaque espèce paramétrée dans notre modèle, quelles molécules confèrent l'activité stimulatrice que nous avons quantifiée.

Inversement, les connaissances acquises sur les autres organismes ou processus mentionnés ci-dessus peuvent servir à améliorer notre modèle, et y être intégrées facilement grâce à sa structure mécaniste. Par exemple, notre modèle de dynamique d'infection des racines par *P. ramosa* (Chapitre 4) est inspiré d'un modèle de dynamique d'une autre espèce d'orobanche (*O. crenata*, Grenz *et al.*, 2005a).

5.1.3. Apports d'un modèle mécaniste pour aider à simplifier la représentation d'un système complexe

La généricité qu'apporte l'approche mécaniste confère à PHERASYS.2 une grande complexité, et le rend plus difficile à utiliser du fait du grand nombre de paramètres et d'entrées à fournir. En revanche, l'intérêt de cette complexité est qu'elle permet d'intégrer un maximum de processus pour ensuite hiérarchiser leurs effets et développer des modèles plus simples à partir des processus les plus influents (Colbach, 2010). C'est de cette façon qu'a été construit le modèle RSCone à partir du modèle ArchiSimple (Pagès *et al.*, submitted)(voir section 1.2.4, Chapitre 1), ou encore qu'un outil d'aide à la décision a été développé à partir de FLORSYS par Colas (2018) pour en faciliter l'utilisation. Cette démarche n'a cependant jamais été effectuée pour étudier les processus majeurs déterminant la dynamique des orobanches (section 1.2.2, Chapitre 1).

Dans ce travail de thèse, nous avons illustré les premières étapes d'une boucle d'amélioration continuelle d'un modèle, incluant une étape de simplification d'un modèle complexe. Nous avons 1) complété les lacunes d'un modèle existant pour produire un modèle plus complexe afin de 2) hiérachiser les effets des processus modélisés et identifier des pistes de simplification de ce modèle complexe en ne gardant que les processus fondamentaux, avant de 3) mettre en évidence de nouvelles lacunes dans notre modèle, etc. Nous avons utilisé le modèle préliminaire PHERASYS (section 1.2.2, Chapitre 1), faisant état des connaissances sur la dynamique de *P. ramosa* et permettant d'identifier les connaissances manquantes, afin de développer PHERASYS.2 sur la base d'une toute nouvelle structure. Grâce aux simulations avec PHERASYS.2, nous avons identifié les processus essentiels à modéliser pour représenter la dynamique de *P. ramosa*, et déduit ceux pour lesquels l'effort de modélisation peut être moindre. Par exemple, en étudiant l'influence des paramètres dans le couplage de FLORSYS avec RSCone, nous avons pu déterminer que, dans le contexte testé (voir sections 5.4.2 et 5.4.3), les règles d'allocation de biomasse dans les plantes entre leur partie aérienne et racinaire sont plus déterminantes pour l'exploration racinaire que la structure du sol (Chapitre 3). En simulant différentes stratégies de gestion des orobanches, nous avons montré que, parmi les quelques techniques testées, le semis tardif et l'implantation de cultures pièges et faux-hôtes, sont les techniques les plus influentes sur la dynamique de *P. ramosa*, alors que le travail du sol a peu d'effet (Chapitre 4). Enfin, nous avons mis en évidence de nouvelles lacunes à combler afin d'améliorer PHERASYS.2 dans le futur (voir section 5.4.4).

Par ailleurs, nous avons montré que les prédictions d'un modèle complexe peuvent être utilisées pour évaluer les prédictions de modèles plus simples. Nous avons ainsi évalué l'indicateur de risque orobanche dû aux adventices, calculé simplement d'après la biomasse des adventices (Colbach *et al.*, 2017a), en le comparant aux prédictions de PHERASYS.2 (section 4.3, Chapitre 4), alors qu'il aurait été difficile de mesurer les variables nécessaires pour l'évaluation au champ. Dans un travail précédent,

d'autres indicateurs ont été développés à partir des sorties de FLORSYS pour estimer la nuisibilité et les services écosystémiques apportés par les adventices (Mézière *et al.*, 2015). Cette approche peut être employée pour construire des indicateurs supplémentaires à partir des sorties de PHERASYS.2, pour évaluer le rôle des adventices dans la colonisation par les mycorhizes ou l'efficacité de couverts pour la biofumigation par exemple (voir section 5.1.2).

5.2. Des connaissances nouvelles sur la dynamique des communautés végétales

Ce travail de thèse a conduit au développement d'un modèle permettant de mieux comprendre la dynamique de communautés végétales complexes comprenant des plantes parasites et non parasites dans les agroécosystèmes (Figure 30). Des connaissances nouvelles ont été acquises sur l'écophysiologie de *P. ramosa* (section 5.2.1), et sur l'assemblage des communautés végétales (section 5.2.2).

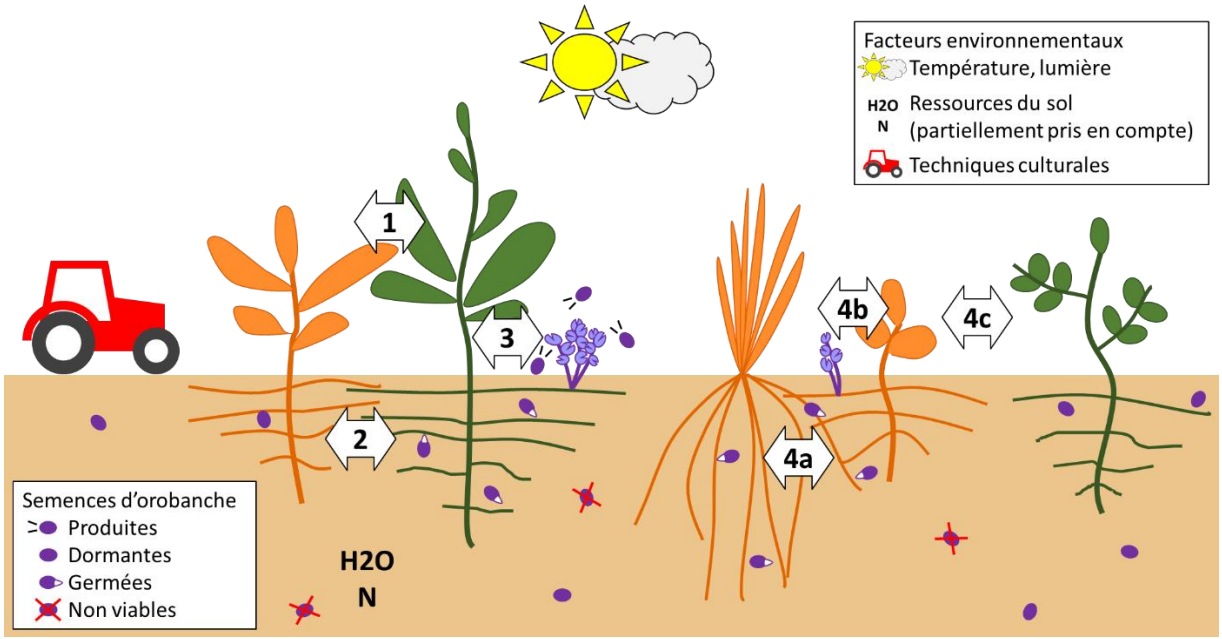

Figure 30 : Interactions entre plantes et facteurs environnementaux pris en compte dans le couplage FLORSYS-RSCone-PHERASYS.2 développé au cours de la thèse, et connaissances nouvelles acquises sur l'écophysiologie de *Phelipanche ramosa* par expérimentation (mortalité, dormance, germination et production de semences). Les cultures sont représentées en vert, les adventices en orange et *P. ramosa* en violet. Les flèches numérotées indiquent différents types d'interactions entre plantes, 1 : compétition pour la lumière, 2 : compétition pour les ressources du sol (partiellement intégré), 3 : parasitisme. Les flèches 4 donnent un exemple d'interaction entre plusieurs plantes pour illustrer l'effet complexe de la communauté adventice et parasite sur les cultures, 4a : une adventice faux-hôte favorise l'infection d'une adventice hôte à proximité en stimulant des germinations de *P. ramosa*, 4b : cette dernière voit sa croissance réduite par le parasitisme, 4c : et exerce donc moins de compétition vis-à-vis de la culture voisine.

5.2.1. Des connaissances nouvelles sur l'écophysiologie de *P. ramosa*

Grâce à la mise en place d'expérimentations, nous avons acquis des connaissances sur la dormance, la mortalité (Chapitre 2) et la production de semences au champ de *P. ramosa* (Chapitre 4), connaissances qui sont relativement rares chez les plantes parasites de manière générale (section 1.1.2, Chapitre 1). Nous avons également mis en évidence la nécessité de considérer l'échelle intraspécifique des pathovars.

Pour la première fois, nous avons observé des différences de comportement notables entre deux populations d'une même espèce de plante parasite dans le processus de dormance (Chapitre 2). L'observation de germinations spontanées en l'absence de plante hôte stimulatrice chez l'une de nos populations est un résultat très original, qui nécessite toutefois d'être confirmé par des analyses complémentaires. Il amène à s'interroger sur l'absolue nécessité pour une plante parasite obligatoire d'être stimulée par les exsudats racinaires d'un hôte. Est-ce que germer spontanément peut constituer une stratégie opportuniste? De nouvelles populations de *P. ramosa* ont été mises en évidence récemment (Stojanova *et al.*, 2019), il est possible que parmi celles-ci certaines présentent des comportements inédits. La population que nous avons étudiée semble adopter un comportement intermédiaire entre celui d'une plante hémiparasite facultative, dont les semences germent sans nécessiter de stimulation par des exsudats racinaires (Yoneyama *et al.*, 2013), et celui d'une plante holoparasite obligatoire, catégorie à laquelle elle appartient car elle est incapable d'effectuer la photosynthèse.

En construisant PHERASYS.2 (Chapitre 4), nous avons rassemblé les connaissances disponibles sur toutes les parties du cycle de vie de *P. ramosa*, ce qui n'avait jamais été fait auparavant (section 1.2.2, Chapitre 1), c'est-à-dire sur les déterminants de la dynamique de son stock semencier, sa phénologie, ses relations trophiques avec ses hôtes (à la fois l'effet du parasitisme sur les hôtes et l'effet des hôtes sur la plante parasite). De nouvelles connaissances sur les interactions entre *P. ramosa* et les autres plantes, que nous avions identifiées comme cruciales à acquérir (section 1.2.2.1, Chapitre 1), ont émergé de cette synthèse. Nous avons établi la liste des espèces cultivées et adventices hôtes et faux-hôtes de *P. ramosa* en distinguant les pathovars. Nous avons explicité, avec des formalismes nouveaux et simples, l'hypothèse générale que les orobanches fixées à leurs hôtes se comportent comme des organes supplémentaires exerçant une compétition pour les ressources principalement avec le compartiment reproducteur (Manschadi *et al.*, 2001; Grenz *et al.*, 2008; Fernández-Aparicio *et al.*, 2016a). Nous avons modélisé les relations trophiques entre *P. ramosa* et ses hôtes en adaptant les relations d'allométrie entre les compartiments des plantes (ex : relation entre biomasse racinaire et totale, entre biomasse foliaire et aérienne… Weiner, 2004) et en considérant que les orobanches fixées se substituent à tout ou partie du compartiment reproducteur.

Enfin, en effectuant des simulations avec FLORSYS-RSCone-PHERASYS.2 (Chapitre 4), nous avons identifié que la durée de cycle de vie de *P. ramosa* est un déterminant majeur de sa dynamique à long-terme dans les agroécosystèmes (*P. ramosa* ne peut se reproduire que sur des hôtes ayant une durée de vie suffisamment longue), alors que certains auteurs considèrent que la plante parasite est capable de s'adapter à la durée de vie de ses hôtes (voir discussion section 5.4.4).

5.2.2. Un outil pour comprendre l'assemblage des communautés

Le modèle résultant du couplage FLORSYS-RSCone-PHERASYS.2 réalisé dans cette thèse est utile pour comprendre comment se structurent les communautés végétales car il prend en compte à la fois la compétition entre plantes pour les ressources (lumière, eau et nutriments, ces deux derniers étant en cours d'intégration, Moreau *et al.*, in prep.) et les relations de parasitisme (Figure 30). Sa représentation individu-centrée, sur le modèle de FLORSYS, permet de simuler des interactions complexes impliquant plusieurs plantes, comme par exemple une adventice A, qui favorise le

parasitisme sur une adventice B voisine, réduit indirectement la compétition qu'exerce cette dernière sur la culture (« moins × moins = plus », exemple 4 sur la Figure 30). Ce type d'interactions semble jouer un rôle prépondérant dans les communautés adventices, comme nous le suggérons dans le Chapitre 3 à la lecture des faibles corrélations des analyses RLQ. Cela avait également déjà été observé dans des études de simulations précédentes (Colbach *et al.*, 2017a) et sur le terrain dans les milieux peu anthropisés (ex : une plante parasite régule une espèce hôte invasive qui exerce une forte compétition avec la communauté végétale native, Prider *et al.*, 2009).

Nos simulations ont déjà permis d'apporter des connaissances originales sur la dynamique des plantes parasites dans les communautés végétales. De manière générale, les relations entre plantes parasites et non-parasites au sein des communautés végétales ont été relativement peu étudiées, particulièrement pour les plantes parasites obligatoires (Cameron and Phoenix, 2013). Dans le Chapitre 4, nous avons montré que la communauté adventice peut diminuer l'infestation de la parcelle par *P. ramosa* plus ou moins efficacement en fonction de sa composition. En revanche, dans le contexte floristique testé, nous n'avons pas observé d'effet du parasitisme sur la communauté adventice, que ce soit en terme de composition ou d'abondance, contrairement à ce qui peut être observé dans les milieux peu anthropisés où les plantes parasites modifient la structure des communautés (Cameron and Phoenix, 2013). Des résultats similaires ont été obtenus pour le piétin échaudage par d'autres travaux de simulations, montrant que le champignon n'affecte pas la dynamique pluriannuelle de l'adventice *Alopecurus myosuroides* (Mézière *et al.*, 2013).

Nos simulations ont également apporté des connaissances sur les relations de compétition entre plantes, justifiant l'importance de considérer l'échelle plante entière (parties aériennes et racinaires). En effet dans le Chapitre 3, l'exploration racinaire des adventices s'est montrée plus fortement influencée par les caractéristiques morphologiques aériennes des plantes que par leurs caractéristiques racinaires (en l'absence de stress lié à l'indisponibilité des ressources du sol, voir section 5.4.1). Par exemple, les espèces ayant un système racinaire de faible envergure et de faible biomasse étaient celles qui occupaient pourtant le sol le plus densément car leurs caractéristiques aériennes (ex : forte surface foliaire initiale) leur permettaient de s'imposer dans la communauté végétale en colonisant rapidement la surface du sol (Liebman and Gallandt, 1997; Colbach *et al.*, 2019).

5.3. Contributions pour la gestion agroécologique des adventices et des plantes parasites

5.3.1. Un outil pour le diagnostic, l'expérimentation virtuelle et la conception de systèmes de culture

Le modèle complexe FLORSYS-RSCone-PHERASYS.2 issu de cette thèse constitue un outil de diagnostic des systèmes de culture car il permet d'évaluer leurs performances, d'identifier les systèmes les plus à risque et de comprendre les déterminants techniques des risques en décortiquant les effets des facteurs en interaction grâce à sa structure mécaniste (voir section 1.2.1). Cela est particulièrement utile pour la gestion de *P. ramosa* puisque (1) de multiples techniques de lutte doivent être combinées (Rubiales and Fernández-Aparicio, 2012), comme le confirment nos simulations (ex : l'emploi de cultures pièges ou faux-hôtes n'est efficace qu'en combinaison avec des techniques réduisant la fréquence de reproduction de *P. ramosa*, Chapitre 4) et que (2) la variabilité due aux interactions entre facteurs peut être telle au champ qu'il est difficile de conclure sur les performances de combinaisons de techniques par expérimentation (ex : effets très variables de combinaisons de différentes dates de semis et modalités d'apport d'engrais sur *P. ramosa*, www.terresinovia.fr/-/en-savoir-plus-sur-l-orobanche-rameuse).

Le Chapitre 4 donne un exemple de diagnostic réalisé avec FLORSYS-RSCone-PHERASYS.2. Nous avons calculé les pertes de rendement dues à *P. ramosa* en comparant la production agricole dans des parcelles infestées et non infestées, ce qui est laborieux voire impossible au champ. En réalisant des simulations dans différents scenarii climatiques, nous avons estimé à la fois des pertes de rendement moyennes et une gamme de variabilité traduisant le risque que les systèmes soient peu performants en fonction des années. En analysant des variables intermédiaires difficiles à mesurer au champ, par exemple la dynamique du stock semencier parasite et du nombre d'orobanches à maturité, nous avons mis en évidence que le semis précoce est une technique à risque car elle permet la reproduction de plusieurs cohortes de *P. ramosa* par an. Ce type de diagnostic devra être complété à plus large échelle, comme cela a été effectué pour les adventices dans des systèmes de culture sur tout le territoire français (Colbach and Cordeau, 2018), pour identifier un maximum de techniques à risque en fonction des situations de production (section 5.4.3). Cela permettra en outre de produire des références réalistes sur les pertes de rendement causées par *P. ramosa* en France, alors que la littérature donne seulement des valeurs extrêmes (90-100%, Gibot-Leclerc *et al.*, 2012; Jestin, 2017), pourtant anecdotiques (X. Pinochet, communication personnelle).

Outre la possibilité d'évaluer des systèmes existants, notre modèle permet également de tester des systèmes prospectifs, c'est-à-dire de faire de l'expérimentation virtuelle. L'avantage par rapport à l'expérimentation au champ est que cela permet d'explorer une très large gamme de systèmes, y compris des systèmes très innovants difficiles à mettre en place au champ à cause de verrous sociologiques (Colas, 2018). En outre, les systèmes peuvent être rapidement évalués sur plusieurs décennies (ex : 30 années simulées en moins de 3h dans le Chapitre 4).

Grâce à ces avantages, l'expérimentation virtuelle peut être employée pour concevoir des systèmes de culture, comme cela a été fait dans d'autres travaux avec FLORSYS et l'outil d'aide à la décision dérivé DECIFLORSYS (Colbach *et al.*, submitted). Par exemple, le diagnostic à partir de simulations de systèmes de cultures existants (comme décrit ci-dessus) peut servir de base pour proposer des améliorations et tester les systèmes résultant virtuellement (Figure 31.B) (Colbach *et al.*, 2017b). Le même type de démarche peut être adopté lors d'ateliers de co-conception avec des agriculteurs, où les systèmes pratiqués par les agriculteurs servent de base à améliorer, et les systèmes proposés par le groupe sont simulés en direct puis discutés et améliorés consécutivement (Figure 31.C) (Colas, 2018; Van Inghelandt *et al.*, 2019). Cette démarche d'implication des acteurs est fondamentale pour favoriser l'adoption de pratiques innovantes (Guichard *et al.*, 2017). Une autre approche consiste à concevoir des systèmes de culture par optimisation informatique, c'est-à-dire que l'ordinateur améliore des modalités techniques (ex : date de semis) itérativement par rapport à un objectif donné (ex : réduire les pertes de rendement dues aux adventices, Figure 31.A) (Bergez *et al.*, 2010; Maillot *et al.*, 2019). Cette méthode permet d'explorer un gamme plus large de systèmes de cultures mais implique peu les acteurs.

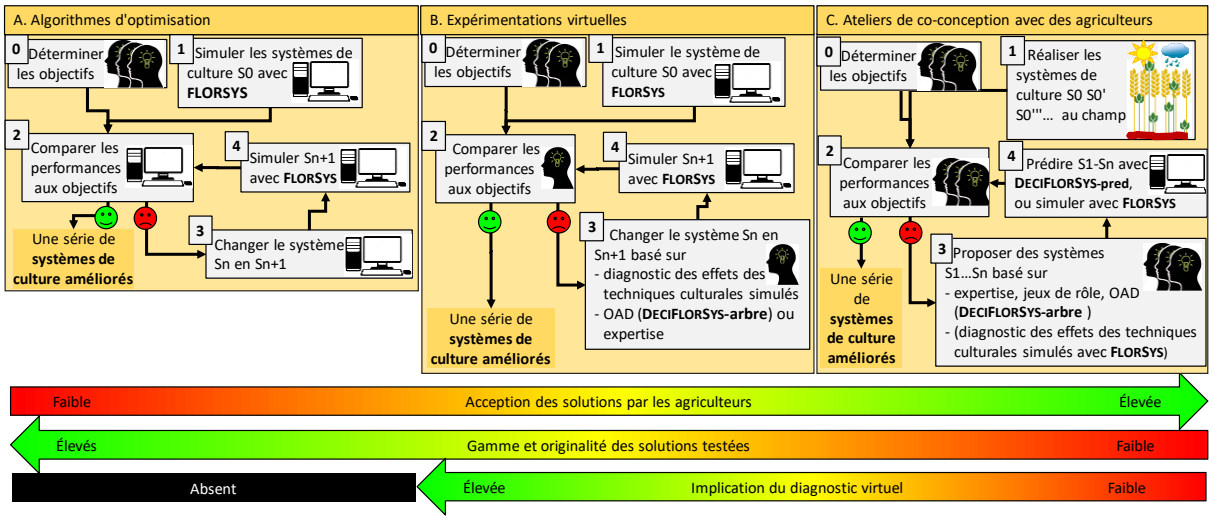

Figure 31 : Trois méthodes d'utilisation de FLORSYS pour concevoir des systèmes de culture innovants via une amélioration pas-à-pas d'un système de culture initial S0. A. Les algorithmes d'optimisation gèrent toutes les étapes en interaction avec FLORSYS, à l'exception des objectifs et contraintes des nouveaux systèmes qui sont déterminés par un groupe d'experts. B. Dans le cas d'expérimentations virtuelles, les experts fixent les objectifs et contraintes, comparent les performances simulées des systèmes à ces objectifs et proposent des innovations, suite à un diagnostic des variables d'état simulées par FLORSYS, de l'expertise et de l'arbre de décision de DECIFLORSYS. C. Les ateliers de co-conception avec les agriculteurs démarrent souvent avec un ou plusieurs systèmes défaillants sur le terrain ; des innovations sont proposées par un groupe d'agriculteurs et d'autres experts utilisant une variété d'outils (dont éventuellement du diagnostic sur base de simulations FLORSYS) et ces systèmes sont évalués en direct par le calculateur de DECIFLORSYS, ce qui peut déclencher un nouveau tour de re-conception (Nathalie Colbach © 2019) (Colbach *et al.*, submitted).

5.3.2. Un outil pour la recherche d'idéoptypes de cultures

L'approche développée dans le Chapitre 3 illustre comment le modèle FLORSYS-RSCone peut être utilisé pour rechercher des idéotypes, c'est-à-dire des plantes idéales théoriques combinant des caractéristiques optimisant leurs performances dans un contexte de production donné (Martre *et al.*, 2015). Cette utilisation présente un intérêt pour la sélection variétale, en particulier dans le cas de *P. ramosa*, car aucune variété de colza résistante n'a été mise au point à ce jour malgré les efforts de recherche (Fernández-Aparicio *et al.*, 2016b). Par exemple, nous avons montré que des cultures moins vigoureuses (c'est-à-dire à faible envergure et vitesse de croissance au niveau aérien et racinaire) pourraient être moins infectées par *P. ramosa*. Cependant, ce résultat ne prend pas en compte les mécanismes du parasitisme, tels que l'avantage compétitif qu'ont les plantes vigoureuses par rapport à *P. ramosa* une fois que celle-ci est fixée (Chapitre 4). L'approche développée dans le Chapitre 3 devra donc être appliquée au modèle complet incluant PHERASYS.2. Cet exemple illustre la complexité des relations entre caractéristiques et performances des plantes, et souligne l'intérêt des modèles mécanistes pour prendre en compte des processus complexes en interaction.

Avec le modèle FLORSYS-RSCone-PHERASYS.2, il est également possible de simuler des variétés virtuelles (c'est-à-dire avec un paramétrage décrivant une combinaison fictive de caractéristiques), ce qui permet de tester une vaste gamme de caractéristiques pour traquer des idéotypes correspondant à différentes situations de production et combinaisons d'objectifs (ex : faibles pertes de rendement dues

à l'orobanche et faible usage d'herbicides). Cela peut être réalisé soit par analyse de sensibilité[10] parmi de nombreuses variétés virtuelles renseignées par l'utilisateur (voir section 5.4.2) (Martre *et al.*, 2015), soit par amélioration automatique pas-à-pas en partant d'une variété décrite en entrée avec des algorithmes d'optimisation (voir section 5.3.1).

Comme notre modèle FLORSYS-RSCone-PHERASYS.2 est capable de prendre en compte les interactions entre plantes dans les communautés végétales (section 5.2.2), il peut également être utile pour aider à concevoir des mélanges de variétés ou d'espèces de cultures, un levier de gestion prometteur de l'agroécologie (Gaudio *et al.*, 2019). L'approche que nous avons développée dans le Chapitre 3 (ex : recherche de caractéristiques qui minimisent le volume racinaire entrecoupé par différentes espèces) peut être adaptée pour identifier des espèces « compatibles » avec des architectures racinaires explorant différentes niches, comme cela a été étudié par expérimentation par Tardy *et al.* (2017). L'avantage de notre modèle par rapport à l'expérimentation est qu'il permet de simuler un grand nombre de mélanges d'espèces ou de variétés, y compris des idéotypes virtuels, et d'étudier leur dynamique en réponse aux changements d'environnement au cours du temps à un pas de temps journalier.

5.3.3. Rôle des adventices dans la transmission de *P. ramosa*

Bien que les interactions entre plantes parasites et non-parasites dans les communautés végétales aient été étudiées sur le terrain (Cameron and Phoenix, 2013), et que des espèces faux-hôtes de *P. ramosa* aient été identifiés parmi les adventices (Gibot-Leclerc *et al.*, 2003), aucune étude à notre connaissance ne s'est intéressée à l'utilisation des communautés végétales pour lutter contre les plantes parasites. Seulement l'inverse, c'est-à-dire utiliser une plante parasite pour réguler les communautés végétales, a été envisagé (Prider *et al.*, 2009).

Les adventices sont généralement considérées comme de potentiels relais de l'infestation de *P. ramosa* qu'il faut désherber rigoureusement (Jestin, 2017). Nos simulations ont montré au contraire que les adventices peuvent aider à gérer *P. ramosa* dans certaines conditions, en stimulant d'abondantes germinations suicides (Chapitre 4). Ce résultat, à condition qu'il soit confirmé après évaluation du modèle FLORSYS-RSCone-PHERASYS.2 (section 5.4.2), amène à reconsidérer la perception traditionnelle des adventices comme organismes uniquement nuisibles. Il ajoute un exemple aux services écosystémiques déjà connus que les adventices peuvent rendre (ex : ressources pour les pollinisateurs, Petit *et al.*, 2011).

L'effet des adventices dans nos simulations dépendait cependant de la flore résiduelle laissée par les différents systèmes de culture, réduisant plus ou moins l'infestation par *P. ramosa*. Ces résultats étaient de plus conditionnés par l'état actuel des connaissances sur la flore adventice (ex : des adventices ont dues être considérées comme non-hôte par manque d'information). Cela montre que développer une gestion agroécologique des bioagresseurs est complexe et requiert des outils adaptés et modulables pour intégrer les connaissances nouvelles à mesures qu'elles sont acquises, tels que le modèle que nous avons développé.

[10] Analyse de sensibilité : Etude de l'influence de différentes sources de variabilité dans les entrées d'un modèle sur la variabilité dans les sorties du modèle (Saltelli et al., 2008a).

5.4. Limites et perspectives

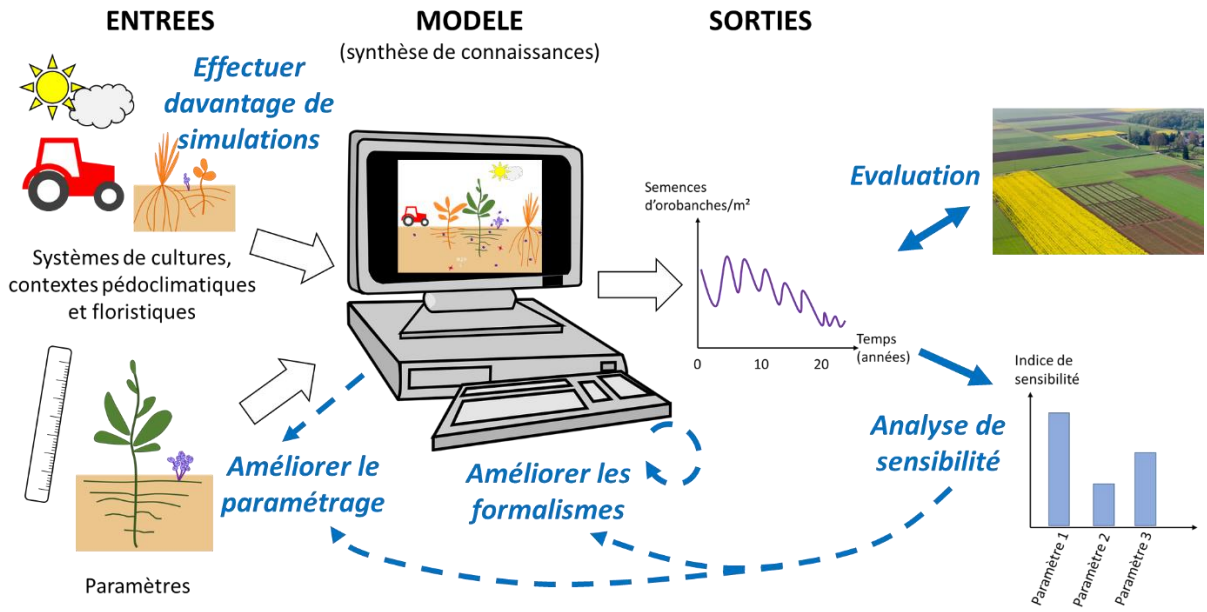

Figure 32 : Perspectives d'amélioration du modèle FLORSYS-RSCone-PHERASYS.2 issu de cette thèse (en bleu) au niveau des entrées et des formalismes implémentés dans le modèle. Les flèches en pointillés montrent comment les améliorations à apporter ont été identifiées (par synthèse des connaissances dans le modèle et par analyse de sensibilité). Source de la photo : www.dijon.inra.fr/Les-Unites/Domaine-experimental.

5.4.1. Le prélèvement racinaire n'est pas encore modélisé

Nous avons présenté notre modèle FLORSYS-RSCone-PHERASYS.2 comme l'un des rares à caractériser les relations de compétition entre plantes dans les couverts hétérogènes et plurispécifique aussi bien au niveau aérien que racinaire (section 5.2.2). En fait, cette conclusion anticipe les travaux en cours dans l'équipe visant à intégrer le prélèvement de ressources par les racines dans le modèle (Moreau *et al.*, 2018; Moreau *et al.*, in prep.). Pour l'instant, le modèle ne prend en compte que la compétition pour la lumière et le parasitisme. Si la lumière a longtemps été considérée comme la source de compétition majeure entre plantes dans les agroécosystèmes intensifs en conditions tempérées (Wilson, 1988a), de récentes études réfutent cette hypothèse et soulignent l'importance de la compétition pour les ressources du sol (Kiær *et al.*, 2013), notamment dans un contexte de réduction d'intrants et de changement climatique. Les analyses du Chapitre 3 visant à identifier les caractéristiques impliquées dans la compétition pour les ressources devront donc être reconduites une fois la fonction de prélèvement racinaire intégrée dans le modèle. En favorisant la croissance des plantes stimulatrices et/ou supportant les fixations de *P. ramosa*, le prélèvement de ressources pourrait augmenter la probabilité d'infection par la plante parasite par exemple.

5.4.2. Le modèle doit être évalué ("validé")

Le modèle FLORSYS-RSCone-PHERASYS.2 issu de cette thèse a été partiellement évalué (uniquement sur la partie non parasite et aérienne des plantes, Chapitre 3) et s'est montré capable de prédire la dynamique des adventices et la production agricole de manière satisfaisante sur 13 ans dans le contexte pédoclimatique et floristique de la Bourgogne. L'évaluation sur d'autres contextes est en cours. Cependant, la qualité de prédiction de la partie parasitisme reste à évaluer. Des données

récoltées dans des essais et dans des parcelles d'agriculteurs par l'institut technique Terres Inovia pourront être utilisées pour cette évaluation (X. Pinochet, communication personnelle), en comparant par exemple le nombre d'orobanches observées à différentes dates dans les parcelles au nombre d'orobanches émergées prédit par le modèle. Nous savons déjà que, pour l'instant, notre modèle n'est pas utilisable dans les systèmes de culture très dépendants d'intrants de synthèse car il ne simule pas les effets de la fertilisation et des herbicides sur *P. ramosa* (seulement l'effet indirect des herbicides via les hôtes est modélisé, Chapitre 4).

Une analyse de sensibilité du modèle FLORSYS-RSCone-PHERASYS.2 devra être conduite pour évaluer l'influence des paramètres du modèle sur les sorties et déduire quels processus doivent être améliorés et quelles connaissances doivent être acquises pour cela. Nous avons amorcé ce travail sur le modèle FLORSYS-RSCone dans le Chapitre 3 (ex : nous avons montré que la structure du sol a peu d'effet sur l'exploration racinaire, et donc qu'il n'était pas nécessaire d'améliorer le formalisme connectant la structure du sol prédite par FLORSYS à l'effet simulé dans RSCone), mais nous n'avons simulé que quelques systèmes de cultures (voir section 5.4.3) avec des valeurs de paramètres réalistes et sans prendre en compte le modèle de parasitisme PHERASYS.2. L'effet de quelques paramètres pressentis comme particulièrement influents (ex : durée de vie de *P. ramosa,* voir section 5.4.4) pourra être testé dans des systèmes de culture simplifiés (ex : une culture et l'itinéraire technique associé, avec une adventice dans un contexte pédoclimatique et floristique une année donnée) par les méthodes d'analyse de sensibilité classiques. La méthode LHS (Latin Hypercube Sampling) pourra être employée pour définir un plan de simulation (les valeurs possibles des différents paramètres et contextes considérés sont combinées aléatoirement, Saltelli *et al.*, 2008a) et des indices de Sobol pour quantifier l'effet des entrées (Saltelli, 2002). En revanche ces méthodes ne sont pas adaptées pour étudier l'influence de l'ensemble des entrées du modèle FLORSYS-RSCone-PHERASYS.2 sur les sorties, car trop de combinaisons d'entrées sont possibles. Les plans de simulation et méthodes d'analyses proposées par Colas (2018) pourront être utilisés pour cela (systèmes de culture existants et aléatoires pour couvrir une large gamme de situations et analyse de forêts aléatoires pour identifier les entrées les plus influentes).

5.4.3. Davantage de simulations doivent être réalisées

Les quelques simulations réalisées dans cette thèse ont servi à illustrer les potentialités du modèle FLORSYS-RSCone-PHERASYS.2. Seulement 15 systèmes de cultures et deux contextes pédoclimatiques (Bourgogne et Poitou-Charentes) ont été simulés. Davantage de systèmes et de contextes doivent donc être simulés pour évaluer le domaine de validité des conclusions obtenues dans cette thèse.

Nous disposons d'une base de données de plus de 900 systèmes de cultures couvrant tout le territoire métropolitain Français et une région d'Espagne, correspondant à des systèmes pratiqués par des agriculteurs, des essais ou des systèmes construits par des experts (Colbach and Cordeau, 2018; Colbach *et al.*, in prep.). Simuler ces systèmes avec le complexe FLORSYS-RSCone-PHERASYS.2 permettrait de prospecter des combinaisons de techniques efficaces et adaptées à chaque situation de production pour lutter contre *P. ramosa* et les adventices, et de s'en servir comme base à améliorer pour proposer des systèmes de culture innovants (voir section 5.3.1).

5.4.4. Pistes de recherche sur la biologie de *P. ramosa* à explorer

En synthétisant des connaissances scientifiques pour construire notre modèle FLORSYS-RSCone-PHERASYS.2, nous avons identifié des pistes de recherche à explorer.

Tout d'abord, le comportement de *P. ramosa* doit être mieux caractérisé à l'échelle intraspécifique. Aucune étude ne compare la production de semences ou les relations trophiques hôte-parasite entre différents pathovars par exemple, alors que des différences existent probablement puisque le poids des semences varie du simple au double en fonction de la population étudiée (Chapitre 4, annex A.3.1).

Nos résultats du Chapitre 2 contribuent à mieux connaître la variabilité intraspécifique de *P. ramosa* dans les processus de mortalité, dormance et de germination des semences et ont montré un fort effet de la population génétique, mais seulement deux populations ont été étudiées. Davantage de populations doivent être testées dans différents lieux pour caractériser les comportements des pathovars.

L'observation inédite de germinations spontanées massives invite à mieux comprendre le processus de germination au champ, en relation avec les caractéristiques physico-chimiques du sol et les microorganismes (voir discussion du Chapitre 2), d'autant que les mycorhizes par exemple peuvent réguler l'infection par les orobanches (Louarn *et al.*, 2012). Les tests de germination sont généralement réalisés au laboratoire sur papier filtre ou gel d'agar, avec des stimulants synthétiques ou des extraits de plantes, et après désinfection des semences (ex : Goldwasser and Yoder, 2001; Fernández-Aparicio *et al.*, 2009; Gibot-Leclerc *et al.*, 2012; Stojanova *et al.*, 2019), mais peu d'études testent des extraits de sol. L'une de ces dernières a révélé que différentes molécules stimulent la germination de *P. ramosa* au laboratoire et dans le sol, possiblement à cause de processus de dégradation par les microorganismes du sol (Auger *et al.*, 2012).

En paramétrant PHERASYS.2 (Chapitre 4), nous nous sommes également rendus compte qu'il nous manquait des informations sur la gamme d'hôtes des différents pathovars. Par exemple, le statut du tournesol, culture de diversification commune, est confus (hôte occasionnel dans des conditions non définies, Jestin *et al.*, 2014). Nous n'avons pas pu trouver de données pour quantifier l'activité stimulatrice de toutes les espèces cultivées et adventices communément trouvées dans les parcelles agricoles sur les populations françaises de *P. ramosa*, en particulier pour les céréales. Ces dernières sont généralement considérées comme non-hôtes (Parker, 2013), alors que certaines sont capable de stimuler des germinations de *P. ramosa* sans permettre de fixations viables au laboratoire (S. Gibot-Leclerc, communication personnelle). Ces céréales pourraient servir de faux-hôtes d'autant plus efficaces que leurs racines occupent densément le sol (Chapitre 3). Les effets de facilitation entre plantes, récemment découverts (Gibot-Leclerc *et al.*, 2013a), n'ont pas non plus pu être intégrés dans le modèle.

L'une des hypothèses fortes de PHERASYS.2 est que la durée du cycle de vie du pathovar modélisé est fixe et indépendante de l'hôte (de l'espèce et de sa vitesse de croissance, Chapitre 4). Bien que cette hypothèse soit soutenue par la littérature (Manschadi *et al.*, 2001; Grenz *et al.*, 2005b; Gibot-Leclerc *et al.*, 2013b; Stojanova *et al.*, 2019), d'autres auteurs considèrent que *P. ramosa* est capable de synchroniser son cycle avec celui de son hôte, sans préciser cependant de quel pathovar il s'agit (Jestin *et al.*, 2014). Notre hypothèse a une forte influence dans notre modèle car elle implique que *P. ramosa* ne peut pas se reproduire sur des plantes hôtes à cycle court. Si elle est fausse, le modèle sous-estime largement l'infection de la parcelle, notamment via les adventices (car les adventices jouent le rôle de plantes pièges du fait de leur cycle court, Chapitre 4). Cette hypothèse est difficile à confirmer car aucune expérimentation de co-culture hôte-parasite n'est conduite jusqu'à reproduction du pathovar colza. De même, nous avons fait l'hypothèse que *P. ramosa* meurt dès que son hôte meurt alors qu'en réalité, les orobanches peuvent continuer à murir après avoir été arrachées à leur hôte (Goldwasser and Rodenburg, 2013). Nous n'avons pu modéliser ce phénomène car les conditions dans lesquelles il se produit n'ont jamais été décrites finement (ex : à partir de quel stade des orobanches ?). Il est donc crucial d'étudier plus précisément les déterminants de la durée du cycle de vie de *P. ramosa*.

Outre les lacunes dans les connaissances propres au parasitisme, nous avons identifié des processus mal connus pour les plantes en général. Par exemple, nous avons modélisé la dynamique de *P. ramosa* à l'échelle de la parcelle, négligeant la dispersion à plus large échelle (section 1.2.1, Chapitre 1). En reprenant les formalismes développés dans FLORSYS pour les plantes non parasites, nous avons la possibilité de modéliser la dispersion des semences via le vent et l'eau en renseignant la hauteur moyenne des orobanches et le poids de leurs semences (Colbach *et al.*, 2018). Les mécanismes majeurs de dispersion, c'est-à-dire via les activités humaines (Goldwasser and Rodenburg, 2013)

restent cependant difficiles à modéliser (Auffret *et al.*, 2014). Par ailleurs, nous avons modélisé l'effet limitant de la compaction du sol sur la croissance racinaire (Chapitre 3), mais n'avons pas pu intégrer l'effet inverse, c'est-à-dire l'ameublissement du sol par l'enracinement, car les mécanismes impliqués sont encore mal connus (Chen and Weil, 2010). Enfin, nous avons montré que l'allocation de biomasse aux racines est plastique en fonction de la disponibilité en nutriments du sol et que cette plasticité ne dépend pas de l'espèce, mais nous avons travaillé avec seulement six espèces (Chapitre 3). Les paramètres quantifiant la capacité des espèces à stimuler les germinations de *P. ramosa* pourraient être utilisés pour estimer la variabilité spécifique de cette plasticité, car les strigolactones (stimulants de germination) ont un rôle majeur dans la modulation du ratio aérien/racinaire en réponse à la disponibilité du sol en nutriments (Yoneyama *et al.*, 2013).

Compte tenu de la multiplicité et de la complexité des questionnements listés ci-dessus, une analyse de sensibilité du modèle aux valeurs de paramètres mais aussi des formalismes choisis serait particulièrement utile pour déterminer quelles pistes de recherche explorer en priorité (ex : simuler diverses durées de cycle de vie de *P. ramosa* ou l'hypothèse que *P. ramosa* à une durée de vie équivalente à celle de ses hôtes, section 5.3.1). En attendant, la cohérence des résultats de simulations avec la littérature et la validation partielle du modèle indiquent que ce dernier peut d'ores et déjà être utilisé pour classer des systèmes de culture en terme de risque parasitaire et de (dis)services liés aux adventices.

5.5. Conclusion générale

En combinant et synthétisant des connaissances de différentes disciplines dans un modèle de simulation, nous avons développé un outil utile pour aider à concevoir des stratégies de gestion de *P. ramosa*, plante parasite causant des pertes de rendement considérables pour une vingtaine de cultures d'importance économique dans le monde entier.

Nous avons montré qu'une gestion agroécologique de *P. ramosa* est possible mais complexe car elle doit combiner de multiples techniques culturales et exploiter les régulations biologiques entre plantes. Bien que nous ayons choisi l'exemple de la gestion de *P. ramosa*, notre modèle permet également de mieux comprendre comment gérer les adventices et, de manière générale, comment les plantes s'assemblent au sein des communautés végétales, par l'analyse d'interactions complexes entre effets (techniques × plantes × climat) à l'échelle des processus.

Notre modèle constitue un outil de transfert prometteur car il est potentiellement utilisable par des chercheurs, conseillers agricoles et agriculteurs au sein de démarches participatives. Les limites que nous avons identifiées définissent le cadre dans lequel le modèle peut être utilisé. Ce cadre est amené à s'élargir car du fait de sa structure mécaniste, notre modèle est facilement améliorable.

D'ailleurs, notre modèle s'inscrit dans une boucle d'amélioration continuelle dont les étapes, illustrées au cours de cette thèse, consistent à 1) synthétiser des connaissances, 2) en déduire les lacunes, 3) hiérarchiser les connaissances à acquérir et 4) intégrer les nouvelles connaissances acquises. Cette démarche fait de notre modèle un outil pertinent d'organisation de la recherche.

Liste des publications

• Articles dans des revues internationales à comité de lecture

Dans le cadre de la thèse

- En preparation:

Pointurier, O., Moreau, D. & Colbach, N. (en cours de soumission). Individual-based 3D modelling of root systems in heterogeneous plant canopies at the multiannual scale. Case study with a weed dynamics model. *Ecological Modelling.*

Pointurier, O., Gibot-Leclerc, S., Moreau, D., Reibel, C., Vieren, E. & Colbach, N. (en préparation). Designing a model to investigate the regulation of parasitic plants by weeds. *European Journal of Agronomy.*

Moreau, D., **Pointurier, O.**, Perthame, L., Beaudoin, N., Munier-Jolain, N., Villerd, J. & Colbach, N. (en préparation). Integrating crop-weed competition for nitrogen in the FLORSYS weed-dynamics simulation model.

Colbach, N., **Pointurier, O.** & Villerd, J. (en préparation). Multicriteria evaluation of weed impacts on crop production and biodiversity in herbicide-sparse cropping systems of the French DEPHY farm network. *Agriculture, Ecosystems & Environment.*

- Soumis ou en revision:

Moreau D, **Pointurier O**, Nicolardot B, Villerd J, Colbach N (en révision). In which cropping systems can residual weeds reduce nitrate leaching and soil erosion? *European Journal of Agronomy*.

Pagès, L., **Pointurier, O.**, Moreau, D., Voisin, A. S. & Colbach, N. (soumis). Simplifying an individual-based 3D root architecture model with virtual experiments. *Plant and Soil*.

- Publiés

Pointurier, O., Gibot-Leclerc, S., Le Corre, V., Reibel, C., Strbik, F. & Colbach, N. (**2019**). Intraspecific seasonal variation of dormancy and mortality of branched broomrape seeds. *Weed Research*. https://onlinelibrary.wiley.com/doi/full/10.1111/wre.12378

Colbach, N., Bockstaller, C., Colas, F., Gibot-Leclerc, S., Moreau, D., **Pointurier, O.** & Villerd, J. (**2017a**). Assessing broomrape risk due to weeds in cropping systems with an indicator linked to a simulation model. *Ecological Indicators* 82: 280-292.

Colbach, N., Colas, F., **Pointurier, O.**, Queyrel, W. & Villerd, J. (**2017b**). A methodology for multi-objective cropping system design based on simulations. Application to weed management. *European Journal of Agronomy* 87: 59-73.

Moreau, D., Gibot-Leclerc, S., Girardin, A., **Pointurier, O.**, Reibel, C., Strbik, F., Fernández-Aparicio, M. & Colbach N. (**2016**). Trophic relationships between the parasitic plant species *Phelipanche ramosa* (L.) and different hosts depending on host phenological stage and host growth rate. *Frontiers in Plant Science* 7: 1033.

Hors cadre de la thèse

Williams, L., **Pointurier, O.** & Deschodt, P. (**2019**). Affect of food provisioning on survival and reproductive success of the olive fruit fly parasitoid, *Psyttalia lounsburyi*, in the field. *Arthropod-Plant Interactions*.

Williams, L., Deschodt, P., **Pointurier, O.** & Wyckhuys, K. A. G. (**2015**). Sugar concentration and timing of feeding affect feeding characteristics and survival of a parasitic wasp. *Journal of Insect Physiology* 79: 10-18.

Colas, F., Colbach, N., Cordeau, S., Jeuffroy, M.-H., Granger, S., Queyrel, W., **Pointurier, O.**, Rodriguez, A., Villerd, J., (soumis). Co-development of a decision support system for integrated weed managment: contribution from future users. *European Journal of Agronomy*.

Colas, F., Colbach, N., **Pointurier, O.**, Villerd, J., (en préparation). Which cultural techniques drive weed dynamics and impact? Sensitivity analysis of a cropping system model to support integrated weed management.

- # Revue nationale sans comité de lecture

Colbach, N., Bockstaller, C., Colas, F., Gibot-Leclerc, S., Granger, S., Guyot, S., Mézière, D., Moreau, D., **Pointurier, O.**, Queyrel, W., Villerd, J. & Voisin, A.-S. (**2017**). Conception de systèmes de culture multiperformants à l'aide de modèles prédisant la nuisibilité et les services dépendant des adventices. *Innovations Agronomiques* 59, 191-203.

- # Mémoire

Pointurier, O. (**2015**). Modélisation des effets des systèmes de culture sur la dynamique de la plante parasite orobanche rameuse en interaction avec la flore adventice. In *UMR Agroécologie, INRA Dijon*, Engineer thesis, 64 p. Montpellier Supagro, Agrocampus Ouest, AgroParisTech. (prix de mémoire de fin d'étude de la fondation Xavier-Bernard)

- # Communications en congrès et colloques

<u>Conférences internationales</u>

Pointurier, O., Gibot-Leclerc, S., Moreau, D., Reibel, C., Strbik, F. & Colbach, N. (**2018**). Modelling cropping system effects on branched broomrape dynamics in interaction with weeds. In *XV^e^ European Society for Agronomy Congress*, Geneva, Switzerland. Poster (premier prix poster étudiant).

Moreau, D., **Pointurier, O.**, Nicolardot, B., Colbach, N. (**2018**). Reduction of nitrate leaching: what is the contribution of the residual weed flora? In *XV^e^ European Society for Agronomy Congress*. Geneva, Switzerland. Oral.

Moreau, D., **Pointurier, O.**, Nicolardot, B., Colbach, N. (**2018**). What is the contribution of the residual weed floras to reduce nitrate leaching? In *18^th^ European Weed Research Society Symposium*, Ljubljana, Slovenia. Oral.

Pointurier, O., Gibot-Leclerc, S., Moreau, D. & Colbach, N. (**2016**). Modelling cropping system effects on branched broomrape dynamics in interaction with weeds. In *23e Conférence du COLUMA: Journées internationales sur la lutte contre les mauvaises herbes*, Dijon, France: AFPP. Poster.

Pointurier, O., Gibot-Leclerc, S., Moreau, D., Darmency, H. & Colbach, N. (**2016**). Modelling cropping system effects on branched broomrape dynamics in interaction with weeds. In *7^th^ International Weed Science Congress*, Prague, Czech Republic. Poster.

Colbach, N., Colas, F., Moreau, D., Gibot-Leclerc, S., **Pointurier, O.**, Queyrel, W., Bockstaller, C. (**2016**). Ex ante evaluation of weed-mediated pests and environmental benefits of cropping systems with simulation-based indicators. In *XIV^e^ European Society for Agronomy Congress*. Edinburgh, Scotland. Poster.

Colas, F., Cordeau, S., Jeuffroy, M.-H., Granger, S., Queyrel, W., **Pointurier, O.**, Rodriguez, A., Villerd, J., Colbach, N. (**2016**). Développement d'un outil d'aide à la décision pour la gestion intégrée des adventices. In *23e Conférence du COLUMA: Journées internationales sur la lutte contre les mauvaises herbes*, Dijon, France: AFPP. Poster.

Séminaires

Pointurier, O., Gibot-Leclerc, S., Le Corre, V., Reibel, C., Strbik, F. & Colbach, N. (**2019**). Les semences de la plante parasite orobanche rameuse ont une dormance saisonnière qui varie au niveau intrespécifique et une faible mortalité au champ. In *Séminaire du Projet de Recherche ANR CoSAC*, Paris, France. Poster.

Pointurier, O., Gibot-Leclerc, S., Moreau, D., Le Corre, V., Reibel, C., Strbik, F. & Colbach, N. (**2019**). Modélisation des effets des systèmes de culture sur la dynamique de la plante parasite orobanche rameuse en interaction avec les adventices. In *Journée des doctorants de l'UMR Agroécologie*, Dijon, France. Oral.

Pointurier, O., Villerd, J., Jolys, O., Munier-Jolain, N., Dubuc, M. & Colbach, N. (**2018**). Simuler les systèmes de culture du réseau DEPHY dans FLORSYS. In *Assemblée générale du Projet de Recherche ANR CoSAC*, Paris, France. Oral.

Pointurier, O. & Colbach, N. (**2018**). Modéliser la dynamique des adventices avec le modèle FLORSYS pour évaluer et concevoir des systèmes de culture multiperformants : Utilisation des données du réseau DEPHY. In *Séminaire DEPHY GCPE 2018*, Dijon, France. Oral.

Pointurier, O., Moreau, D., Pagès, L. & Colbach, N. Modélisation de l'architecture racinaire dans FLORSYS et perspectives : Application à la modélisation du parasitisme par l'orobanche rameuse (**2018**). In *2ème Journée de présentation de modèles de l'atelier thématique modélisation de l'UMR Agroécologie*, Dijon, France. Oral.

Pointurier, O. & Colbach, N. (**2017**). Prédire la dynamique des adventices dans les parcelles agricoles avec le modèle FLORSYS. In *Rencontres GIS PIC lég*, Marseille, France. Oral.

Pointurier, O., Gibot-Leclerc, S., Moreau, D. & Colbach, N. (**2017**). Modélisation des effets des systèmes de culture sur la dynamique de l'orobanche rameuse en interaction avec les adventices. In *Séminaire de Restitution à mi-parcours du Projet de Recherche ANR CoSAC*, Paris, France. Poster.

Colas, F., Cordeau, S., Jeuffroy, M.-H., Granger, S., Queyrel, W., **Pointurier, O.**, Rodriguez, A., Villerd, J., Colbach, N. (**2017**). Développement d'un outil d'aide à la décision pour la gestion intégrée des adventices : implication des futurs utilisateurs. In *Séminaire de restitution à mi-parcours du projet de recherche ANR CoSAC*, Paris, France. Poster.

Colbach, N., Colas, F., **Pointurier, O.**, Queyrel, W., Villerd, J. (**2017**). Proposition d'une méthodologie de conception multi-objective de systèmes de culture à partir de simulations. Application à la gestion des adventices. In *Séminaire de restitution à mi-parcours du projet de recherche ANR CoSAC*, Paris, France. Oral.

Pagès, L., Moreau, D., **Pointurier, O.**, Poulain, A., Sauvage, S., Serra, V. & Colbach, N. (**2017**). Modélisation de l'architecture racinaire dans le projet COSAC : pourquoi et comment ? In *Séminaire de Restitution à mi-parcours du Projet de Recherche ANR CoSAC*, Paris, France. Poster.

Villerd, J., Brun, F., Jolys, O., Métais, P., Munier-Jolain, N., Pointurier, O. & Vuillemi, F. (**2017**). L'hétérogénéité des données au sein du projet Cosac : Enjeux et solutions. In *Séminaire de Restitution à mi-parcours du Projet de Recherche ANR CoSAC*, Paris, France. Poster.

Pointurier, O. & Colbach, N. (**2016**). Prédire la dynamique des adventices dans les parcelles agricoles avec le modèle FLORSYS. In *Journée technique Carottes de France*, Saint-Jean-d'Illac, France. Oral.

Pointurier, O., Gibot-Leclerc, S., Moreau, D., Le Corre, V., Reibel, C., Strbik, F. & Colbach, N. (**2016**). Modélisation des effets des systèmes de culture sur la dynamique de la plante parasite orobanche rameuse en interaction avec la flore adventice. In *Séminaire des doctorants du Laboratoire de Mathématiques de Besançon*, Besançon, France. Oral.

Pointurier, O., Deschodt, P., Wyckhuys, K. & Williams, L. (**2014**). Nutritional ecology of a parasitic wasp - Sugar concentration and timing of feeding affect survival. In *Colloque des Entomophagistes*, Louvain-la-Neuve, Belgium. Poster.

Curriculum vitae

Olivia Pointurier
5, avenue du Maréchal Foch, 21000 Dijon
olivia.pointurier@gmail.com
+33 6 33 29 02 89

Formation et diplômes

- **2016-en cours Thèse de doctorat en modélisation appliquée à l'agronomie** (gestion de la plante parasite orobanche rameuse), INRA, Dijon
- **2011-2015 Diplôme d'ingénieur agronome**, spécialisée en Protection des Plantes et Environnement, Supagro, Montpellier, dont un semestre à Wageningen University, Pays-Bas
- **2009-2011 Classes Préparatoires aux Grandes Ecoles** BCPST (Biologie, Chimie, Physique et Sciences de la Terre), Lycée Victor Hugo, Besançon
- **2009 Baccalauréat Scientifique**, spécialité Sciences de la Vie et de la Terre, mention TB, Lycée Victor Hugo, Besançon

Expérience professionnelle

- **Ingénieur d'étude en modélisation de dynamique des adventices et programmation, préparation d'une thèse en parallèle, INRA Dijon, 2016-2019**

Recherche : modélisation, lancement de simulations, élaboration d'un protocole expérimental, analyse de données, écriture d'articles scientifiques, préparation d'une thèse

Informatique : programmation, contribution au développement d'un programme informatique de transfert de données entre deux systèmes d'information

Communication : formation et accompagnement des utilisateurs d'un modèle (chercheurs, conseillers et agriculteurs), contribution à la rédaction du manuel d'utilisation, présentations dans des conférences nationales et internationales

Autre : reconnaissance des adventices, expert extérieur dans un jury de mémoire d'ingénieur agronome

- **Aide technique de laboratoire, INRA Dijon, 2015 (3 mois)**

Expérimentation en laboratoire

- **Assistant chercheur (stagiaire), 2013-2015**

Modélisation de la dynamique de la plante parasite orobanche rameuse dans les agroécosytèmes, INRA Dijon, 2015 (6 mois, stage de fin d'études)

Entretiens d'agriculteurs pour comprendre leurs trajectoires post-installation en Massif Central, JA Auvergne-INRA Clermont-Ferrand, 2013-2014 (6 mois)

Lutte biologique contre la mouche de l'olive, EBCL (European Biological Control Laboratory, US Department of Agriculture), 2013 (5 mois)

Elaboration d'un protocole pour mener des entretiens (guide d'entretien et échantillonnage), expérimentations au laboratoire (dont quarantaine) et en plein champ, entretiens individuels auprès d'agriculteurs, analyse de données (quantitatives et qualitatives), modélisation, synthèse des résultats (écriture d'un mémoire, contribution à l'écriture d'articles scientifiques), présentation des résultats dans un colloque international

- **Ouvrier agricole (stagiaire), 2012-2014**

Elevage ovin-caprin avec transformation fromagère et maraîchage (2 mois)

Horticulture en protection biologique intégrée (2 mois)

Autres compétences

- **Communication**

Anglais couramment parlé et écrit (B2 - C1), TOEIC (870 points), bonne maîtrise de l'Espagnol (A2)

- **Informatique**

Bureautique (Word, Excel, Powerpoint), statistiques (R), programmation (C/C++), gestion de références (EndNote)

Connaissances basiques en conception de sites Internet, traitement de bases de données (Access) et Systèmes d'Information Géographique (QGis)

- **Permis B**

Récompenses

- **Premier prix poster étudiant** du XVe European Society for Agronomy Congress, Genève, Suisse, 2018
- **Prix de mémoire de fin d'études** de la fondation Xavier-Bernard, Académie d'Agriculture de France, 2015

Références

Agreste (2012). Recensement agricole 2010 - Grandes cultures. In *Agreste Poitou-Charentes*, Vol. n°1. http://agreste.agriculture.gouv.fr/IMG/pdf/R5412A01.pdf (accessed on 14.10.19)

Altieri, M. (1995). Agroecology: principles and strategies for designing sustainable farming systems. (Ed FAO). http://www.fao.org/agroecology/database/detail/fr/c/893012/ (accessed on 14.10.19)

Arslan, Z. & Uygur, N. (2013). Potency of some synthetic stimulants and root exudates on the germination of *Phelipanche* spp. *Tarım Bilimleri Dergisi – Journal of Agricultural Sciences* 19: 198-206.

Auffret, A. G., Berg, J. & Cousins, S. A. O. (2014). The geography of human-mediated dispersal. *Diversity and Distributions* 20(12): 1450-1456.

Auger, B., Pouvreau, J. B., Pouponneau, K., Yoneyama, K., Montiel, G., Le Bizec, B., Yoneyama, K., Delavault, P., Delourme, R. & Simier, P. (2012). Germination stimulants of *Phelipanche ramosa* in the rhizosphere of *Brassica napus* are derived from the glucosinolate pathway. *Molecular Plant-Microbe Intercations* 25(7): 993-1004.

Aziz, M. M., Palta, J. A., Siddique, K. H. M. & Sadras, V. O. (2017). Five decades of selection for yield reduced root length density and increased nitrogen uptake per unit root length in Australian wheat varieties. *Plant And Soil* 413(1): 181-192.

Barber, S. A. (1984). *Soil Nutrient Bioavailability: A Mechanistic Approach.* New York: John Wiley & Sons.

Barker, E. R., Press, M. C., Scholes, J. D. & Quick, W. P. (1996). Interactions between the parasitic angiosperm *Orobanche aegyptiaca* and its tomato host: Growth and biomass allocation. *The New Phytologist* 133(4): 637-642.

Bengough, A. G. & Mullins, C. E. (1990). Mechanical impedance to root-growth - a review of experimental-techniques and root-growth responses. *Journal of Soil Science* 41(3): 341-358.

Bengough, A. G., McKenzie, B. M., Hallett, P. D. & Valentine, T. A. (2011). Root elongation, water stress, and mechanical impedance: a review of limiting stresses and beneficial root tip traits. *J Exp Bot* 62(1): 59-68.

Benharrat, H., Boulet, C., Theodet, C. & Thalouarn, P. (2005). Virulence diversity among branched broomrape (*Orobanche ramosa* L.) populations in France. *Agronomy for Sustainable Development* 25: 123-128.

Benjamin, L. R., Milne, A. E., Parsons, D. J. & Lutman, P. J. W. (2010). A model to simulate yield losses in winter wheat caused by weeds, for use in a weed management decision support system. *Crop Protection* 29(11): 1264-1273.

Berger, A. G., McDonald, A. J. & Riha, S. J. (2013). Simulating root development and soil resource acquisition in dynamic models of crop–weed competition. In *Enhancing understanding and quantification of soil–root growth interactions*, 229-244 (Eds D. Timlin and L. R. Ahuja). Madison, WI: American Society of Agronomy, Crop Science Society of America, Soil Science Society of America.

Bergez, J. E., Colbach, N., Crespo, O., Garcia, F., Jeuffroy, M. H., Justes, E., Loyce, C., Munier-Jolain, N. & Sadok, W. (2010). Designing crop management systems by simulation. *European Journal of Agronomy* 32(1): 3-9.

Blackshaw, R. E., Molnar, L. J. & Janzen, H. H. (2004). Nitrogen fertilizer timing and application method affect weed growth and competition with spring wheat. *Weed Science* 52(4): 614-622.

Bockstaller, C., Guichard, L., Makowski, D., Aveline, A., Girardin, P. & Plantureux, S. (2008). Agri-environmental indicators to assess cropping and farming systems. A review. *Agronomy for Sustainable Development* 28(1): 139-149.

Bodner, G., Leitner, D., Nakhforoosh, A., Sobotik, M., Moder, K. & Kaul, H.-P. (2013). A statistical approach to root system classification. *Frontiers in Plant Science* 4(292).

Bonhomme, R. (2000). Bases and limits to using ‘degree.day’ units. *European Journal of Agronomy* 13(1): 1-10.

Bonneu, A., Dumont, Y., Rey, H., Jourdan, C. & Fourcaud, T. (2012). 2012-01 - A minimal continuous model for simulating growth and development of plant root systems. *Plant And Soil* 354.

Bouaziz, A. & Bruckler, L. (1989). Modeling wheat seedling growth and emergence. I. Seedling growth affected by soil water potential. *Soil Sci. Soc. Am. J.* 53: 1832-1838.

Boulet, C., Labrousse, P., Arnaud, M. C., Zehhar, N. & Fer, A. (2001). Weed species present various responses to *Orobanche ramosa* L. attack. In *7th International Parasitic Weed Symposium*, Nantes, France.

Boulet, C., Pineault, D., Benharrat, H., Bozec, D., Delavault, P. & Simier, P. (2007). Adventices du colza et orobanche. In *20ème conférence du COLUMA. Journées internationales sur la lutte contre les mauvaises herbes.*, Dijon, France.

Boulet, C., Molenat, D., Benharrat, H., Delavault, P. & Simier, P. (2013). Étude de la sensibilité des adventices vis-à-vis de l'orobanche rameuse (*Phelipanche ramosa* (L.) Pomel) en vue d'une lutte intégrée. In *22ème conférence du COLUMA. Journées internationales sur la lutte contre les mauvaises herbes.*, Dijon, France.

Bradford, K. J. (2002). Applications of hydrothermal time to quantifying and modeling seed germination and dormancy. *Weed Science* 50(2): 248-260.

Brault, M., Betsou, F., Jeune, B., Tuquet, C. & Sallé, G. (2007). Variability of *Orobanche ramosa* populations in France as revealed by cross infestations and molecular markers. *Environmental and Experimental Botany* 61(3): 272-280.

Brisson, N., Mary, B., Ripoche, D., Jeuffroy, M. H., Ruget, F., Nicoullaud, B., Gate, P., Devienne-Barret, F., Antonioletti, R., Dürr, C., Richard, G., Beaudoin, N., Recous, S., Tayot, X., Plenet, D., Cellier, P., Machet, J. M., Meynard, J. M. & Delecolle, R. (1998). STICS: a generic model for the simulation of crops and their water and nitrogen balances. I. Theory and parameterization applied to wheat and corn. *Agronomie* 18(5-6): 311-346.

Brisson, N., Ruget, F., Gate, P., Lorgeou, J., Nicoullaud, B., Tayot, X., Plenet, D., Jeuffroy, M.-H., Bouthier, A., Ripoche, D., Mary, B. & Justes, E. (2002). STICS: a generic model for simulating crops and their water and nitrogen balances. II. Model validation for wheat and maize. *Agronomie* 22(1): 69-92.

Brisson, N., Gary, C., Justes, E., Roche, R., Mary, B., Ripoche, D., Zimmer, D., Sierra, J., Bertuzzi, P., Burger, P., Bussiere, F., Cabidoche, Y. M., Cellier, P., Debaeke, P., Gaudillere, J. P., Henault, C., Maraux, F., Seguin, B. & Sinoquet, H. (2003). An overview of the crop model STICS. *European Journal of Agronomy* 18: 309-332.

Brouwer, R. (1962). Nutritive influences on the distribution of dry matter in the plant. *Netherlands Journal Of Agricultural Science* 10: 399-408.

Brown, R. & Edwards, M. (1944). The germination of the seed of *Striga lutea*: I. Host influence and the progress of germination. *Ann Bot* 8(2-3): 131-148.

Brun, F., Richard-Molard, C., Pagès, L., Chelle, M. & Ney, B. (2010). To what extent may changes in the root system architecture of Arabidopsis thaliana grown under contrasted homogenous nitrogen regimes be explained by changes in carbon supply? A modelling approach. *Journal of Experimental Botany* 61: 2157-2169.

Bui, H. H., Serra, V. & Pagès, L. (2015). Root system development and architecture in various genotypes of the Solanaceae family. *Botany* 93: 465-474.

Cameron, D. D. & Phoenix, G. K. (2013). Ecology of hemiparasitic Orobanchaceae with special reference to their interaction with plant communities. In *Parasitic Orobanchaceae : Parasitic mechanisms and control strategies*, 287-305 (Eds D. M. Joel, J. Gressel and L. J. Musselman). Springer-Verlag Berlin Heidelberg.

Casper, B. B., Schenk, H. J. & Jackson, R. B. (2003). Defining a plant's belowground zone of influence. *Ecology* 84(9): 2313-2321.

Cassab, G. I., Eapen, D. & Campos, M. E. (2013). Root hydrotropism: An update. *American Journal of Botany* 100(1): 14-24.

Castel, T., Lecomte, C., Richard, Y., Lejeune-Hénaut, I. & Larmure, A. (2017). Frost stress evolution and winter pea ideotype in the context of climate warming at a regional scale. *OCL* 24(1): D106.

Castro-Tendero, A. J. & García-Torres, L. (1995). SEMAGI — an expert system for weed control decision making in sunflowers. *Crop Protection* 14(7): 543-548.
Chatelin, M. H., Aubry, C., Poussin, J. C., Meynard, J. M., Masse, J., Verjux, N., Gate, P. & Le Bris, X. (2005). DéciBlé, a software package for wheat crop management simulation. *Agricultural Systems* 83(1): 77-99.
Chauvel, B., Darmency, H., Munier-Jolain, N. & Rodriguez, A. (2018). *Gestion durable de la flore adventice des cultures.* Versailles: Editions Quae.
Chen, G. & Weil, R. R. (2010). Penetration of cover crop roots through compacted soils. *Plant And Soil* 331(1): 31-43.
Cheng, F. & Cheng, Z. (2015). Research progress on the use of plant allelopathy in agriculture and the physiological and ecological mechanisms of allelopathy. *Frontiers in Plant Science* 6: 1020.
Cohen, Y., Roei, I., Blank, L., Goldshtein, E. & Eizenberg, H. (2017). Spatial spread of the root parasitic weed *Phelipanche aegyptiaca* in processing tomatoes by using ecoinformatics and spatial analysis. *Frontiers in Plant Science* 8(973).
Colas, F. (2018). Co-développement d'un modèle d'aide à la décision pour la gestion intégrée de la flore adventice. Méta-modélisation et analyse de sensibilité d'un modèle mécaniste complexe (FLORSYS) des effets des systèmes de culture sur les services et disservices écosystémiques de la flore adventice., PhD thesis, 333 p.
Colas, F., Gauchi, J.-P., Villerd, J. & Colbach, N. (in revision). Simplifying a complex computer model: sensitivity analysis and metamodelling of the complex process-based model FLORSYS. *Ecological Modelling*.
Colbach, N., Clermont-Dauphin, C. & Meynard, J. M. (2001). GENESYS: a model of the influence of cropping system on gene escape from herbicide tolerant rapeseed crops to rape volunteers. I. Temporal evolution of a population of rapeseed volunteers in a field. *Agriculture, Ecosystems and Environment* 83: 235-253.
Colbach, N. (2006). Modélisation des effets des systèmes de culture sur les bioagresseurs. "Mémoire d'habilitation à diriger les recherches" thesis, 110 p. Université de Bourgogne.
Colbach, N., Busset, H., Yamada, O., Dürr, C. & Caneill, J. (2006a). ALOMYSYS: Modelling black-grass (*Alopecurus myosuroides* Huds.) germination and emergence, in interaction with seed characteristics, tillage and soil climate: II. Evaluation. *European Journal of Agronomy* 24(2): 113-128.
Colbach, N., Dürr, C., Roger-Estrade, J., Chauvel, B. & Caneill, J. (2006b). ALOMYSYS: Modelling black-grass (*Alopecurus myosuroides* Huds.) germination and emergence, in interaction with seed characteristics, tillage and soil climate: I. Construction. *European Journal of Agronomy* 24(2): 95-112.
Colbach, N., Chauvel, B., Gauvrit, C. & Munier-Jolain, N. M. (2007). Construction and evaluation of ALOMYSYS modelling the effects of cropping systems on the blackgrass life-cycle: From seedling to seed production. *Ecological Modelling* 201(3): 283-300.
Colbach, N. (2010). Modelling cropping system effects on crop pest dynamics: how to compromise between process analysis and decision aid. *Plant Science* 179: 1-13.
Colbach, N., Kurstjens, D. A. G., Munier-Jolain, N. M., Dalbiès, A. & Doré, T. (2010). Assessing non-chemical weeding strategies through mechanistic modelling of blackgrass (*Alopecurus myosuroides* Huds.) dynamics. *European Journal of Agronomy* 32(3): 205-218.
Colbach, N., Abdennebi-Abdemessed, N. & Gibot-Leclerc, S. (2011). A preliminary approach for modelling the effects of cropping systems on the dynamics of broomrape (*Phelipanche ramosa*) in interaction with the non-parasitic weed flora. *OCL* 18(1): 39-45.
Colbach, N., Biju-Duval, L., Gardarin, A., Granger, S., Guyot, S. H. M., Mézière, D., Munier-Jolain, N. M. & Petit, S. (2014a). The role of models for multicriteria evaluation and multiobjective design of cropping systems for managing weeds. *Weed Research* 54: 541–555.
Colbach, N., Busset, H., Roger-Estrade, J. & Caneill, J. (2014b). Predictive modelling of weed seed movement in response to superficial tillage tools. *Soil & Tillage Research* 138: 1-8.
Colbach, N., Collard, A., Guyot, S. H. M., Mézière, D. & Munier-Jolain, N. M. (2014c). Assessing innovative sowing patterns for integrated weed management with a 3D crop:weed competition model. *European Journal of Agronomy* 53: 74-89.

Colbach, N., Bertrand, M., Busset, H., Colas, F., Dugué, F., Farcy, P., Fried, G., Granger, S., Meunier, D., Munier-Jolain, N. M., Noilhan, C., Strbik, F. & Gardarin, A. (2016). Uncertainty analysis and evaluation of a complex, multi-specific weed dynamics model with diverse and incomplete data sets. *Environmental Modelling & Software* 86: 184-203.

Colbach, N., Bockstaller, C., Colas, F., Gibot-Leclerc, S., Moreau, D., Pointurier, O. & Villerd, J. (2017a). Assessing broomrape risk due to weeds in cropping systems with an indicator linked to a simulation model. *Ecological Indicators* 82: 280-292.

Colbach, N., Colas, F., Pointurier, O., Queyrel, W. & Villerd, J. (2017b). A methodology for multi-objective cropping system design based on simulations. Application to weed management. *European Journal of Agronomy* 87: 59-73.

Colbach, N. & Cordeau, S. (2018). Reduced herbicide use does not increase crop yield loss if it is compensated by alternative preventive and curative measures. *European Journal of Agronomy* 94: 67-78.

Colbach, N., Cordeau, S., Garrido, A., Granger, S., Laughlin, D., Ricci, B., Thomson, F. & Messéan, A. (2018). Landsharing vs landsparing: How to reconcile crop production and biodiversity? A simulation study focusing on weed impacts. *Agriculture, Ecosystems & Environment* 251: 203-217.

Colbach, N., Gardarin, A. & Moreau, D. (2019). The response of weed and crop species to shading: Which parameters explain weed impacts on crop production? *Field Crops Research* 238: 45-55.

Colbach, N., Pointurier, O. & Villerd, J. (in prep.). Multicriteria evaluation of weed impacts on crop production and biodiversity in herbicide-sparse cropping systems of the French DEPHY farm network. *Agriculture, Ecosystems & Environment*.

Colbach, N., Colas, F., Cordeau, S., Maillot, T., Moreau, D., Queyrel, W. & Villerd, J. (in revision). Modelling crop-weed canopies as a tool to investigate the role of crop diversification in agroecological cropping systems. *European Journal of Agronomy*.

Colbach, N., Cordeau, S., Queyrel, W., Maillot, T., Villerd, J. & Moreau, D. (submitted). Du champ virtuel au champ réel - ou comment utiliser un modèle de simulation pour diagnostiquer des stratégies durables de gestion des adventices? *Agriculture, Environnement et Sociétés*.

Colombi, T., Torres, L. C., Walter, A. & Keller, T. (2018). Feedbacks between soil penetration resistance, root architecture and water uptake limit water accessibility and crop growth – A vicious circle. *Science of The Total Environment* 626: 1026-1035.

Cook, R. J. (2003). Take-all of wheat. *Physiological and Molecular Plant Pathology* 62(2): 73-86.

de Willigen, P., Heinen, M., Mollier, A. & Noordwijk, M. V. (2002). Two-dimensional growth of a root system modelled as a diffusion process. I. Analytical solutions. *Plant And Soil* 240(2): 225-234.

Denev, I., Deneva, B. & Batchvarova, R. (2007). The biosynthetic origin of germination stimulants for O*robanche ramosa* (l.) in tobacco and *Arabidopsis*. *Biotechnology & Biotechnological Equipment* 21(1): 54-57.

Dennis, P. G., Miller, A. J. & Hirsch, P. R. (2010). Are root exudates more important than other sources of rhizodeposits in structuring rhizosphere bacterial communities? *FEMS Microbiology Ecology* 72(3): 313-327.

Díaz, J., Norambuena, H. & López-Granados, F. (2006). Characterization of the holoparasitism of *Orobanche ramosa* on tomatoes under field conditions. *Agricultura Técnica* 66: 223-234.

Disciglio, G., Lops, F., Carlucci, A., Gatta, G., Tarantino, A., Frabboni, L., Carriero, F. & Tarantino, E. (2016). Effects of different methods to control the parasitic weed *Phelipanche ramosa* (L.) Pomel in processing tomato crops. *Italian Journal of Agronomy* 11:681: 39-46.

Données Ephy - Anses (2018). Le catalogue des produits phytopharmaceutiques et de leurs usages, des matières fertilisantes et des supports de culture autorisés en France. https://ephy.anses.fr/ (accessed on 08.10.18)

Doré, T. (2006). Introduction générale. In *L'agronomie aujourd'hui*, 23-30 (Eds T. Doré, M. Le Bail, P. Martin, B. Ney and J. Roger-Estrade). Versailles: Editions Quae.

Doré, T. & Meynard, J.-M. (2006). I. Itinéraire technique, système de culture : de la compréhension du foncionnement du champ cultivé à l'évoluation des pratiques agricoles. Introdution générale.

In *L'agronomie aujourd'hui*, 33-42 (Eds T. Doré, M. Le Bail, P. Martin, B. Ney and J. Roger-Estrade). Versailles: Editions Quae.
Dray, S. & Dufour, A.-B. (2007). The ade4 package: Implementing the duality diagram for ecologists. *Journal of Statistical Software* 22.
Drouet, J. L. & Pagès, L. (2003). GRAAL: a model of GRowth, Architecture and carbon ALlocation during the vegetative phase of the whole maize plant: Model description and parameterisation. *Ecological Modelling* 165(2): 147-173.
Drouet, J. L., Pagès, L. & Serra, V. (2005). Dynamics of leaf mass per unit leaf area and root mass per unit root volume of young maize plants: implications for growth models. *European Journal of Agronomy* 22(2): 185-193.
Dulout, A., Lucas, P., Sarniguet, A. & Doré, T. (1997). Effects of wheat volunteers and blackgrass in set-aside following a winter wheat crop on soil infectivity and soil conduciveness to take-all. *Plant And Soil* 197(1): 149-155.
Dunbabin, V. M., Postma, J. A., Schnepf, A., Pagès, L., Javaux, M., Wu, L., Leitner, D., Chen, Y. L., Rengel, Z. & Diggle, A. J. (2013). Modelling root–soil interactions using three–dimensional models of root growth, architecture and function. *Plant And Soil* 372(1): 93-124.
Dupuy, L., Gregory, P. J. & Bengough, A. G. (2010). Root growth models: towards a new generation of continuous approaches. *Journal of Experimental Botany* 61(8): 2131-2143.
Dürr, C., Aubertot, J. N., Richard, G., Dubrulle, P., Duval, Y. & Boiffin, J. (2001). SIMPLE: A model for SIMulation of PLant Emergence predicting the effects of soil tillage and sowing operations. *Soil Science Society of America Journal* 65(2): 414-423.
Eizenberg, H., Colquhoun, J. & Mallory-Smith, C. (2005). A predictive degree-days model for small broomrape (*Orobanche minor*) parasitism in red clover in Oregon. *Weed Science* 53(1): 37-40.
Eizenberg, H., Lande, T., Achdari, G., Smirnov, Y. & Hershenhorn, J. (2009). PICKIT- a decision support system for rational control of *Phelipanche aegyptiaca* in tomato. In *10th World Congress of Parasitic Plants*, Kusadasi, Turquie.
Eizenberg, H., Aly, R. & Cohen, Y. (2012a). Technologies for smart chemical control of broomrape (*Orobanche* spp. and *Phelipanche* spp.). *Weed Science* 60: 316-323.
Eizenberg, H., Hershenhorn, J., Achdari, G. & Ephrath, J. E. (2012b). A thermal time model for predicting parasitism of *Orobanche cumana* in irrigated sunflower—Field validation. *Field Crop Research* 137: 49-55.
Eizenberg, H. & Goldwasser, Y. (2018). Control of egyptian broomrape in processing tomato: A summary of 20 years of research and successful implementation. *Plant Dis* 102(8): 1477-1488.
Ephrath, J. E. & Eizenberg, H. (2010). Quantification of the dynamics of *Orobanche cumana* and *Phelipanche aegyptiaca* parasitism in confectionery sunflower. *Weed Research* 50(2): 140-152.
Faverjon, L., Escobar-Gutiérrez, A., Pagès, L., Migault, V. & Louarn, G. (2019). Root growth and development do not directly relate to shoot morphogenetic strategies in temperate forage legumes. *Plant And Soil* 435: 277-294.
Fayaud, B., Coste, F., Corre-Hellou, G., Gardarin, A. & Durr, C. (2014). Modelling early growth under different sowing conditions: A tool to predict variations in intercrop early stages. *European Journal of Agronomy* 52: 180-190.
Fernandez-Aparicio, M., Kisugi, T., Xie, X., Rubiales, D. & Yoneyama, K. (2014). Low strigolactone root exudation: a novel mechanism of broomrape (*Orobanche* and *Phelipanche* spp.) resistance available for faba bean breeding. *J Agric Food Chem* 62(29): 7063-7071.
Fernández-Aparicio, M., Flores, F. & Rubiales, D. (2009). Recognition of root exudates by seeds of broomrape (*Orobanche* and *Phelipanche*) species. *Ann Bot* 103(3): 423-431.
Fernández-Aparicio, M., García-Garrido, J. M., Ocampo, J. A. & Rubiales, D. (2010). Colonisation of field pea roots by arbuscular mycorrhizal fungi reduces *Orobanche* and *Phelipanche* species seed germination. *Weed Research* 50(3): 262-268.
Fernández-Aparicio, M., Yoneyama, K. & Rubiales, D. (2011). The role of strigolactones in host specificity of *Orobanche* and *Phelipanche* seed germination. *Seed Science Research* 21: 55-61.

Fernández-Aparicio, M., Flores, F. & Rubiales, D. (2016a). The effect of *Orobanche crenata* infection severity in faba bean, field pea, and grass pea productivity. *Frontiers in Plant Science* 7(1409).
Fernández-Aparicio, M., Reboud, X. & Gibot-Leclerc, S. (2016b). Broomrape weeds. Underground mechanisms of parasitism and associated strategies for their control: A review. *Frontiers in Plant Science* 7: 135.
Fowler, D. B., Limin, A. E. & Gusta, L. V. (1999). Low-temperature tolerance in cereals : Model and genetic interpretation. *Crop Science* 39: 626-633.
Freckelton, R. P. & Stephens, P. A. (2009). Predictive models of weed population dynamics. *Weed Research* 49(3): 225-232.
Gadkar, V., David-Schwartz, R., Kunik, T. & Kapulnik, Y. (2001). Arbuscular mycorrhizal fungal colonization. Factors involved in host recognition. *Plant Physiology* 127(4): 1493-1499.
García-Torres, L., Castejón-Muñoz, M., Jurado-Expósito, M. & López-Granados, F. (1996). Modelling the economics of controlling nodding broomrape (*Orobanche cernua*) in sunflower (*Helianthus annuus*). *Weed Science* 44(3): 591-595.
Gardarin, A., Dürr, C. & Colbach, N. (2011). Prediction of germination rates of weed species: relationships between germination parameters and species traits. *Ecological Modelling* 222: 626-636.
Gardarin, A., Dürr, C. & Colbach, N. (2012). Modeling the dynamics and emergence of a multispecies weed seed bank with species traits. *Ecological Modelling* 240: 123-138.
Gardarin, A. & Colbach, N. (2015). How much of seed dormancy in weeds can be explained by seed traits? *Weed Research* 55: 14-25.
Gaudin, Z. (2013). Place de l'azote dans l'interaction plante - plante parasite : *Brassica napus* L. – *Phelipanche ramosa* (L.) Pomel. PhD thesis, 452 p. Université de Nantes -Faculté des sciences et des techniques.
Gaudio, N., Escobar-Gutiérrez, A. J., Casadebaig, P., Evers, J. B., Gérard, F., Louarn, G., Colbach, N., Munz, S., Launay, M., Marrou, H., Barillot, R., Hinsinger, P., Bergez, J.-E., Combes, D., Durand, J.-L., Frak, E., Pagès, L., Pradal, C., Saint-Jean, S., Van Der Werf, W. & Justes, E. (2019). Current knowledge and future research opportunities for modeling annual crop mixtures. A review. *Agronomy for Sustainable Development* 39(2): 20.
Gauthier, M., Véronési, C., El-Halmouch, Y., Leflon, M., Jestin, C., Labalette, F., Simier, P., Delourme, R. & Delavault, P. (2012). Characterisation of resistance to branched broomrape, *Phelipanche ramosa*, in winter oilseed rape. *Crop Protection* 42: 56-63.
Gbèhounou, G., Pieterse, A. H. & Verkleij, J. A. C. (2003). Longevity of *Striga* seeds reconsidered: results of a field study on purple witchweed (*Striga hermonthica*) in Bénin. *Weed Science* 51(6): 940-946.
Gérard, F., Blitz-Frayret, C., Hinsinger, P. & Pagès, L. (2017). Modelling the interactions between root system architecture, root functions and reactive transport processes in soil. *Plant And Soil* 413(1): 161-180.
Gibot-Leclerc, S., Brault, M., Pinochet, X. & Sallé, G. (2003). Potential role of winter rape weeds in the extension of broomrape in Poitou-Charentes. *Comptes Rendus de Biologie* 326: 645-658.
Gibot-Leclerc, S. (2004). Etude épidémiologique, écophysiologique et agronomique du couple *Orobanche ramosa* L./*Brassica napus*. PhD thesis, 182 p. Université Pierre et Marie Curie.
Gibot-Leclerc, S., Corbineau, F., Sallé, G. & Côme, D. (2004). Responsiveness of *Orobanche ramosa* L. seeds to GR 24 as related to temperature, oxygen availability and water potential during preconditioning and subsequent germination. *Plant Growth Regulation* 43: 63-71.
Gibot-Leclerc, S., Pinochet, X. & Sallé, G. (2006). Orobanche rameuse (*Orobanche ramosa* L.) du colza : un risque émergent sous surveillance. *OCL* 13(2-3): 200-205.
Gibot-Leclerc, S., Sallé, G., Reboud, X. & Moreau, D. (2012). What are the traits of *Phelipanche ramosa* (L.) Pomel that contribute to the success of its biological cycle on its host *Brassica napus* L.? *Flora* 207: 512-521.
Gibot-Leclerc, S., Abdennebi-Abdemessed, N., Reibel, C. & Colbach, N. (2013a). Non-host facilitators, a new category that unexpectedly favors parasitic weeds. *Agronomy for Sustainable Development* 33: 787-793.

Gibot-Leclerc, S., Reibel, C., Dessaint, F. & Le Corre, V. (2013b). *Phelipanche ramosa* (L.) Pomel populations differ in life-history and infection response to hosts. *Flora* 208(4): 247-252.
Gibot-Leclerc, S., Reibel, C., Le Corre, V. & Dessaint, F. (2015). Unexpected fast development of branched broomrape on slow-growing Brassicaceae. *Agronomy for Sustainable Development* 35: 151-156.
Gibot-Leclerc, S., Perronne, R., Dessaint, F., Reibel, C. & Le corre, V. (2016). Assessment of phylogenetic signal in the germination ability of *Phelipanche ramosa* on *Brassicaceae* hosts. *Weed Research* 56(6): 452-461.
Gilligan, C. A. (1980). Zone of potential infection between host roots and inoculum units of *Gaeumannomyces graminis*. *Soil Biology and Biochemistry* 12(5): 513-514.
Goldwasser, Y. & Yoder, J. I. (2001). Differential induction of *Orobanche* seed germination by *Arabidopsis thaliana*. *Plant Science Letters* 160: 951-959.
Goldwasser, Y. & Rodenburg, J. (2013). Integrated agronomic management of parasitic weed seed banks. In *Parasitic Orobanchaceae : Parasitic mechanisms and control strategies*, 393-413 (Eds D. M. Joel, J. Gressel and L. J. Musselman). Springer-Verlag Berlin Heidelberg.
Gouzy, D. (2009). Contribution à l'optimisation de l'association entre deux espèces, le pois et la fétuque portegraine : caractérisation de la levée et de la croissance précoce. In *Agrocampus Ouest*, Engineer in horticulture thesis, 61 p. ESA.
Gregory, P. J., Palta, J. A. & Batts, G. R. (1995). Root systems and root:mass ratio-carbon allocation under current and projected atmospheric conditions in arable crops. *Plant And Soil* 187(2): 221-228.
Grenz, J. H., Manschadi, A. M., De Voil, P., Meinke, H. & Sauerborn, J. (2005a). Assessing strategies for *Orobanche* sp. control using a combined seedbank and competition model. *Agronomy Journal* 97: 1551-1559.
Grenz, J. H., Manschadi, A. M., Uygur, F. N. & Sauerborn, J. (2005b). Effects of environment and sowing date on the competition between faba bean (*Vicia faba*) and the parasitic weed *Orobanche crenata*. *Field Crops Research* 93(2): 300-313.
Grenz, J. H., Iştoc, V. A., Manschadi, A. M. & Sauerborn, J. (2008). Interactions of sunflower *(Helianthus annuus*) and sunflower broomrape (*Orobanche cumana*) as affected by sowing date, resource supply and infestation level. *Field Crops Research* 107(2): 170-179.
Guichard, L., Dedieu, F., Jeuffroy, M.-H., Meynard, J.-M., Reau, R. & Savini, I. (2017). Le plan Ecophyto de réduction d'usage des pesticides en France : décryptage d'un échec et raisons d'espérer. *Cahiers Agricultures* 26(1): 14002.
Guinet, M. (2019). Quantification des flux d'azote induits par les cultures de légumineuses et étude de leurs déterminants : comparaison de dix espèces de légumineuses à graines. PhD thesis, 251 p. Université de Bourgogne Franche-Comté.
Gummerson, R. J. (1986). The effect of constant temperatures and osmotic potentials on the germination of sugar beet. *Journal of Experimental Botany* 37: 729-741.
Gutteridge, R. J., Jenkyn, J. F. & Bateman, G. L. (2006). Effects of different cultivated or weed grasses, grown as pure stands or in combination with wheat, on take-all and its suppression in subsequent wheat crops. *Plant Pathology* 55(5): 696-704.
Haidar, M. A., Bibi, W. & Sidahmed, M. M. (2003). Response of branched broomrape (*Orobanche ramosa*) growth and development to various soil amendments in potato. *Crop Protection* 22(2): 291-294.
Hasegawa, S. & Sato, T. (1987). Water uptake by roots in cracks and water movement in clayey subsoil. *Soil Science* 143(5): 381.
Hauggaard-Nielsen, H., Jørnsgaard, B., Kinane, J. & Jensen, E. (2008). Grain legume - cereal intercropping: The practical application of diversity, competition and facilitation in arable and organic cropping systems. *Renewable Agriculture and Food Systems* 23(1): 3-12.
Heide-Jørgensen, H. S. (2013). Introduction: The parasitic syndrome in higher plants. In *Parasitic Orobanchaceae : Parasitic mechanisms and control strategies*, 1-18 (Eds D. M. Joel, J. Gressel and L. J. Musselman). Springer-Verlag Berlin Heidelberg.
Hibberd, J. M., Quick, W. P., Press, M. C. & Scholes, J. D. (1998). Can source–sink relations explain responses of tobacco to infection by the root holoparasitic angiosperm *Orobanche cernua*? *Plant, Cell & Environment* 21(3): 333-340.

Holst, N., Rasmussen, I. A. & Bastiaans, L. (2007). Field weed population dynamics: a review of model approaches and applications. *Weed Research* 47: 1-14.
Hosseini, P., Ahmadvand, G., Oveisi, M., Morshedi, P. & Gonzalez-Andujar, J. L. (2017). A modelling approach for predicting the initial phase of Egyptian broomrape (*Phelipanche aegyptiaca*) parasitism in potato. *Crop Protection* 100: 51-56.
Jégo, G., Chantigny, M., Pattey, E., Bélanger, G., Rochette, P., Vanasse, A. & Goyer, C. (2014). Improved snow-cover model for multi-annual simulations with the STICS crop model under cold, humid continental climates. *Agricultural and Forest Meteorology* 195-196: 38-51.
Jestin, C., Boulet, C., Molenat, D., Leflon, M., Benharrat, H., Baraton, E., Legros, S. & Simier, P. (2014). Évaluation de l'efficacité de différentes pratiques culturales dans la lutte contre l'orobanche rameuse par une méthode de quantification du stock grainier et cartographie du parasite sur le territoire français. *Innovations Agronomiques* 34: 157-173.
Jestin, C. (2017). Orobanche rameuse du colza : la plante parasite exige une grande attention. *Perspectives agricoles* 444: 28-32.
Jeuffroy, M.-H., Casadebaig, P., Debaeke, P., Loyce, C. & Meynard, J.-M. (2014). Agronomic model uses to predict cultivar performance in various environments and cropping systems. A review. *Agronomy for Sustainable Development* 34(1): 121-137.
Joel, D. M. (2013a). Seed production and dispersal in the Orobanchaceae. In *Parasitic Orobanchaceae : Parasitic mechanisms and control strategies*, 143-146 (Eds D. M. Joel, J. Gressel and L. J. Musselman). Springer-Verlag Berlin Heidelberg.
Joel, D. M. (2013b). The haustorium and the life cycles of parasitic Orobanchaceae. In *Parasitic Orobanchaceae : Parasitic mechanisms and control strategies*, 21-23 (Eds D. M. Joel, J. Gressel and L. J. Musselman). Springer-Verlag Berlin Heidelberg.
Joel, D. M. (2013c). The seed and the seedling. In *Parasitic Orobanchaceae : Parasitic mechanisms and control strategies*, 147-165 (Eds D. M. Joel and H. Bar). Springer-Verlag Berlin Heidelberg.
Joel, D. M. (2013d). Functional structure of the mature haustorium. In *Parasitic Orobanchaceae : Parasitic mechanisms and control strategies*, 25-60 (Eds D. M. Joel, J. Gressel and L. J. Musselman). Springer-Verlag Berlin Heidelberg.
Keating, B. A., Carberry, P. S., Hammer, G. L., Probert, M. E., Robertson, M. J., Holzworth, D., Huth, N. I., Hargreaves, J. N. G., Meinke, H., Hochman, Z., McLean, G., Verburg, K., Snow, V., Dimes, J. P., Silburn, M., Wang, E., Brown, S., Bristow, K. L., Asseng, S., Chapman, S., McCown, R. L., Freebairn, D. M. & Smith, C. J. (2003). An overview of APSIM, a model designed for farming systems simulation. *European Journal of Agronomy* 18(3): 267-288.
Kebreab, E. & Murdoch, A. J. (1999). A quantitative model for loss of primary dormancy and induction of secondary dormancy in imbibed seeds of *Orobanche* spp. *Journal of Experimental Botany* 50(331): 211-219.
Kiær, L. P., Weisbach, A. N. & Weiner, J. (2013). Root and shoot competition: a meta-analysis. *Journal of Ecology* 101(5): 1298-1312.
Kirkegaard, J. A. & Sarwar, M. (1998). Biofumigation potential of brassicas. *Plant And Soil* 201(1): 71-89.
Kutschera, L. & Lichtenegger, E. (1960). *Wurzelatlas mitteleuropäischer Ackerunkräuter und Kulturpflanzen.* Frankfurt am Main: DLG-Verlag.
Labrousse, P., Delmail, D., Arnaud, M. C. & Thalouarn, P. (2010). Mineral nutrient concentration influences sunflower infection by broomrape (Orobanche cumana). *Botany* 88: 839-849.
Lacoste, M. & Powles, S. (2017). RIM: Anatomy of a weed management decision support system for adaptation and wider application. *Weed Science* 63(3): 676-689.
Le Corre, V., Reibel, C. & Gibot-Leclerc, S. (2014). Development of microsatellite markers in the branched broomrape *Phelipanche ramosa* l. (pomel) and evidence for host-associated genetic divergence. *International Journal of Molecular Sciences* 15: 994-1002.
Lê, S., Josse, J. & Husson, F. (2008). FactoMineR: An R package for multivariate analysis. *Journal of Statistical Software* 25(1): 1-18.
Lecomte, C., Giraud, A. & Aubert, V. (2003). Testing a predicting model for frost resistance of winter wheat under natural conditions. *Agronomie* 23(1): 51-66.

Liebman, M. & Gallandt, E. R. (1997). Many little hammers: Ecological management of crop-weed interactions. In *Ecology in agriculture*, 291-343 (Ed L. E. Jackson). Academic Press.
Lins, R. D., Colquhoun, J. B. & Mallory-Smith, C. A. (2007). Effect of small broomrape (*Orobanche minor*) on red clover growth and dry matter partitioning. *Weed Science* 55(5): 517-520.
López-Granados, F. & García-Torres, L. (1996). Effects of environmental factors on dormancy and germination of crenate broomrape (*Orobanche crenata*). *Weed Science* 44: 284-289.
López-Granados, F. & García-Torres, L. (1997). Modelling the demography of crenate broomrape (*Orobanche crenata*) as affected by broadbean (*Vicia faba*) cropping frequency and planting date. *Weed Science* 45: 261-268.
López-Granados, F. & García-Torres, L. (1999). Longevity of crenate broomrape (*Orobanche crenata*) seed under soil and laboratory conditions. *Weed Science* 47(2): 161-166.
Louarn, J., Carbonne, F., Delavault, P., Bécard, G. & Rochange, S. (2012). Reduced germination of *Orobanche cumana* seeds in the presence of arbuscular mycorrhizal fungi or their exudates. *PLOS ONE* 7(11): e49273.
Lynch, J. P., Nielsen, K. L., Davis, R. D. & Jablokow, A. G. (1997). SimRoot: Modelling and visualization of root systems. *Plant And Soil* 188(1): 139-151.
Ma, Z., Guo, D., Xu, X., Lu, M., Bardgett, R. D., Eissenstat, D. M., McCormack, M. L. & Hedin, L. O. (2018). Evolutionary history resolves global organization of root functional traits. *Nature* 555: 94.
Maillot, T., Mion, M., Vioix, J.-B. & Colbach, N. (2019). Conception de systèmes de cultures par algorithmes d'optimisation. In *Gestion des adventices dans un contexte de changement - Séminaire CoSAC*, Paris, France.
Malagoli, P. & Le Deunff, E. (2014). An updated model for nitrate uptake modelling in plants. II. Assessment of active root involvement in nitrate uptake based on integrated root system age: measured versus modelled outputs. *Ann Bot* 113(6): 1007-1019.
Mangnus, E. M., Stommen, P. L. A. & Zwanenburg, B. (1992). A standardized bioassay for evaluation of potential germination stimulants for seeds of parasitic weeds. *Journal of Plant Growth Regulation* 11(2): 91-98.
Manschadi, A. M., Sauerborn, J. & Stützel, H. (2001). Quantitative aspects of *Orobanche crenata* infestation in faba beans as affected by abiotic factors and parasite soil seedbank. *Weed Research* 41(4): 311-324.
Manschadi, A. M., Wang, E., J. Robertson, M., Meinke, H. & Sauerborn, J. (2003). Development of a parasite module in APSIM - Case study: the parasitic weed *Orobanche crenata* infesting faba bean. In *11th Australian Agronomy Conference*, Geelong, Victoria: Australian Society of Agronomy.
Manschadi, A. M., Hargreaves, J. N. G., Grenz, J., DeVoil, P. & Meinke, H. (2004). Simulating damage effects of parasitic weeds in APSIM: a generic cohort-based approach. In *Fourth International Crop Science Conference*, Brisbane, Australia.
Marie, G. & Simioni, G. (2014). Extending the use of ecological models without sacrificing details: a generic and parsimonious meta-modelling approach. *Methods in Ecology and Evolution* 5(9): 934-943.
Martre, P., Quilot-Turion, B., Luquet, D., Memmah, M.-M. O.-S., Chenu, K. & Debaeke, P. (2015). Chapter 14 - Model-assisted phenotyping and ideotype design. In *Crop Physiology (Second Edition)*, 349-373 (Eds V. O. Sadras and D. F. Calderini). San Diego: Academic Press.
Mauromicale, G., Monaco, A. L., Longo, A. M. G. & Restuccia, A. (2005). Soil solarization, a nonchemical method to control branched broomrape (*Orobanche ramosa*) and improve the yield of greenhouse tomato. *Weed Science* 53(6): 877-883.
Mauromicale, G., Monaco, A. L. & Longo, A. M. G. (2008). Effect of branched broomrape (*Orobanche ramosa*) infection on the growth and photosynthesis of tomato. *Weed Science* 56(4): 574-581.
Metcalfe, H., Milne, A. E., Coleman, K., Murdoch, A. J. & Storkey, J. (2019). Modelling the effect of spatially variable soil properties on the distribution of weeds. *Ecological Modelling* 396: 1-11.
Mézière, D., Lucas, P., Granger, S. & Colbach, N. (2013). Does integrated weed management affect the risk of crop diseases? A simulation case study with a grass weed and a soil-borne cereal disease. *European Journal of Agronomy* 47: 33-43.

Mézière, D., Petit, S., Granger, S., Biju-Duval, L. & Colbach, N. (2015). Developing a set of simulation-based indicators to assess harmfulness and contribution to biodiversity of weed communities in cropping systems. *Ecological Indicators* 48: 157-170.

Miegel, D., Hayton, D. & Matthews, J. (2013). Banched broomrape seed production. *Compendium of branched broomrape research. Section 3. Seed biology. A compilation of research reports from the branched broomrape eradication program South Australia.* , 13-15: Government of South Australia. https://data.environment.sa.gov.au/Content/Publications/BBR_Res_Comp_3.pdf (accessed on 14.10.19).

Molenat, D., Boulet, C. & Leflon, M. (2013). Introduction des cultures pièges ou non-hôtes dans les systèmes culturaux afin de lutter contre l'orobanche rameuse : du laboratoire au terrain. In *Colloque : l'orobanche rameuse en France*, Poitier, France.

Moreau, D., Milard, G. & Munier-Jolain, N. (2013). A plant nitrophily index based on plant leaf area response to soil nitrogen availability. *Agronomy for Sustainable Development* 33(4): 809-815.

Moreau, D., Busset, H., Matejicek, A. & Munier-Jolain, N. (2014). The ecophysiological determinants of nitrophily in annual weed species. *Weed Research* 54(4): 335-346.

Moreau, D., Pivato, B., Bru, D., Busset, H., Deau, F., Faivre, C., Matejicek, A., Strbik, F., Philippot, L. & Mougel, C. (2015). Plant traits related to nitrogen uptake influence plant-microbe competition. *Ecology* 96(8): 2300-2310.

Moreau, D., Gibot-Leclerc, S., Girardin, A., Pointurier, O., Reibel, C., Strbik, F., Fernandez-Aparicio, M. & Colbach, N. (2016). Trophic relationships between the parasitic plant species *Phelipanche ramosa* (L.) and different hosts depending on host phenological stage and host growth rate. *Frontiers in Plant Science* 7.

Moreau, D., Abiven, F., Busset, H., Matejicek, A. & Pagès, L. (2017). Effects of species and soil-nitrogen availability on root system architecture traits – study on a set of weed and crop species. *Annals Of Applied Biology* 171(1): 103-116.

Moreau, D., Busset, H., Matejicek, A., Perrot, C. & Colbach, N. (2018). The response of weed species to water stress. In *18th European Weed Research Society Symposium*, Ljubljana, Slovenia.

Moreau, D., Bardgett, R. D., Finlay, R. D., Jones, D. L. & Philippot, L. (2019). A plant perspective on nitrogen cycling in the rhizosphere. *Functional Ecology* 33: 540-552.

Moreau, D., Pointurier, O., Perthame, L., Beaudoin, N., Villerd, J. & Colbach, N. (in prep.). Integrating crop-weed competition for nitrogen in the FLORSYS weed-dynamics simulation model.

Morlon, P. (2010). Adventice. In *Les mots de l'agronomie.* https://lorexplor.istex.fr/mots-agronomie.fr/index.php/Adventice (accessed on 17.09.18)

Mortensen, Bastiaans & Sattin (2000). The role of ecology in the development of weed management systems: an outlook. *Weed Research* 40(1): 49-62.

Munier-Jolain, N. M., Guyot, S. H. M. & Colbach, N. (2013). A 3D model for light interception in heterogeneous crop:weed canopies. Model structure and evaluation. *Ecological Modelling* 250: 101-110.

Munier-Jolain, N. M., Collard, A., Busset, H., Guyot, S. H. M. & Colbach, N. (2014). Investigating and modelling the morphological plasticity of weeds in multi-specific canopies. *Field Crops Research* 155: 90-98.

Murdoch, A. J. & Kebreab, E. (2013). Germination ecophysiology. In *Parasitic Orobanchaceae : Parasitic mechanisms and control strategies*, 195-219 (Eds D. M. Joel, J. Gressel and L. J. Musselman). Springer-Verlag Berlin Heidelberg.

Niu, G.-Y., Yang, Z.-L., Mitchell, K. E., Chen, F., Ek, M. B., Barlage, M., Kumar, A., Manning, K., Niyogi, D., Rosero, E., Tewari, M. & Xia, Y. (2011). The community Noah land surface model with multiparameterization options (Noah-MP): 1. Model description and evaluation with local-scale measurements. *Journal of Geophysical Research: Atmospheres* 116(D12).

Norris, R. F. (2005). Ecological bases of interactions between weeds and organisms in other pest categories. *Weed Science* 53: 909-913.

Novotny, V. (1999). Diffuse pollution from agriculture — A worldwide outlook. *Water Science and Technology* 39(3): 1-13.

Oerke, E.-C. (2006). Crop losses to pests. *Journal of Agricultural Science* 144: 31-43

Pagès, L. (2011). Links between root developmental traits and foraging performance. *Plant, Cell & Environment* 34(10): 1749-1760.
Pagès, L., Bruchou, C. & Garre, S. (2012). Links between root length density profiles and models of the root system architecture. *Vadose Zone Journal* 11(4).
Pagès, L., Bécel, C., Boukcim, H., Moreau, D., Nguyen, C., Sterckeman, T. & Voisin, A.-S. (2014). Calibration and evaluation of ArchiSimple, a parsimonious model of the root system architecture. *Ecological Modeling*: in press.
Pagès, L. & Picon-Cochard, C. (2014). Modelling the root system architecture of Poaceae. Can we simulate integrated traits from morphological parameters of growth and branching? *New Phytologist* 204: 149-158.
Pagès, L. & Kervella, J. (2018). Seeking stable traits to characterize the root system architecture. Study on 60 species located at two sites in natura. *Ann Bot* 122(1): 107-115.
Pagès, L., Pointurier, O., Moreau, D., Voisin, A. S. & Colbach, N. (submitted). Simplifying an individual-based 3D root architecture model with virtual experiments. *Plant And Soil*.
Pannell, D. J., Stewart, V., Bennett, A., Monjardino, M., Schmidt, C. & Powles, S. B. (2004). RIM: a bioeconomic model for integrated weed management of *Lolium rigidum* in Western Australia. *Agricultural Systems* 79(3): 305-325.
Papy, F. (2013). Système de culture. In *Les mots de l'agronomie*. https://lorexplor.istex.fr/mots-agronomie.fr/index.php/Syst%C3%A8me_de_culture (accessed on 17.09.18)
Parker, C. & Riches, C. (1993). *Parasitic Weeds of the World: Biology and Control*. Wallingford, UK: CAB International.
Parker, C. (2013). The parasitic weeds of the Orobanchaceae. In *Parasitic Orobanchaceae : Parasitic mechanisms and control strategies*, 313-344 (Eds D. M. Joel, J. Gressel and L. J. Musselman). Springer-Verlag Berlin Heidelberg.
Parsons, D. J., Benjamin, L. R., Clarke, J., Ginsburg, D., Mayes, A., Milne, A. E. & Wilkinson, D. J. (2009). Weed Manager—A model-based decision support system for weed management in arable crops. *Computers and Electronics in Agriculture* 65(2): 155-167.
Pedersen, A., Zhang, K., Thorup-Kristensen, K. & Jensen, L. S. (2010). Modelling diverse root density dynamics and deep nitrogen uptake—A simple approach. *Plant And Soil* 326(1): 493-510.
Pérez-de-Luque, A., Flores, F. & Rubiales, D. (2016). Differences in crenate broomrape parasitism dynamics on three legume crops using a thermal time model. *Frontiers in Plant Science* 7: 1910.
Perronne, R., Gibot-Leclerc, S., Dessaint, F., Reibel, C. & Le Corre, V. (2017). Is induction ability of seed germination of *Phelipanche ramosa* phylogenetically structured among hosts? A case study on *Fabaceae* species. *Genetica* 145(6): 481-489.
Perthame, L., Colbach, N., Brunel-Muguet, S., Busset, H., Lilley, J. M., Matejicek, A. & Moreau, D. (submitted). How to quantify the nitrogen demand of individual plants in heterogeneous canopies? Case study with crop-weed canopies. *Ann Bot*.
Petit, S., Boursault, A., Le Guilloux, M., Munier-Jolain, N. & Reboud, X. (2011). Weeds in agricultural landscapes. A review. *Agronomy for Sustainable Development* 31(2): 309-317.
Pointurier, O., Gibot-Leclerc, S., Moreau, D., Reibel, C., Strbik, F. & Colbach, N. (2018). Modelling cropping system effects on branched broomrape dynamics in interaction with weeds. In *XV^e European Society for Agronomy Congress*, Geneva, Switzerland.
Pointurier, O., Gibot-Leclerc, S., Le Corre, V., Reibel, C., Strbik, F. & Colbach, N. (2019). Intraspecific seasonal variation of dormancy and mortality of branched broomrape seeds. *Weed Research*.
Pointurier, O., Moreau, D. & Colbach, N. (submission in progress). Individual-based 3D modelling of root systems in heterogeneous plant canopies at the multiannual scale. Case study with a weed dynamics model.
Postma, J. A. & Lynch, J. P. (2012). Complementarity in root architecture for nutrient uptake in ancient maize/bean and maize/bean/squash polycultures. *Ann Bot* 110(2): 521-534.
Postma, J. A., Kuppe, C., Owen, M. R., Mellor, N., Griffiths, M., Bennett, M. J., Lynch, J. P. & Watt, M. (2017). OpenSimRoot: widening the scope and application of root architectural models. *New Phytologist* 215(3): 1274-1286.

Potier, D. (2014). Pesticides et agro-écologie. Les Champs du possible. 252 p. http://agriculture.gouv.fr/rapport-de-dominique-potier-pesticides-et-agro-ecologie-les-champs-du-possible (accessed on 08.10.18).
Press, M. C. & Phoenix, G. K. (2005). Impacts of parasitic plants on natural communities. *New Phytol* 166(3): 737-751.
Prider, J., Watling, J. & Facelli, J. M. (2009). Impacts of a native parasitic plant on an introduced and a native host species: implications for the control of an invasive weed. *Ann Bot* 103(1): 107-115.
Prider, J., Correll, R. & Warren, P. (2012). A model for risk-based assessment of *Phelipanche mutelii* (branched broomrape) eradication in fields. *Weed Research* 52(6): 526-534.
Prider, J. & Craig, A. (2013). Seasonal changes in germination response of buried branched broomrape seeds. *Compendium of branched broomrape research. Section 3. Seed biology. A compilation of research reports from the branched broomrape eradication program South Australia.*, 41-47: Government of South Australia. https://data.environment.sa.gov.au/Content/Publications/BBR_Res_Comp_3.pdf (accessed on 14.10.19).
Prider, J., Ophel Keller, K. & McKay, A. (2013). Molecular diagnosis of parasite seed banks. In *Parasitic Orobanchaceae : Parasitic mechanisms and control strategies*, 357-368 (Eds D. M. Joel, J. Gressel and L. J. Musselman). Springer-Verlag Berlin Heidelberg.
Prider, J. (2015). The reproductive biology of the introduced root holoparasite *Orobanche ramosa* subsp. *mutelii* (Orobanchaceae) in South Australia. *Australian Journal of Botany* 63(5): 426-434.
Qasem, J. R. & Foy, C. L. (2007). Screening studies on the host range of branched broomrape (*Orobanche ramosa*). *The Journal of Horticultural Science and Biotechnology* 82(6): 885-892.
R Core Team (2016). R: A language and environment for statistical computing. R Foundation for Statistical Computing, Vienna, Austria. URL http://www.R-project.org/.
R Core Team (2019). R: A Language and Environment for Statistical Computing. Vienna: R Foundation for Statistical Computing. https://www.R-project.org (accessed on 08.10.18)
Raleigh, M. S., Landry, C. C., Hayashi, M., Quinton, W. L. & Lundquist, J. D. (2013). Approximating snow surface temperature from standard temperature and humidity data: New possibilities for snow model and remote sensing evaluation. *Water Resources Research* 49(12): 8053-8069.
Raun, W. R. & Johnson, G. V. (1999). Improving nitrogen use efficiency for cereal production. *Agronomy Journal* 91(3): 357-363.
Regan, T. J., Chadès, I. & Possingham, H. P. (2011). Optimally managing under imperfect detection: a method for plant invasions. *Journal of Applied Ecology* 48(1): 76-85.
Renton, M. & Chauhan, B. S. (2017). Modelling crop-weed competition: Why, what, how and what lies ahead? *Crop Protection* 95(Supplement C): 101-108.
Réseau de Réflexion et de Recherches sur les Résistances aux Pesticides (2018). Cas de résistance aux PPP en France. https://www.r4p-inra.fr/fr/statut-des-resistances-en-france/ (accessed on 08.10.18).
Roberts, D. W. A. (1979). Duration of hardening and cold hardiness in winter wheat. *Canadian Journal of Botany* 57: 1511-1517.
Roger-Estrade, J., Richard, G., Caneill, J., Boizard, H., Coquet, Y., Defossez, P. & Manichon, H. (2004). Morphological characterisation of soil structure in tilled fields: from a diagnosis method to the modelling of structural changes over time. *Soil and Tillage Research* 79(1): 33-49.
Rubiales, D., Fernandez-Aparicio, M., Wegmann, K. & Joel, D. M. (2009). Revisiting strategies for reducing the seedbank of *Orobanche* and *Phelipanche* spp. *Weed Research* 49: 23-33.
Rubiales, D. & Fernández-Aparicio, M. (2012). Innovations in parasitic weeds management in legume crops. A review. *Agronomy for Sustainable Development* 32(2): 433-449.
Saatkamp, A., Poschlod, P. & Venable, D. L. (2014). The functional role of soil seed banks in natural communities. In *Seeds: the ecology of regeneration in plant communities*, 263-295.
Saltelli, A. (2002). Making best use of model evaluations to compute sensitivity indices. *Computer Physics Communications* 145(2): 280-297.

Saltelli, A., Ratto, M., Andres, T., Campolongo, F., Cariboni, J., Gatelli, D., Saisana, M. & Tarantola, S. (2008a). Experimental designs. In *Global sensitivity analysis. The primer.*, 53-107: John Wiley & Sons, Ltd.
Saltelli, A., Ratto, M., Andres, T., Campolongo, F., Cariboni, J., Gatelli, D., Saisana, M. & Tarantola, S. (2008b). Introduction to sensitivity analysis. In *Global sensitivity analysis. The primer.*, 1-51: John Wiley & Sons, Ltd.
Samejima, H. & Sugimoto, Y. (2018). Recent research progress in combatting root parasitic weeds. *Biotechnology & Biotechnological Equipment* 32(2): 221-240.
Sánchez, M., Manzoli, O. L. & Guimarães, L. J. N. (2014). Modeling 3-D desiccation soil crack networks using a mesh fragmentation technique. *Computers and Geotechnics* 62: 27-39.
Schneeweiss, G. M. (2013). Phylogenetic relationships and evolutionary trends in Orobanchaceae. In *Parasitic Orobanchaceae : Parasitic mechanisms and control strategies*, 243-265 (Eds D. M. Joel, J. Gressel and L. J. Musselman). Springer-Verlag Berlin Heidelberg.
Schnell, H., Kunisch, M., Saxena, M. & Sauerborn, J. (1996). Simulation of the seed bank dynamics of *Orobanche crenata* forsk. in some crop rotations common in Northern Syria. *Experimental Agriculture* 32(4): 395-403.
Sebillote, M. (1990). Système de culture, un concept operatoire pour les agronomes. In *Les systèmes de culture*, 165-196 (Eds L. Combe and D. Picard). Paris (France): INRA.
Seneze J. (2018). Etude de la diversité intra- et inter-spécifique de l'architecture racinaire des légumineuses, en lien avec la croissance et la nutrition azotée. In *INRA Dijon*, Engineer in Agronomy thesis, 57 p. UniLaSalle, Beauvais.
Shishkova, S., Rost, T. L. & Dubrovsky, J. G. (2008). Determinate root growth and meristem maintenance in angiosperms. *Ann Bot* 101(3): 319-340.
Siberchicot, A., Julien-Laferrière, A., Dufour, A.-B., Thioulouse, J. & Dray, S. (2017). adegraphics: An s4 lattice-based package for the representation of multivariate data. *R Journal* 9: 198-212.
Simier, P., Boulet, C., Voisin, M., Quenouille, J., Molenat, D., Duffe, P., Leflon, M., Legros, S., Dauvergne, X., Benharrat, H., Delgrange, S., Schmidt, J., Pouvreau, J. B., Jestin, C., Delourme, R. & Delavault, P. (2013). Variabilité génétique de l'orobanche rameuse et son spectre d'hôtes In *Colloque : l'orobanche rameuse en France*, Poitier, France.
Stojanova, B., Delourme, R., Duffé, P., Delavault, P. & Simier, P. (2019). Genetic differentiation and host preference reveal non-exclusive host races in the generalist parasitic weed *Phelipanche ramosa*. *Weed Research* 59(2): 107-118.
Tardieu, F. (1994). Growth and functioning of roots and of root systems subjected to soil compaction. Towards a system with multiple signalling? *Soil and Tillage Research* 30(2): 217-243.
Tardy, F., Damour, G., Dorel, M. & Moreau, D. (2017). Trait-based characterisation of soil exploitation strategies of banana, weeds and cover plant species. *PLOS ONE* 12(3): e0173066.
Terres Inovia (2018a). Classement des variétés de colza vis-à-vis de l'orobanche rameuse - 2006 à 2018. http://www.terresinovia.fr/fileadmin/cetiom/regions/Ouest/InfoTK/2018/co_classement_var_orobanche_2006-2018.pdf (accessed on 08.10.18)
Terres Inovia (2018b). Enquêtes de surveillance. Questionnaire orobanche. http://www.terresinovia.fr/orobanche/carte.php (accessed on 08.10.18)
Thorsen, S. M., Roer, A.-G. & Oijen, M. v. (2010). Modelling the dynamics of snow cover, soil frost and surface ice in Norwegian grasslands. *Polar Research* 29(1): 110-126.
Timko, M. P. & Scholes, J. D. (2013). Host reaction to attack by root parasitic plants. In *Parasitic Orobanchaceae : Parasitic mechanisms and control strategies*, 115-141 (Eds D. M. Joel, J. Gressel and L. J. Musselman). Springer-Verlag Berlin Heidelberg.
Tippe, D. E., Rodenburg, J., van Ast, A., Anten, N. P. R., Dieng, I., Kayeke, J., Cissoko, M. & Bastiaans, L. (2017). Delayed or early sowing: Timing as parasitic weed control strategy in rice is species and ecosystem dependent. *Field Crops Research* 214: 14-24.
Trnka, M., Kocmánková, E., Balek, J., Eitzinger, J., Ruget, F., Formayer, H., Hlavinka, P., Schaumberger, A., Horáková, V., Možný, M. & Žalud, Z. (2010). Simple snow cover model for agrometeorological applications. *Agricultural and Forest Meteorology* 150(7): 1115-1127.

Turral, H., Burke, J. & Faurès, J. M. (2011). Climate change, water and food security. *FAO water reports*, 200 Rome: FAO. http://www.fao.org/tempref/docrep/fao/meeting/013/ai783e.pdf (accessed on 14.10.19).
UCLA: Statistical Consulting Group (2015). Nonlinear Regression in SAS. http://www.ats.ucla.edu/stat/sas/library/SASNLin_os.htm (accessed on 27/08/15)
Union des Industries de la Protection des Plantes (2018). Repères 2017-2018. http://www.uipp.org/Ressources/Publications/?tag=11 (accessed on 08.10.18).
Van Hezewijk, M. J., Linker, K. H., López-Granados, F., Al-Menoufi, O. A., García-Torres, L., Saxena, M. C., Verkleij, J. A. C. & Pieterse, A. H. (1994). Seasonal changes in germination response of buried seeds of *Orobanche crenata* Forsk. *Weed Research* 34(5): 369-376.
Van Inghelandt, B., Queyrel, W., Cavan, N., Colas, F., Guyot, B. & Colbach, N. (2019). Combiner expertise et modèles en ateliers de co-conception de systèmes de culture pour une gestion durable des adventices : apports méthodologiques et perspectives. In *Gestion des adventices dans un contexte de changement - Séminaire CoSAC*, Paris, France.
Van Mourik, T., Stomph, T. J. & Westerman, P. (2003). Estimating *Striga hermonthica* seed mortality under field conditions. *Aspect of Applied Biology* 69: 1-8.
Vico, G., Hurry, V. & Weih, M. (2014). Snowed in for survival: Quantifying the risk of winter damage to overwintering field crops in northern temperate latitudes. *Agricultural and Forest Meteorology* 197: 65-75.
Villa-Vialaneix, N., Follador, M., Ratto, M. & Leip, A. (2012). A comparison of eight metamodeling techniques for the simulation of N2O fluxes and N leaching from corn crops. *Environmental Modelling & Software* 34: 51-66.
Violle, C., Navas, M.-L., Vile, D., Kazakou, E., Fortunel, C., Hummel, I. & Garnier, E. (2007). Let the concept of trait be functional! *Oikos* 116(5): 882-892.
Weiner, J. (2004). Allocation, plasticity and allometry in plants. *Perspectives in Plant Ecology, Evolution and Systematics* 6(4): 207-215.
Westwood, J. H. (2000). Characterization of the *Orobanche–Arabidopsis* system for studying parasite–host interactions. *Weed Science* 48(6): 742-748.
Wilson, J. B. (1988a). Shoot competition and root competition. *Journal of Applied Ecology* 25(1): 279-296.
Wilson, J. B. (1988b). A review of evidence on the control of shoot: root ratio, in relation to models. *Ann Bot* 61(4): 433-449.
Yoneyama, K., Ruyter-Spira, C. & Bouwmeester, H. (2013). Induction of germination. In *Parasitic Orobanchaceae : Parasitic mechanisms and control strategies*, 167-194 (Eds D. M. Joel, J. Gressel and L. J. Musselman). Springer-Verlag Berlin Heidelberg.
Zehhar, N., Labrousse, P., Arnaud, M.-C., Boulet, C., Bouya, D. & Fer, A. (2003). Study of resistance to *Orobanche ramosa* in host (oilseed rape and carrot) and non-host (maize) plants. *European Journal of Plant Pathology* 109(1): 75-82.

Annexes

In the following sections, population O and H refer to *Phelipanche ramosa* seeds collected on oilseed rape (*Brassica napus*) and hemp (*Cannabis sativa*) respectively. GR24 is a growth regulator used to trigger broomrape seed germination.

A.1. Annexes du chapitre 2

A.1.1. Additional experiments

A.1.1.1. Testing soil-sand mixtures for seed bags

Prior to the experiments, different mixtures of soil and sand were tested to optimize seed recovery from the buried seed bags without affecting germinability. A hundred (100) *P. ramosa* seeds collected on hemp were buried in bags, either with 200 g of a soil-sand mixture (1/3 sand and 2/3 soil), or with 40 g of sand, with two bags per mixture. The soil was taken from the INRA Dijon experimental station (47°14'26″N, 05°06'51″E, 220 m; Côte d'Or, France) and sterilized in an autoclave at 121 °C for 3 hours. Seeds were recovered following the protocol of Brault-Hernandez (2006)**.** With the sand-soil mixtures, 44-66 seeds were recovered, depending on the repetition. When seeds were mixed with only sand, 100% of the initial seeds were recovered. Germination tests were carried out on the recovered seeds after conditioning according to the protocol in section 2.2.3.5. The results were compared to a control where seeds were directly assessed for germination without the retrieval protocol being applied.

Table S1: Effect of the seed retrieval protocol on *P. ramosa* seed germination

	Seed bag filled with		Control
	1/3 sand, 2/3 soil	sand	
Number of seeds per bag	100	100	NA
Number of retrieved seeds	44-66[£]	100	134[$]
Number of germinated seeds	36-58[£]	85	107
Proportion of germinated seeds¤	0.82-0.88[£]	0.85	0.80

[$]Number of seeds in the control seed lot

[£]Two replicates in the soil-sand mixture treatment

¤Proportion of germinated seeds among retrieved seeds

A.1.1.2. Effect of conditioning seeds on viability and dormancy

Every six months (16 March and 14 September 2015 for population O, and 13 April and 19 October 2015 for population H), one additional basket was excavated for each population, and germination and viability tests were carried out without conditioning to assess the impact of this procedure on seed germination and viability results. The effect of conditioning on seed viability (germinated seeds and ungerminated seeds reacting to tetrazolium) and germinability (total germination rate) was tested with a generalized linear model using a logit transformation and a binomial distribution glm function of R (R Core Team, 2015). The effect of conditioning on germination parameters (time to first germination, time to mid-germination and shape parameter) was tested with a linear model lm function of R (R Core Team, 2015).

Table S 2: Effect of seed conditioning on *P. ramosa* seed viability and germination for population O and H

Excavation date and parameter	***Phelipanche ramosa* population**					
	O			**H**		
	p-value	Comparison of means		p-value	Comparison of means	
		With conditioning	Without conditioning		With conditioning	Without conditioning
Seed viability – proportion of germinated seeds and ungerminated seeds reacting to tetrazolium						
16/03/2015 or 13/04/2015[$]	**0.0350**	0.972 A	0.935 B	**0.0438**	0.952 A	0.909 B
14/09/2015 or 19/10/2015	0.748	**0.949 A**	**0.943 A**	**0.0284**	0.931 B	0.970 A
Total germination rate						
16/03/2015 or 13/04/2015	0.432	**0.0730 A**	**0.0566 A**	0.838	**0.834 A**	**0.841 A**
14/09/2015 or 19/10/2015	0.452	**0.943 A**	**0.957 A**	NA[§]	**0.774**	**0.960**
Germination lag (x_0, °C·days)						
16/03/2015 or 13/04/2015	0.0626	**53.6 A**	**147 A**	0.135	**58.6 A**	**44.5 A**
14/09/2015 or 19/10/2015	0.976	**49.1 A**	**48.7 A**	NA[§]	59.9	50.7
Mid-germination (x_{50}, °C·days)						
16/03/2015 or 13/04/2015	0.296	**124 A**	**195 A**	**0.00171**	**85.9 A**	**52.7 B**
14/09/2015 or 19/10/2015	0.782	**67.0 A**	**68.3 A**	NA[§]	60.7	57.1
Germination shape (b, no unit)						
16/03/2015 or 13/04/2015	0.402	**1.18 A**	**0.976 A**	0.556	**3.20 A**	**2.56 A**
14/09/2015 or 19/10/2015	0.809	**2.22 A**	**2.78 A**	NA[§]	**0.255**	**2.83**

Means of a given line and *P. ramosa* population followed by the same letter are not significantly different at p=0.05

[$] Excavation dates for populations O and H, respectively. [§] Insufficient seed number for a valid test.

A.1.1.3. Effect of GR 24 addition on germination rate

On 19 October 2015, two additional baskets were excavated for population H (with one already mentioned in section A.1.1.2), to compare germination and viability of seeds with and without adding germination stimulant to the seeds. These seeds were not conditioned. The effect of GR 24 on seed viability (germinated seeds and ungerminated seeds reacting to tetrazolium) and germinability (total germination rate) was tested with a generalized linear model using a logit transformation and a binomial distribution glm function of R (R Core Team, 2015). The effect of GR24 on germination parameters (time to first germination, time to mid-germination and shape parameter) was tested with a linear model lm function of R (R Core Team, 2015).

Table S 3: Effect of GR 24 on *P. ramosa* seed viability and germination in population H

Parameter	p-value	Comparison of means	
		With GR 24	Without GR 24
Seed viability[§]	**<0.0001**	0.970 A	0.745 B
Total germination rate	**<0.0001**	0.960 A	0.791 B
Germination lag (x_0, °C·days)	0.903	51.2 A	50.7 A
Mid-germination ($x_{50,}$ °C·days)	0.289	**57.1 A**	**58.0 A**
Germination shape (b, no unit)	0.365	**2.83 A**	**1.95 A**

Means of a given line followed by the same letter are not significantly different at p=0.05.
[§] Proportion of germinated and ungerminated seeds reacting to tetrazolium.

A.1.2. Additional details on the burial experiment

A.1.2.1. Excavation dates

Table S 4: Excavation dates of *P. ramosa* seeds of population O and H

Excavation	***Phelipanche ramosa* population**	
	O	**H**
1	18 September 2014	1 December 2014
2	4 November 2014	15 January 2015
3	15 December 2014	2 March 2015
4 (and 4')	30 January 2015	13 April 2015
5 (and 5')	16 March 2015	1 June 2015
6	30 April 2015	20 July 2015
7	15 June 2015	2 September 2015
8 (and 8' and 8'')	27 July 2015	19 October 2015
9 (and 9')	14 September 2015	18 January 2016
10	2 November 2015	7 March 2016
11	18 December 2015	18 April 2016
12	15 February 2016	6 June 2016
13	11 April 2016	11 July 2016
14	13 June 2016	
15	25 July 2016	

A.1.2.2. Additional statistics

A.1.2.2.1. Fitting viability vs. time

The proportion of viable seeds pV_{dr} with time over the two years was analysed with a linear regression inspired by Gardarin *et al.* (2010).

[a] $1 - pV_{dr} = a \cdot t_d + t_d{:}b_{age\ class}$ + error where the factor "age class" is "young" if seeds are less than one year old or "old" else, and t_d the age of the buried seeds (in years).

A.1.2.2.2. Fitting dormancy vs. time

The proportion of non-dormant seeds pND_{dr} was analysed over time t_d (days since July 17) with another broken-sticks regression, using the generic seed dormancy model proposed by Gardarin *et al*. (Gardarin & Colbach, 2015, Gardarin *et al.*, 2012):

[b]
$$pND_d = maxND \quad \text{if } t_d < tio$$
$$pND_d = maxND + (maxND - minND)/(tio - tie) \cdot (t_{d-tio}) \quad \text{if } t_d \in [tio,tie]$$
$$pND_d = minND \quad \text{if } t_d \in [tie, tbo]$$
$$pND_d = minND + (minND - maxND)/(tbo - tbe) \cdot (t_{d-tbo}) \quad \text{if } t_d \in [tbo,tbe]$$
$$pND_d = maxND \quad \text{if } t_d \in [tbe, tio + tlag]$$
$$pND_d = maxND + (maxND - minND)/(tio - tie) \cdot (t_d - (tio+tlag)) \quad \text{if } t_d \in [tio+ tlag,tie+ tlag]$$
$$pND_d = minND \quad \text{if } t_d \in [tie+ tlag, tbo+ tlag]$$
$$pND_d = minND + (minND - maxND)/(tbo - tbe) \cdot (t_d - (tbo+tlag)) \quad \text{if } t_d \in [tbo+ tlag,tbe+ tlag]$$
$$pND_d = maxND \quad \text{if } t_d > tbe+ tlag$$

With the following parameters:

Timing in young seeds (days since burial on July 17)	
Onset of dormancy induction	**tio**
End of dormancy induction	**tie**
Onset of dormancy break-up	**tbo**
End of dormancy break-up	**tbe**
Timing in old seeds	
Delay vs. young seeds (days)	**tlag**
Proportion of non-dormant seeds	
Maximum (summer-autumn)	**maxND**
Minimum (winter-spring)	**minND**

A.1.3. Additional results

A.1.3.1. Genetic analysis

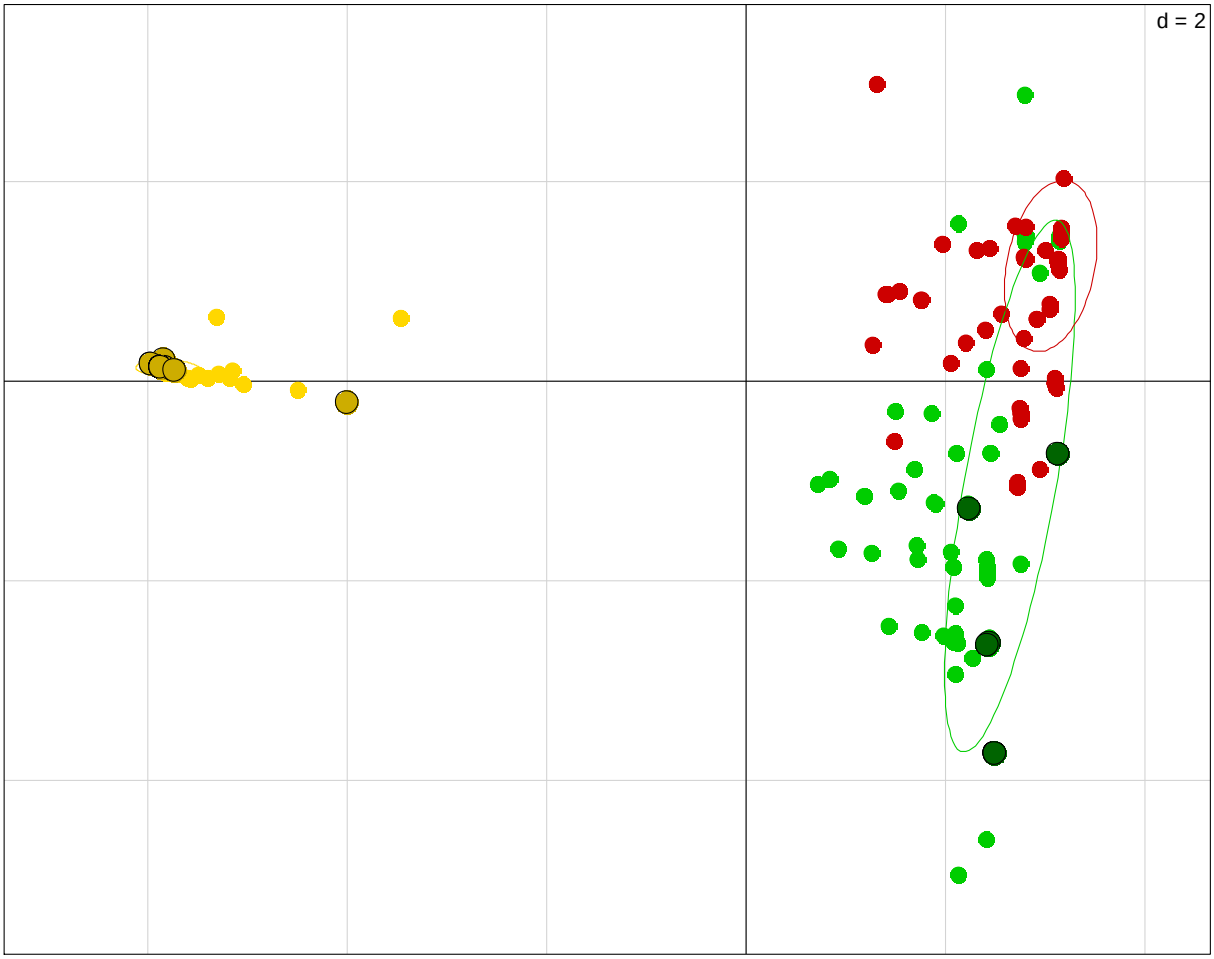

Figure S 1: Genetic variation at 10 microsatellite markers in 973 individuals of *P. ramosa* collected in 32 French fields cultivated with oilseed rape (yellow), hemp (green) and tobacco (red). The two populations used in our study (bigger and darker dots, yellow-colored for population O, green-colored for population H) are projected with data from previous studies (Le Corre *et al.*, 2014 and unpublished data) on the two first axes of a Principal Component Analysis.

A.1.3.2. Loss of seed viability over time

Table S 5: Analysis of variance table of the linear model fitting the proportion of viable seeds vs. age and age class ("young" or "old") of *P. ramosa* seeds for population O (A) and H (B)

A. Population O

Complete model: $1 - pV_{dr} = 0 + a \cdot t_d + t_d{:}b_{age\ class}$ + error (equation [a])

	DF	Sum of Squares	Mean Square	F Value	Pr > F
Seed age (t_d)	1	0.135079	0.135079	39.5907	<0.0001
Interaction (t_d:age class)	1	0.000252	0.000252	0.0739	0.7885
Residuals	21	0.071650	0.0034121		

Model retained after backward selection: $1 - pV_{dr} = a \cdot t_d$ + error

	DF	Sum of Squares	Mean Square	F Value	Pr > F
Seed age (t_d)	1	0.135079	0.135079	41.331	<0.0001
Residuals	22	0.071902	0.003268		

Parameter	Estimate	Std error	t value	Pr(>|t|)
a	0.0689	0.01072	6.429	<0.0001

Adjusted R-squared: 0.6368

B. Population H

Complete model: $1 - pV_{dr} = 0 + a \cdot t_d + t_d{:}b_{age\ class}$ + error

	DF	Sum of Squares	Mean Square	F Value	Pr > F
Seed age (t_d)	1	0.077980	0.077980	27.4785	<0.0001
Interaction (t_d:age class)	1	0.002024	0.002024	0.7133	0.4035
Residuals	39	0.110676	0.002838		

Model retained after backward selection: $1 - pV_{dr} = a \cdot t_d$ + error

	DF	Sum of Squares	Mean Square	F Value	Pr > F
Seed age (t_d)	1	0.07798	0.077980	27.677	<0.0001
Residuals	40	0.11270	0.002817		

Parameter	Estimate	Std error	t value	Pr(>|t|)
a	0.041841	0.007953	5.261	<0.0001

Adjusted R-squared: 0.3942

Table S 6: Analysis of variance table of the linear model fitting the proportion of viable seeds as a function of seed age and *P. ramosa* population

Complete model: $1 - pV_{dr} = 0 + a \cdot t_d + b_{population} + t_d{:}c_{population} + error$

	DF	Sum of Squares	Mean Square	F Value	Pr > F
Seed age (t_d)	1	0.200348	0.200348	68.1881	<0.0001
Population	2	0.019243	0.009622	3.2747	0.04469
Interaction (t_d:population)	1	0.001780	0.001780	0.6059	0.43939
Residuals	60	0.176289	0.002938		

Model retained after backward selection: $1 - pV_{dr} = 0 + a \cdot t_d + b_{population} + error$

	DF	Sum of Squares	Mean Square	F Value	Pr > F
Seed age (t_d)	1	0.200348	0.200348	68.632	<0.0001
Population	2	0.019243	0.009622	3.296	0.04373
Residuals	61	0.178070	0.002919		

Parameter	Estimate	Std error	t value	Pr(>|t|)
a	0.03551	0.01204	2.951	0.00449
b population H	0.01029	0.01360	0.757	0.45222
b population O	0.03939	0.01602	2.458	0.01681

Adjusted R-squared	0.5302

A.1.3.3. Inconsistent data in seed viability

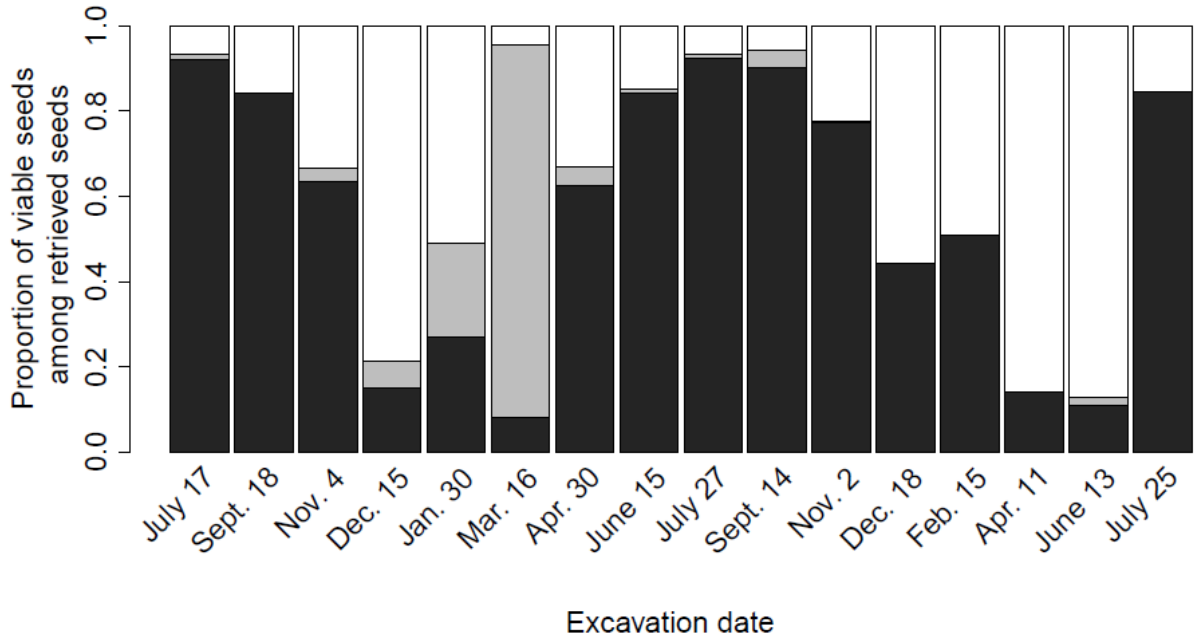

Figure S 2: Mean proportion of germinated seeds (black) and seeds reactive to tetrazolium (grey) among retrieved *P. ramosa* seeds of population O at each excavation date.

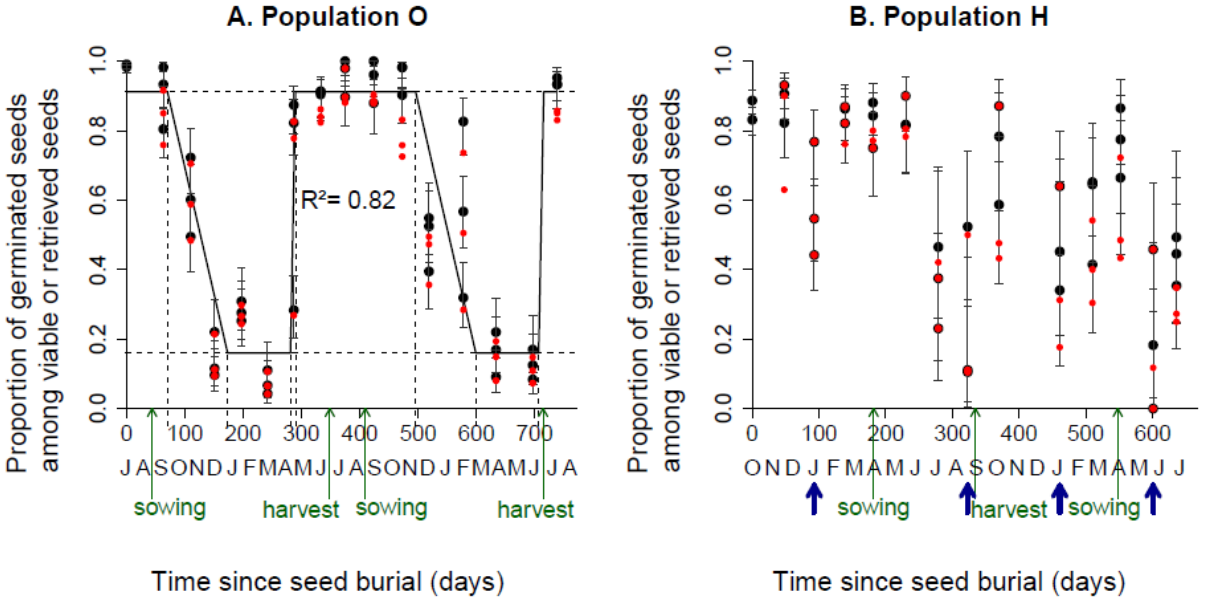

Figure S 3: Proportion of germinated *P. ramosa* seeds over two years for populations O (A) and H (B) among viable (black dots) and retrieved seeds (red dots). Each point is the proportion of seeds germinating after seed-bag recovery, conditioning and addition of GR24. Lines and arrows: see Figure 8.

A.1.3.4. Germination parameters

Table S 7: Distribution of germination parameter values of *P. ramosa* seeds of population O (A) and H (B) and quality of non-linear regression fits (examples of models represented in Figure 9).

A. Population O

Distribution	Fitting quality pseudo-R^2	Germination lag (x_0, °C·days)	Mid-germination (x_{50}, °C·days)	Germination shape (b, no unit)
Minimum	0.862	0.000	12.0	0.315
5% percentile	0.972	0.000	31.6	0.480
Median	1.000	59.6	88.4	1.05
Mean	*0.992*	*57.9*	*98.3*	*1.72*
95% percentile	1.000	103	176	5.43
Maximum	1.000	174	290	8.36

B. Population H

Distribution	Fitting quality pseudo-R^2	Germination lag (x_0, °C·days)	Mid-germination (x_{50}, °C·days)	Germination shape (b, no unit)
Minimum	0.955	0.000	28.2	0.167
5% percentile	0.982	0.000	30.5	0.365
Median	1.000	49.8	59.7	2.54
Mean	*0.997*	*39.4*	*61.9*	*2.58*
95% percentile	1.000	60.0	90.1	5.57
Maximum	1.000	86.7	102	5.77

Table S 8: Effects of burial length, seed age class and seasonal non-dormancy on germination parameters of *P. ramosa* seeds of population O and H.

Effect	***Phelipanche ramosa* population**					
	O			**H**		
	p-value	R^2		p-value	R^2	
Germination lag (x_0, °C·days)						
Time since burial (days)	**0.0141**	**0.11**	y = 36.3 + 0.0444·x	0.230		log(y+1) = 2.73 + 0.00132·x
Seed age class (young vs. old, days)	**0.0129**	**0.11**	**young: 42.2, old: 61.4**	0.388		young: 18.8, old: 28.2
Proportion of non-dormant seeds	0.176		log(y+1) = 3.14 + 0.727·x	0.183		log(y+1) = 3.86 -1.15·x
Mid-germination (x_{50}, °C·days)						
Time since burial (days)	0.123		log(y) = 4.22 + 0.000559·x	0.294		y = 68.4 -0.0162·x
Seed age class (young vs. old)	0.122		young: 73.5, old: 93.4	0.413		young: 65.4, old: 60.3
Proportion of non-dormant seeds	0.0648		y= 113 -31.3·x	0.298		y = 55.5 + 12.6·x
Germination shape (b, no unit)						
Time since burial (days)	0.135		log(y) = 0.486 - 0.000785·x	0.407		y = 2.24 + 0.00114·x
Seed age class (young vs. old)	0.108		young: 1.48, old: 1.03	0.793		young: 2.67, old: 2.52
Proportion of non-dormant seeds	0.125		log(y) = 0.482 -0.470·x	0.490		y = 3.06 -0.744·x

Table S 9: Effects of *P. ramosa* population on germination parameters.

Parameter	p-value	Means	
		Population O	Population H
Germination lag (x_0, °C·days)	**0.00477**	52.8 A	37.3 B
Mid-germination (x_{50}, °C·days)	**<0.0001**	94.1 A	63.2 B
Germination shape (b, no unit)	**0.0315**	1.21 B	1.83 A

Means of a given line followed by the same letter are not significantly different at p=0.05

A.2. Annexes du chapitre 3

A.2.1. Metamodelling a 3D architectural root system model to provide a simple model based on key processes and species functional groups

Loïc Pagès[1], Olivia Pointurier[2], Delphine Moreau[2], Anne-Sophie Voisin[2], Nathalie Colbach[2*]

[1] UR 1115 PSH, INRA Centre PACA, Site Agroparc, 94914 Avignon Cedex 9, France

[2] Agroécologie, AgroSup Dijon, INRA, Univ. Bourgogne, Univ. Bourgogne Franche-Comté, F-21000 Dijon, France

* Address for correspondence
Nathalie Colbach
INRA
UMR1347 Agroécologie
BP 86510
17 rue Sully
21065 Dijon Cedex
France
Nathalie.Colbach@inra.fr
Tel 033-380693033

A.2.1.1. Abstract

Aims. The architecture of root systems determines where and how much resources plants can extract from the soil, how they compete for soil resources, and how they interact with soil organisms. We aimed to develop a 3D root-system model called RSCone for future inclusion into multispecies individual-based canopy models suitable to design integrated weed management or intercropping strategies.

Methods. We (1) proposed a conceptual root-system model consisting of empirical equations predicting root-system envelope, root length and biomass distribution from environmental conditions, species and plant stage, (2) calibrated the model from simulations with an existing architectural root-system model (ArchiSimple) to benefit from its knowledge on root functioning and the many parameterized crop and weed species, (3) identified the root-system architectural processes driving the key root state variables and (4) established species functional groups with Principal Component Analyses and clustering.

Results. RSCone consists of 17 equations and 14 parameters; it was calibrated for 22 weeds and 22 crop species and varieties. Six species functional groups were established, depending on their family (*Poaceae*, *Fabaceae*, other), root-extension rates, specific root length (SRL) and the time to reach maximum SRL.

Conclusion. RSCone is ready to be included into multispecies (crop and/or weed) dynamics models.

Keywords. Calibration, weed, cover crop, ArchiSimple, simulation

A.2.1.2. Introduction

Understanding root system development and growth, as well as root distribution in the soil is crucial to understand plant functions and responses to environmental conditions. The architecture of the root system determines where and how much resources the plant can extract from the soil (Barber, 1984), and thus how plants compete for soil resources such as nitrogen or water (Gérard *et al.*, 2017). The root system also determines over which soil volume plants spread root exudates, and thus how plants interact with organisms, whether beneficial (e.g. microorganisms described in Moreau *et al.*, 2019) or harmful (e.g. parasitic plants, Grenz *et al.*, 2005a).

Many models have been developed to represent root development and growth and/or root distribution that we can classify into two main categories: density models and architecture models. Density models (see examples in Dupuy *et al.*, 2010) aim to describe distributions of particular root attributes (usually length or biomass) in the soil, particularly across soil layers. They are particularly useful when the root system must be described at a large scale, i.e. the whole crop canopy. Most of them use simple mathematical formalisms, either spatial functions or differential equations when the dynamics are considered. Such models are usually used in crop models simulating homogenous monospecies canopies from soil and weather inputs (e.g. STICS, Brisson *et al.*, 2003; APSIM, Keating *et al.*, 2003). However, these models remain abstract, relatively far from the root structures and processes, and they are often impossible to up or downscale. It can be difficult to estimate their parameters, which often have no direct biological meaning and vary with numerous environmental factors as well as with plant phenology. Such models can thus not be used in heterogeneous, particularly multispecies canopies.

Architectural models (e.g., Pagès *et al.*, 2014) explicitly represent root systems, usually in 3D, in which the individual roots are split into segments and have precise locations in space. Most of them are dynamic and developmental models and represent individual plants. Their basic concepts are rather concrete and simple, close to the biological processes, and fit nicely with above-ground function-structure plant models (see examples in Gaudio *et al.*, 2019). But, the combination of several developmental sub-processes makes these models more complex than the density models. Moreover, the number of individual objects in a root system is usually very high in a mature plant, so that these models are restricted to individual plants to limit simulation time and computer memory. This point is a serious limitation when the objective is to investigate plant populations or communities with plant-plant interactions. This is particularly the case for multispecies crop mixtures or crop-weed canopies whose heterogeneity in terms of plant emergence date, location and morphology requires a 3D individual-based modelling approach to correctly simulate plant-plant interactions (Munier-Jolain *et al.*, 2013; Renton and Chauhan, 2017; Gaudio *et al.*, 2019; Colbach *et al.*, in revision).

New models, somewhere between these two categories, are required, as pointed by Pedersen et al (2010). These could feed homogeneous-canopy models such as STICS or APSIM to improve the modelling of soil-plant interactions (mainly, uptake and use of soil resources) as well as 3D individual-based models which do not need to represent each leaf or root as function-structure models but specifically represent plant-plant interactions (mainly, the competition for soil resources among neighbour plants) (see examples in Gaudio *et al.*, 2019). The new root models should be conceptually simple and also easy and quick to compute, particularly when aiming to include them in individual-based models.

This new root-system model could be either built *de novo*, starting from scratch, or by simplifying an existing complex and mechanistic root-architecture model. The latter allows recycling data collection, formalisation and evaluation. One simplification technique is metamodeling, which aims at emulating the original model, linking inputs and outputs by less detailed but faster equations fitted to a huge simulated data set. This principle has been successfully applied to various fields, e.g. root depth density distribution (Pagès *et al.*, 2012), forest growth (Marie and Simioni, 2014), bio-geo-chemical cycles (Villa-Vialaneix *et al.*, 2012) or 3D individual-based light interception (Colas *et al.*, in

revision). These empirical metamodels replace the initial mechanistic models, using the same inputs and producing the same outputs. The metamodeling procedure includes a sensitivity analysis to identify minor inputs that can be ignored and thus produces new knowledge on the key input variable driving the analysed system. However, this approach requires a huge simulation plan to cover every contingency, and the prediction quality may decline when inputs are close to the limits of the simulated input ranges (Colas *et al.*, in revision).

In this paper, we proposed a conceptual simplified root-system model consisting of a succession of empirical equations linked to environmental conditions and carbon resource supply, and suitable for future inclusion into population or individual-based models. Our new model was based on an existing architectural root-system model (ArchiSimple, Pagès *et al.*, 2014), which was used to run virtual experiments in order to fit the equations and estimate species and genotype parameters. The resulting simplified root-system model aimed to predict the key state variables relevant for plant-soil and plant-plant interactions, i.e. the envelope of the root system as well as the distribution of root biomass and root length inside this envelope. It was then calibrated for a large range of contrasting species to identify the root-system architectural processes driving these key state variables and establish species functional groups.

The architectural model chosen as a starting point had to be sufficiently generic and realistic to be used in virtual experiments for contrasting crop and weed species, which is the case of ArchiSimple (Pagès *et al.*, 2014). This model has been parameterized and tested for many contrasting species (including crops and weeds, monocot and dicots, legumes and non-legumes) and crop genotypes with different growth strategies (Drouet *et al.*, 2005; Pagès *et al.*, 2014; Pagès and Picon-Cochard, 2014; Bui *et al.*, 2015; Moreau *et al.*, 2017; Pagès and Kervella, 2018; Faverjon *et al.*, 2019).

A.2.1.3. Material and methods

A.2.1.3.1. The ArchiSimple model used for the virtual experiments

The ArchiSimple model was presented in detail by Pagès et al (2014). It is a dynamic architectural model, in which the root system is represented as a set of root segments (of some millimetres) and meristems (examples in Figure S 4). Each day, the virtual root system is modified through the combination of several developmental and growth submodels which formalize the main processes: emission of new adventitious roots from the shoot, elongation of existing roots, acropetal branching, radial growth and self-pruning following root decay.

Source and sink concepts are integrated in a very simple way. Each day, the resource supply (i.e. the root biomass provided by photosynthesis) is given as input. The demand for root biomass of all roots is then summed throughout the root system and compared to the available supply to determine a satisfaction coefficient. Actual growth (i.e. elongation, branching etc) is calculated from potential growth using this coefficient, as well as soil temperature, mechanical constraints (Table S 10) and species parameters (Table S 11). These parameters are species properties implicated in the processes driving root architecture and their number is rather small (22) but the detailed representation of the root-system architecture, locating and representing each individual root segment slows down simulations, with 20 seconds for a single plant over only 80 days on a 2 GHz processor with 16 Go RAM. Together with the need for memory for storing the various root segments data, this is incompatible with the thousands of plants that must be simulated over decades in a 3D individual based crop-weed model.

A.2.1.3.2. Proposing the conceptual simplified root-system model RSCone

The new simplified root-system model was called RSCone (Root System seen as a Cone). It is a numerical model simulating the root system of a plant at a daily time step, to make it compatible with

modelling processes such as photosynthesis or soil-resource take-up, whether in homogeneous-canopy models such as STICS (Brisson *et al.*, 2003) or in 3D individual-based multispecies models (Colbach *et al.*, in revision). RSCone's root system is enclosed by an extending 3D envelope, resulting from the superposition of a cylinder sitting on top of a spilled cone (Figure S 4). This envelope represents the root influence zone of the plant (Casper *et al.*, 2003), and the combination of the two volumes allows to cover the multitude of possible root-system shapes presented by the usual crop and weed species from agroecosystems (Kutschera and Lichtenegger, 1960). Three state variables determine the envelope, i.e. the depth and extent (radius) of the cylinder-shaped part of the root system, and the total root-system depth (Figure S 4).

Each day, the root-system envelope grows, depending on plant age, mechanical soil constraints and soil temperature as well as species parameters. Two key root attributes are specified within the envelope: root-biomass density (i.e. dry root biomass per unit soil volume inside the root-system envelope) and root-length density (i.e. the cumulated root length per unit soil volume) which is derived from biomass density via the specific root length (SRL, i.e. root length per unit of root biomass) and also depends on plant age. Once the root-system model is included in homogeneous-canopy models or 3D individual-based models, these attributes are essential to simulate extraction of soil resources (Malagoli and Le Deunff, 2014; Aziz *et al.*, 2017) and/or the attachment of root pathogens or parasites (Grenz *et al.*, 2005a).

A.2.1.3.3. Building RSCone

To determine the shape of the equations driving the extension of the root-system envelope, biomass and root length from plant age and environmental conditions, contrasting root systems were simulated with ArchiSimple. To ensure that the equations were sufficiently generic and applied to both crops and weeds, we chose root systems that contrasted the most for the functions to be analysed. The choice was based on the expert knowledge of the ArchiSimple authors and previous ArchiSimple simulations (e.g., Pagès and Picon-Cochard, 2014; Pagès and Kervella, 2018). Each root system was repeated on five plants to account for stochastic effects in ArchiSimple, and simulated over 80 days, in non-limiting conditions, i.e. at optimal soil temperature, without soil compaction or gravel content, and without root biomass provision being limited by photosynthesis. In terms of actual plant age, these 80 days under optimal temperature conditions (e.g., 24 °C for maize) cover the duration of root-system growth of most species. For each root-system state variable, we here presented the two or three most contrasting examples to demonstrate the adequacy and genericity of the equations to be used in RSCone. Simulated data were analysed, using lm() and nls() functions of R (R Core Team, 2016) for linear and non-linear regressions, respectively.

A.2.1.3.4. Parameterizing RSCone

A series of 35 weed and crop species (including 10 genotypes for *Pisum sativum*) were parameterized for ArchiSimple (Table S 11), from our own experiments and literature (Drouet *et al.*, 2005; Pagès *et al.*, 2014; Pagès and Picon-Cochard, 2014; Bui *et al.*, 2015; Moreau *et al.*, 2017; Pagès and Kervella, 2018) (section A.1 online). For each species, three plants (considered as replicates) were simulated over 70 days, in non-limiting conditions in terms of soil structure, soil temperature and biomass provision. The simulations of section A.2.1.3.3 had shown that fewer replicates and days were sufficient to estimate species parameters. Then, the RSCone parameters were estimated by fitting the RSCone equations to the simulated output of each plant, using lm() and nls() of R (R Core Team, 2016). These parameter values were then averaged over the three plants of each species. One RSCone parameter necessary to simulate the effect of soil constraints on root-system state variables could be directly calculated from an ArchiSimple parameter (Table S 11.B). Two others, base and optimal

temperatures, were mostly taken from crop and weed models (e.g., STICS, Brisson *et al.*, 2003; FlorSys, Colbach *et al.*, in revision).

As ArchiSimple includes stochastic processes, the calibration script was run twice over 21 weed species and 14 crop species, among which 10 pea varieties (Table S 15) and Pearson correlation coefficients were calculated between the parameter values of the two runs for each RSCone parameter, using the cor() function of R.

A.2.1.3.5. Functional species groups

Correlations among RSCone parameters were investigated with a Principal Component Analysis (PCA), followed by a Ward ascendant hierarchy classification to cluster crop and weed species into functional groups, depending on their root-system parameters, using the PCA() and hclust() functions of the FactoMineR package (Lê *et al.*, 2008) of R (R Core Team, 2016). To identify which ArchiSimple parameters were the major determinants of root-system characteristics in RSCone, the ArchiSimple parameters were projected onto the PCA axes. Pearson correlation coefficients were also calculated between ArchiSimple and RSCone parameters.

A.2.1.4. Results

A.2.1.4.1. Daily steps in RSCone

In addition to species parameters (Table S 12), RSCone needs daily soil temperature and mechanical constraints as well as root biomass provision resulting from photosynthesis as inputs (Table S 10), i.e. the same inputs as ArchiSimple. The equations are run daily to drive root-system growth for the virtual plant in RSCone and are presented in Table S 13, the list of state variables describing the root system in Table S 14. Time is in days since seed germination; the slowing down of root growth and development by too cold or too hot conditions is accounted for by temperature-dependant corrective functions.

The following sections explain the various equations and how they were chosen.

Depth of the root system envelope

The total depth of the root system is the distance from soil surface to the peak of the spilled cone (Figure S 4). In non-limiting conditions (i.e. no soil compaction, optimal soil temperature, non-limiting root biomass provision), the potential root-system depth $Dpot_d$ solely depends on plant age for a given species. To identify a generic equation linking root-system depth to plant age, we ran ArchiSimple simulations for a series of root-system types contrasting in terms of emergence timing, root elongation and emission rates, importance of gravitropism etc. Figure S 5 shows the three most contrasting systems. The first system represents the linear growth of a tap-rooted system as can be found in pea (*Pisum sativum*). The taproot started growing after a lag of several days following germination, and continued to grow until the end of the simulation. The second system represents a determinate growth pattern (Shishkova *et al.*, 2008). Elongation stopped to grow after approximately two months. In the third system which is common in *Poaceae* species, the seminal root was the deepest until day 40, and was then outgrown by faster growing adventitious roots, without stopping until the simulation end.

The same equation (equation 4 of Table S 13) satisfactorily fitted all three behaviours (Figure S 5). The lag from germination to root-system extension in depth (t0) could directly be linked to two ArchiSimple parameters, as the sum of the plant age when meristems are mature plus the inverse of the emission rate of seminal roots (Table S 12).

Lateral root-system extension

Lateral extent defines the radius of both the cylinder and the cone base (Figure S 4). It was calculated to enclose 95% of the root segments and tested on a series of contrasting root systems, three of which can be seen in Figure S 4. In the first case (Figure S 4.A), the lateral roots emerging from the radicle extended slowly and were overtaken by adventitious roots with a higher elongation rate after 25 days. The second case (Figure S 4.B) presented a rather constant expansion rate due to vigorous lateral roots as well as vigorous and precocious adventitious roots. The third root system (Figure S 4.C) presented a significant gravitropism in lateral roots. The curvature of these lateral roots induced a gradual decrease of the lateral extension rate with time. As for root-system depth, a broken-stick linear regression was sufficiently generic to approximate all situations (eq 5 in Table S 13, section B.2 online).

Depth of the cylinder-shaped part of the root system

The same principle was used to determine the shape of the equation driving the depth of the cylinder-shaped part of the root system (Figure S 4) from plant age and species parameters. ArchiSimple was run for a series of contrasting root systems. The depth of the cylinder was defined by first locating % root segments that were located furthest from the central plant axis, and then calculating the 95-percentile of their depths (Figure S 4). After a lag of a few days, this depth increased linearly with plant age, irrespective of the tested root system. The first root system (Figure S 4.A) presented vigorous adventitious roots emitted from day 12 onwards, with a low gravitropism common in *Solanaceae* species. In the second system (Figure S 4.B), lateral root-system expansion was driven by the vigorous acropetal lateral roots of the taproot common among *Brassicaceae* such as *Brassica napus*. In the third system common in *Poaceae* species (Figure S 4.C), the lateral expansion started almost immediately, with vigorous adventitious roots and a strong gravitropism.

The analysis of the ratio of the cylinder depth vs the root-system depth showed that this ratio was constant regardless of plant age (section **B.2** online). The lag between seed germination and the time when the cylinder started to grow in depth (**t0+ tcyl0)** was longer than the lag for total root-system depth increase (**t0**). Consequently, RSCone uses the same extension rate (**rD**) for both cylinder and total depths, multiplying the result by a parameter (**rCD**), and increases the initial lag by a further lag (**tcyl0**) for cylinder depth growth (eq 6 in Table S 13).

Effect of soil constraints

The growth of root-system depth is usually limited by two soil characteristics: temperature and soil resistance to root penetration, due to soil compaction. These characteristics are given as input variables, with one value per 1-cm thick soil layer (Table S 10). They are transformed into relative coefficients, reflecting relative reduction in root-system expansion, ranging from 0 (i.e. no root growth) to 1 (no limitation in root growth due to soil compaction, too cold or too hot temperature).

The effect of temperature is supposed to follow a sinusoidal curve (section B.1 online), increasing from 0 when soil temperature ($Tsoil_{dl}$) equates the base temperature (**Tbase**) of the species to 1 when the optimal species temperature (**Topt**) is reached (equation 1 in Table S 13). This effect is calculated for each 1-cm thick soil layer and then averaged over the current root depth.

The effect of the mechanical constraint (eq. 2 in Table S 13) was inspired by literature (Bengough and Mullins, 1990) and is assumed to be a linear function of the penetration resistance ($Psoil_{dl}$), decreasing from 1 when soil offers no resistance to roots, to 0 when soil resistance allows the species maximum penetration ability (**Pmax**). This parameter Pmax was directly calculated from an ArchiSimple parameter (i.e. maximum root tip diameter dmax): Pmax increases from 0.7 to 1 cm/cm (no effect of

soil constraints) when the maximum root tip diameter increases from 0.3 to 1.2 mm (section B.1 online). As for temperature, the soil resistance effect is calculated for each soil layer and then averaged over root depth.

The two effects are combined (eq 3 in Table S 13) and then applied to potential root depth to get actual root depth (eq 7). The same principle is applied to the depth and radius of the cylinder-shaped part of the root system (eq 8 and 9). Once the actual dimensions of the root envelope are known, the root-system lateral extent (i.e. radius) inside the cone can be calculated as a linear regression (eq 10), making the extent shrink from its maximum value EC_d at the top of the cone (soil layer l = DC_d) to zero at the base of the cone, i.e. depth of the root system (layer l= D_d).

Root biomass density

RSCone does not consider the horizontal variations of biomass distribution, only its vertical variation along soil depth. For this purpose, we made a large number of simulations of various types and ages of root systems, assuming that biomass provision to roots resulting from photosynthesis was non-limiting, and visually explored the variations of biomass density on graphs (root biomass per 1-cm soil layer divided by soil layer volume inside root-system envelope, eq. 11 in Table S 13). This exploration showed that the biomass distribution could greatly vary, depending on the root system architecture. The simplest generic approach was to consider that root biomass density was constant in the cylinder-shaped part of the root system and then linearly decreased to zero at the tip of the cone (eq. 12). This equation only needed a single parameter, i.e. maximum root biomass density. If a greater precision of root biomass vs depth is needed, more complicated equations can be used but these need one or two additional parameters (e.g. a two-parameter Weibull equation, section B.4 online).

When investigating root biomass density variations with plant age in contrasting root systems, we could not find a relationship with plant age. So, **RBDmax** simply is the mean of the maximum root biomass densities estimated by fitting eq. 12 to plants older than 25 days, to eliminate stochasticity in values which is very high in young plants.

Root-system biomass

The potential root biomass $RBMpot_d$ depends on root-system dimensions, integrating root biomass density over the root-system volume (eq 13 in Table S 13). The actual root biomass of the day also depends on biomass provision resulting from photosynthesis which is an input variable in both ArchiSimple and RSCone (Table S 10). Actual biomass is the minimum between the potential and the actual provided biomass (eq 14 in Table S 13). The ratio of these two biomasses ($rPhoto_d$) is then used to determine the day's actual root biomass density, accounting for insufficient photosynthesis (eq 14 in Table S 13). Insufficient biomass provision to roots from photosynthesis does not affect root-system dimensions. Indeed, insufficient resources primarily limit the emission and elongation of fine roots rather than those of primary root axes, which define the shape and size of the root-system envelope.

Specific root length

In order to calculate root length density from biomass density, we also need the specific root length (SRL) over time, i.e. the total root length divided by the total root biomass. As previously, we tested different root systems, and two contrasting examples can be found in Figure S 6. Both root systems showed the same basic pattern in the change in SRL. In the root system with thick roots and radial growth (such as *Pisum sativum*), SRL started at a low level, increased during 10 days until it reached a constant value approximating three times the initial value. The second system, with thinner roots and without radial growth (e.g. *Poaceae*), started with nearly ten times the SRL of the first root system.

The increase lasted for more than a month, before reaching a level again approximately three times the initial value.

Whatever the root-system type, the change in SRL with plant age can be modelled with a broken-stick regression (eq. 16 in Table S 13), depending on initial and final values (**srl0**, **srlmax**) and the timing of the onset and end of the period of SRL increase (**t0**, **tsrlmax**). Root length density in a given soil layer l can then simply be calculated by multiplying root biomass density on the layer by the day's specific root length (eq 17).

A.2.1.4.2. Species typology

Thirty-five species of 11 families, among which 22 weed and 12 crop species, including 10 genotypes of *Pisum sativum* (Table S 15), were calibrated for RSCone by fitting the equations of Table S 13 to root-system architecture simulated with ArchiSimple. The comparison of the parameter values of the two calibration runs showed them to be very stable (Pearson correlation coefficients ranging from 0.96 to 1 between the parameter values of the two runs, data not shown), despite ArchiSimple stochasticity. With the exception of the timing of root-system growth (**t0**), the RSCone parameters varied considerably among the calibrated species (Figure S 7).

Some RSCone parameters were correlated. Generally, the species and varieties with the greatest lateral root-system extent (**Emax**) were also those with the fastest growth speed, in terms of extent (**rE**), depth (**rD**) and cylinder-depth (**rCD**) (Figure S 8.A). They also started the growth of the cylinder-shaped part of the root system earlier (opposite to **t0cyl**). Species and varieties with a large specific root length SRL during early growth stages (**srl0**) were also able to reach much larger SRL later in their life (**srlmax**), but tended to be less resistant to soil compaction (low **Pmax**). There were no other strong correlations among RSCone parameters (Figure S 8.C). Particularly, the onset of root-system growth (**t0**) and the age when the maximum SRL was reached (**tSRLmax**) and the maximum root biomass density (**RBDmax**) were little correlated to any other parameter (Figure S 8.A and C).

Six functional groups in terms of root-system growth could be determined from the RSCone parameters (Figure S 8.B). Group C consisted of all tested *Poaceae* species except maize (ZEAMX) and these were essentially characterised by a delayed maximum SRL (**tSRLmax**), and a large and fast lateral root-system extent (**Emax, rE**). Non-legume dicotyledonous species were essentially split into two groups. Group B was closest to *Poaceae* species, but reaching maximum SRL slightly earlier (**tSRLmax**) and a fast vertical rather than lateral root-system extent (**rD** on Figure S 8.D). It consisted of only four species, from four different families. All the other non-legume dicots (except sunflower, HELAN) were included in group A, characterized by slow root-system growth (low **rE, rD, rCD**), low resistance to soil compaction (low **Pmax**) but higher specific root length (**srl0**).

Fabaceae (legume species) were also essentially split into two groups. Group F comprised four (low **rE, rD**) legume species with a slow root-system growth. The other legumes were all in group D which was roughly the opposite of group A in terms of attributes. The only exception were the two pea varieties with a very low seed mass (Table S 15), i.e. PI186093 and NepalA, which were in group A with the majority of non-legume dicotyledonous species.

Group E, consisting of the tall summer annuals *Helianthus annuus* (HELAN) and *Zea mays* (ZEAMX), was particular insofar as it shared many characteristics with the *Poaceae* group C and the *Fabaceae* group F (Figure S 8.B) but it differed from all groups with its slightly later onset of root-system growth (**t0**, Figure S 8.D).

A.2.1.4.3. Which ArchiSimple parameters drive root-system extension?

When using ArchiSimple parameters to discriminate the species, the species typology was much simpler (section A.2 online), with roughly *Poaceae*, *Fabaceae* and non-legume dicotyledons. *H. annuus* and *Z. mays* were again set apart, differing from all other groups and from each other.

Among the 22 ArchiSimple parameters, only a few were highly correlated to RSCone parameters (Figure S 8), and thus need to be estimated with greatest care in the future. The identified correlations were consistent with the rules underlying root-system growth in ArchiSimple. Species with larger maximum diameter primary-root tips (dmax) had roots that penetrated better into compacted soil in RSCone (**Pmax**), and their root system grew faster and larger (**Emax, rD, rE**, **rCD**) though their specific root length SRL tended to be lower (**srl0, srlmax**) (Figure S 8.A). Low SRL in RSCone was associated to large minimum diameters in primary roots tips in ArchiSimple (large dmin) and an early onset of adventitious-root emission (low ageadvemis). Species that, in RSCone, reached their maximum SRL late (**tsrlmax**) were usually monocots (opposite to dicot), presented a large maximum number of seminal roots (nbmaxsem), with a high emission rate of adventitious roots (emissrateadv), a low radial growth coefficient (opposite to radgrowth) and narrow seminal roots (opposite to propdiamsem).

The other parameters were less closely linked (Figure S 8.C). Species that, in RSCone, grew faster in terms of root-system depth (**rD**) also presented a high root elongation rate relatively to root-tip diameter in ArchiSimple (elongvsdiam). Other links could not be seen on the dimension presented in Figure S 8. For instance, a late onset of root growth in RSCone (**t0**) was linked to a low emission rate of seminal roots in ArchiSimple (emissratesem, Pearson correlation coefficient = 1).

A.2.1.5. Discussion

A.2.1.5.1. A fast and simple dynamic model, with a low number of parameters

This modelling approach is a new means to make a simple and dynamic representation of the root system of individual plants. Such representations are necessary to take into account several issues related to soil-plant relations, especially when considering multispecies and heterogeneous canopies. While 3D-individual based models all consider plant-plant competition for light, competition for soil resources is still rarely considered (Gaudio *et al.*, 2019), and the present model will be an essential step toward this goal.

Simplicity is an important criterion to achieve this task, for several reasons. In most cases, it is important to use a model that is easy to understand, from a conceptual point of view, and easy and quick to program and to compute. Moreover, the number of parameters and state variables describing the root system must be as low as possible. RSCone only uses 14 parameters compared to ArchiSimple's 22 (or several dozens of parameters as in some models, Dunbabin *et al.*, 2013), and these parameters all have a straightforward biological meaning. Most of them can be calibrated independently from real data (measured in greenhouse or field experiments) or, even better, from virtual data produced from models such as ArchiSimple as we did here. The parameters can thus be estimated from different data sources, which is a major advantage compared to conventional metamodels whose structure and parameter values are very dependent on the source model used to build the metamodel. The main simplification though lies in the simplification of the root-system structure, simulating an envelope filled in by root biomass and length, instead of explicitly simulating the size and location of each root segment as in ArchiSimple (Pagès *et al.*, 2014) or other models (Dunbabin *et al.*, 2013). Despite the simplification, the RSCone structure allows to predict the key state variables for plant-plant interaction while dividing the simulation time by more than 20 compared to ArchiSimple. Moreover, the daily steps are sufficiently independent to allow increasing complexity,

e.g. a more precise albeit more parameter-hungry equation can be used to simulate root biomass density with depth.

Several authors have emphasized this need for simple models (e.g., Pedersen *et al.*, 2010) and rather simple models of the root system have been developed during the last years (de Willigen *et al.*, 2002; Dupuy *et al.*, 2010; Bonneu *et al.*, 2012) based on differential equations to describe the dynamics of root density. But, these model do not discriminate the root zone of individual plants, they are calibrated from root density maps observed in pure stands in fields, and are thus not adapted to simulate plant-plant interactions in heterogeneous multispecies canopies (see section A.2.1.5.3). RSCone is substantially different, and closer to the model of Pedersen et al. (2010), but with several key advantages (see next section).

However, as for root density models (see examples in Dupuy *et al.*, 2010), the RSCone representation does not make sense for the very young root systems before they have reached a significant extension and/or branching. This limit has though little effect in many conditions. Indeed, nitrogen availability has little effect on very young plants (e.g., before 150-200 °Cdays approximately, Fayaud *et al.*, 2014) and young roots are still too small to attract many parasites (Gibot-Leclerc *et al.*, 2012). Conversely, lack of water can limit pre-emergent growth (Bouaziz and Bruckler, 1989), and radicle growth must thus be modelled (Dürr *et al.*, 2001; Gardarin *et al.*, 2012).

Another structural limit of RSCone for 3D canopy modelling is its assumption that the plant's root system is symmetric, with homogeneous root characteristics per horizontal soil layer. Both soil structure and resources not only vary vertically but also horizontally (Roger-Estrade *et al.*, 2004; Metcalfe *et al.*, 2019) and root systems tend to grow toward resources or away from constraints (Cassab *et al.*, 2013). If the aim is to work at such a detailed scale (rather than at the cropping-system scale for instance), then function-structure models might be more appropriate (see examples in Gaudio *et al.*, 2019).

A.2.1.5.2. Simplify virtual rather than actual reality, or why a metamodel rather than an empirical model?

Pedersen et al (2010) built their model from scratch, using field observations. While this has the advantage of investigating reality, the model's structure and domain of validity are highly conditional on the studied species and environmental conditions. Using a detailed architectural root-system model based on generic and universally valid processes as virtual reality results in a model with a larger domain of validity and whose structure should be sufficiently generic to cover most plant species. Pagès et al (2012) used a similar approach, building root density functions from intensive simulation and sensitivity analysis of a very simple root-system architecture model. Here, we went a step further, starting with a more complex root-system architecture model, testing a larger diversity of root system types, predicting a larger number of root-system state variables and accounting for the effect of environmental limiting factors.

Basing the simple root-system model on a process-based mechanistic model allowed checking which limiting factors should be considered in the simplified progeny model. For instance, the rules driving root-system architecture in non-legumes were shown to be little affected by nitrogen nutrition status (Brun *et al.*, 2010; Moreau *et al.*, 2017). The root-system parameters in RSCone thus do not need to vary with nitrogen availability even though the root-system state variables will be affected indirectly via root biomass provision (Brun *et al.*, 2010; Moreau *et al.*, 2017) which is an input of RSCone. So, RSCone is probably able to account for differences in plant root distribution in soil due to nitrogen limitation resulting from competition for nitrogen. By analogy, it may also allow reflecting differences in plant root distribution due to competition for light (the most frequent limiting resource in crop-weed canopies). Indeed, shading decreases both plant biomass production and biomass provision to roots (Brouwer, 1962).

Starting from the mechanistic model also improves the quality of the parameter measurements. It is easier to measure, for instance, minimum root-tip diameter in controlled conditions than the empirical parameters of RSCone (e.g., root penetration force) or Pedersen's model (2010). Moreover, basing the new model on an existing model allows to capitalize knowledge. Indeed, ArchiSimple has been parameterized for a wide range of species and genotypes (Dicot vs. monocot, legume vs. non legume, weed vs crop…) (Drouet *et al.*, 2005; Pagès *et al.*, 2014; Pagès and Picon-Cochard, 2014; Bui *et al.*, 2015; Moreau *et al.*, 2017; Pagès and Kervella, 2018) and still continues to be parameterized for new species and genotypes (Faverjon *et al.*, 2019) and be linked to new models (Gérard *et al.*, 2017). All these species and genotypes can therefore be easily, rapidly and cheaply parameterized for RSCone via simulations (running approximately for an hour per species).

The main drawback of the present modelling approach is its conditionality on the prediction quality of the underlying mechanistic model, here ArchiSimple. As ArchiSimple only considers root-system architecture, disregarding its functions as well as other plant organs, it is very difficult to evaluate with independent field data. But, field trials have shown that ArchiSimple well predicts specific root length, root-system depth and root biomass at two dates (Pagès and Picon-Cochard, 2014), or that key species parameters such as root-tip diameter measured in 60 species were similar in two sites contrasting in terms of region, habitat, soil, and weather (Pagès and Kervella, 2018).

Transforming ArchiSimple into the simpler RSCone which can be more easily connected to homogeneous-canopy models and 3D individual based models opens the door for checking the consistency of its predictions. Indeed, these models predict realistic crop and weed state variables which are comparable to usual field measurements (e.g. plant biomass, crop yield). Such a comparison does not actually check whether the details of the root system are correctly predicted but rather whether the root-system variables relevant for the plant functioning and reproduction are. And, to think even further, once these canopy-scaled models are used to evaluate and design cropping systems, it will be essential to verify whether they (as the result of many interacting submodels) allow to take the right decisions in terms of crop management.

A.2.1.5.3. Integration into homogeneous-canopy models and 3D individual based models

Though RSCone does not explicitly model plant-plant interactions or the effects of pedoclimate and cropping techniques, its inputs and outputs are tailored to make this possible when linked to other models. Once connected to soil models predicting soil temperature and structure from pedoclimate and cropping techniques, RSCone allows simulating the effect of the latter two environmental variables on root systems. Once the actual biomass provision (i.e. $RBMact_d$ in eq. 14 in Table S 13) is predicted by ecophysiological functions considering light interception and shading by neighbouring plants, the effect of plant-plant competition for light on the root systems will be included. Finally, the predicted root-system state variables will allow to determine where and how much soil resources are extracted from the soil, and thus how roots of neighbouring plants interact.

When connecting RSCone to models simulating homogeneous monospecies canopies (e.g. STICS, Brisson *et al.*, 2003; APSIM, Keating *et al.*, 2003), RSCone simply represents an average plant and the horizontal root-system extension can be ignored. However, the vertical distribution of root length density and root depth are key state variables to simulate the extraction of soil resources and tolerance to drought (e.g. Barber, 1984). But, root density models (see examples in Dupuy *et al.*, 2010) would allow reaching the same goal.

The main target of RSCone are 3D individual-based models simulating heterogeneous multispecies canopies from pedoclimate and cropping techniques, particularly those running over several years (Renton and Chauhan, 2017; Gaudio *et al.*, 2019; Colbach *et al.*, in revision). Indeed, in the past, the investigation of plant-plant competition focused on light as soil resources were usually sufficient in the

intensively managed cropping system of temperate climates. But, recently because of environmental and health issues, national and European policies require farmers to switch to integrated crop production using fewer or no chemical inputs. In this context, RSCone allows to tackle plant-plant competition for soil resources, by reducing resource uptake of plants whose root systems overlap in resource-limited soil areas. Including this process is essential both in crop-weed canopies to control the most harmful pest for crop production (Oerke, 2006) and in intercrops as one of the key levers of agroecological crop production (Hauggaard-Nielsen *et al.*, 2008).

A.2.1.5.4. Similar architectural rules can lead to different root systems

The RSCone model allowed to identify some of the emergent properties of the underlying root-system architectural model. We were able to identify functional species types in terms of root-system attributes and to link those to key ArchiSimple parameters, i.e. close to the biological processes driving root-system growth and architecture. Interestingly, the RSCone parameters (which result from the aggregation of several processes) allowed to discriminate sub-groups among non-legume dicots, among legumes and even among pea genotypes that could not be identified with the process-close ArchiSimple parameters. It is though difficult to compare our RSCone or ArchiSimple functional groups to those established on root-system observations from fields. Indeed, the latter are the result of both root-architecture rules and biomass provision whereas the former solely account for architecture rules, either directly (ArchiSimple) or indirectly (RSCone). But, the correlations between RSCone and ArchiSimple parameters demonstrated architecture rules observed *in situ* and/or included in ArchiSimple were preserved in RSCone such as the decrease in specific root length with increasing root diameter (Ma *et al.*, 2018), the difference between *Poaceae*, legumes and non-legumes in terms of root system morphology or, more interestingly, similar discriminations inside these groups, e.g. *Vicia sativa* (VICSA) behaving differently from other legumes (Bodner *et al.*, 2013). Moreover, our analysis allowed us to identify the key ArchiSimple parameters driving root-system architecture, showing for instance that the minimum root-tip diameter Dmin is more influential than the maximum root-tip diameter Dmax, or that radial growth (radgrowth) substantially modifies the dynamics of specific root length SRL.

A good knowledge of the inter- or intra-specific differences in root traits allows hypothesizing differences among species or genotypes in their ability to take up nutrients, depending on their location and mobility. For instance, species or genotypes with a high root ability to penetrate the soil and a high rate of root-system increase in depth (right hand of Figure S 8.B) are assumed to better access the deepest soil resources, such as water and leached nitrate (Dunbabin *et al.*, 2013). Besides, species or genotypes with a high specific root length (top left hand of Figure S 8.B) are generally associated to a high uptake efficiency of relatively immobile nutrients, such as phosphorus (Eissenstat, 1992)(Pagès, 2011), due to a high colonization of the soil volume increasing the probability to reach poorly mobile nutrients. However, only considering the values of the parameters is insufficient to definitely conclude on the outcome of plant-plant competition. As other factors interact (such as the date of emergence of plants, their phenology, their access to light, the effects of techniques and pedoclimate), simulations are essential to better understand and predict interactions among plants.

A.2.1.6. Acknowledgements

This project was supported by INRA and the French project CoSAC (ANR-15-CE18-0007). They authors are grateful to Maé Guinet, Marlène Lefèbvre, Mathieu Chanis and Juliette Senèze for contributing to the provision of datasets on legume species and genotypes.

Table S 10: Input variables illustrating environmental constraints on day d and in soil layer l (cm from soil surface) driving root-system growth and development in both ArchiSimple and RSCone

Variable	Meaning	Unit
$Csoil_{dl}$	Soil constraints due to soil compaction and gravel content in soil layer l, ranging from 0 = allowing no root growth to 1 = no effect on root growth	cm cm^{-1}
$RBMact_{d}$	Root biomass provided by photosynthesis since seed germination	g $plant^{-1}$
$\underline{Tsoil_{dl}}$	Soil temperature in soil layer l	°C

Table S 11: Species parameters driving root growth in the architectural model ArchiSimple (based on Pagès *et al.*, 2014), with range of variation of values (Drouet *et al.*, 2005; Pagès *et al.*, 2014; Pagès and Picon-Cochard, 2014; Bui *et al.*, 2015; Moreau *et al.*, 2017; Pagès and Kervella, 2018) and present paper for the crop and weed species calibrated later for RSCone

			Range of variation in species calibrated for RSCone		
Parameter	Meaning	Unit	mean	min	max
dicot	Clade (0: monocotyledon, 1: dicotyledon)		0.85	0.00	1.00
emissratesem	Emission rate of seminal roots	day^{-1}	0.98	0.50	1.00
propdiamsem	Ratio of the diameter of seminal roots to maximum root diameter		0.95	0.60	1.00
nbmaxsem	Maximum number of seminal roots		1.02	1.00	2.00
ageadvemis	Plant age when it starts to emit adventitious roots	day	4574	5	10000
distmaxadv	Maximum distance of adventitious roots to the root base	mm	11.5	10.0	80.0
emissrateadv	Emission rate of adventitious roots	day^{-1}	0.20	0.00	1.68
propdiamadv	Ratio of the diameter of adventitious roots to maximum root diameter		0.90	0.90	1.00
nbmaxadv	Maximum number of adventitious roots		17	0	148
dmin	Root-tip diameter below which elongation is impossible (diameter of the finest roots)	mm	0.16	0.08	0.36
dmax	Maximum tip diameter of primary roots	mm	1.00	0.44	2.06
elongvsdiam	Slope of the potential elongation rate versus root-tip diameter	$mm \cdot mm^{-1} \cdot day^{-1}$	26.0	11.9	49.2
tgravi	Direction of tropism (plagiotropism; negative geotropism; positive geotropism; exotropism)		All positive geotropism		
igravi	Intensity of tropism		0.0045	0.0020	0.0080
durdp	Plant age when meristems are mature	days	5.00	5.00	5.00
ibd	Inter-primordium distance	mm	2.02	0.56	3.74
dldm	Average ratio of the diameter of the daughter root to that of the mother root	mm^{-1}	0.32	0.12	0.52
vard	Relative variation of the daughter root diameter		0.28	0.10	0.67
tmd	Root tissue density	$g \cdot cm^{-3}$	0.11	0.03	0.30
growthdur	Slope of the growth duration versus squared tip diameter	$day \cdot mm^{-2}$	323	170	350
lifeexp	Slope of the life duration versus tip diameter and tissue mass density	$day \cdot mm\ mg^{-1}$	2513	2500	2800
radgrowth	Proportionality coefficient between section area of the segment and the sum of distal section areas (radial growth coefficient)		0.13	0.00	0.25

Table S 12: Species parameters driving root-system growth and development in RSCone, with values for maize (*Zea mays*) as an example

A. Timing and extent of root system

Parameter	Meaning	Maize values	Unit	Estimation method[§]
t0	Timing of root growth onset	7	Days since germination (under optimal temperature)	Durdp + (1/emissratesem)
t0cyl	Delay from t0 to when the cylinder part of the root system starts to grow in depth	31	Days since t0 (under optimal temperature)	Fit eq. 6, or min of d-t0 where E_d > 0.01 cm
tmax	Timing of root growth end	infinite	Days since germination (under optimal temperature)	Fit eq. 4
tSRLmax	Timing of maximum specific root length (SRL)	59.2	Days since germination (under optimal temperature)	Fit eq. 16
Emax	Maximum extent (radius) of the root system	24.7	cm	Fit eq. 5
RBDmax	Root biomass density in cylinder part of the root system, disregarding constraints	$2.28\ 10^{-4}$	$g \cdot cm^{-3}$	Calculated from eq. 13
rD	Speed at which root-system depth increases	1.11	$cm \cdot day^{-1}$ (under optimal temperature)	Fit eq. 4
rE	Speed at which root-system extent (radius) increases	0.608	$cm \cdot day^{-1}$ (under optimal temperature)	Fit eq. 5
rCD	Ratio of speed at which depth of cylinder-shaped part of root system increase vs speed of total root-system depth increase	0.144	$cm \cdot day^{-1}\ cm^{-1}\ day^{-1}$ (under optimal temperature)	Mean of DC_d/D_d if d>**t0**+**t0cyl**
srl0	Specific root length when roots start to grow	552	$cm \cdot g^{-1}$	Fit eq. 16
srlmax	Maximum specific root length	3170	$cm \cdot g^{-1}$	Fit eq. 16

B. Effect of environmental conditions

Parameter	Meaning	Maize values	Unit	Estimation method[§]
Pmax	Ability of roots to penetrate the soil	1	cm/cm, ranging from 0 (unable) to 1 (no limitation)	If dmin x < 0.3, Pmax = 0.7 Else if dmin < 1.2 Pmax = 0.6 + 0.33 dmin Else Pmax = 1
Tbase	Base temperature for growth and development	8	°C	Literature
Topt	Optimal temperature for growth and development	24	°C	Literature

[§] Directly calculated from ArchiSimple parameters (Table S 11), estimated by fitting equations of Table S 13 to state variables (Table S 14) simulated with ArchiSimple, or calculated from state variables simulated with ArchiSimple.

Table S 13: Comprehensive list of equations for simulating the root system in RSCone, with a daily time step (d=days since germination) and according to soil layer l (cm from soil surface). State variables in standard black with definitions in Table S 14, species parameters in **bold blue** with definitions in Table S 12, inputs in *italic* with definitions in Table S 10

N°	Process	Equation
Environmental constraints on root-system growth		
1	Root growth limitation due to soil temperature	If $\underline{Tsoil_{dl}}$ < **Tbase** then $rTsoil_{dl} = 0$ else if $\underline{Tsoil_{dl}}$ < **Topt** then $rTsoil_{dl} = \sin(0.5 \cdot \pi \cdot (\underline{Tsoil_{dl}} - \mathbf{Tbase}) / (\mathbf{Topt} - \mathbf{Tbase}))$ else $rTsoil_{dl} = 1$ $rTsoil_d$ = mean of $rTsoil_{dl}$ with $l \leq D_{d-1}$
2	Root growth limitation due to soil structure	If $Psoil_{dl} \geq$ **Pmax** then $rPen_{dl} = 0$ else $rPen_{dl} = 1 - Psoil_{dl} /$ **Pmax** $rPen_d$ = mean of $rPen_{dl}$ with $l \leq D_{d-1}$
3	Root growth limitation due to soil constraints (temperature and compaction)	$rSoil_d = rTsoil_d \cdot rPen_d$
Potential root system dimensions (disregarding soil constraints)		
4	Potential root system depth	If d < **t0**, then $Dpot_d = 0$ else if d < **tmax**, then $Dpot_d =$ **rD** $\cdot$ (d – **t0**) else $Dpot_d =$ **rD** $\cdot$ (**tmax** – **d0**)
5	Potential root system lateral extent (radius of the cylinder-shaped part of root system)	if d ≤ **t0**, then $ECpot_d = 0$ else if d < **t0** + **Emax** / **rE**, then $ECpot_d =$ **rE** $\cdot$ (d –**t0**) else $ECpot_d =$ **Emax**
6	Potential depth at which root system extent (radius) is maximal (depth of cylinder-shaped part of root system)	If d < **t0** + **t0cyl**, then $DCpot_d = 0$ else $DCpot_d$ = (d - **t0** - **t0cyl**) $\cdot$**rD**$\cdot$ **rCD**
Actual root system dimensions (accounting for soil constraints)		
7	Actual root system depth	$D_d = Dpot_d \cdot rSoil_d$
8	Actual depth at which root-system extent (radius) is maximal	$DC_d = DCpot_d \cdot rSoil_d$
9	Actual maximum root-system extent (radius)	$EC_d = ECpot_d \cdot rSoil_d$
10	Lateral root system extent (radius) in soil layer l	If $l < DC_d$, then $E_{dl} = EC_d$ else if $l < D_d$, then $E_{dl} = EC_d \cdot (1 - \frac{l+0.5-DC_d}{D_d-DC_d}$ else $E_{dl} = 0$
Root-system biomass		
11	Volume of root layer l inside the root-system envelope	If $l < DC_d$ then $vol_{dl} = \pi \cdot EC_d^2 \cdot l$ else if $l < D_d$ then $vol_{dl} = \pi \cdot EC_d^2 \cdot DC_d^2 + \pi \cdot 0.25 \cdot EC_d^2 \cdot (D_d - DC_d) - \pi \cdot 0.25 \cdot EC_d^2 \cdot (D_d - l)^3 / (D_d - DC_d)^2$ else $vol_{dl} = 0$
12	Potential biomass density per soil layer (disregarding insufficient photosynthesis but accounting for soil constraints)	If $l < DC_d$ then $RBDpot_{dl} =$ **RBDmax** else if $l < D_d$ then $RBDpot_{dl} =$ **RBDmax** $\cdot$ $(D_d - l) / (D_d - DC_d)$ else $RBDpot_{d.} = 0$
13	Potential root-system biomass (disregarding insufficient photosynthesis but accounting for soil constraints)	If d < **t0**, then $RBMpot_d = 0$ else $RBMpot_d =$ **RBDmax** $\cdot 0.25 \cdot \pi \cdot E_d^2 \cdot (3 \cdot DC_d + D_d)$
14	Actual root biomass (accounting for soil and photosynthesis constraints)	$RBM_d = \min(RBMpot_d, RBMact_d)$ If $RBMpot_d > 0$ then $rPhoto_d = RBM_d / RBMpot_d$ else $rPhoto_d = 0$
15	Actual root biomass density in soil layer l (accounting for soil and photosynthesis constraints)	$RBD_{dl} = rPhoto_d \cdot RBDpot_{dl}$
Root length density (accounting for soil and photosynthesis constraints)		
16	Specific root length density	if d ≤ **t0**, $srl_d =$ **srl0** else if d < **tsrlmax**, $srl_d =$ (**srlmax** – **srl0**) $\cdot$ (d - **t0**) / (**tsrlmax** –**t0**) + **srl0** else $srl_d =$ **srlmax**
17	Root length density in soil layer l	If $l \leq D_d$, then $RLD_{dl} = srl_d \cdot RBD_{dl}$ else $RLD_{dl} = 0$

Table S 14: Root-system state variables on day d predicted by RSCone for a virtual plant

Variable	Meaning	Drivers (other than species)	Unit
$Csoil_d$	Average soil constraints due to soil compaction and gravel content, ranging from 0 = allowing no root growth to 1 = no effect on root growth	Soil constraints in each soil layer (input)	cm cm^{-1}
DC_d	Actual depth of the cylinder-shaped part of the root system (considering soil constraints)	Potential depth at which the root system width starts to shrink, soil constraints	cm
$DCpot_d$	Potential depth of the cylinder-shaped part of the root system (disregarding soil constraints)	Plant age	cm
D	Actual root-system depth (considering soil constraints)	Potential root-system depth, soil constraints	cm
$Dpot_d$	Potential root-system depth (disregarding soil constraints)	Plant age	cm
EC_d	Actual extent (radius) of the cylinder-shaped part of the root system (considering soil constraints)	Potential root-system extent, soil constraints	cm
$ECpot_d$	Potential extent (radius) of the cylinder-shaped part of the root system (disregarding soil constraints)	Plant age	cm
E_{dl}	Root-system extent (radius) in soil layer l	Actual root-system extent, soil layer	cm
RBD_{dl}	Root biomass density in soil layer l	Actual root biomass in soil layer l, volume of layer l inside root-system envelope	$g \cdot cm^{-3}$
RBM_{dl}	Actual root biomass in soil layer l	Actual root biomass	g $plant^{-1}$
RBM_d	Actual root biomass	Potential root biomass, root biomass allocation by photosynthesis (input)	g $plant^{-1}$
$RBMpot_d$	Potential root-system biomass	Actual root-system dimensions, plant age	g $plant^{-1}$
RLD_{dl}	Root length density in soil layer l	Root biomass density in soil layer, specific root length	$cm \cdot cm^{-3}$
$rPen_{dl}$	Relative reduction in root-system expansion due to root penetration resistance exerted by the soil (due to soil compaction and gravel content) in soil layer l	Penetration resistance of soil layer l (input)	cm cm^{-1}
$rPen_d$	Average relative reduction in root-system expansion due to root penetration resistance exerted by the soil (due to soil compaction and gravel content)	Relative reduction in root-system expansion due to root penetration resistance in soil layer l	cm cm^{-1}
$rPhoto_d$	Relative reduction in root biomass due to insufficient photosynthesis	Potential root biomass, root biomass provided by photosynthesis	g g^{-1}
$rSoil_d$	Relative reduction in root-system expansion due to soil constraints (temperature, compaction)	Relative reduction in root-system expansion due to mechanical constraints, idem due to temperature	cm cm^{-1}
$rTsoil_{dl}$	Relative reduction in in root-system expansion due to low soil temperature in soil layer l	Soil temperature (input)	cm cm^{-1}
$rTsoil_d$	Average relative reduction in in root-system expansion due to low soil temperature	Relative reduction in in root-system expansion due to low soil temperature in soil layer l	cm cm^{-1}
srl_d	Specific root length	Plant age	$cm \cdot g^{-1}$
vol_{dl}	Volume of soil layer l inside root-system envelope	Root-system dimensions	cm^3

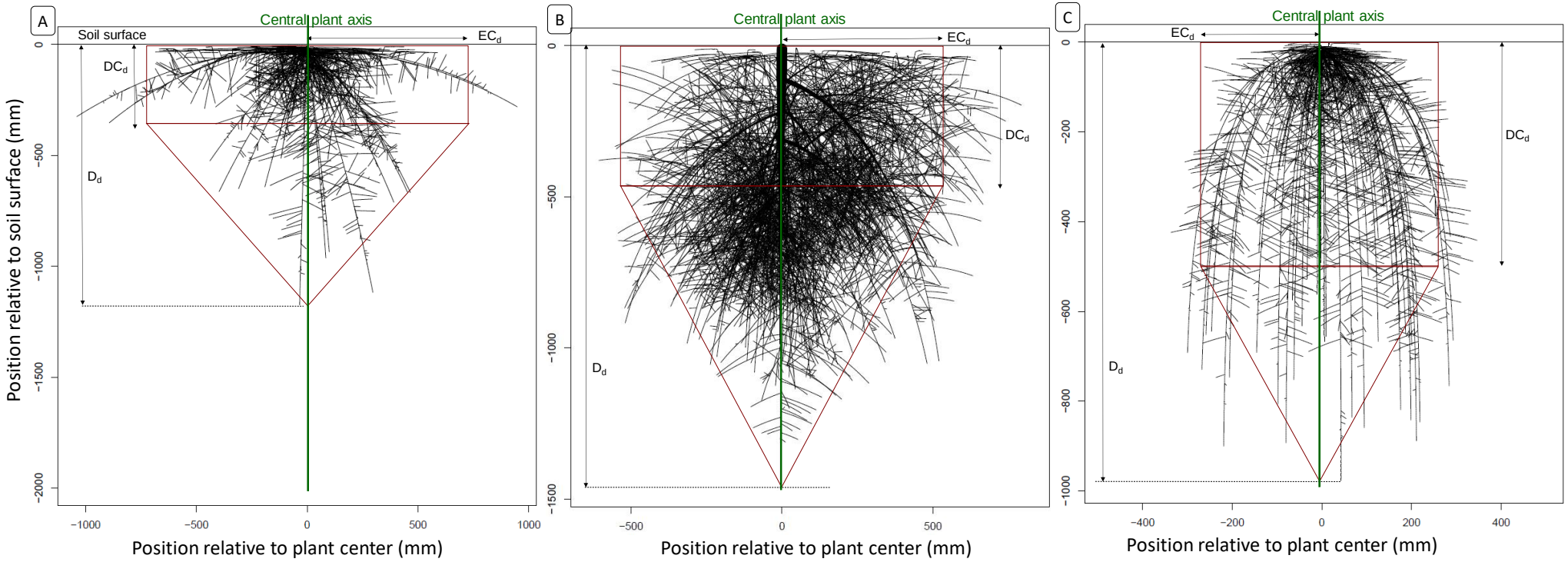

Figure S 4: Examples of root systems (A. Slow lateral roots and fast adventitious roots; B. Vigorous lateral roots, vigorous and early adventitious roots; C. Lateral roots with strong gravitropism) simulated with ArchiSimple and the corresponding RSCone envelope. In ArchiSimple, each root is a succession of segments whose advent and elongation are driven by processes such as emission of new adventitious roots from the shoot, elongation of existing roots, acropetal branching, radial growth and self-pruning following root decay. The RSCone envelope consists of a cylinder (depth DC_d, radius EC_d) on top of a spilled cone (height = D_d – DC_d). Please note the difference in scales between the three graphs, a scaled representation can be found in section C.3 in supplementary material online. (Loïc Pagès & Nathalie Colbach © 2019)

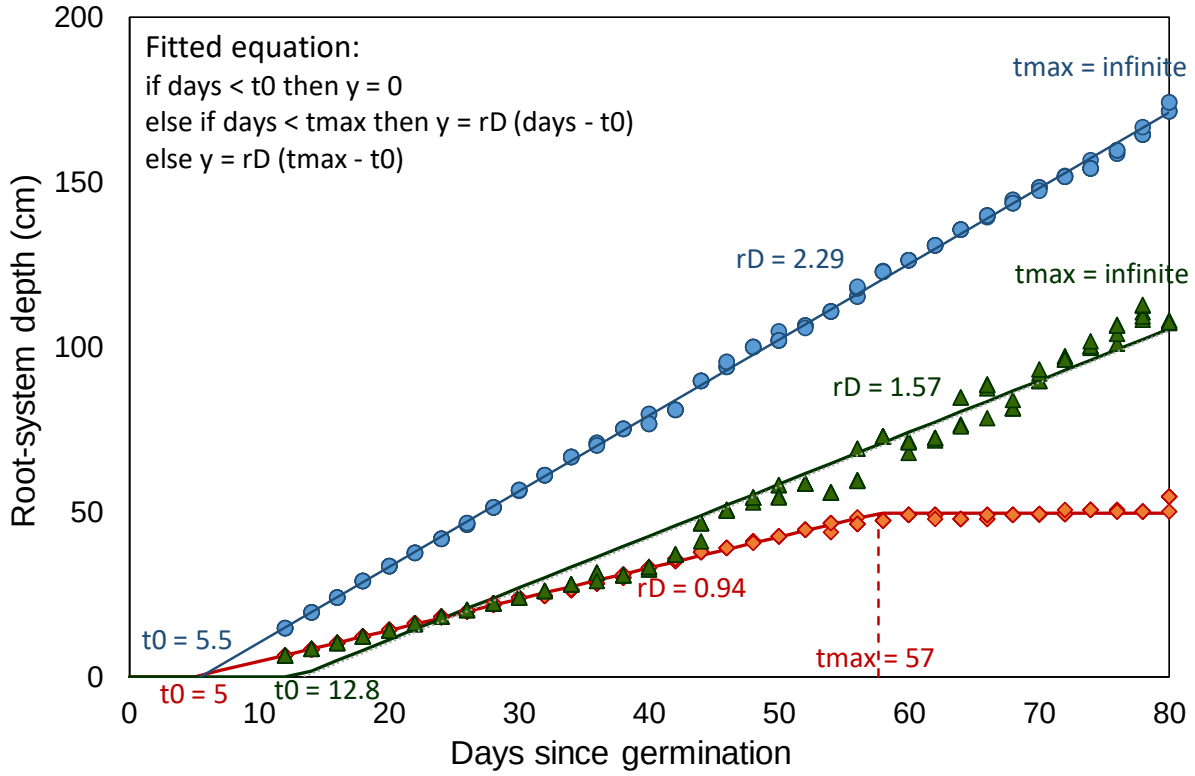

Figure S 5: Root depth versus plant age simulated with ArchiSimple for three contrasting root-system types (● tap-rooted system, ◆ determinate growth pattern, ▲ determinate seminal followed by indeterminate adventitious growth) in non-limiting conditions (no soil compaction, optimal soil temperature, non-limiting root biomass provision), with five replicates for each system. The pictures of the root systems can be found in section C.1 online (Loïc Pagès & Nathalie Colbach © 2019)

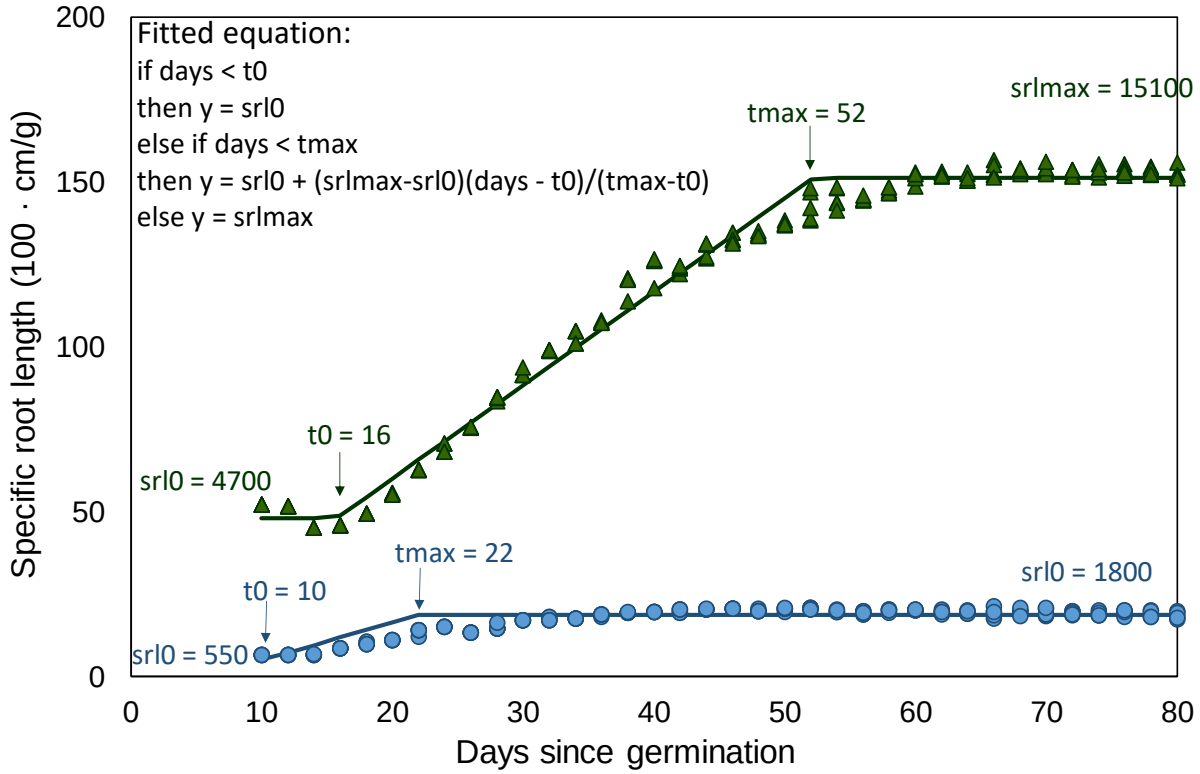

Figure S 6: Specific root length (cumulated root length divided by root biomass) versus plant age simulated with ArchiSimple for two contrasting root-system types (● thick root with radial growth, ▲thin roots without radial growth) in non-limiting conditions (no soil compaction, optimal soil temperature, non-limiting root biomass provision), with five replicates for each system. The pictures of the root systems can be found in section B.4 online (Loïc Pagès & Nathalie Colbach © 2019)

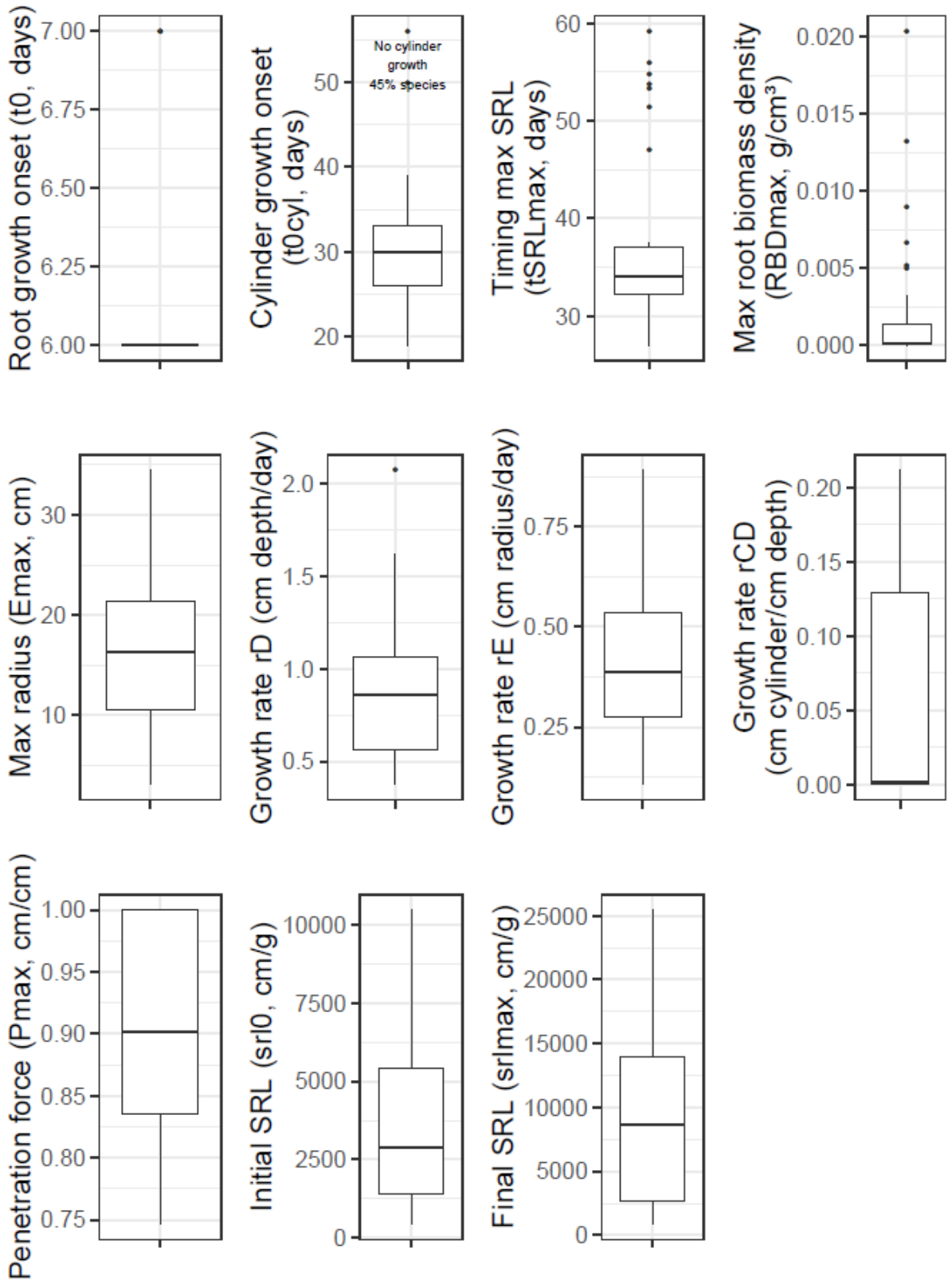

Figure S 7: Distribution of species parameters driving root-system state variables in RSCone. Parameters were estimated by fitting the equations of Table S 13 to simulations with ArchiSimple parameterized for the 45 species and varieties of Table S 15. For further information on RSCone parameters, see Table S 12.

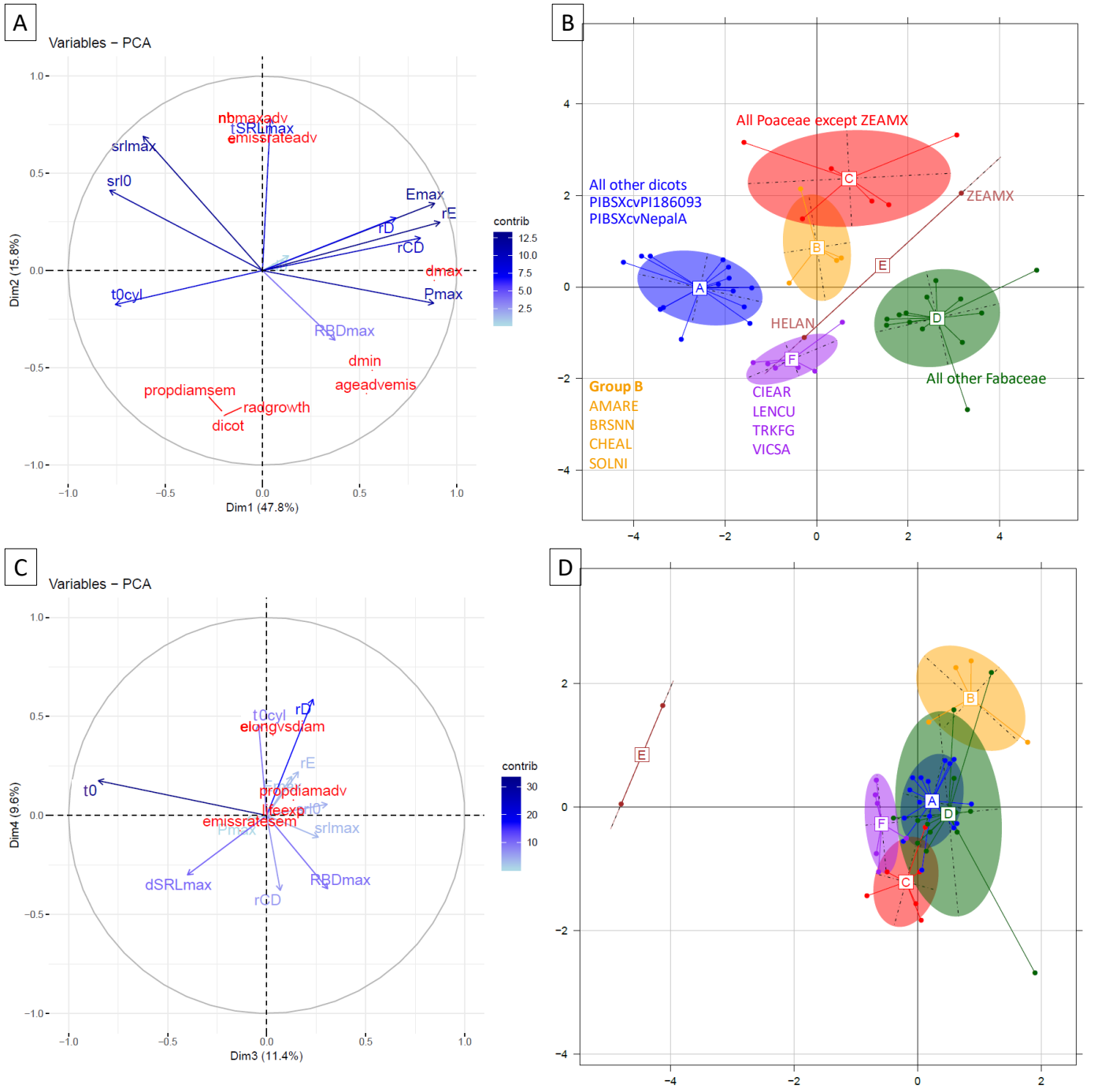

Figure S 8: Typology of crop and weed species based on a Principal Component Analysis on the RSCone parameters and the 45 species and varieties of Table S 15. Correlation circles with RSCone parameters in blue (see Table S 12 for meaning), with the five most important ArchiSimple parameters projected in red for the first two (A) and the last two axes (C), colouring variables according to their contribution to the analysis. Crop and weed species individuals clustered into groups, following a Ward ascendant hierarchy classification for the first two (B) and the last two axes (D). Species names are EPPO codes (Nathalie Colbach and Loïc Pagès © 2019)

Table S 15: List of crop and weed species used in ArchiSimple simulations to estimate RSCone parameters

Species	EPPO code	Variety	Family	Status	Seed mass (mg)
Alopecurus myosuroides	ALOMY		Poaceae	Weed	2.3
Amaranthus retroflexus	AMARE		Amaranthaceae	Weed	0.38
Avena fatua	AVEFA		Poaceae	Weed	18.5
Brassica napus	BRSNN	Kadore	Brassicaceae	Crop	4.4
Bromus hordeaceus (mollis)	BROMO		Poaceae	Weed	2.77
Capsella bursa-pastoris	CAPBP		Brassicaceae	Weed	0.14
Centaurea cyanus	CENCY		Asteraceae	Weed	5.3
Chenopodium album	CHEAL		Amaranthaceae	Weed	0.56
Cicer arietinum	CIEAR	Twist	Fabaceae	Weed	382
Echinochloa crus-galli	ECHCG		Poaceae	Weed	2.24
Fallopia convolvulus	POLCO		Polygonaceae	Weed	6.52
Galium aparine	GALAP		Rubiaceae	Weed	7.37
Geranium molle	GERMO		Geraniaceae	Weed	1.07
Glycine max	GLXMA	Sultana	Fabaceae	Crop	216
Helianthus annuus	HELAN		Asteraceae	Crop	41.0
Lens culinaris	LENCU	Anicia	Fabaceae	Crop	31.0
Lupin album	LUPAL	Feodora	Fabaceae	Crop	218
Phaseolus vulgaris	PHSVX	Flavert	Fabaceae	Crop	162
Pisum sativum	PIBSX	Amino	Fabaceae	Crop	203
Pisum sativum	PIBSX	Austin	Fabaceae	Crop	292
Pisum sativum	PIBSX	Cameor	Fabaceae	Crop	152
Pisum sativum	PIBSX	Cuzco 1	Fabaceae	Crop	182
Pisum sativum	PIBSX	Isard	Fabaceae	Crop	199
Pisum sativum	PIBSX	Kayanne 1[§]	Fabaceae	Crop	na
Pisum sativum	PIBSX	Kayanne 2	Fabaceae	Crop	216
Pisum sativum	PIBSX	Kayanne 3	Fabaceae	Crop	249
Pisum sativum	PIBSX	L1073	Fabaceae	Crop	253
Pisum sativum	PIBSX	Livioletta	Fabaceae	Crop	125
Pisum sativum	PIBSX	NepalA	Fabaceae	Crop	41.7
Pisum sativum	PIBSX	PI186093	Fabaceae	Crop	116
Polygonum aviculare	POLAV		Polygonaceae	Weed	1.52
Polygonum persicaria	POLPE		Polygonaceae	Weed	1.9
Senecio vulgaris	SENVU		Asteraceae	Weed	6.52
Solanum nigrum	SOLNI		Solanaceae	Weed	1.90
Sonchus asper	SONAS		Asteraceae	Weed	0.26
Stellaria media	STEME		Caryophyllaceae	Weed	0.80
Teucrium botrys	TEUBO		Lamiaceae	Weed	0.30
Trigonella foenum-graecum	TRKFG	Fenufix	Fabaceae	Crop	0.40
Tripleurospermum inodorum	MATIN		Asteraceae	Weed	0.27
Triticum aestivum	TRZAX	Caphorn	Poaceae	Crop	42.0
Veronica hederifolia	VERHE		Plantaginaceae	Weed	3.52
Vicia faba	VICFX	Espresso	Fabaceae	Crop	359
Vicia narbonensis	VICNA	Clara	Fabaceae	Crop	231
Vicia sativa	VICSA	Candy	Fabaceae	Crop	82.0
Vulpia myuros	VLPMY		Poaceae	Weed	0.83
Zea mays	ZEAMX		Poaceae	Crop	252

[§] *P. sativum* cv Kayanne was grown three times, in three different experimental series.

A.2.2. Equations, variables, parameters and inputs used in the FLORSYS-RSCone connection

Table S 16: Equations in the FLORSYS-RSCone connection, with d: date in days, l: soil layer in cm, s: species, i: individual, c: cohort (all plants of the same species emerging on the same day). Shaded cells show equations from (Pagès *et al.*, submitted), unshaded cells show equations required for connecting both models. Parameters are in blue (see meaning in Table S 17 and Table S 18), inputs are in **bold** (see meaning in Table S 19), FLORSYS state variables and variables added for the connection are in black plain font (see meaning in Table S 20) and RSCone variables in red (see meaning Table S 21).

N°	When	Process	Equation
Phenology			
[1]	∀d, ∀s, ∀c	Thermal time since cohort emergence on day d=dem_c	$TTE_{dsc} = \sum_{d'=dem_c}^{d}(T_{d'} - Tbase_s)$ (Colbach *et al.*, 2014c)
[2]	∀d, ∀s, ∀c	Converting durations of root development stages in optimal days since germination into day since emergence (considering that root system starts to grow the day of emergence)	$t0e_s = 0$ $tSRLmaxe_s = tSRLmax_s - t0_s$
[3]	∀d, ∀s, ∀c	Calibrating root development stages from plant phenology	$t_{sc} = t_s \cdot rPheno_{sc}$ with $t_{sc} = t0cyl_{sc}$ or $tSRLmaxe_{sc}$ and $t_s = t0cyl_s$ or $tSRLmaxe_s$ and $rPheno_{sc} = TTE_{sc\ death}/\min(TTE_{sc\ death})$
Environmental constraints on root-system growth			
[4]	∀s	Root-growth limitation due to soil structure	If $l \leq 29$ then $rPen_{dls} = pen_s \cdot (1 - rSmax \cdot (c\Delta_{dl} + 1/2 \cdot b\Delta_{dl} +$ **Stone**$) / (100 +$ **Stone**$))$
[5]			else if $l \geq 30$ and $l \leq$ **soil depth** then $rPen_{dls} = rPen_{d29s}$ else if $l >$ **soil depth** then $rPen_{dls} = 0$
[6]	∀s	Root-growth limitation due to soil temperature	If $l \leq 29$ then If $Tsoil_{dl} < Tbase_s$ then $rTsoil_{dls} = 0$ else if $Tsoil_{dl} < Topt_s$ then $rTsoil_{dls} = \sin(0.5 \cdot \pi \cdot (Tsoil_{dl} - Tbase_s) / (Topt_s - Tbase_s))$ else $rTsoil_{dls} = 1$
[7]			else if $l \geq 30$ and $l \leq$ **soil depth** then $rTsoil_{dls} = rTsoil_{d29s}$ else if $l >$ **soil depth** then $rTsoil_{dls} = 0$
[8]	∀s	Root growth limitation due to soil constraint (temperature and structure)	$rSoil_{dls} = rTsoil_{dls} \cdot rPen_{dls}$
Potential root-system dimensions (disregarding soil constraints)			
[9]	∀d, ∀s, ∀c	Potential root-system depth	$Dpot_{dsc} = rD_s \cdot te_{dsc}$
[10]	∀d, ∀s, ∀c	Potential root-system lateral extent (radius of the cylinder-shaped part of root system)	if $te_{dsc} < Emax_s/rE_s$ then $ECpot_{dsc} = rE_s \cdot te_{dsc}$ else $ECpot_{dsc} = Emax_s$
[11]	∀d, ∀s, ∀c	Potential depth at which root-system extent (radius) is maximal (depth of	If $te_{dsc} < t0cyl_{sc}$ then $DCpot_{dsc} = 0$ else $DCpot_{dsc} = (te_{dsc} - t0cyl_{sc}) \cdot rD_s \cdot rCD_s$

N°	When	Process	Equation
		cylinder-shaped part of root system)	
Actual root-system dimensions (accounting for soil constraints)			
[12]	∀d, ∀s, ∀c	Environmental constraints over potential root depth	$rSoilR_{dsc} = \frac{1}{\max(L,1)} \sum_{l=0}^{\max(L,1)} rSoil_{dls}$ with L = $Dpot_{dsc}$ $DCpot_{dsc}$ and DC_{dsc} for subsequent use in equations [13], [14] and [15] respectively
[13]	∀d, ∀s, ∀c	Actual root-system depth (cannot shrink except if frost damage)	$D_{dsc} = Dpot_{dsc} \cdot rSoilR_{dsc}$ If $D_{dsc} < D_{d-1sc}$ and $\mathbf{Tmin_d} > Tfrost_{sc}$ then $D_{dsc} = D_{d-1sc}$
[14]	∀d, ∀s, ∀c	Actual depth at which root-system extent (radius) is maximal (cannot shrink except if frost damage)	$DC_{dsc} = DCpot_{dsc} \cdot rSoilR_{dsc}$ If $DC_{dsc} < DC_{d-1sc}$ and $\mathbf{Tmin_d} > Tfrost_{sc}$ then $DC_{dsc} = DC_{d-1sc}$
[15]	∀d, ∀s, ∀c	Actual maximum root-system extent (radius) (cannot shrink except if frost damage)	$EC_{dsc} = ECpot_{dsc} \cdot rSoilR_{dsc}$ If $EC_{dsc} < EC_{d-1sc}$ and $\mathbf{Tmin_d} > Tfrost_{sc}$ then $EC_{dsc} = EC_{d-1sc}$
[16]	∀d, ∀s, ∀c	Lateral root-system extent (radius) in soil layer l	If $l < DC_{dsc}$ then $E_{dscl} = EC_{dsc}$ else if $l < D_{dsc}$ then $E_{dscl} = EC_{dsc} \cdot (1 - \frac{l+0.5-DC_{dsc}}{D_{dsc}-DC_{dsc}})$ else $E_{dscl} = 0$
Remobilization: onset and end			
[17]	If d=mowing	Remobilization starts if mowing or frost damage (Colbach *et al.*, 2014c) (annex A.2.3.2)	$ABM_{dsi} = f(ABM_{d-1si}, \mathbf{mowing\ height})$ $Remob_{dsi} = 1$ $ABMini_{si} = ABM_{dsi}$
[18]	$\mathbf{Tmin_d} < Tfrost_{sc}$		$ABM_{dsi} = f(ABM_{d-1si}, \mathbf{Tmin_d}, Tfrost_{sc})$ $RBM_{dsi} = f(RBM_{d-1si}, \mathbf{Tmin_d}, Tfrost_{sc})$ $Remob_{dsi} = 1$ $ABMini_{si} = ABM_{dsi}$
[19]	∀d, ∀s, ∀c If $Remob_{dsi} = 1$	Remobilization stops when the aboveground biomass has reached again the value before remobilization	If $ABM_{dsi} \geq ABMini_{si}$ $Remob_{dsi} = 0$
Biomass allocation to roots			
[20]	∀d, ∀s, ∀c, ∀i If $SI_{dsi} < 0.05$	Proportion of total biomass that is allocated to roots when plants are not yet competing for light.	If $TBM_{d-1si} > 0$ then $RBR_{dsi} = \frac{aa1_s \cdot TBM_{d-1si}^{a2_s}}{TBM_{d-1si}}$ else $RBR_{dsi} = 0$ If $RBR_{dsi} > 1$ then $RBR_{dsi} = RBRmax$ else if $RBR_{dsi} < 0$ then $RBR_{dsi} = 0$
[21]	∀d, ∀s, ∀c, ∀i If $SI_{dsi} < 0.05$	Plant growth when plants are not yet competing for light.	$ABM_{dsi} = f(TTE_{dsc})$ (Colbach *et al.*, 2014c) $RBMall_{dsi} = ABM_{dsi} \cdot \frac{RBR_{dsi}}{1-RBR_{dsi}}$
[22]	∀d, ∀s, ∀c, ∀i If $SI_{dsi} \geq 0.05$	Photosynthesis (as a function of photosynthetically active radiation intercepted by plants) and respiration of roots and aboveground organs when plants are competing for light.	$BMps_{dsi} = f(PAR_{dsi})$ (Colbach *et al.*, 2014c) $ABMr_{dsi} = (LBM_{d-1si} \cdot cr_{leaf} + StBM_{d-1si} \cdot cr_{stem} + SeBM_{d-1si} \cdot cr_{seeds}) \cdot Teffect$ with $Teffect = f(\mathbf{T_d})$ (Colbach *et al.*, 2014c) $RBMr_{dsi} = RBM_{d-1si} \cdot cr_{roots} \cdot Teffect$
[23]	∀d, ∀s, ∀c, ∀i If $SI_{dsi} \geq 0.05$	Proportion of total biomass that is allocated to roots when plants are competing for light.	$TBM_{dsi} = TBM_{d-1si} + BMps_{dsi} - ABMr_{dsi} - RBMr_{dsi}$ If $TBM_{dsi} > 0$ then $RBR_{dsi} = \frac{aa1_s \cdot TBM_{dsi}^{a2_s} \cdot 10^{a3 \cdot Nstress_{d-1si}}}{TBM_{dsi}}$ else $RBR_{dsi} = 0$ If $RBR_{dsi} > 1$ then $RBR_{dsi} = RBRmax$ If $RBR_{dsi} < 0$ then $RBR_{dsi} = 0$

N°	When	Process	Equation
[24]	∀d, ∀s, ∀c, ∀i If $SI_{dsi} \geq 0.05$ If $TTE_{dsc} < TTflo_{sc}$ and if $Remob_{dsi} = 0$	Plant growth when plants are competing for light before flowering onset and if there is no remobilization following a mowing operation or frost damage	$RBMall_{dsi} = RBM_{d-1si} + RBR_{dsi} \cdot BMps_{dsi} - RBMr_{dsi}$ If $RBMall_{dsi} < 0$ then $RBMall_{dsi} = 0$ $ABM_{dsi} = ABM_{dsi} + (1- RBR_{dsi}) \cdot BMps_{dsi} - ABMr_{dsi}$ If $ABM_{dsi} < 0$ then $ABM_{dsi} = 0$
[25]	∀d, ∀s, ∀c, ∀i If $SI_{dsi} \geq 0.05$ If p ≥ flowering or $Remob_{dsi} = 1$	Plant growth when plants are competing for light from the beginning of flowering onward, or during remobilization following a mowing operation or frost damage.	$RBMall_{dsi} = RBM_{d-1si} - RBMr_{dsi} - ABMr_{dsi}$ If $RBMall_{dsi} < 0$ then $RBMall_{dsi} = 0$ $ABM_{dsi} = ABM_{dsi} + BMps_{dsi}$
[26]	∀d, ∀s, ∀c, ∀i	Plant mortality due to biomass loss (insufficient photosynthesis due to shading, mowing, frost)	If $TBM_{dsi} = 0$ then plant i dies
Root-system biomass			
[27]	∀d, ∀s, ∀c	Potential biomass density per soil layer (disregarding insufficient photosynthesis but accounting for soil constraints)	If $l < DC_{dsc}$ then $RBDpot_{dscl} = RBDmax_s$ else if $l < D_{dsc}$ then $RBDpot_{dscl} = RBDmax_s \cdot (D_{dsc} - l) / (D_{dsc} - DC_{dsc})$ else $RBDpot_{dscl} = 0$
[28]	∀d, ∀s, ∀c	Potential root-system biomass (disregarding insufficient photosynthesis but accounting for soil constraints)	If $te_{dsc} = 0$ then $RBMpot_{dsc} = 0$ else $RBMpot_{dsc} = RBDmax_s \cdot 0.25 \cdot \pi \cdot EC_{dsc}^2 \cdot (3 \cdot DC_{dsc} + D_{dsc})$
[29]	∀d, ∀s, ∀c, ∀i	Actual root biomass (accounting for soil and photosynthesis constraints)	$RBM_{dsi} = \min(RBMpot_{dsc}, RBMall_{dsi})$ If $RBMpot_{dsc} > 0$ then $rPhoto_{dsi} = RBM_{dsi} / RBMpot_{dsc}$ else $rPhoto_{dsi} = 0$
[30]	∀d, ∀s, ∀c, ∀i	Actual root-biomass density in soil layer l (accounting for soil and photosynthesis constraints)	$RBD_{dsil} = rPhoto_{dsi} \cdot RBDpot_{dscl}$
Root-length density (accounting for soil and photosynthesis constraints)			
[31]	∀s, ∀c, ∀p, ∀i	Specific root length	If $te_{dsc} = 0$ then $srl_{dsc} = srl0_s$ else if $te_{dsc} \leq tSRLmaxe_{sc}$ then $srl_{dsc} = (srlmax_s - srl0_s) \cdot te_{dsc} / tSRLmaxe_{sc} + srl0_s$ else $srl_{dsc} = srlmax_s$
[32]	∀s, ∀c, ∀p, ∀i	Root-length density in soil layer l	If $l \leq D_{dsc}$ then $RLD_{dsil} = srl_{dsc} \cdot RBD_{dsil}$ else $RLD_{dsil} = 0$

Table S 17: Species parameters used in FLORSYS-RSCone, with d: date in days, l: soil layer in cm, s: species, i: individual, c: cohort (all plants of the same species emerging the same day).

Parameter	Meaning	Source	Unit	Range of variation in simulated species
$aa1_s = 10^{a1_s}$	Root biomass when total plant biomass is near zero for species s	Estimated from data on root and total plant biomass (section 3.2.4.1.3)	$g \cdot g^{-1}$	0.112-0.261
$a2_s$	Slope of allometric relationship of root vs total plant biomass for species s		no unit	0.817-1.04
$Emax_s$	Maximum extent (radius) of the root system	RSCone parameter	cm	87.9-423
pen_s	Ability of roots to penetrate the soil (from 0: no penetration, to 1: no soil constraint on root growth)	RSCone parameter	no unit	0.747-1.00
$RBDmax_s$	Root-biomass density in the cylinder part of the root system, disregarding constraints	RSCone parameter	$g \cdot cm^{-3}$	$1.95 \cdot 10^{-5}$-$9.85 \cdot 10^{-3}$
rCD_s	Ratio of speed at which depth of cylinder-shaped part of root system increase vs speed of total root-system depth increase	RSCone parameter	$cm \cdot day^{-1} \cdot (cm \cdot day^{-1})^{-1}$ (under optimal temperature)	0.00-0.253
rD_s	Speed at which root-system depth increases	RSCone parameter	$cm \cdot day^{-1}$ (under optimal temperature)	0.950-3.66
rE_s	Speed at which root-system extent (radius) increases	RSCone parameter	$cm \cdot day^{-1}$ (under optimal temperature)	0.200-0.889
$srl0_s$	Specific root length when roots start to grow	RSCone parameter	$cm \cdot g^{-1}$	519-19200
$srlmax_s$	Maximal specific root length	RSCone parameter	$cm \cdot g^{-1}$	1380-30700
$t0cyl_s$	Delay from $t0_s$ to when the cylinder part of the root system starts to grow in depth	RSCone parameter	Days since $t0_s$ (under optimal temperature)	20-365
$t0_s$	Timing of root growth onset since germination	RSCone parameter	Days since germination (under optimal temperature)	6-7
$Tbase_s$	Base temperature for growth and development	FLORSYS parameter	°C	
$Topt_s$	Optimal temperature for growth and development	FLORSYS parameter	°C	
$Tfrost_{sc}$	Temperature threshold for frost damage of cohort c	FLORSYS parameter (details in annex A.2.3.1)	°C	
$tSRLmax_s$	Timing of maximum specific root length (SRL) since germination	RSCone parameter	Days since germination (under optimal temperature)	26-49

Parameter	Meaning	Source	Unit	Range of variation in simulated species
TTE_{scp}	Thermal time from emergence to onset of stage p {vegetative, flowering onset, maturity onset, death} depending on the time of emergence	FLORSYS parameter	°C·days	

Table S 18: Species-independent parameters used in FLORSYS-RSCone.

Parameter	Meaning	Source	Unit
a3	Slope of nitrogen-stress effect on root biomass, regardless of species	Estimated from data on root and total plant biomass (section 3.2.4.1.3)	No unit
cr_{leaf}, cr_{stem}, cr_{seeds}, cr_{roots}	Coefficients for respiration of leaves, stems, seeds and roots respectively (Colbach *et al.*, 2014c)	FLORSYS parameter	$g \cdot g^{-1}$
rSmax	Maximal root growth reduction exerted by soil constraints	STICS parameter (CONTRDAMAX =0.5)	
RBRmax	Maximum leaf biomass ratio, i.e. maximum proportion of plant biomass allocated to roots	Estimated from data on root and total plant biomass (section 3.2.4.1.3)	$g \cdot g^{-1}$

Table S 19: Inputs of FLORSYS-RSCone.

Parameter	Meaning	Unit
T_d	Average air temperature	°C
$Tmin_d$	Minimum air temperature	°C
Stone	Proportion of stones in the soil	

Table S 20: Plant and environment state variables predicted by FLORSYS and added for connecting RSCone, with d: date in days, l: soil layer in cm, s: species, i: individual, c: cohort (all plants of the same species emerging the same day), p: stage ∈ {cotyledon, seedling, vegetative, flowering, disseminating}.

Variable	Meaning	Value	Unit
ABM_{dsi}	Aboveground biomass		$g \cdot plant^{-1}$
$ABMini_{si}$	Aboveground biomass of plant i before mowing or frost damage		$g \cdot plant^{-1}$
$ABMr_{dsi}$	Aboveground biomass lost by respiration on day d		$g \cdot plant^{-1}$
$BMps_{dsi}$	Biomass accumulated by photosynthesis on day d		$g \cdot plant^{-1}$
$b\Delta_{dl}$	Proportion of bΔ soil clods in soil layer l	[0,1]	
$c\Delta_{dl}$	Proportion of cΔ soil clods in soil layer l	[0,1]	
LBM_{dsi}	Leaf biomass		$g \cdot plant^{-1}$
$Nstress_{dsi}$	Nitrogen stress index	Close to 0 under optimum nitrogen nutrition, positive under nitrogen deficiency, and negative under nitrogen excess (Perthame *et al.*, submitted).	
RBR_{dsi}	Root biomass ratio, i.e. proportion of total biomass that is allocated to roots	Depends on total plant biomass, stress index and growth stage	$g \cdot g^{-1}$
$RBMall_{dsi}$	Biomass allocated to roots by FLORSYS	Depends on the stage, the biomass and the nitrogen stress index of the plant	$g \cdot plant^{-1}$
$RBMr_{dsi}$	Root biomass lost by respiration on day d		$g \cdot plant^{-1}$
$Remob_{dsi}$	Boolean indicating whether there is still remobilization each day following a cutting operation or a frost event	0: no remobilization, or 1: remobilization.	
$SeBM_{dsi}$	Seed biomass		$g \cdot plant^{-1}$
$StBM_{dsi}$	Stem biomass		$g \cdot plant^{-1}$
TBM_{dsi}	Total plant biomass	Root biomass + aboveground biomass	$g \cdot plant^{-1}$
te_{dsc}	Number of days since emergence of cohort c of species s		days
$Tsoil_{dl}$	Temperature in soil layer l		°C
TTE_{dsc}	Age since emergence of cohort c on day d	Depends on daily air temperature (Colbach *et al.*, 2014c)	°C·days
PAR_{dsi}	Photosynthetically active radiation intercepted by plant i on day d		J
$t0cyl_{sc}$	Delay from $t0_s$ to when the cylinder part of the root system starts to grow in depth under real temperatures	Time of emergence	Days since the root system starts to grow

Variable	Meaning	Value	Unit
$t0e_s$	Timing of root growth onset since emergence under optimal temperature		Days since emergence (under optimal temperature)
$tSRLmaxe_s$	Timing of maximum specific root length (SRL) since emergence under optimal temperature		Days since emergence (under optimal temperature)
$tSRLmaxe_{sc}$	Timing of maximum specific root length (SRL) since emergence under real temperatures	Time of emergence	Days since emergence
$rPheno_{sc}$	Ratio taking into account that the duration of root development stages depends on the phenology of the plant	Depends on minimal and maximal life-cycle durations of species s (life-cycle duration depending on the time of emergence)	$°C \cdot days \cdot °C^{-1} \cdot days^{-1}$

Table S 21: Variables predicted by RSCone (from Pagès *et al.*, submitted), with d: date in days, l: soil layer in cm, s: species, i: individual, c: cohort (all plants of the same species emerging on the same day), p: stage ∈ {cotyledon, seedling, vegetative, flowering, disseminating}.

Variable	Meaning	Drivers (other than species)	Unit
DC_{dsc}	Actual depth of the cylinder-shaped part of the root system (considering soil constraints)	Potential depth at which the root-system width starts to shrink, soil constraints	cm
$DCpot_{dsc}$	Potential depth of the cylinder-shaped part of the root system (disregarding soil constraints)	Plant age	cm
D_{dsc}	Actual root-system depth (considering soil constraints)	Potential root-system depth, soil constraints	cm
$Dpot_{dsc}$	Potential root-system depth (disregarding soil constraints)	Plant age	cm
EC_{dsc}	Actual extent (radius) of the cylinder-shaped part of the root system (considering soil constraints)	Potential root-system extent, soil constraints	cm
$ECpot_{dsc}$	Potential extent (radius) of the cylinder-shaped part of the root system (disregarding soil constraints)	Plant age	cm
E_{dscl}	Root-system extent (radius) in soil layer l	Actual root-system extent, soil layer	cm
RBD_{dsil}	Root-biomass density in soil layer l	Actual root biomass in soil layer l, volume of layer l inside root-system envelop	$g \cdot cm^{-3}$
$RBDpot_{dscl}$	Potential root-biomass density in soil layer l	Actual root-system dimensions, soil layer	$g \cdot cm^{-3}$
RBM_{dsi}	Actual root biomass	Potential root biomass, root biomass allocated by FLORSYS	$g.plant^{-1}$
$RBMpot_{dsc}$	Potential root-system biomass	Actual root-system dimensions, plant age	$g.plant^{-1}$
RLD_{dsil}	Root-length density in soil layer l	Root-biomass density in soil layer, specific root length	$cm \cdot cm^{-3}$
$rPen_{dls}$	Relative reduction in root-system expansion due to root penetration resistance exerted by the soil (due to soil compaction and gravel content) in soil layer l	Soil structure and gravel content	$cm \cdot cm^{-1}$
$rPhoto_{dsi}$	Relative reduction in root biomass due to insufficient allocation from FLORSYS	Potential root biomass, root biomass provided by FLORSYS	$g \cdot g^{-1}$
$rSoil_{dls}$	Relative reduction in root-system expansion due to soil constraints (temperature, compaction) in soil layer l	Relative reduction in root-system expansion due to soil compaction and temperature in soil layer l	$cm \cdot cm^{-1}$
$rSoilR_{dsc}$	Average relative reduction in in root-system expansion due to soil constraints (temperature, compaction) over several soil layers	Relative reduction in in root-system expansion due to soil constraints (temperature, compaction), soil layers considered	$cm \cdot cm^{-1}$
$rTsoil_{dls}$	Relative reduction in in root-system expansion due to low soil temperature in soil layer l	Soil temperature	$cm \cdot cm^{-1}$
srl_{dsc}	Specific root length	Plant age	$cm \cdot g^{-1}$

A.2.3. Details on FLORSYS submodels

A.2.3.1. Insulating snow effect in FLORSYS (extract of FLORSYS manual)

(Colbach N. & Pointurier O. (2018) Adapting the FLORSYS model to Northern German conditions - Final project report. INRA, Dijon, France, 12 p.

Colbach N., Collard A., Guyot S. H. M., Mézière D. & Munier-Jolain N. M. (2014) Assessing innovative sowing patterns for integrated weed management with a 3D crop:weed competition model. European Journal of Agronomy 53, 74-89, http://dx.doi.org/10.1016/j.eja.2013.09.019.)

A.2.3.1.1. Protection again frost damage by snow cover

FLORSYS uses daily weather data as inputs to predict soil climate, plant phenology and frost damage. A new function was added to predict the amount of snow covering the soil and its insulating effect from these weather inputs as in Jégo *et al.* (2014). The daily snowfall is predicted from the daily amount of rain and minimum and maximum temperatures. The snow cover on a particular day is the amount of snow accumulated over past days minus the amount of snow that has melted during the day. Minimum and maximum temperatures driving biological and physical processes in FLORSYS are then corrected according to the insulating effect of the snow cover which depends on its depth (the thicker the snow cover, the more it insulates). The amount of rain of the day entering the soil is also corrected as the amount of precipitation minus the amount of snowfall plus the amount of melted snow. Corrected temperatures and precipitation are then used to predict soil climate and frost damage on plants depending on plant heights compared to the snow cover depth. If a plant is totally snow-covered, corrected temperatures approximating within-snow temperatures are used to predict biomass reduction due to frost. On the contrary, if the plant is higher than the snow cover, snow surface temperature is used. Plant mortality due to frost is calculated from corrected temperatures whatever the plant height assuming that even a partial snow cover prevent the plant from dying (Jégo, personal communication). Snow surface temperature is used instead of air temperature because it is generally lower than air temperature (Raleigh *et al.*, 2013) and calculations from air temperature may underestimate frost damages above snow cover (Castel, personal communication). Snow surface temperature is approximated by the dew point temperature (Raleigh *et al.*, 2013) which is calculated from the minimum air temperature (Brisson *et al.*, 1998; Brisson *et al.*, 2002; Brisson *et al.*, 2003).

The snow cover model was parameterized with data from the literature. Three models were tested in Jégo *et al.* (2014) and were calibrated for different regions in the world (Thorsen *et al.*, 2010; Trnka *et al.*, 2010; Jégo *et al.*, 2014). The model of Trnka *et al.* (2010) was chosen because it was parameterized with data from Hohenau (Austria) where snow depth dynamics are very similar to Rostock (see Table S 22). Snow depth was used as a criterion because it determines the snow cover behaviour (freezing, melting, compaction…) (Castel, personal communication, Niu *et al.*, (2011)).

Equations are in Table S 22.

A.2.3.1.2. Biomass loss and plant mortality

If the minimum daily temperature perceived by the plant descends below both the species and the plant's frost sensitivity threshold, the plant's biomass is reduced linearly with frost intensity. If the perceived temperature descends even further, plants start to die, with a probability increasing linearly with frost intensity. The surviving plants' frost sensitivity threshold is decreased to 5°C below the current minimum temperature; this reduced sensitivity remains for a month. For many species, sensitivity thresholds vary with plant stage. Generally, as for cultivated species, weed plants are most sensitive at cotyledon stage and again during the reproductive stage; they are least sensitive during seedling and vegetative stages (Roberts, 1979; Fowler *et al.*, 1999).

Equations are in Table S 23.

A.2.3.1.3. Damage to flowers

Based on expertise (Christophe Lecomte (Lecomte *et al.*, 2003; Castel *et al.*, 2017)), a further function was added to the frost damage submodel to make flowers die in case of frost. Once a cohort has started to flower, a minimum day temperature below TF1 (temperature setting off biomass loss) kills off all flowers. Plants will only die if temperature drops below TF2 but they will not produce seeds.

Table S 22: Comprehensive list of equations relating state variables in the snow-cover submodel in FLORSYS, with d=day. For explanations on **parameters** and **input variables** see Table S 24 and Table S 25

Eq.	When	Process	Equation	Explanation
[1]	At the beginning of the simulation	Snow accumulation	if $\mathbf{Tmin_d} \leq$ TA2 then $SA_d = \mathbf{Pr_d}$ if $\mathbf{Tmin_d} \geq$ TA1 then $SA_d = 0$ if $\mathbf{Tmin_d} \in$]TA2,TA1[then $SA_d = (1-(\mathbf{Tmin_d}-TA2)/(\lvert TA1 - TA2\rvert))\cdot\mathbf{Pr_d}$	SA_d = daily snow accumulation (mm snow water equivalent) (Trnka *et al.*, 2010) $\mathbf{Tmin_d}$ and $\mathbf{Tmax_d}$ = minimum and maximum daily air temperatures (°C) $\mathbf{Pr_d}$ = daily precipitation (mm) TA1 and TA2 = temperature thresholds to determine the amount of precipitation in the form of snow, with TA1 > TA2 (°C)
[2]	At the beginning of the simulation	Snow melting	if $\mathbf{Tmin_d} <$ TM1 or if $\mathbf{Tmin_d} \leq 0$ and $\mathbf{Tmax_d} <$ TM2 then $SM_d = 0$ if $\mathbf{Tmin_d} \geq$ TM1 and $\mathbf{Tmax_d} \geq$ TM2 then $SM_d = \min(SC_{d-1}+SA_d, rM\cdot(\mathbf{Tmin_d}+\lvert TM1\rvert))$	SM_d = daily snow melting (mm snow water equivalent) (Trnka *et al.*, 2010) TM1 and TM2 = temperature thresholds to determine the amount of snow melting, with TM1 < TM2 (°C) SC_d = snow cover depth (mm snow water equivalent) (Trnka *et al.*, 2010) rM = daily melting rate of snow (mm snow water equivalent °C^{-1} day^{-1})
[3]	At the beginning of the simulation	Snow depth	if $SC_{d-1} \leq$ SCS then $SC_d = SA_d - SM_d$ else $SC_d = SA_d - SM_d -$ sub	SCS = snow cover depth above which sublimation is taken into account (mm snow water equivalent) sub = amount of snow allowed to sublimate when conditions are met (mm snow water equivalent day^{-1})
[4]	At the beginning of the simulation	Insulating effect of the snow cover	if $SC_d >$ SCI and $\mathbf{Tmin_d} \leq$ TS1 then $TminS_d =$ TS1 if $SC_d >$ SCI and $\mathbf{Tmax_d} \leq$ TS2 then $TmaxS_d =$ TS2 if $SC_d \in$ [0, SCI] and $\mathbf{Tmin_d} \leq$ TS1 then $TminS_d =$ TS1-(1-SC_d/SCI)·(|$\mathbf{Tmin_d}$|+TS1) if $SC_d \in$ [0, SCI] and $\mathbf{Tmax_d} \leq$ TS2 then $TmaxS_d =$ TS2-(1-SC_d/SCI)·(-$\mathbf{Tmax_d}$) if $SC_d > 0$ and $\mathbf{Tmin_d} >$ TS1, $TminS_d = 0$	$TminS_d$, $TmaxS_d$ and TS_d = minimum, maximum and average daily air temperatures corrected to take into account the insulating effect of snow cover (°C) (Jégo *et al.*, 2014) $TminS_d$, $TmaxS_d$ and TS_d = minimum, maximum and

Eq.	When	Process	Equation	Explanation
			if $SC_d > 0$ and $\mathbf{Tmax_d} >$ TS2, $TmaxS_d = 0$ if $SC_d = 0$, $TminS_d = \mathbf{Tmin_d}$ and $TmaxS_d = \mathbf{Tmax_d}$ $TS_d = (TminS_d + TmaxS_d)/2$	average daily air temperatures corrected to take into account the insulating effect of snow cover (°C) (Jégo *et al.*, 2014) TS1 and TS2 = temperature thresholds to take into account the insulating effect of snow cover, with TS1 < TS2 (°C)
[5]	At the beginning of the simulation	Water budget	$PrS_d = \mathbf{Pr_d} - SA_d + SM_d$	PrS_d = daily precipitation in the form of rain (mm) (Jégo *et al.*, 2014)

Table S 23: Comprehensive list of equations relating state variables in the frost damage submodel in FLORSYS, with d=day, s=species, i=individual. For explanations on **parameters** and **input variables** see Table S 24 and Table S 25

Eq.	When	Process	Equation	Explanation
[6]	∀d,i If $Tmin_d < Tsen_{di}$	Biomass reduction	if $T <$ $TF3_{sp}$ then $rR_{dsi} = 1$ if $T \in [TF3_{sp}, TF1_{sp}]$ then $rR_{dsi} = (T - TF1_{sp}) / (TF3_{sp} - TF1_{sp})$ if $T >$ $TF1_{sp}$ then $rR_{dsi} = 0$ with $T = TminS_d$ if $H_{dsi} < 10 \cdot SC_d$, $T = \mathbf{Tmin_d} -$ correcT else	$Tsen_{di}$ = temperature threshold (°C) for frost sensitivity rR_{dsi} = biomass reduction rate by frost $TF1_{sp}$ and $TF3_{sp}$ = temperature thresholds (°C) depending on phenology *p*, with $T1_{sp} > T3_{sp}$ $\mathbf{Tmin_d}$ = minimum daily air temperature (°C) $TminS_d$ = minimum daily air temperatures corrected to take into account the insulating effect of snow cover (°C) H_{dsi} = plant height (cm) correcT = temperature to substract to $Tmin_d$ to estimate dew point temperature (°C)
[7]	∀d,i	Biomass reduction	$BM_{dsi} = (1-rR_{dsi}) \cdot BM_{dsi}$	
[8]	∀d,i If $Tmin_d < Tsen_{dsi}$	Mortality	if $TminS_d <$ $TF3_{sp}$ then $pM_{dsi}=1$ if $TminS_d \in [TF3_{sp}, TF2_{sp}]$ then $pM_{dsi} = (TminS_d - TF2_{sp}) / (TF3_{sp} - TF2_{sp})$ if $TminS_d >$ $TF2_{sp}$ then $pM_{dsi} = 0$	pM_{dsi} = probability of being killed by frost $TF2_{sp}$ = temperature threshold (°C) depending on phenology *p*, with $TF1_{sp} > TF2_{sp} > TF3_{sp}$
[9]	∀d,i	Mortality	prob = *random*(0,1) if prob < pM_{dsi} then P_{si} dies and $nP_{ds} = nP_{ds} - 1$	
[10]	∀d,i	Frost sensitivity	if $nDF_{sdi} > 30$ then $Tsen_{dsi} = 0$ if $TminS_d <$ *min*($Tsen_{di}$, $T1_{sp}$) then $Tsen_{dsi} = TminS_d - 5$ and $nDF_{sdi} = 0$ else $nDF_{sdi} = nDF_{sdi} + 1$	nDF_{sdi} = days since the last frost

d=day, s=species (weed or crop), i=individual, g=gap, p=stage

Variables starting with n are number of individuals in the field map, with d are density of individuals (individuals/m²), with p are probabilities, with r are rates.

min(x_1, x_2) returns the smaller values of x_1 and x_2

Table S 24: List of species parameters used in the FLORSYS frost-damage and snow-cover submodel. For crops, parameters can differ between varieties.

Symbol	Meaning and unit	Source
correcT	temperature to substract to minimum daily air temperature to estimate dew point temperature (°C)	STICS
rM	daily melting rate of snow (mm snow water equivalent $°C^{-1}$ day^{-1}, species-independent)	(Trnka *et al.*, 2010)
SCI	snow cover depth necessary to insulate efficiently crops against frost (mm snow water equivalent, species-independent)	(Trnka *et al.*, 2010)
SCS	snow cover depth above which sublimation is taken into account (mm snow water equivalent, species-independent)	(Trnka *et al.*, 2010)
sub	amount of snow allowed to sublimate when conditions are met (mm snow water equivalent day^{-1}, species-independent)	(Trnka *et al.*, 2010)
TA1, TA2	temperature thresholds to determine the amount of precipitation in the form of snow, with TA1 > TA2 (°C, species-independent)	(Trnka *et al.*, 2010)
$TF1_{sp}$, $TF2_{sp}$, $TF3_{sp}$	temperature thresholds for species sensitivity to frost depending on phenology *p*, with $TF1_{sp} > TF2_{sp} > TF3_{sp}$ (°C)	STICS for crops, expert knowledge (Christophe Lecomte) for varieties. Three types of weeds: winter, spring and summer, based on expertise
TM1, TM2	temperature thresholds to determine the amount of snow melting, with TM1 < TM2 (°C, species-independent)	(Trnka *et al.*, 2010)
TS1, TS2	Temperature thresholds to take into account the insulating effect of snow cover, with TS1 < TS2 (°C, species-independent)	(Trnka *et al.*, 2010; Jégo *et al.*, 2014; Vico *et al.*, 2014)

Phenological stage p ∈ {cotyledon, plantlet, vegetative, flowering, disseminating}; *s* is a crop or a weed species

Table S 25: Input variables of the FLORSYS frost damage and snow-cover submodel.

Input variable	Symbol	Options or units
Pedoclimatic conditions		
Average air temperature on day *d*	$\mathbf{T_d}$	°C
Minimum air temperature on day *d*	$\mathbf{Tmin_d}$	°C
Maximum air temperature on day *d*	$\mathbf{Tmax_d}$	°C
Precipitation on day *d*	Pr_d	mm

A.2.3.2. Effect of harvest, mowing, cutting, residue shredding (extract of FLORSYS manual)

A.2.3.2.1. What are the differences between these operations?

Harvest is any operation that exports part of the crop plants and kills all crop plants. Mowing or cutting are operations that export part of the crop plants but leave them alive to produce new biomass. In FLORSYS, the last mowing operation in a grassland before tilling the soil for the next crops is considered to be a harvest, terminating the grassland crop before moving on to the next crop. Mowing or cutting can also leave the cut biomass in the field.

Residue shredding are operations carried out after crop harvest to chop the residues left by previous crops. In FLORSYS, they are assimilated to mowing or cutting with a cutting height of 0 cm. There are no seed movements in the soil.

A.2.3.2.2. Effect on plant growth and development

(Colbach N., Cordeau S., Garrido A., Granger S., Laughlin D., Ricci B., Thomson F. & Messéan A. (2018) Landsharing vs landsparing: How to reconcile crop production and biodiversity? A simulation study focusing on weed impacts. Agriculture, Ecosystems & Environment 251, 203-217, https://doi.org/10.1016/j.agee.2017.09.005.)

Principle

When a field or grass strip is mown, cut plants (whether annual or multi-annual) produce new shoots if they have not yet started to produce seeds (Colbach *et al.*, 2018). Their flowering and maturation are delayed compared to uncut plants, and their biomass accumulation through photosynthesis is reduced because of leaf-area loss. However, belowground biomass is remobilized to increase aboveground biomass faster and to make up for lost leaf area.

In FLORSYS, this remobilization after mowing increases with species remobilization efficiency, biomass prior to mowing (as a proxy for root biomass which is not yet predicted in FLORSYS) and daily air temperature. Remobilization decreases when plants start to flower, and stops when they start to mature. Once plant biomass exceeds the biomass prior to mowing, remobilization stops. Cutting height determines which plants are affected.

Each plant p belongs to an emergence cohort c consisting of all the plants of species s that have emerged on the same day. To date, only aboveground plant biomass is predicted in FLORSYS. The following subsections describe (1) how plants are cut during mowing, resulting in aboveground biomass loss as well as a reduction in plant size and leaf area, and (2) how they grow after mowing, both via photosynthesis from their reduced leaf area, and via remobilization from belowground plant reserves, using pre-mowing aboveground plant biomass as a proxy.

Inputs and state variables

Each mowing, cutting or harvest operation is characterized by the following input variables:

- Date t_{mowing},
- Height H_{mowing} (cm),
- Mode, i.e. the mown biomass is exported or left in the field,
- Rate of crop seed loss (seeds/seeds).

Crop and weed species are characterized by the following species traits:

- Remobilization coefficient $remob_s$ (g g^{-1} °C $^{-1}$)
- Shortest possible duration of vegetative stage $TTveg_s$ (°C days)
- Efficiency of photosynthesis εb_s (g MJ^{-1})

- Respiration coefficients for leaves, stems and seeds, respectively, rl_s, rt_s and rs_s (g carbohydrates / g dry matter)

Crop and weed cohorts are characterized by the following daily state variables, for each species s and emergence cohort c:

- Plant stage $stage_{sc}$, in {SEEDLING,COTYLEDON,VEGETATIVE,FLOWER,MATURATION}
- Thermal time since cohort emergence TT_{sc} (°C days)
- Plant density P_{sc} (plants/m²)
- Specific plant width in sunny conditions $W0_{sc}$ (cm/g)
- Specific leaf area in sunny conditions $LA0_{sc}$ (cm²/g)
- Sensitivity of specific plant width to shading μw_{sc} (no unit)
- Sensitivity of specific leaf area to shading μl_{sc} (no unit)
- Shape parameter for plant width b_{sc} (no unit)
- Thermal time from cohort emergence to flowering onset $TTflo_{sc}$ (°C days)
- Thermal time from cohort emergence to maturation onset $TTmat_{sc}$ (°C days)

Crop and weed plants are characterized by the following daily state variables, for each species s, emergence cohort c and plant p:

- Plant height H_{scp} (cm)
- Aboveground plant biomass B_{scp} (g)
- Aboveground plant biomass before mowing BM_{scp} (g)
- Total leaf area LA_{scp} (cm²)
- Leaf area between soil surface and height h $LA_{scp}(h)$ (cm²)
- Leaf biomass LB_{scp} (g)
- Stem biomass TB_{scp} (g)
- Seed biomass SB_{scp} (g)
- Shading index, i.e. cumulated shading since plant emergence SI_{scp} (PAR/PAR), predicted by 3D light interception submodel (Munier-Jolain *et al.*, 2013)
- Biomass produced by photosynthesis Ph_{scp} (g)
- Biomass lost through respiration R_{scp} (g)
- Photosynthetically active radiation absorbed by plant $PARa_{scp}$ (MJ), predicted by 3D light interception submodel (Munier-Jolain *et al.*, 2013)

Steps

When a field is mown, plants that are smaller than the mowing height are not affected. All plants that have started to mature and are taller than the mowing height, die (eq. [1] in Table S 26).

Younger plants that exceed the mowing height have their current aboveground biomass stored in other variables for future calculation, and then reduced [2]. All biomass variables (total aboveground, leaves, stems) are multiplied by the plant leaf area below mowing height relative to their total leaf area. Seed biomass remains nil as the plants have not yet started to mature.

Plant size is also adapted [3]: plants are now no taller than the mowing height, and their width and leaf area are reduced, depending on their new biomass and past shading conditions.

If the cohort has started to flower, the stage of the cut plants regresses [4], subtracting half the minimum duration of the vegetative stage from the time since the cohort emerged. This adjusted thermal time is compared to the time needed to start flowering or maturing to adjust cohort stage if necessary. These cut and regressed plants constitute a new cohort as their phenology will be delayed compared to uncut plants having emerged on the same day.

On any day, plants produce biomass through photosynthesis [5], depending on the light intercepted by the plant, the conversion efficiency of the species and the air temperature. They also lose biomass, depending on their relative amounts of leaves, stems and seeds, as well as on temperature [6]. The difference between the two is the daily biomass production due to plant metabolism; it can be negative when respiration exceeds photosynthesis [7].

Cut plants can also produce biomass through remobilization from belowground biomass during the days following mowing. This additional biomass is proportional to the plant biomass prior to mowing (as a proxy for plant root biomass which is not yet predicted in FLORSYS) and to air temperature relative to the species base temperature [8]. Remobilization decreases when plants have started to flower and stops when they start to mature [9] (Figure S 9). Moreover, the smaller the biomass due to remobilization gets relative to the one accumulated through metabolism, the faster is decreases [10] (Figure S 10). The new plant biomass is the sum of the old one, the biomass accumulated via metamobolism and the one due to remobilization [11]. If the biomass becomes negative or lower than 10% of the maximum biomass reached during plant life, then the plant dies [13]. If the new plant biomass exceeds the biomass prior to mowing, this stored biomass will be put to zero to stop remobilization [14].

The new biomass and the past plant shading are then used to determine the new plant height, width and leaf area [15]. For details on plant growth, see previous FLORSYS papers (Colbach *et al.*, 2014c; Munier-Jolain *et al.*, 2014).

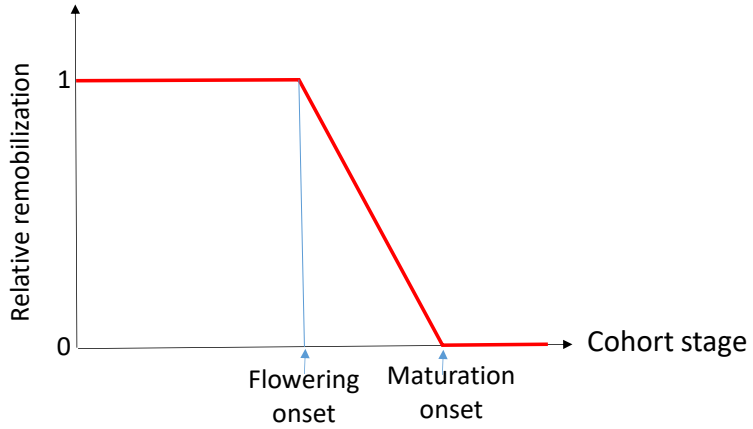

Figure S 9: Effect of plant stage on remobilization after the plant was cut by mowing or harvesting operations.

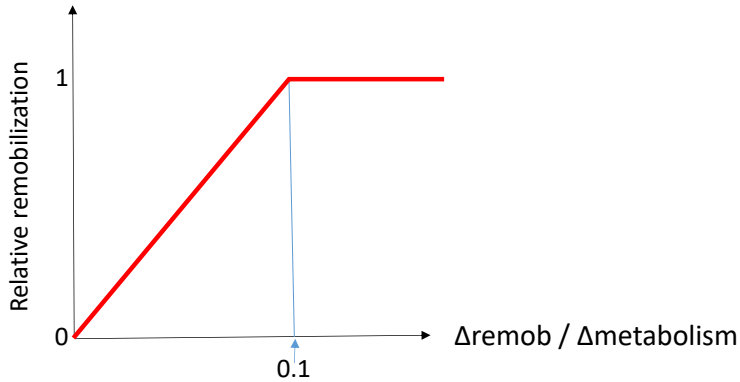

Figure S 10: Gradual decrease in remobilization of cut plants when metabolism starts to take over again.

Table S 26: Submodel for remobilization from belowground plant reserves after mowing in FLORSYS. For explanations on variable and parameter names, see section A.2.3.2.2 (Colbach *et al.*, 2018)

	Timing	**Process**
	Mowing day	**Plant death**
[1]	$d=d_{mowing}$ $\forall s,c,p$ If $H_{scp} > H_{mowing}$ If $stage_{sc} \geq$ MATURATION or $remob_s = 0$	Plant scp dies $P_{sc} = P_{sc} - 1$
	Mowing day	**Plant biomass and size reduction**
[2]	$d=d_{mowing}$ $\forall s,c,p$ If $H_{scp} > H_{mowing}$ If $stage_{sc}$ < MATURATION and $remob_s > 0$	$BM_{scp} = B_{scp}$ $BMax_{scp} = B_{scp}$ $B_{scp} = B_{scp} \cdot LA_{scp}(H_{mowing}) / LA_{scp}$ $LB_{scp} = LB_{scp} \cdot LA_{scp}(H_{mowing}) / LA_{scp}$ $TB_{scp} = TB_{scp} \cdot LA_{scp}(H_{mowing}) / LA_{scp}$ $SB_{scp} = 0$
[3]		$H_{scp} = H_{mowing}$ $W_{scp} = W0_{sc} \cdot B_{scp}^{bsc} \cdot \exp(\mu w_{sc} \cdot SI_{scp})$ $LA_{scp} = LA0_{sc} \cdot LB_{scp} \cdot \exp(\mu l_{sc} \cdot SI_{scp})$
	Mowing day	**Plant stage reduction ⇨ cohort c becomes cohort c'**
[4]	$d=d_{mowing}$ $\forall s,c,p$ If $H_{scp} > H_{mowing}$ If $stage_{sc}$ = FLOWER and $remob_s > 0$	$TT_{sc'} = TT_{sc} - TTveg_s / 2$ If $TT_{sc'} < TTflo_{sc}$ then $stage_{sc'}$ = VEGETATIVE Else if $TT_{sc'} < TTmat_{sc}$ then $stage_{sc'}$ = FLOWER
	Any day	**Photosynthesis and respiration**
[5]	$\forall d$	$Ph_{scp} = PARa_{scp} \cdot \varepsilon b_s \cdot f(temperature)$
[6]	$\forall s,c,p$	$R_{scp} = (rl_s \cdot LB_{scp} + rt_s \cdot TB_{scp} + rs_s \cdot SB_{scp}) \cdot f(temperature)$
[7]		$\Delta metabolism_{scp} = Ph_{scp} - R_{scp}$
	After mowing for cut plants	**Remobilization**
[8]	$\forall d > d_{mowing}$	$\Delta remob_{scp} = remob_s \cdot BM_{scp} \cdot \min(0, T_d - Tbase_s)$
[9]	$\forall s,c,p$ If $BM_{scp} = 0$	If $stage_{sc}$ = MATURATION then $\Delta remob_{scp} = 0$ Else if $stage_{sc}$ = FLOWER then $\Delta remob_{scp} = \Delta remob_{scp} \cdot (TTmat_{sc} - TT_{sc}) / (TTmat_{sc} - TTflo_{sc})$
[10]		If $\Delta remob_{scp} / \Delta metabolism_{scp} < 0.1$ then $\Delta remob_{scp} = \Delta remob_{scp} \cdot 10 \cdot \Delta remob_{scp} / \Delta metabolism_{scp}$
[11]		$B_{scp} = B_{scp} + \Delta metabolism_{scp} + \Delta remob_{scp}$
[12]		$BMax_{scp} = \max(BMax_{scp}, B_{scp})$
[13]		If $B_{scp} < 0$ or $B_{scp} < 0.1 \cdot BMax_{scp}$ then plant scp dies and $P_{sc} = P_{sc} - 1$
[14]		If $B_{scp} > BM_{scp}$ then $BM_{scp} = 0$
	Any day	**Growth**
[15]	$\forall d$ $\forall s,c,p$	H_{scp}, W_{scp}, $LA_{scp} = f(B_{scp}, SI_{scp})$ See (Colbach *et al.*, 2014c)

A.2.4. Details on the simulated cropping systems

A.2.4.1. Pedoclimatic context

Table S 27: Synthetic description of the experimental site used for the evaluation of FLORSYS-RSCone (Colbach *et al.*, 2016).

Latitude, elevation	47°20' N, 211m
Soil texture (%clay, silt, sand)	44-50-6
Soil type	Clayey eutric cambisol
Weather: mean annual temperatures (mean monthly temperatures for January and July)	10.9°C (2.5, 19.9)
Cumulated annual precipitation	709 mm

A.2.4.2. Initial weed flora

Table S 28: Initial seed bank measured at the onset of the cropping system trial at Epoisses in 1999. Cells were coloured as a function of increasing density or biomass (Colbach *et al.*, 2016).

	Seeds/m^2 in each field									
	A1	A5	A6	A7	A8	D1	D2	D3	D4	D5
EPPO code	No herbicides[#]	IWM All	IWM NMW	Inten-sive	IWM NP	Inten-sive	IWM NP	IWM NMW	IWM All	No herbicides
ALOMY	0	0	447	0	0	138	0	0	293	0
AMARE	101	585	164	19	610	4141	107	245	334	16009
AVEFA	0	0	0	0	0	0	0	0	0	0
CAPBP	503	699	2272	94	13	63	25	38	138	43
CHEAL	38	101	302	170	239	164	617	189	283	25
ECHCG	126	19	53	13	13	13	53	0	6	182
GALAP	38	37	6	37	6	0	37	6	126	365
GERDI	0	6	0	0	0	0	6	0	6	0
POLAV	63	403	3298	13	220	13	25	473	157	63
POLCO	409	220	837	1429	208	120	680	459	220	6
POLPE	478	1126	208	88	1561	315	69	50	13	189
SENVU	1	0	1	0	1	8	1	8	1	1
SOLNI	23567	138	76	6	44	25	19	497	69	31
SONAS	6	19	19	6	10	19	13	0	63	21
STEME	76	3216	13	13	4	6	6	25	6	6
VERHE	0	19	132	13	0	47	63	6	0	47
MATIN	0	0	38	0	0	0	0	0	0	0
POAAN	38	0	38	38	0	0	0	0	0	0
VERPE	0	384	308	195	0	6	0	6	0	13

Type of cropping system: Intensive = intensive herbicide-based, IWM = integrated weed management, All = integrating all cultural levers, NMW = no mechanical weeding, NP = no mouldboard ploughing

A.2.4.3. Cropping systems

Table S 29: Crop sequences, soil tillage, crop sowing periods and weed control programs on the 10 fields. Crops written in parenthesis were grown as cover crops or undersown crops. In IWM systems, herbicides were occasionally applied on weed patches only. MP = Mouldboard ploughing, SC = shallow cultivation (Colbach *et al.*, 2016).

Cropping system	Standard		IWM, reduced tillage		IWM, no mechanical weeding		IWM, mechanical weeding		IWM, no herbicides	
Block	D	A	D	A	D	A	D	A	D	A
Tillage		MP+2SC		MP+3SC	MP+2SC		3SC	MP+1SC	MP+2SC	
Harvest 2000	Oilseed rape Late Aug. 2 herbicides	Soybean Early may 3 herbicides	Oilseed rape Late Aug. 3 herbicides	Sunflower Late April 1 herbicide 1 hoe	Sunflower Late April 1 herbicide	W-Wheat Mid Oct 1 herbicide	Sunflower Late April 1 herbicide 1 hoe	Soybean Early may 4 herbicides	Sunflower Late April 1 herbicide 1 hoe	W-Wheat Mid Oct. 3 herbicides
Tillage	MP+3SC	MP+2SC	3SC	2SC	2SC	MP+3SC	3SC	2SC	2SC	MP+4SC
Harvest 2001	W-Wheat Early Oct. 2 herbicides	W-Wheat Early Oct. 3 herbicides	W-Wheat Late Oct. 1 herbicide	W-Wheat Late Oct. 1 herbicide	W-Wheat Late Oct. 2 herbicides	(Mustard) Soybean Early May 2 herbicides	W-Wheat Late Oct. 1 herbicide	W-Wheat Late Oct.. 1 herbicide 2 harrow	W-Wheat Late Oct. 0 herbicide 1 harrow	W-Barley Early Oct. 0 herbicide 1 harrow
Tillage	MP+2SC	MP+2SC	3SC	4SC	MP+2SC	2SC	MP+2SC	MP+3SC	MP+2SC	MP+4SC
Harvest 2002	W-Barley Early Oct. 1 herbicide	Oilseed rape Late Aug. 3 herbicides	W-Barley Mid Oct. No herbicide	(Oat) Soybean Early May 3 herbicides	Oilseed rape Late Aug. 1 herbicide	W-Wheat Early Nov 1 herbicides	(Oilseed rape) Oilseed rape Early Sept.. 0 herbicide 1 harrow	(Mustard) S-Barley Early March 0 herbicide 2 harrow	W-barley Mid Oct. 0 herbicide 2 harrow	Oilseed rape Early Aug. 0 herbicide 1 harrow, 1hoe
Tillage	MP+1SC	MP+3SC	9SC	2SC	5SC	MP+4SC	5SC	4SC	4SC	4SC
Harvest 2003	Oilseed rape Late Aug. 2 herbicides 1 hoe	W-Wheat Early Oct. 3herbicides	Soybean Mid April 2 herbicides	W-Wheat Late Oct. 1 herbicide	W-Wheat Late Oct. 1 herbicide	(Phacelia) Mustard Mid March 2 herbicides	W-Wheat Late Oct. 0 herbicide 4 harrow	Oilseed rape Early Aug. 1 herbicide 3 harrow	Oilseed rape Late Aug. 0 herbicide 3 hoe	W-Wheat Late Oct. 0 herbicide 3 harrow
Tillage	MP+2SC	MP+3SC	4SC	2SC	MP+3SC	2SC	MP+5SC	5SC	MP+3SC	MP+4SC
Harvest 2004	W-Wheat Early Oct. 3 herbicides	W-Barley Early Oct. 4 herbicides	W-Wheat Late Oct. 1 herbicides	Oilseed rape Early Aug. 1 herbicide	(Oat) Soybean Early may 1 herbicide	W-Wheat Late Oct. 1herbicides	Sugar Beet Late March 4 banded herb. 6 hoe	W-Wheat Late Oct. 1 herbicide 2 harrow	W-Wheat Late Oct. 0 herbicide 3 harrow	W-barley Mid Oct. 0 herbicide 2 harrow
Tillage	MP+1SC	MP+2SC	1SC	4SC	2SC	MP+1SC	3SC	MP+4SC	MP+5SC	MP+4SC
Harvest 2005	W-barley Early Oct. 2 herbicides	Oilseed rape Late Aug. 4 herbicides	Oilseed rape Early Aug. 2 herbicides	W-Wheat Early Nov. 3 herbicides	S-Barley Mid March 1 herbicide	Oilseed rape Early Sept. 1 herbicide	S-Barley Mid March 2 herbicide	Sugar beet Mid March 4 banded herb. 5 hoe	Sunflower Mid April No herbicide 1 harrow, 3hoe	S-Faba bean Early Feb. No herbicide 2 harrow, 1 hoe
Tillage	MP+2SC	MP+3SC	3SC	3SC	MP+3SC	3SC	MP+4SC	3SC	2SC	2SC
Harvest 2006	Oilseed rape Late Aug. 2 herbicides	W-Wheat Early Oct. 3 herbicides	Triticale Late Oct. 1 herbicides	S-Barley Mid March 1 herbicide	S-Oats Mid March 1 herbicide	Triticale Late Oct. 1 herbicides	W-Faba bean Late Oct. 1 herbicide 1 harrow, 3hoe	Triticale Late Oct. 1 herbicide 1 harrow, 3 hoe	Triticale Late Oct. 0 herbicide 1harrow, 2 hoe	Triticale Late Oct. 0 herbicide 1 hoe
Tillage	MP+2SC	MP+2SC	3SC	7SC	3SC	8SC	3SC	MP+6SC	MP+3SC	MP+2SC
Harvest 2007	W-Wheat Early Oct. 2 herbicides	W-Barley Early Oct. 3 herbicides	W-Barley (Clover) Late Feb. 1 herbicide	Sorghum Early May 2 herbicides	Faba bean Late Oct. No herbicide	Maize Late April 3 herbicides	Triticale Late Oct. 1 herbicide	Faba bean Early March 1 herbicide 5 hoe	White lupin Early March 0 herbicide 1 harrow, 5 hoe	Oilseed rape Early Aug. 0 herbicide 4 hoe
Tillage	MP+3SC	MP+3SC	2SC	No tillage	MP+4SC	MP+1SC	MP+3SC	6SC	6SC	5SC
Harvest 2008	W-Barley Early Oct. 3 herbicides	Oilseed rape Late Aug. 2 herbicides	(Mixture[%]) Sorghum Late May 4 herbicides	Faba bean Late Oct. 0 herbicide	Oilseed rape Late Aug. No herbicide	Faba bean Late Oct. 1 herbicide	Oilseed rape Early Sept. 0 herbicide 2 harrow, 5 hoe	W-Wheat Late Oct. 2 herbicides 1 harrow	W-Wheat Late Oct. 0 herbicide 1 harrow,4 hoe	W-Wheat Late Oct. 0 herbicide 2 hoe
Tillage	MP+3SC	MP+3SC	No tillage	2SC	4SC	6SC	4SC	MP+3SC	7SC	9SC
Harvest 2009	(Oilseed rape) Oilseed rape Mid Sept. 3 herbicides	W-Wheat Early Oct. 2 herbicides	Faba bean Mid Nov. No herbicides 2 rotary hoe	(Mustard) Triticale Mid Oct. 1 herbicide	W-Wheat Late Oct. 1 herbicide	W-Wheat Late Oct. 1 herbicide	W-Wheat Late Oct. 1 herbicide 1 harrow	Oilseed rape Early Sept. 0 herbicide 4 hoe	Lucerne Mid Aug. 0 herbicide	Sorghum Early may 0 herbicide 3 hoe
Tillage	MP+2SC	MP+4SC	2SC	2SC	MP+7SC	8SC	7SC	6SC		MP+2SC
Harvest 2010	W-Wheat Early Oct. 1 herbicide	W-Barley Early Oct. 2 herbicides	(Mixture[&]) W-Wheat Late Oct. 2 herbicides	(O. rape) Oilseed rape Early Sept. 2 herbicides	Sorghum Mid may 1 herbicide	S-Barley Mid March 1 herbicide	(Mixture[¥]) Maize Late April 2 herbicides	W-Wheat Late Oct. 1 herbicide 1 harrow	1 harrow	Faba bean Late Oct. 0 herbicide 2 harrow,1 hoe
Tillage	MP+2SC	MP+3SC	No tillage	No tillage	MP+2SC	MP+3SC	MP+2SC	8SC		5SC
Harvest 2011	W-Barley Mid Oct 1 herbicide	Oilseed rape Mid Sept. 2 herbicides	O. rape + lentils Late July 4 herbicides	W-Wheat Mid Oct. 3 herbicides	Faba bean Early Nov. 1 herbicide	(O. rape) Lentils Mid Sept. 0 herbicide	W.Wheat Late Oct. 1 herbicide 2 harrow	Maize Mid April 0 herbicide 2 hoe	1 harrow	W-Wheat Late Oct. 0 herbicide 4 harrow
Tillage	MP+5SC	MP+2SC	No tillage	No tillage	5SC	5SC	7SC	MP+1SC	MP+7SC	4SC
Harvest 2012	Oilseed rape Mid Sept. 1 herbicide	W-Wheat Early Oct. 2 herbicides	(Mixture[$]) W-Wheat Early Oct. 2 herbicides	(Mixture[#]) S-Barley Early March 2 herbicides	Triticale Mid Oct. 1 herbicide	W-Wheat Late Oct 1 herbicide	S-Barley Mid March 1 herbicide 1 harrow	W-Wheat Late Oct. 1 herbicide 2 harrow	W-Wheat Late Oct. 0 herbicide 2 harrow, 2 hoe	Lucerne Early Sept. 0 herbicide 1 harrow

Cover crop mixtures: [%] Vetch, Rye, Triticale; [&]Phacelia, Niger, Egyptian clover, Sorghum, Sunflower, Mustard; [$]Faba bean, Fodder pea, Lentils; [#]Oats, Vetch, Phacelia; [¥]Sunflower, Sorghum, Mustard, Vetch

A.2.5. Allometric relationship between root and total plant biomass

A.2.5.1. Effect of species, nitrogen and light

Table S 30: Effect of log10(plant biomass), species, nitrogen stress, shading and two-way interactions on log10(root biomass) in data from experiment E1 (see Table 7). Data on fescue was excluded from the analysis because otherwise the effect of the interaction between light and species could not be tested (because data under shading had to be removed for fescue, Table 7). The effect of the interaction between log10(plant biomass) and nitrogen stress was not significant. R^2 =0.99.

	Sum Sq	Df	F value	Pr(>F)	partial R^2
(Intercept)	13.7	1	898	<0.001	0.193
log10(plant biomass)	43.0	1	2819	<0.001	0.606
Species	3.77	4	61.8	<0.001	0.0531
Nitrogen stress	1.34	1	88.0	<0.001	0.0189
Light	4.66	1	305	<0.001	0.0656
log10(plant biomass)×species	1.00	4	16.3	<0.001	0.0140
log10(plant biomass)×light	0.0879	1	5.75	0.0167	0.00124
Species×nitrogen stress	0.874	4	14.3	<0.001	0.0123
Species×light	2.38	4	38.9	<0.001	0.0335
Nitrogen stress×light	0.203	1	13.3	<0.001	0.00285
Residuals	11.9	780			

A.2.5.2. Effect of species and nitrogen after removing the effect of light

Table S 31: Effect of log10(plant biomass), species and nitrogen stress and two-way interactions on log10(root biomass) in data from experiment E1 (Table 7). Data on fescue under shading was excluded from the analysis. A. Anova results. B. Parameters.

A.

	Sum Sq	Df	F value	Pr(>F)	partial R^2
(Intercept)	71.0	1	1797	<0.001	0.259
log10(plant biomass)	188	1	4761	<0.001	0.687
Species	9.57	5	48.4	<0.001	0.0349
Nitrogen stress	1.40	1	35.4	<0.001	0.00510
log10(plant biomass)×species	2.15	5	10.9	<0.001	0.00786
log10(plant biomass)×nitrogen stress	0.167	1	4.24	0.0398	0.000611
Species×nitrogen stress	1.51	5	7.64	<0.001	0.00551
Residuals	34.0	861			

B.

Coefficients	Estimate	Std. Error	t value	Pr(>|t|)
(Intercept)	-0.712	0.0168	-42.4	<0.001
log10(plant biomass)	1.02	0.0148	69.0	<0.001
T. aestivum	-0.0692	0.0264	-2.63	0.00879
B. napus	-0.270	0.0235	-11.5	<0.001
S. arundinaceus	0.296	0.0553	5.34	<0.001
G. molle	-0.214	0.0267	-8.01	<0.001
M. sativa	-0.0329	0.0279	-1.18	0.238
Nitrogen stress	0.278	0.0468	5.95	<0.001
log10(plant biomass)×*T. aestivum*	0.114	0.0235	4.87	<0.001
log10(plant biomass)×*B. napus*	0.000362	0.0208	0.0174	0.986
log10(plant biomass)×*S. arundinaceus*	-0.147	0.0478	-3.08	0.00211
log10(plant biomass)×*G. molle*	0.0793	0.0218	3.64	<0.001
log10(plant biomass)×*M. sativa*	0.0406	0.0247	1.64	0.100
log10(plant biomass)×nitrogen stress	0.0549	0.0267	2.06	0.0398
T. aestivum×nitrogen stress	0.118	0.0791	1.49	0.137
B. napus×nitrogen stress	0.146	0.0617	2.37	0.0181
S. arundinaceus×nitrogen stress	-0.189	0.0689	-2.74	0.00636
G. molle×nitrogen stress	0.132	0.0744	1.77	0.0768
M. sativa×nitrogen stress	0.0484	0.0848	0.570	0.569

A.2.5.3. Final allometric model with nitrogen effect

Table S 32: Effect of log10(plant biomass), species and nitrogen stress and two-way interactions (apart from the interaction species×nitrogen stress) on log10(root biomass) in data from experiment E1 (Table 7). Data on fescue under shading was excluded from the analysis. The effect of the interaction log10(plant biomass)×nitrogen stress was not significant. R^2 =0.97.

	Sum Sq	Df	F value	Pr(>F)	partial R^2
(Intercept)	77.4	1	1888	<0.001	0.248
log10(plant biomass)	212	1	5172	<0.001	0.679
Species	10.4	5	50.6	<0.001	0.0332
Nitrogen stress	10.1	1	246	<0.001	0.0322
log10(plant biomass)×species	2.63	5	12.8	<0.001	0.00842
Residuals	35.6	867			

A.2.5.4. Effect of experimental set-up

Table S 33: Effect of log10(plant biomass), species and experimental set-up and two-way interactions (apart from the interaction species×experimental set-up which could not be tested since all species were not tested in all experiments) on log10(root biomass) in data described in Table 7. R^2 =0.98.

	Sum Sq	Df	F value	Pr(>F)	partial R^2
(Intercept)	6.46	1	470	<0.001	0.285
log10(plant biomass)	2.72	1	198	<0.001	0.120
Experiment	1.71	9	13.9	<0.001	0.076
Species	8.16	36	16.5	<0.001	0.360
log10(plant biomass)×experiment	0.474	9	3.84	<0.001	0.021
log10(plant biomass)×species	3.13	36	6.33	<0.001	0.138
Residuals	16.1	1176			

A.2.5.5. Data at early and late stages

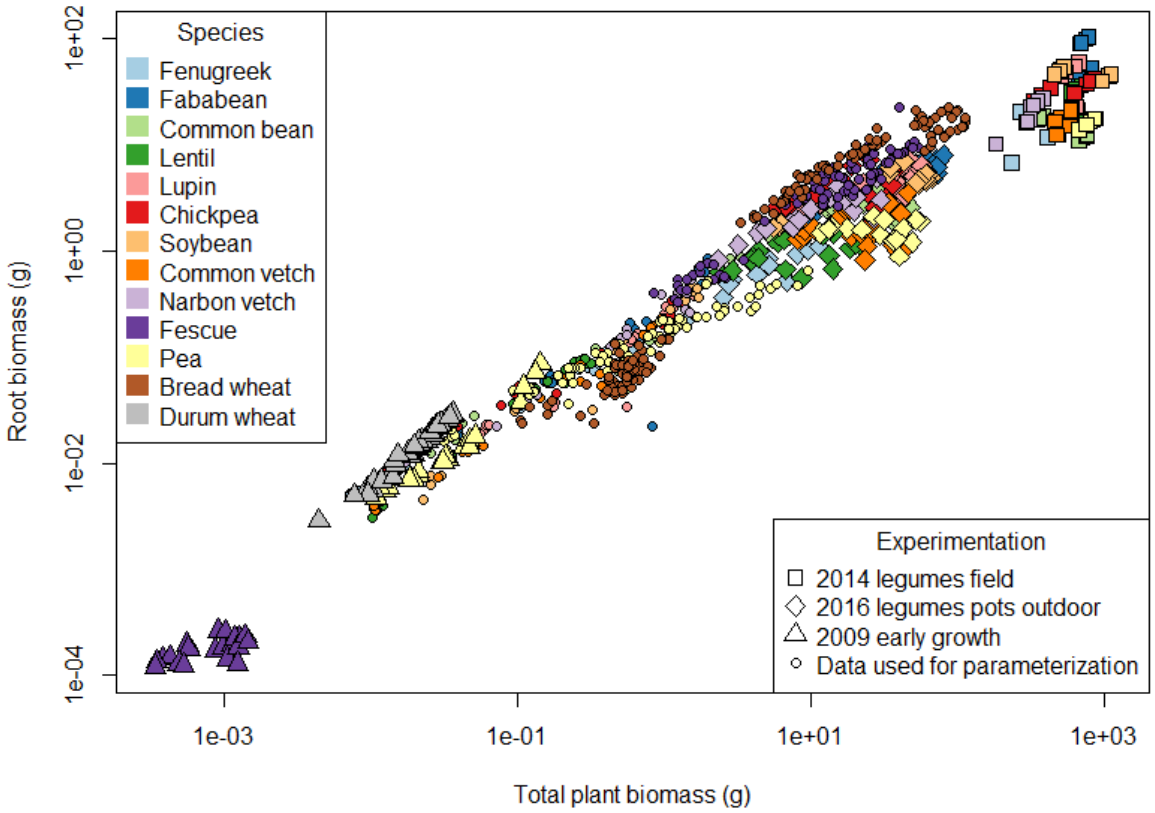

Figure S 11: Root biomass as a function of total plant biomass for 12 species of crops. Data used to parameterize the species (round dots, data described in Table 7) is compared to data collected at earlier (emergence) and later stages (flowering and harvest) from other experiments (Table S 34). Each dot represents a plant or several plants (for experiments at late stages, see Table S 34), each colour a species and each symbol an experimentation. Different varieties of the same species are used depending on the experiment (e.g. pea cv Hardy was used in the early growth experiment whereas cv Kayanne was used in other experiment, see Table S 34).

Table S 34: Data used to study the relationship between root and total plant biomass at early and late developmental stages.

Exp.	Species tested	Nitrogen treatment	Growth medium	Sampling stages	Ref.
ES1	Chickpea (*Cicer arietinum*) cv Twist, common bean (*Phaseolus vulgaris*) cv Flavert, common vetch (*Vicia sativa*) cv Candy, faba bean (*Vicia faba*) cv Espresso, fenugreek (*Trigonella foenum-graecum*) cv Hanka, lentil (*Lens culinaris*) cv Anicia, lupine (*Lupinus albus*) cv Feodora, Narbonne vetch (*Vicia narbonensis*) cv Clara, pea (*Pisum sativum*) cv Kayanne, soybean (*Glycine max*) cv Sultana	5 kg N/ha provided at sowing	Field	Flowering and harvest	(Guinet, 2019)
ES2	Chickpea (*Cicer arietinum*) cv Vulcano, common bean (*Phaseolus vulgaris*) cv Flavert, common vetch (*Vicia sativa*) cv Candy, faba bean (*Vicia faba*) cv Espresso, fenugreek (*Trigonella foenum-graecum*) cv Fenu-fix, lentil (*Lens culinaris*) cv Anicia, lupine (*Lupinus albus*) cv Feodora, Narbonne vetch (*Vicia narbonensis*) cv Clara, pea (*Pisum sativum*) cv Kayanne, soybean (*Glycine max*) cv Sultana	0.625 mM	Substrate in pots outdoor	Flowering and harvest	
ES3	Wheat (*Triticum durum*) cv Acalou, fescue (*Schedonorus arundinaceus*) cv Tomahawk, pea (*Pisum sativum*) cv Hardy	10.5 mM	Substrate (sand) in pots or boxes in greenhouses	Emergence	(Gouzy, 2009)

A.2.6. Parameters determining soil-resource uptake, competition for soil resource and infection by parasitic plants

A.2.6.1. Crops

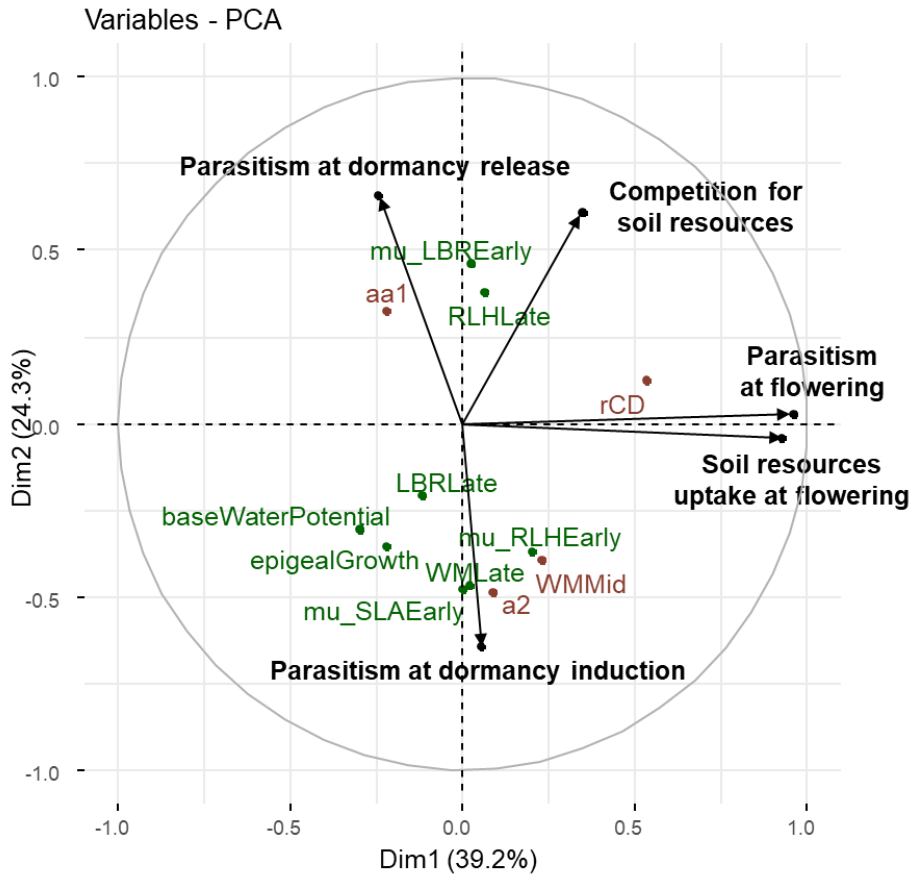

Figure S 12: Principal component analysis on proxy variables for potential soil-resource uptake, competition for soil resource and infection by *Phelipanche ramosa* in crops. Root (in brown) and aboveground parameters (in green) were added to the graph for information to show relationships between parameters and proxy variables but were not included in the principal component analysis. Only most correlated parameters are shown (correlation coefficients ≥|0.60| with at least one of the proxy variable, see Table S 35).

Table S 35: Pearson correlations between parameters and proxy variables for soil-resource uptake, competition for soil resource and infection by *Phelipanche ramosa* in crops. Correlations between proxy variables are in blue. Correlations between parameters and a high potential uptake, competitiveness for soil resource and a low risk of parasitism are in green, opposite correlations are in red. The darker the colour, the stronger the correlation. Only significant correlations are presented. Some parameters were calculated at different stages: after emergence in young seedlings ("Early"), during vegetative stage ("Mid") and from flowering onwards ("Late").

Proxy / Parameter/proxy	Parasitim at dormancy induction (autumn)	Parasitim at dormancy release (summer)	Parasitim at crop flowering	Soil-resource uptake at crop flowering	Competition for soil resource at crop flowering
Proxies					
Parasitism at dormancy induction			0.091		-0.107
Parasitism at dormancy release					0.107
Parasitism at crop flowering	0.091			0.851	0.269
Soil-resource uptake at crop flowering			0.851		0.111
Competition for soil resource at crop flowering	-0.107		0.269		
Root parameters					
Timing of root growth onset since germination (t0, days under optimal temperature)	0.082	0.323	-0.367	-0.263	-0.239
Delay from t0 to when the cylinder part of the root system starts to grow in depth (t0Cyl, days under optimal temperature)		0.099	-0.410	-0.342	-0.280
Timing of maximum SRL (tSRLmax, days under optimal temperature)	-0.326		0.357	0.520	0.216
Root-biomass density in the cylinder part of the root system, disregarding constraints (RBDmax $g \cdot cm^{-3}$)		0.089	-0.400	-0.280	-0.202
Maximum root-system extent (Emax, cm)	0.550	-0.260	0.061		0.063
Speed at which root-system depth increases (rD, cm per day under optimal temperature)	0.504			-0.097	0.195
Speed at which root-system extent increases (rE, cm per day under optimal temperature)	0.392	-0.352	0.308	0.328	0.233
Ratio of speed at which depth of cylinder-shaped part of root system increase vs speed of total root-system depth increase (rCD, cm per day under optimal temperature)	-0.271		0.484	0.635	0.275
Ability of roots to penetrate the soil (pen, no unit)	-0.373			0.244	
SRL when roots start to grow (srl0, $cm \cdot g^{-1}$)	0.473	-0.227	0.069		0.063
Maximum SRL (srlmax, $cm \cdot g^{-1}$)	0.321	-0.381	0.494	0.335	0.299
Root biomass when total plant biomass is near zero (aa1, $g \cdot g^{-1}$)	-0.610	0.264		-0.090	-0.170
Slope of allometric relationship of root vs total plant biomass (a2, no unit)	0.647	-0.304			
Parameters for early growth					
Relative growth rate (RGR, $cm^2 \cdot cm^{-2} \circ C day^{-1}$)	0.563		-0.221	-0.235	
Leaf area at emergence (LA0, cm^2)	-0.100		-0.232	-0.246	-0.261
Epigeal preemergent growth (1=epigeal, 0=	0.622	-0.088		-0.350	

Parameter/proxy	Proxy	Parasitim at dormancy induction (autumn)	Parasitim at dormancy release (summer)	Parasitim at crop flowering	Soil-resource uptake at crop flowering	Competition for soil resource at crop flowering
hypogeal)						
Base temperature for germination (°C)		0.442		-0.353	-0.338	-0.171
Base water potential for germination (Mpa)		0.661		-0.308	-0.313	-0.142
Maximum shoot length during preemergent seedling growth (shootLength, mm)		-0.429			-0.056	-0.209
Germination speed (time to 50% of final germination rate, °Cdays^{-1})		-0.408		-0.229		-0.292
Parameters for potential aboveground morphology in unshaded conditions						
Specific leaf area (total leaf area vs. total leaf biomass, SLA, cm^2·g^{-1})	Early	0.298		-0.319	-0.493	-0.090
	Mid	0.319	0.319	-0.368	-0.473	-0.085
	Late		0.090	-0.373	-0.479	-0.134
Leaf biomass ratio (leaf biomass vs. aboveground biomass, LBR, g·g^{-1})	Early			0.458	0.470	0.299
	Mid	-0.077		0.290	0.336	0.141
	Late	0.696	0.082			
Specific plant height (height per unit of aboveground biomass, HM, cm·g^{-1})	Early				-0.268	-0.122
	Mid		0.418			0.053
	Late		0.258		-0.084	0.086
Impact of biomass on plant height (the larger the parameter, the more height increases with biomass, b_HM, no unit)	Early	-0.248		-0.364	-0.455	-0.264
	Mid			-0.425	-0.530	-0.187
	Late	0.450	0.102	-0.496	-0.590	-0.266
Specific plant width (width per unit of aboveground biomass, WM, cm·g^{-1})	Early		-0.262	0.070		-0.099
	Mid	0.686	-0.256			0.141
	Late	0.665	-0.268		-0.054	
Impact of biomass on plant width (the larger the parameter, the more width increases with biomass, b_WM, no unit)	Early	-0.440				-0.128
	Late				0.072	0.074
Median relative leaf height (relative plant height below which 50% leaf area are located, RLH, cm·cm^{-1})	Early	0.064			-0.271	-0.060
	Late	-0.688			0.061	
Impact of biomass on leaf distribution along plant height (the lower the parameter, the more uniformly leaves are distributed along plant height, b_RLH, no unit)	Early		0.066			
	Mid			0.220		0.167
	Late	0.083		0.283	0.272	0.206
Parameters for response to shading						
Increase of specific leaf area under shading (mu_SLA, no unit)	Early	0.600	-0.318		-0.083	
	Mid	0.535	-0.336			
	Late	0.257				
Increase of leaf biomass ratio under shading (mu_LBR, no unit)	Early	-0.635	0.266	0.058	0.100	
	Mid	-0.556	0.276	0.091		
	Late	-0.597			0.085	-0.054
Increase of specific plant height under shading (mu_HM, no unit)	Early	0.575	-0.270			-0.094
	Mid	0.355	-0.297		0.078	
	Late			0.060	-0.074	-0.087
Increase of specific plant width under	Early		-0.306		0.085	-0.094

Parameter/proxy	Proxy	Parasitim at dormancy induction (autumn)	Parasitim at dormancy release (summer)	Parasitim at crop flowering	Soil-resource uptake at crop flowering	Competition for soil resource at crop flowering
shading (mu_WM, no unit)	Mid		0.281			-0.188
	Late					-0.136
Distribution of leaf area towards the top of the plant under shading (mu_RLH, no unit)	Early	0.636	-0.271		0.076	0.141
	Mid	0.375	-0.361	0.371	0.275	0.289
	Late	0.541	-0.252	0.314	0.294	0.235
Other morphological parameters						
Maximum plant height (max_height, cm)		0.374		-0.094		-0.054
Maximum plant width (max_width, cm)		0.234				-0.130
Maximum harvest index (BMseed_BMair1, $g \cdot g^{-1}$)		-0.409		0.260		0.211
Plant growth form: climbing ("climb")		0.079				-0.114
Plant growth form: prostrate		0.058		0.084		0.072
Plant growth form: rosette		-0.079			0.090	
Seed trait						
Seed weight (mg)		-0.351	0.094			-0.227
Taxonomy						
Dicot species (vs monocot species)		0.520		-0.387	-0.516	-0.207
Photosynthetic pathway						
C4 species (vs C3)			0.248	-0.055		-0.072
Life-cycle parameters						
Minimum plant lifespan (MinLifespan, months)		-0.072			0.058	
Maximum plant lifespan (MaxLifespan, months)		-0.096				
Seasonal type: summer annual		0.094	0.402	-0.462	-0.323	-0.269
Seasonal type: winter annual			-0.487	0.514	0.516	0.251
Parameters for sensitivity to temperatures						
Minimum temperature for photosynthesis (tPhoto1, °C)			0.431	-0.377	-0.349	-0.175
Temperature above which photosynthesis is maximal (tPhoto2, °C)			0.322	-0.468	-0.356	-0.277
Temperature above which photosynthesis starts to decrease (tPhoto3, °C)			0.249	-0.554	-0.476	-0.348
Maximum temperature for photosynthesis (tPhoto4, °C)		-0.532		0.062		
Temperature below which plants start to loose biomass due to frost (tFrost1, °C)	Early		0.398	-0.480	-0.350	-0.327
	Mid		0.390	-0.360	-0.243	-0.239
	Late	-0.104	0.403	-0.410	-0.392	-0.182
Temperature below which plants start to die due to frost (tFrost2, °C)	Early	0.301	0.365	-0.436	-0.308	-0.254
	Mid	0.357	0.313	-0.433	-0.396	-0.257
	Late		0.397	-0.439	-0.365	-0.202
Temperature below which all plants die due to frost (tFrost3, °C)	Early	0.287	0.345	-0.532	-0.495	-0.281
	Mid	0.246	0.359	-0.533	-0.493	-0.284
	Late		0.294	-0.509	-0.504	-0.291

A.2.6.2. Weeds

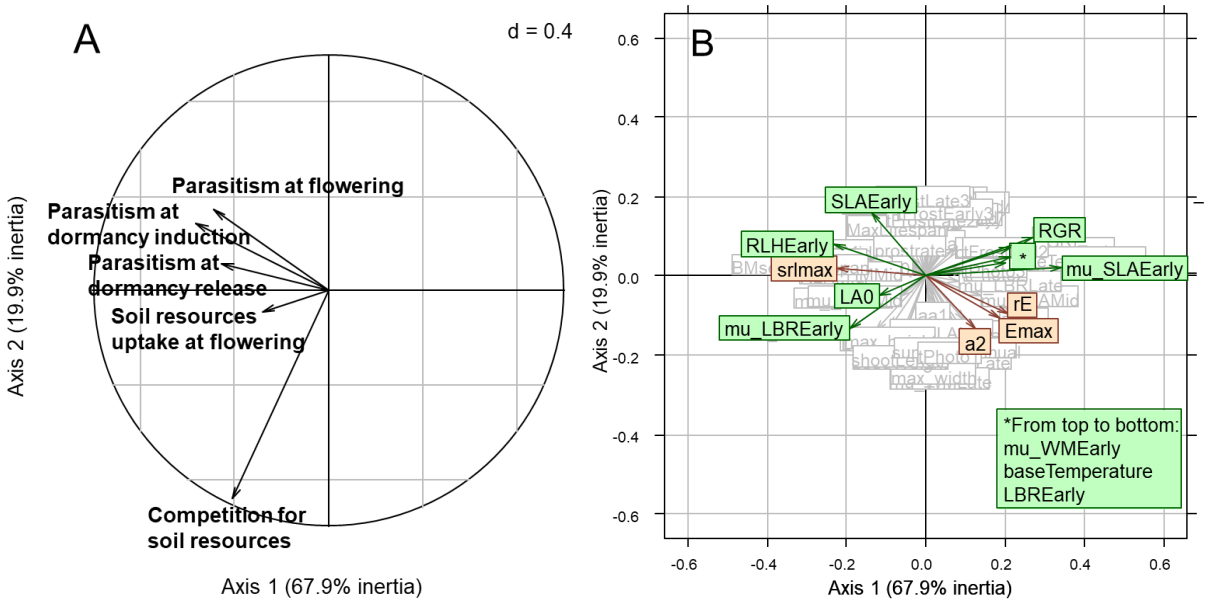

Figure S 13: Weed parameters involved in potential soil-resource uptake, competition for soil resource and infection by *Phelipanche ramosa*. Proxy variables (A) for soil-resource uptake (root biomass), competition for soil resource (crop root volume intercepted by weed root volume) and *P. ramosa* infection (cumulated root length over 30cm depth), and parameters (B) are projected on the two first RLQ axes. Only parameters significantly correlated with at least one of the proxy variables according to the fourth-corner analysis are shown. Most correlated parameters are coloured (correlation coefficienst >|0.10| with at least one of the proxy variable, see Table S 36), in brown for root parameters and in green for aboveground parameters.

Table S 36: Correlations between parameters and proxy variables for soil-resource uptake, competition for soil resource and broomrape infection in weeds. Correlations between proxies are Pearson correlations (in blue), and correlations between proxies and parameters are results from the fourth-corner analysis (in red and green). Correlations between parameters and a high potential uptake, competitiveness for soil resource and risk of parasitism are in red, opposite correlations are in green. The darker the colour, the stronger the correlation. Only significant correlations are shown. Some parameters were calculated at different stages: after emergence in young seedlings ("Early"), during vegetative stage ("Mid") and from flowering onwards ("Late").

Proxy / Parameter/proxy		Parasitim at dormancy induction (autumn)	Parasitim at dormancy release (summer)	Parasitim at crop flowering	Soil-resource uptake at crop flowering	Competition for soil resource at crop flowering
Proxies						
Parasitism at dormancy induction			0.355	0.343	0.370	0.284
Parasitism at dormancy release		0.355		0.865	0.783	0.518
Parasitism at crop flowering		0.343	0.865		0.847	0.471
Soil-resource uptake at crop flowering		0.370	0.783	0.847		0.480
Competition for soil resource at crop flowering		0.284	0.518	0.471	0.480	
Root parameters						
Timing of root growth onset since germination (t0, days under optimal temperature)				0.020	0.027	
Root-biomass density in the cylinder part of the root system, disregarding constraints (RBDmax $g \cdot cm^{-3}$)		0.023				-0.030
Maximum root-system extent (Emax, cm)		-0.116				
Speed at which root-system depth increases (rD, cm per day under optimal temperature)					-0.044	
Speed at which root-system extent increases (rE, cm per day under optimal temperature)		-0.121			-0.038	
Ability of roots to penetrate the soil (pen, no unit)			-0.063			
SRL when roots start to grow (srl0, $cm \cdot g^{-1}$)			0.062		0.057	
Maximum SRL (srlmax, $cm \cdot g^{-1}$)		0.112			0.064	
Root biomass when total plant biomass is near zero (aa1, $g \cdot g^{-1}$)		-0.024				
Slope of allometric relationship of root vs total plant biomass (a2, no unit)		-0.106	-0.050			
Parameters for early growth						
Relative growth rate (RGR, $cm^2 \cdot cm^{-2} \cdot °C day^{-1}$)			-0.139	-0.105		-0.129
Leaf area at emergence (LA0, cm^2)		0.101				
Base temperature for germination (°C)		-0.050	-0.115			
Maximum shoot length during preemergent seedling growth (shootLength, mm)		0.059				
Parameters for potential aboveground morphology in unshaded conditions						
Specific leaf area (total leaf area vs. total leaf biomass, SLA, $cm^2 \cdot g^{-1}$)	Early	0.104	0.059			
	Mid		0.055			

Parameter/proxy	Proxy	Parasitim at			Soil-resource uptake at	Competition for soil resource at
		dormancy induction (autumn)	dormancy release (summer)	crop flowering	crop flowering	crop flowering
	Late		-0.061			
Leaf biomass ratio (leaf biomass vs. aboveground biomass, LBR, $g \cdot g^{-1}$)	Early	-0.118	-0.065	-0.069		
	Mid					-0.081
	Late				0.060	
Specific plant height (height per unit of aboveground biomass, HM, $cm \cdot g^{-1}$)	Early	-0.043				
	Mid	-0.051				
	Late				-0.046	
Impact of biomass on plant height (the larger the parameter, the more height increases with biomass, b_HM, no unit)	Mid			-0.043		
Specific plant width (width per unit of aboveground biomass, WM, $cm \cdot g^{-1}$)	Early	-0.070				
	Mid	-0.070				
	Late	0.075				0.099
Impact of biomass on plant width (the larger the parameter, the more width increases with biomass, b_WM, no unit)	Early					-0.082
	Mid	-0.049				
	Late					0.043
Median relative leaf height (relative plant height below which 50% leaf area are located, RLH, $cm \cdot cm^{-1}$)	Early	0.116		0.118		0.047
	Mid	0.062	0.047			0.045
	Late		-0.042			
Impact of biomass on leaf distribution along plant height (the lower the parameter, the more uniformly leaves are distributed along plant height, b_RLH, no unit)	Early	-0.055				-0.059
	Mid	-0.044		-0.041		
Parameters for response to shading						
Increase of specific leaf area under shading (mu_SLA, no unit)	Early	-0.124	-0.160	-0.149	-0.118	
	Mid		-0.040			
	Late			-0.043		
Increase of leaf biomass ratio under shading (mu_LBR, no unit)	Early	0.057				0.120
	Mid			0.042		0.047
	Late		-0.034			
Increase of specific plant height under shading (mu_HM, no unit)	Early			0.049		-0.058
	Mid			0.048	0.047	
	Late					0.036
Increase of specific plant width under shading (mu_WM, no unit)	Early	-0.103				
	Mid		0.046			0.031
	Late	-0.053		-0.049		
Other morphological parameters						
Maximum plant height (max_height, cm)		0.063				
Maximum plant width (max_width, cm)				-0.059		0.093

Parameter/proxy \ Proxy		Parasitim at dormancy induction (autumn)	Parasitim at dormancy release (summer)	Parasitim at crop flowering	Soil-resource uptake at crop flowering	Competition for soil resource at crop flowering
Maximum harvest index (BMseed_BMair1, $g \cdot g^{-1}$)						0.049
Plant growth form: prostrate			0.032		0.026	
Seed trait						
Seed weight (mg)		0.051				
Photosynthetic pathway						
C4 species (vs C3)						-0.070
Life-cycle parameters						
Minimum plant lifespan (MinLifespan, months)						0.040
Maximum plant lifespan (MaxLifespan, months)				0.044		
Seasonal type: summer annual				-0.057		
Seasonal type: winter annual				0.057		
Parameters for sensitivity to temperatures						
Minimum temperature for photosynthesis (tPhoto1, °C)				-0.049		0.044
Temperature above which photosynthesis is maximal (tPhoto2, °C)					-0.032	-0.036
Temperature above which photosynthesis starts to decrease (tPhoto3, °C)				-0.050	-0.032	-0.038
Maximum temperature for photosynthesis (tPhoto4, °C)		0.054				-0.063
Temperature below which plants start to loose biomass due to frost (tFrost1, °C)	Early					-0.044
	Late	0.068				-0.061
Temperature below which plants start to die due to frost (tFrost2, °C)	Early	0.064				-0.065
	Mid			-0.043		
	Late				-0.044	-0.047
Temperature below which all plants die due to frost (tFrost3, °C)	Early	0.045	-0.053			
	Late	0.065				-0.064

A.3. Annexes du chapitre 4

A.3.1. Equations, variables and parameters used in the PHERASYS.2 model

Table S 37: Equations of the PHERASYS.2 model representing branched broomrape dynamics and the effect of parasitism on host growth. Meaning of indices: a = seed age class (young vs. old), d = day, l = soil layer, ph = plant p of species h. Parameters are in bold.

Eq.	when	Process	Equation	Explanation
Broomrape dynamics				
[1]	∀d	Seed mortality	da = 1-(365-**am**·age_a)/(365-**am**·(age_a-1)) SB_{lda}= (1-da)·$SB_{l(d-1)a}$	da = daily seed mortality rate of broomrape seeds (in $days^{-1}$) (Gardarin *et al.*, 2012) **am** = annual mortality rate of broomrape seeds (in $year^{-1}$) (Pointurier *et al.*, 2019) age_a = broomrape seed age (in days) SB_{lda} = viable broomrape seeds in soil layers/m²
[2]	∀d If d ∈ [**dFr$_{ph}$**,**d0**] If $\Psi_{ld} \geq$ **Ψ$_{min\ cond}$**	Thermal time accumulated during conditioning of fresh seeds	If $T_{ld} \in$ [**T$_{min\ cond}$**,**T$_{opt\ cond}$**], $TT_{cond\ ld} = TT_{cond\ l(d-1)} + (T_{ld}$-**T$_{min\ cond}$**) If $T_{ld} \in$]**T$_{opt\ cond}$**, **T$_{max\ cond}$**], $TT_{cond\ ld} = TT_{cond\ l(d-1)} + ($**T$_{max\ cond}$**-**$T_{ld}$) If $T_{ld} <$ **T$_{min\ cond}$** or $T_{ld} >$ **T$_{max\ cond}$**, $TT_{cond\ ld} = TT_{cond\ l(d-1)}$ + 0	**dFr$_{ph}$** = date of fructification of broomrape (in julian days, see equation [20]) **d0** = date of dormancy release of fresh broomrape seeds (first day when $TT_{cond\ ld} \geq$ 250 °C·days) $TT_{cond\ ld}$ = thermal time accumulated by broomrape seeds since they were released from the mother plant (in °C·days) T_{ld} = daily mean soil temperature in layer l (in °C) **T$_{min\ cond}$** = minimum temperature for conditioning of broomrape seeds (in °C) **T$_{max\ cond}$** = maximum temperature for conditioning of broomrape seeds (in °C) **T$_{opt\ cond}$** = optimum temperature for conditioning of broomrape seeds (in °C) **Ψ$_{min\ cond}$** = minimum water potential for conditioning of broomrape seeds (in MPa) Ψ_{ld} = daily water potential in soil layer l (in MPa)
[3]	If $age_a <$ **d0** Else	Dormancy release of fresh seeds (conditioning)	If a = young, $pND_{lda} = pND'_{lda} \cdot \left[1 - e^{-\ln(2)\left(\frac{TT_{cond\ ld}}{TT_{50\ cond}}\right)^{bprec}}\right]$ $pND_{lda} = pND'_{lda}$	pND_{lda} = proportion of non-dormant broomrape seeds pND'_{lda} = proportion of non-dormant broomrape seeds over seasons (before conditioning in case of fresh seeds) **TT$_{50\ cond}$** = thermal time when 50% of fresh broomrape seeds are conditioned (in °C·days) **b$_{cond}$** = shape parameter in the equation modelling conditioning of

Eq.	when	Process	Equation	Explanation
				fresh seeds
[4]	 If d ∈]$\mathbf{d4_a}$,$\mathbf{d1_a}$] If d ∈]$\mathbf{d1_a}$,$\mathbf{d2_a}$] If d ∈]$\mathbf{d2_a}$,$\mathbf{d3_a}$] If d ∈]$\mathbf{d3_a}$,$\mathbf{d4_a}$] If d >$\mathbf{d4_a}$	Seasonal dormancy • Low dormancy • Dormancy induction • Dormancy • Dormancy release • Low dormancy	 pND'_{lda} = $\mathbf{ndmax_a}$ pND'_{lda} = $\mathbf{ndmax_a}$-(d-$\mathbf{d1_a}$)·(**ndmax-ndmin**)/($\mathbf{d2_a}$-$\mathbf{d1_a}$) pND'_{lda} = **ndmin** pND'_{lda} = **ndmin**+(d-$\mathbf{d3_a}$)·(**ndmax -ndmin**)/($\mathbf{d4_a}$-$\mathbf{d3_a}$) pND'_{lda} = **ndmax**	$\mathbf{d1_a}$ = date of seasonal dormancy induction onset for broomrape seeds of age class a $\mathbf{d2_a}$ = date of seasonal dormancy induction end $\mathbf{d3_a}$ = date of seasonal dormancy release onset $\mathbf{d4_a}$ = date of seasonal dormancy release end **ndmin** = minimum proportion of non-dormant broomrape seeds **ndmax** = maximum proportion of non-dormant broomrape seeds (Pointurier *et al.*, 2019)
[5]	If d ∈ [de_{ph},$dfle_{ph}$] ∀ h	Potential root stimulating volume	$VS_{ldph} = \pi\cdot(\mathbf{d_{max\text{-}stimu}} + \mathbf{rd_h/2})^2\cdot RLD_{ldph}$, with $RLD_{ldph} = SRL_{dph} \cdot VSR_{ldph} \cdot RBD_{ldph} \cdot 1000$	de_{ph} = emergence date of the stimulating plant p $dfle_{ph}$ = date of end of flowering of the stimulating plant p $\mathbf{d_{max\text{-}stimu}}$ = maximum distance from a stimulating root for broomrape seeds to perceive germination stimulants (in m) VS_{ldph} = proportion of soil volume in layer l permeated with germination stimulants exuded by roots of plant p (in $m^3 \cdot m^{-3}$) $\mathbf{rd_h}$ = root tip diameter of species h (in m) RLD_{ldph} = cumulated root length density of stimulating plant p in soil layer l (in $m \cdot m^{-2}$) SRL_{dph} = specific root length of stimulating plant p (in $m \cdot g^{-1}$) (Pagès *et al.*, submitted) VSR_{ldph} = proportion of soil volume in layer l occupied by the root system of stimulating plant p (in $m^3 \cdot m^{-3}$) (Pagès *et al.*, submitted) RBD_{ldph} = root biomass density of stimulating plant p in soil layer l (in $g \cdot dm^{-3}$) (Pagès *et al.*, submitted)
[6]	If d ∈ [de_{ph},$dfle_{ph}$] If h = stimulating species	Germination triggering	$pNDS_{lda} = pND_{lda} \cdot \sum_h \boldsymbol{\alpha_{h/GR24}} [\sum_p^{N_{dh}} (VS_{ldph} - VS_{l(d-1)ph})]$ $NDS_{lda} = SB_{lda} \cdot pNDS_{lda}$	$pNDS_{lda}$ = proportion of non-dormant seeds stimulated by root exudates of all stimulating plants in soil layer l $\boldsymbol{\alpha_{h/GR24}}$ = broomrape-stimulating ability of species h relative to GR24 N_{dh} = number of plants of species h stimulating broomrape germination/m^2 NDS_{lda} = non-dormant seeds stimulated/m^2
[7]	∀d	Cumulated germination Merging consecutive germination flushes	If $HTT_{ld} \geq x_0$, $CG_{lda} = NDS_{lda} \cdot \left[1 - e^{-\ln(2)\left(\frac{HTT_{ld} - \mathbf{x_0}}{x_{50} - \mathbf{x_0}}\right)^{\boldsymbol{b}}}\right]$ If $HTT_{ld} < x_0$, $CG_{lda} = 0$ If $HTT_{ld}1 < 2.5 * x_{50}1$, $m=\min(1; m_1+m_2)$	CG_{lda} = cumulated number of germinated broomrape seeds/m^2 on day d HTT_{ld} = hydrothermal time accumulated by broomrape seeds in soil layer l on day d since germination triggering by root exudates (in °C·MPa·MPa^{-1}·days) $\mathbf{x_0}$ = hydrothermal time from germination triggering to first germinated broomrape seeds (in °C·MPa·MPa^{-1}·days)

Eq.	when	Process	Equation	Explanation
			$x_0=(m_1 \cdot x_0 1 + m_2 \cdot \max(x_{02};HTT_{ld}1))/m$ $x_{50}=(m_1 \cdot x_{50} 1 + m_2 \cdot (x_{50}2+HTT1_{ld}1))/m$ $b=b_1+b_2$ $HTT_{ld}=HTT_{ld1}$	**x_{50}** = hydrothermal time from germination triggering to 50% of final germination of broomrape seeds (in °C·MPa·MPa^{-1}·days) **b** = shape parameter in the equation modelling germination dynamics of broomrape seeds (Pointurier *et al.*, 2019) $HTT_{ld}1$ = hydrothermal time accumulated during the ongoing germination flush, with m1, $x_0 1$, $x_{50}1$ and b1 its parameters m2, $x_0 2$, $x_{50}2$ and b2 = parameters of the new germination flush
[8]	∀d	Hydrothermal time accumulated since the first triggering in the current moist period, following the merging of germination flushes	If $T_{ld} \geq \mathbf{T_{base}}$ and $\Psi ld \geq \mathbf{\Psi_{base}}$, $HTT_{ld} = HTT_{l(d-1)} + (T_{ld}-\mathbf{T_{base}}) \cdot (\Psi_{ld}-\mathbf{\Psi_{base}}) / (\Psi_{opt}-\mathbf{\Psi_{base}})$ If $T_{ld} < \mathbf{T_{base}}$ and $\Psi ld \geq \mathbf{\Psi_{base}}$, $HTT_{ld} = HTT_{l(d-1)} + 0$, If $\Psi_{ld} < \mathbf{\Psi_{base}}$ or if tillage which dilutes root exudates, $HTT_{ld} = 0$	**T_{base}** = base temperature for germination of broomrape seeds (in °C) **Ψ_{base}** = base water potential for germination of broomrape seeds (in MPa) Ψ_{opt} = optimal soil water potential for seed germination (=0 MPa)
[9]	∀d	Daily number of germinated seeds	$G_{lda} = CG_{lda} - CG_{l(d-1)a}$ $SB_{lda}' = SB_{lda} - G_{lda}$	G_{lda} = germinated broomrape seeds/m² SB_{lda}' = viable broomrape seeds/m² after germination losses
[10]	∀d If h = host species	Attachment zone around stimulating roots	$VF_{ldph} = \pi \cdot (\mathbf{d_{max}} + \mathbf{rd_h}/2)^2 \cdot RLD_{ldph}$	VF_{ldph} = proportion of soil volume in layer l where broomrape seeds are close enough to the roots of host plant p to attach it (in $m^3 \cdot m^{-3}$) **d_{max}** = maximum distance from a stimulating root for broomrape seeds to attach to the root (in m)
[11]	∀d If h = host species	Total attachments on all host plants (before competition between attachments for host ressources)	$F_{ld} = (G_{ld\ young} + G_{ld\ old}) \cdot \sum_p VF_{ldph}$	F_{ld} = total number of attachments among germinated broomrape seeds in soil layer l before competition between attachments for host resources
[12]	∀d If h = host species	Attachments on individual host plants (before competition between attachments for host ressources)	$F_{ldph} = F_{ld} \cdot VF_{ldph} / \sum_p VF_{ldph}$	F_{ldph} = number of attachments on roots of host plant p in soil layer l before competition between attachments for host resources
[13]	If d = $dros_{ph}$ If h = host species	Host carrying capacity	If $BHros_{ph} \leq \mathbf{BH_{min}}$, $\gamma_{ph} = 0$ Else $\gamma_{ph} = \mathbf{\delta} \cdot (BHros_{ph} - \mathbf{BH_{min}})$ If $\gamma_{ph} \geq 20$, $\gamma_{ph} = 20$	$dros_{ph}$ = date when host plant p reaches rosette stage γ_{ph} = maximum number of broomrapes supported by host plant p **δ** = maximum number of attached broomrapes supported per gram of plant p at rosette stage (in g^{-1}) $BHros_{ph}$ = biomass of infected host plant p at rosette stage (in g) **BH_{min}** = minimum biomass of a host plant at rosette stage to allow the complete development of broomrapes (in g)
[14]	If d = $dros_{ph}$	Cumulated attachments	$Fros_{ph} = \sum_{de_{ph}}^{dFr_{ph}} \sum_l F_{ldph}$	$Fros_{ph}$ = total number of broomrapes attached on host plant p at

Eq.	when	Process	Equation	Explanation
	If h = host species	at host rosette stage		rosette stage before competition between attachments for host resources
[15]	If d = $dros_{ph}$ If h = host species	Competition between attachments at host rosette stage	If $\gamma_{ph} > 0$, $Fr_{dph} = \gamma_{ph} \cdot (1\text{-}e^{-Fros_{ph}/\gamma_{ph}})$ Else $Fr_{dph} = 0$	Fr_{dph} = total number of attachments on host plant p on day d
[16]	If d > $dros_{ph}$ If h = host species	Competition between attachments after host rosette stage	If $\gamma_{ph} > 0$ $\Delta FS_{dph} = e^{-\sum_l F_{ldph}/\gamma_{ph}} \cdot \sum_l F_{ldph}$ Else $\Delta FS_{dph} = 0$	ΔFS_{dph} = daily number of attachments after host rosette stage
[17]	If d∈] $dros_{ph}$, dFr_{ph}] If h = host species	Total number of attached broomrapes	$Fr_{dph} = Fr_{d\text{-}1ph} + \Delta FS_{dph}$	
[18]	If d∈] $dros_{ph}$, dFr_{ph}] If h = host species	Total number of attached broomrapes	If host p dies $Fr_{dph} = 0$	
[19]	If d∈] $dros_{ph}$, dFr_{ph}] If h = host species	Broomrape biomass at seed shed	$BP_{ph} = \mathbf{b1} \cdot Fr_{ph}^{\mathbf{b2}}$	BP_{ph} = biomass of each broomrape at fructification stage on host plant p (in g) **b1** and **b2** = coefficients relating broomrape biomass per individual to the number of broomrapes per host plant
[20]	If d ≥ de_{ph} If h = host species	Thermal time accumulated by broomrape since host emergence	If $T_d \geq T_{base}$, $TT_{ldph} = TT_{l(d-1)ph} + (T_d\text{-}T_{base})$ If $T_d < T_{base}$, $TT_{ldph} = TT_{l(d-1)ph} + 0$ dFr_{ph} = first day when $TT_{ldph} \geq 1709$ °C·days	TT_{ldph} = thermal time accumulated by broomrape since host p emerged (in °C·days) T_d = daily mean air temperature (in °C)
[21]	If d ≥ $dros_{ph}$ If h = host species	Total broomrape biomass on a host over time	$BPT_{dph} = BP_{ph} \cdot Fr_{ph} \cdot \left[1 - e^{-\ln(2)\left(\frac{TT_{ldph}}{TT_{50\,BP}}\right)^{b_{BP}}}\right]$ $BPT_{dph} = \min(BPT_{dph}, ABH_{phd})$	BPT_{dph} = total broomrape biomass on host plant p on day d (in g) $\mathbf{TT_{50\,BP}}$ = thermal time accumulated by broomrape from host emergence up to 50% of the total broomrape biomass is reached (in °C·days) $\mathbf{b_{BP}}$ = shape parameter in the equation modelling broomrape biomass accumulation over time ABH_{phd} = above-ground biomass of the pathosystem p (including attached broomrapes in infected hosts, in g) (Colbach *et al.*, 2014c)
[22]	If d=dFr_{ph} If h = host species	Broomrape seed production	$NC_{ph} = \mathbf{c} \cdot BPT_{dph} \cdot (1\text{-}\mathbf{ci})$ $SP_{ph} = NC_{ph} \cdot \mathbf{CW} / \mathbf{SW} \cdot \mathbf{v}$	NC_{ph} = number of seed capsules produced per broomrape attached on host plant p **c** = number of seed capsules per gram of broomrape (in g^{-1})

Eq.	when	Process	Equation	Explanation
				ci = proportion of broomrape seed capsules that will not produce mature seeds (capsules with immature seeds, eaten by insects or atrophied) SP_{ph} = number of viable broomrape seeds produced on host plant p **CW** = mean weight of broomrape seeds per capsule (in g) **SW** = mean weight of a broomrape seed (in g) **v** = proportion of viable broomrape seeds at seed shed (Pointurier *et al.*, 2019)
[23]	If d=dFr_{ph} If h = host species	Seed return to seed bank	$SB_{ld\ young} = (SB_{l\ young}' + \sum_p SP_{ph})$, with l=0	
Effect of parasitism on host growth				
[24]	∀d If h = host species	Effect of parasitism on host growth	If d ≥ $dflb_{ph}$ and $\sum_{de_{ph}}^{dFr_{ph}} \sum_l F_{ldph}$>0, $BH_{phd} = BH_{ph\ d-1} + \Delta BH_{phd} \cdot$ **rBH** Else, $BH_{phd} = BH_{ph\ d-1} + \Delta BH_{phd}$	$dflb_{ph}$ = date of beginning of flowering of host plant p BH_{phd} = pathosystem p (=host p + attached broomrapes) biomass on day d (in g) ΔBH_{phd} = new biomass produced by plant p on day d through photosynthesis after deduction of respiration loss (in g) (Colbach *et al.*, 2014c) **rBH** = rate of biomass reduction due to parasitism in the pathosystem (host + attached broomrapes, in $g^1 \cdot g^{-1}$)
[25]	∀d If h = host species	Effect of parasitism on biomass allocation in host roots	If d ≥ $dros_{ph}$ and $\sum_{de_{ph}}^{dFr_{ph}} \sum_l F_{ldph}$>0, $RBH_{phd} = RBH_{phd-1} + \Delta BH_{phd} \cdot$ **rBH** $\cdot RBR_{ph} \cdot$ **rRBH** Else $RBH_{phd} = RBH_{phd-1} + \Delta BH_{phd} \cdot RBR_{ph}$	RBH_{phd} = root biomass of host plant p (in g) RBR_{ph} = proportion of biomass allocated to roots in healthy plant p (in g) (Pointurier *et al.*, submission in progress) **rRBH** = rate of reduction in biomass allocation to roots due to parasitism in the pathosystem (host + attached broomrapes, in $g^2 \cdot g^{-2}$)
[26]	∀d If h = host species	Effect of parasitism on biomass allocation in host above-ground organs	$ABH_{phd} = BH_{phd} - RBH_{ph}$ $LBH_{phd} = LBR_{phd} \cdot ABH_{phd}$	LBH_{phd} = leaf biomass of host plant p (in g) (Colbach *et al.*, 2014c) LBR_{phd} = leaf vs. above-ground biomass ratio in host plant p (in $g \cdot g^{-1}$) (Colbach *et al.*, 2014c)
[27]	When plant p is at seed production stage If h = host species	Seed production in healthy hosts	$SeBHh_{phd} =$ **HI_s** $\cdot ABH_{phd}^{\mathbf{bHI_s}}$	$SeBHh_{phd}$ = seed biomass in healthy plant p (in g) (Colbach *et al.*, 2014c) **HI_s** = harvest index of host species h (seed vs. above-ground biomass ratio, in $g \cdot g^{-1}$) **bHI_s** = shape parameter for seed vs. above-ground biomass

Eq.	when	Process	Equation	Explanation
				relationship of host species h
[28]	When plant p is at seed production stage If h = host species	Biomass allocation to seeds and broomrapes in infected hosts	If $\sum_{de_{ph}}^{dFr_{ph}} \sum_l F_{ldph}$>0, $SHPB_{phd} = SeBHh_{phd} \cdot$ **rSPBH**	$SHPB_{phd}$ = biomass allocated to host seeds and attached broomrapes in the above-ground part of the pathosystem p (=host p + attached broomrapes, in g) **rSPBH** = proportion of healthy reproductive compartment allocated to host seeds and broomrapes in the above-ground part of the pathosystem (host + attached broomrapes, in $g^2 \cdot g^{-2}$)
[29]	When plant p is at seed production stage If h = host species	Seed production in infected hosts	If $SHPB_{phd} > BPT_{dph}$, $SeBHp_{phd} = SHPB_{phd} - BPT_{dph}$ Else $SeBHp_{phd} = 0$	$SeBHp_{phd}$ = host seed biomass in infected host plant p (in g)

Table S 38: Parameters used in PHERASYS.2. Parameters specific to host species (rd_h and $\alpha_{h/GR24}$) are listed in Table S 40.

Parameter	Meaning and unit	Estimated value	
		Oilseed rape pathovar	Hemp pathovar
am	Annual mortality rate of broomrape seeds (in $year^{-1}$)	0.0689 ± 0.0107	0.0418 ± 0.00795
v	Proportion of viable broomrape seeds at seed shed	0.933 ± 0.0185*	0.927 ± 0.0158*
b_{cond}	Shape parameter in the equation modelling conditioning of fresh seeds	1.80 ± 1.70	NA
BH_{min}	Minimum biomass of a host plant at rosette stage to allow the development of broomrapes (in g)	2.01 ± 0.368	NA
d0	Date of dormancy release of fresh broomrape seeds (in julian days)	First day when $TT_{cond\ ld} \geq 250$ °C·days	NA
$d1_a$	Date of seasonal dormancy induction onset (in julian days) for - Young seeds - Old seeds	267 ± 0.00 + 61 ± 11.1	NA NA
$d2_a$	Date of seasonal dormancy induction end (in julian days) for - Young seeds - Old seeds	5 ± 14.4 + 61 ± 11.1	NA NA
$d3_a$	Date of seasonal dormancy release onset (in julian days) for - Young seeds - Old seeds	113 ± 3.23 + 61 ± 11.1	NA NA
$d4_a$	Date of seasonal dormancy release end (in julian days) for - Young seeds - Old seeds	122 ± NA + 61 ± 11.1	NA NA
d_{max}	Maximum distance from a stimulating root for broomrape seeds to attach to the root (in m)	0.004**	
$d_{max\text{-}stimu}$	Maximum distance from a stimulating root for broomrape seeds to perceive germination stimulants (in m)	0.036**	
ndmax	Maximum proportion of non-dormant broomrape seeds	0.911 ± 0.0334	NA
ndmin	Minimum proportion of non-dormant broomrape seeds	0.159 ± 0.0448	NA
T_{base}	Base temperature for germination of broomrape seeds (in °C)	5**	NA
$T_{max\ cond}$	Maximum temperature for conditioning of broomrape seeds (in °C)	36.7 ± 3.55	NA
$T_{min\ cond}$	Minimum temperature for conditioning of broomrape seeds (in °C)	0.00 ± 3.17	NA
$T_{opt\ cond}$	Optimum temperature for conditioning of broomrape seeds (in °C)	18.0 ± 2.67	NA
$TT_{50\ cond}$	Thermal time when 50% of fresh broomrape seeds are conditioned (in °C·days)	70.0 ± 10.7	NA
δ	Maximum number of attached broomrapes supported per gram of plant p at rosette stage (in g^{-1})	3.41 ± 0.428	NA
Ψ_{base}	Base water potential for germination of broomrape seeds (in MPa)	-3.5**	NA
$\Psi_{min\ cond}$	Minimum water potential for conditioning of broomrape seeds (in MPa)	-2	NA

Parameter	Meaning and unit	Estimated value	
		Oilseed rape pathovar	Hemp pathovar
CW	Mean weight of broomrape seeds per capsule (in g)	$5.49 \cdot 10^{-4}$ $\pm 8.18 \cdot 10^{-5}$*	NA
SW	Mean weight of a broomrape seed (in g)	$2.09 \cdot 10^{-6}$ $\pm 2.63 \cdot 10^{-7}$*	$5.41 \cdot 10^{-6}$
x_0	Hydrothermal time from germination triggering to first germinated broomrape seeds (in °C·MPa·MPa^{-1}·days)	57.9 ± 34.4*	39.4 ± 21.2*
x_{50}	Hydrothermal time from germination triggering to 50% of final germination of broomrape seeds (in °C·MPa·MPa^{-1}·days)	98.3 ± 50.2*	61.9 ± 18.0*
b	Shape parameter in the equation modelling germination dynamics of broomrape seeds	1.72 ± 1.73*	2.58 ± 1.64*
b1	Coefficient relating broomrape biomass per individual to the number of broomrapes per host plant (in g·g^{-1})	2.95 ± 0.527	NA
b2	Coefficient relating broomrape biomass per individual to the number of broomrapes per host plant (no unit)	-0.615 ± 0.127	NA
c	Number of seed capsules per gram of broomrape (in g^{-1})	7.72 ± 3.20	NA
ci	Proportion of broomrape seed capsules that will not produce mature seeds (capsules with immature seeds, eaten by insects or atrophied)	0.0848	NA
rBH	Rate of biomass reduction due to parasitism in the pathosystem (host + attached broomrapes, in $g^1 \cdot g^{-1}$)	0.725 ± 0.0497	NA
rRBH	Rate of reduction in biomass allocation to roots due to parasitism in the pathosystem p (host p + attached broomrapes, in $g^2 \cdot g^{-2}$)	0.787 ± 0.0397	NA
rSPBH	Proportion of healthy reproductive compartment allocated to host seeds and broomrapes in the pathosystem (host + attached broomrapes, in $g^2 \cdot g^{-2}$)	1.55 ± 0.148	NA
$TT_{50\ BP}$	Thermal time accumulated by broomrape from host emergence up to 50% of the total broomrape biomass is reached (in °C·days)	1130 ± 40.3	NA
b_{BP}	Shape parameter in the equation modelling broomrape biomass accumulation over time	7.40 ± 2.57	NA
dFr_{ph}	Date of fructification of broomrape (in degree-days, base 5°C, days since host emergence)	1709°C·days ***	NA

Parameters are estimated by linear or non-linear regressions (parameter value ± standard error), or by calculating mean values ± standard deviation (*) or from the literature (** (Gibot-Leclerc *et al.*, 2004) ***(Gibot-Leclerc, 2004)).

Table S 39: Name, meaning and unit of variables in PHERASYS.2. Meaning of indices: a = seed age class (young vs. old), d = day, l = soil layer, ph = plant p of species h.

Variable	Meaning	Unit	Predicted by
Da	Daily seed mortality rate of broomrape seeds (Gardarin *et al.*, 2012)	$days^{-1}$	PHERASYS.2
age_a	Broomrape seed age	days	PHERASYS.2
SB_{lda}	Density of viable broomrape seeds in soil layers	$seeds \cdot m^{-2}$	PHERASYS.2
$TT_{cond\ ld}$	Thermal time accumulated by broomrape seeds since they were released from the mother plant	°C·days	PHERASYS.2
T_{ld}	Daily mean soil temperature in layer l	°C	FLORSYS
Ψ_{ld}	Daily water potential in soil layer l	MPa	FLORSYS
pND_{lda}	Proportion of non-dormant broomrape seeds	$seeds \cdot seeds^{-1}$	PHERASYS.2
pND'_{lda}	Proportion of non-dormant broomrape seeds over seasons (before conditioning in case of fresh seeds)	$seeds \cdot seeds^{-1}$	PHERASYS.2
de_{ph}	Emergence date of the stimulating plant p	Julian days	FLORSYS
$dfle_p$	Date of end of flowering of the stimulating plant p	Julian days	FLORSYS
VS_{ldph}	Proportion of soil volume in layer l permeated with germination stimulants exuded by roots of plant p	$m^3 \cdot m^{-3}$	PHERASYS.2
RLD_{ldph}	Cumulated root length density of stimulating plant p in soil layer l	$m \cdot m^{-2}$	FLORSYS
SRL_{dph}	Specific root length of stimulating plant p (Pagès *et al.*, submitted)	$m \cdot g^{-1}$	FLORSYS
VSR_{ldph}	Proportion of soil volume in layer l occupied by the root system of stimulating plant p (Pagès *et al.*, submitted)	$m^3 \cdot m^{-3}$	FLORSYS
RBD_{ldph}	Root biomass density of stimulating plant p in soil layer l (Pagès *et al.*, submitted)	$g \cdot dm^{-3}$	FLORSYS
$pNDS_{lda}$	Proportion of non-dormant broomrape seeds stimulated by root exudates of all stimulating plants in soil layer l	$seeds \cdot seeds^{-1}$	PHERASYS.2
N_{dh}	Density of plants of species h stimulating broomrape germination	$plants \cdot m^{-2}$	PHERASYS.2
NDS_{lda}	Density of non-dormant broomrape seeds stimulated by root exudates	$seeds \cdot m^{-2}$	PHERASYS.2
CG_{lda}	Cumulated number of germinated broomrape seeds in soil layer l on day d	$seeds \cdot m^{-2}$	PHERASYS.2
HTT_{ld}	Hydrothermal time accumulated by broomrape seeds in soil layer l on day d since germination triggering by root exudates	$°C \cdot MPa \cdot MPa^{-1} \cdot days$	PHERASYS.2
G_{lda}	Density of germinated broomrape seeds	$seeds \cdot m^{-2}$	PHERASYS.2
SB_{lda}'	Density of viable broomrape seeds after germination losses	$seeds \cdot m^{-2}$	PHERASYS.2
VF_{ldph}	Proportion of soil volume in layer l where broomrape seeds are close enough to the roots of host plant p to attach it	$m^3 \cdot m^{-3}$	PHERASYS.2
F_{ld}	Total number of attachments among germinated broomrape seeds in soil layer l before competition between attachments for host resources	$Attachments \cdot host^{-1}$	PHERASYS.2
F_{ldph}	Number of attachments on roots of host plant p in soil layer l before competition between attachments for host resources	$Attachments \cdot host^{-1}$	PHERASYS.2
$dros_{ph}$	Date when host plant p reaches rosette stage	Julian days	FLORSYS

Variable	Meaning	Unit	Predicted by
γ_{ph}	Maximum number of broomrapes supported by host plant p	Attachments ·host^{-1}	PHERASYS.2
$BHros_{ph}$	Biomass of infected host plant p at rosette stage	g	FLORSYS
$Fros_{ph}$	Total number of broomrapes attached on host plant p at rosette stage before competition between attachments for host resources	Attachments ·host^{-1}	PHERASYS.2
ΔFS_{dph}	Daily number of broomrapes attached on host plant p after host rosette stage	Attachments ·host^{-1}	PHERASYS.2
Fr_{ph}	Total number of broomrapes attached on host plant p on day d	Broomrapes ·host^{-1}	PHERASYS.2
BP_{ph}	Biomass of each broomrape at fructification stage on host plant p	g·broomrape^{-1}	PHERASYS.2
TT_{ldph}	Thermal time accumulated by broomrape since host plant p emerged	°C·days	PHERASYS.2
T_d	Daily mean air temperature	°C	FLORSYS input
BPT_{dph}	Total broomrape biomass on host plant p on day d	g·host^{-1}	PHERASYS.2
ABH_{phd}	Above-ground biomass of the pathosystem p (including attached broomrapes in infected hosts) (Colbach *et al.*, 2014c)	g·host^{-1}	FLORSYS
NC_{ph}	Number of seed capsules produced per attached broomrape on host plant p	broomrape^{-1}	PHERASYS.2
SP_{ph}	Number of viable broomrape seeds produced on host plant p	host^{-1}	PHERASYS.2
$dflb_{ph}$	Date of beginning of flowering of host plant p	Julian days	FLORSYS
BH_{phd}	Pathosystem (=host p + attached broomrapes) biomass on day d	g·host^{-1}	FLORSYS and PHERASYS.2
ΔBH_{phd}	New biomass produced by host plant p on day d through photosynthesis after deduction of respiration loss (Colbach *et al.*, 2014c)	g·host^{-1}	FLORSYS
RBH_{phd}	Root biomass of host plant p	g·host^{-1}	FLORSYS and PHERASYS.2
RBR_{ph}	Proportion of biomass allocated to roots in healthy plant p (Pointurier *et al.*, submission in progress)	g·g^{-1}	FLORSYS
LBH_{phd}	Leaf biomass of host plant p (Colbach *et al.*, 2014c)	g·host^{-1}	FLORSYS
LBR_{phd}	Leaf vs. above-ground biomass ratio in host plant p (Colbach *et al.*, 2014c)	g·g^{-1}	FLORSYS
$SeBHh_{phd}$	Seed biomass in healthy plants p (Colbach *et al.*, 2014c)	g·host^{-1}	FLORSYS
$SHPB_{phd}$	Biomass allocated to host seeds and attached broomrapes in the pathosystem p (=host p + attached broomrapes)	g·host^{-1}	PHERASYS.2
$SeBHp_{phd}$	Host seed biomass in infected host plant p	g·host^{-1}	PHERASYS.2

Table S 40: Specific parameters of crop and weed species included in FLORSYS characterizing their interaction with branched broomrape. Species in bold were actually simulated. In case of missing data, data from a close species (*), from another pathovar (**) or from number of attachments instead of germination rate for $\alpha_{h/GR24}$ (***, section 4.2.4.1.3) were used. Root tip diameters originate from parameters of the root architecture model ArchiSimple (Pagès *et al.*, 2014, Pagès, pers. comm.; Moreau *et al.*, 2017; Seneze J., 2018; Guinet, 2019). When it was unknown, the mean diameter calculated over all other species was used.

Species	**Ability to stimulate broomrape germination relative to GR24 ($\alpha_{h/GR24}$)**	**Ability to support broomrape development**	**Root tip diameter (rd_h, in m)**	**Reference for stimulating activity and host status**
Oat (*Avena sativa*)	0.125**	No**	NA	(Parker and Riches, 1993; Fernández-Aparicio *et al.*, 2009)
Small oat (*Avena strigosa*)	0.125*	No*	NA	Same as oat
Beet (*Beta vulgaris*)	0	No	NA	(Qasem and Foy, 2007; Fernández-Aparicio *et al.*, 2009; Molenat *et al.*, 2013; Jestin *et al.*, 2014)
Wheat (*Triticum aestivum*)	0	No	0.000802	(Qasem and Foy, 2007; Molenat *et al.*, 2013; Jestin *et al.*, 2014)
Oilseed rape (*Brassica napus*)	0.656	Yes	0.000377	(Parker and Riches, 1993; Gibot-Leclerc *et al.*, 2003; Brault *et al.*, 2007; Fernández-Aparicio *et al.*, 2009; Auger *et al.*, 2012; Gauthier *et al.*, 2012; Gibot-Leclerc *et al.*, 2012; Gibot-Leclerc *et al.*, 2013b; Simier *et al.*, 2013)
Fenugreek (*Trigonella foenum-graecum*)	0.307**	Yes**	0.000656	(Fernández-Aparicio *et al.*, 2009; Molenat *et al.*, 2013; Jestin *et al.*, 2014)
Faba bean (*Vicia faba*)	0.443**	No	0.000819	(Parker and Riches, 1993; Fernández-Aparicio *et al.*, 2009; Fernández-Aparicio *et al.*, 2011; Molenat *et al.*, 2013)
Chickling pea (*Lathyrus sativus*)	0.00247*	Yes	NA	(Fernández-Aparicio *et al.*, 2009; Molenat *et al.*, 2013; Jestin *et al.*, 2014)
Field bean (*Phaseolus vulgaris*)	0.00388**	No**	0.000519	(Qasem and Foy, 2007; Arslan and Uygur, 2013)
Lentil (*Lens culinaris*)	0.0549**	Yes	0.000511	(Parker and Riches, 1993; Fernández-Aparicio *et al.*, 2009; Arslan and Uygur, 2013; Molenat *et al.*, 2013; Jestin *et al.*, 2014)
Lens nigricans	0.0549*	Yes*	0.000511	Same as lentil
Flax (*Linum usitatissimum*)	0.399**	No	NA	(Parker and Riches, 1993; Fernández-Aparicio *et al.*, 2009; Arslan and Uygur, 2013; Molenat *et al.*, 2013; Jestin *et al.*, 2014)
Birdsfoot trefoil (*Lotus corniculatus*)	1.59	No	NA	(Parker and Riches, 1993; Perronne *et al.*, 2017)
Lucerne (*Medicago sativa*)	0.0154*	No	NA	(Parker and Riches, 1993; Boulet *et al.*, 2007; Molenat *et al.*, 2013; Perronne *et al.*, 2017)

Species	**Ability to stimulate broomrape germination relative to GR24 ($\alpha_{h/GR24}$)**	**Ability to support broomrape development**	**Root tip diameter (rd_h, in m)**	**Reference for stimulating activity and host status**
Maize (*Zea mays*)	0.450**	No	0.000965	(Parker and Riches, 1993; Zehhar *et al.*, 2003; Qasem and Foy, 2007; Fernández-Aparicio *et al.*, 2009; Fernández-Aparicio *et al.*, 2011; Molenat *et al.*, 2013)
Black medick (*Medicago lupulina*)	0.0154	No*	NA	(Perronne *et al.*, 2017)
White mustard (*Sinapis alba*)	0.654*	Yes	NA	(Parker and Riches, 1993; Fernández-Aparicio *et al.*, 2009; Molenat *et al.*, 2013; Jestin *et al.*, 2014)
Niger (*Guizotia abyssinica*)	0	No	NA	(Parker and Riches, 1993; Molenat *et al.*, 2013; Jestin *et al.*, 2014)
Barley (*Hordeum vulgare*)	0	No	NA	(Qasem and Foy, 2007; Fernández-Aparicio *et al.*, 2009; Molenat *et al.*, 2013; Jestin *et al.*, 2014)
Phacelia (*Phacelia tanacetifolia*)	0	No	NA	(Molenat *et al.*, 2013; Jestin *et al.*, 2014)
Winter pea (*Pisum sativum*)	0	No	0.000751 to 0.000758 depending on pea genotypes	(Qasem and Foy, 2007; Fernández-Aparicio *et al.*, 2009; Fernández-Aparicio *et al.*, 2011; Arslan and Uygur, 2013; Molenat *et al.*, 2013; Jestin *et al.*, 2014)
Spring pea (*Pisum sativum*)	0	No	0.000528	(Qasem and Foy, 2007; Fernández-Aparicio *et al.*, 2009; Fernández-Aparicio *et al.*, 2011; Arslan and Uygur, 2013; Molenat *et al.*, 2013; Jestin *et al.*, 2014)
Potato (*Solanum tuberosum*)	0.219***	Yes**	NA	(Parker and Riches, 1993)
Radish (*Raphanus sativus*)	0.507*	No**	NA	(Qasem and Foy, 2007)
Soybean (*Glycine max*)	0	No	0.000720	(Arslan and Uygur, 2013; Molenat *et al.*, 2013; Jestin *et al.*, 2014)
Sorghum (*Sorghum bicolor*)	0	No	NA	(Qasem and Foy, 2007; Fernández-Aparicio *et al.*, 2009; Molenat *et al.*, 2013; Jestin *et al.*, 2014)
Sunflower (*Helianthus annuus*)	0.443**	Yes	0.000535	(Parker and Riches, 1993; Fernández-Aparicio *et al.*, 2009; Fernández-Aparicio *et al.*, 2011; Molenat *et al.*, 2013; Simier *et al.*, 2013)
Berseem clover (*Trifolium alexandrinum*)	0.0224*	Yes	NA	(Fernández-Aparicio *et al.*, 2009; Molenat *et al.*, 2013; Jestin *et al.*, 2014)
White clover (*Trifolium repens*)	0.0399	No	NA	(Molenat *et al.*, 2013; Jestin *et al.*, 2014; Gibot-Leclerc *et al.*, 2016)
Red clover (*Trifolium*	0.00487	No	NA	(Molenat *et al.*, 2013)

Species	Ability to stimulate broomrape germination relative to GR24 ($\alpha_{h/GR24}$)	Ability to support broomrape development	Root tip diameter (rd_h, in m)	Reference for stimulating activity and host status
pratense)				
Triticale (x *Triticosecale*)	0.470**	No	NA	(Fernández-Aparicio *et al.*, 2009; Molenat *et al.*, 2013)
Common vetch (*Vicia sativa*)	0.00513*	Yes	0.000466	(Fernández-Aparicio *et al.*, 2009; Molenat *et al.*, 2013)
Abutilon theophrasti	No data in the literature			
Aethusa cynapium	NA	Yes	NA	(Boulet *et al.*, 2013)
Alopecurus myosuroides	0	No	0.000418	(Simier *et al.*, 2013)
Amaranthus retroflexus	0	No	0.000541	(Qasem and Foy, 2007)
Ambrosia artemisiifolia	No data in the literature			
Ammi majus	0.267***	Yes	NA	(Boulet *et al.*, 2007; Simier *et al.*, 2013)
Anagallis arvensis	0.176***	No	NA	(Boulet *et al.*, 2001; Simier *et al.*, 2013)
Arabidopsis thaliana	0.881	Yes	NA	(Goldwasser and Yoder, 2001; Boulet *et al.*, 2007; Denev *et al.*, 2007; Auger *et al.*, 2012; Simier *et al.*, 2013; Gibot-Leclerc *et al.*, 2015; Gibot-Leclerc *et al.*, 2016) (Westwood, 2000)
Avena fatua	0	No	0.000604	(Simier *et al.*, 2013)
Bromus sterilis	0	No	0.000407	(Simier *et al.*, 2013)
Capsella bursa-pastoris	0.0467	Yes	0.000316	(Gibot-Leclerc *et al.*, 2003; Simier *et al.*, 2013; Gibot-Leclerc *et al.*, 2015; Gibot-Leclerc *et al.*, 2016; Moreau *et al.*, 2016)
Cyanus segetum	NA	Yes	0.000454	(Simier *et al.*, 2013)
Chenopodium album	0	No	0.000474	(Boulet *et al.*, 2001; Boulet *et al.*, 2007)
Datura stramonium	0.0386***	No	NA	(Boulet *et al.*, 2001)
Digitaria sanguinalis	NA	No	NA	(Boulet *et al.*, 2001; Simier *et al.*, 2013)
Echinochloa crus-galli	0	No	0.000640	(Boulet *et al.*, 2001; Boulet *et al.*, 2007)
Euphorbia helioscopia	0.137***	Yes	NA	(Gibot-Leclerc *et al.*, 2003)
Galium aparine	2.50***	Yes	0.000343	(Boulet *et al.*, 2001; Boulet *et al.*, 2007; Simier *et al.*, 2013)
Geranium dissectum	0.481***	Yes	0.000333	(Gibot-Leclerc *et al.*, 2003; Boulet *et al.*, 2007; Simier *et al.*, 2013)
Lapsana communis	1.18***	No	NA	(Boulet *et al.*, 2001; Boulet *et al.*, 2007)
Lolium multiflorum	0	No	NA	(Parker and Riches, 1993; Gibot-Leclerc *et al.*, 2003; Molenat *et al.*, 2013; Simier *et al.*, 2013)
Matricaria chamomilla	0.0394***	Yes	0.000406	(Qasem and Foy, 2007; Simier *et al.*, 2013)
Tripleurospermum	0.0394***	Yes	0.000406	(Simier *et al.*, 2013)

Species	Ability to stimulate broomrape germination relative to GR24 ($\alpha_{h/GR24}$)	Ability to support broomrape development	Root tip diameter (rd_h, in m)	Reference for stimulating activity and host status
inodorum				
Mercurialis annua	0.137***	Yes	NA	(Gibot-Leclerc *et al.*, 2003; Boulet *et al.*, 2007)
Panicum miliaceum	0	No	NA	(Qasem and Foy, 2007)
Papaver rhoeas	0.137***	Yes	NA	(Gibot-Leclerc *et al.*, 2003; Simier *et al.*, 2013)
Poa annua	No data in the literature			
Polygonum aviculare	NA	Yes	0.000363	(Gibot-Leclerc *et al.*, 2003; Boulet *et al.*, 2007)
Fallopia convolvulus	NA	Yes	0.000480	(Boulet *et al.*, 2007)
Persicaria maculosa	0	No	0.000431	(Boulet *et al.*, 2001)
Raphanus raphanistrum	0.507	Yes	NA	(Boulet *et al.*, 2001; Gibot-Leclerc *et al.*, 2003; Boulet *et al.*, 2007; Simier *et al.*, 2013; Gibot-Leclerc *et al.*, 2016)
Senecio vulgaris	0.381***	Yes	0.000411	(Boulet *et al.*, 2001; Boulet *et al.*, 2007)
Setaria viridis	NA	No	NA	(Simier *et al.*, 2013)
Sinapis alba	0.654*	Yes	NA	(Parker and Riches, 1993; Fernández-Aparicio *et al.*, 2009; Molenat *et al.*, 2013; Jestin *et al.*, 2014)
Sinapis arvensis	0.654	No	NA	(Gibot-Leclerc *et al.*, 2003; Simier *et al.*, 2013; Gibot-Leclerc *et al.*, 2015; Gibot-Leclerc *et al.*, 2016)
Solanum nigrum	3.28***	No	0.000583	(Boulet *et al.*, 2001; Boulet *et al.*, 2007)
Sonchus asper	2.26***	Yes	0.000429	(Boulet *et al.*, 2001; Gibot-Leclerc, 2004; Boulet *et al.*, 2007; Simier *et al.*, 2013)
Stellaria media	0	No	0.000329	(Boulet *et al.*, 2001)
Veronica hederifolia	0.0427*	Yes	0.000286	(Simier *et al.*, 2013)
Veronica persica	0.0427***	Yes*	NA	Same as *V. hederifolia*
Viola arvensis	NA	Yes	NA	(Simier *et al.*, 2013)

A.3.2. Effect of temperature and humidity during conditioning and germination

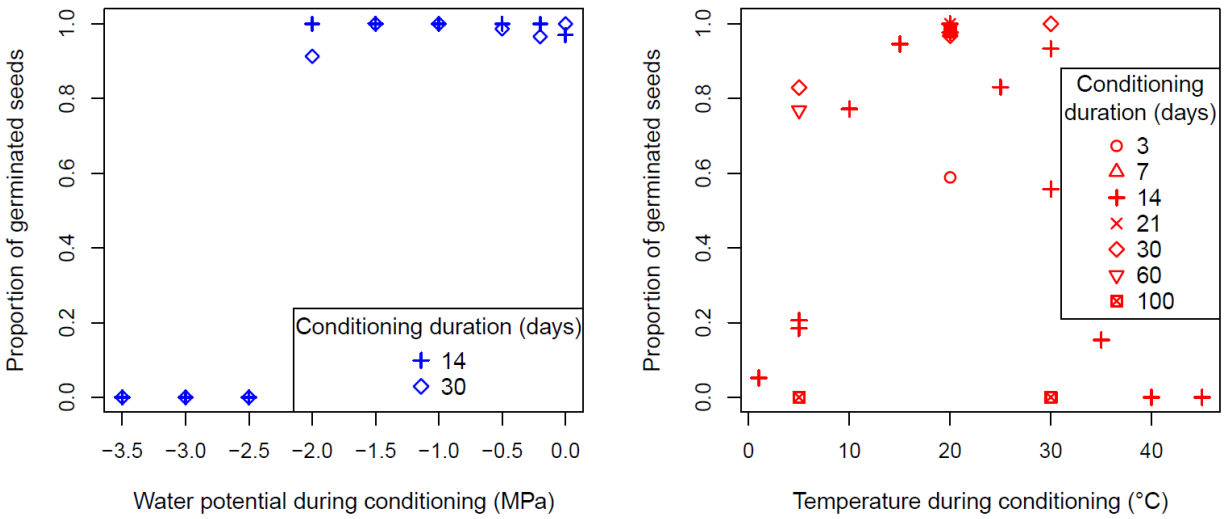

Figure S 14: Effect of water potential (left) and temperature (right) during different durations of conditioning on the proportion of germinated seeds in branched broomrape. Germination rate was measured after 10 to 20 days after stimulation with GR24 at 1 mg.L^{-1} at 20 °C. Data from (Gibot-Leclerc *et al.*, 2004).

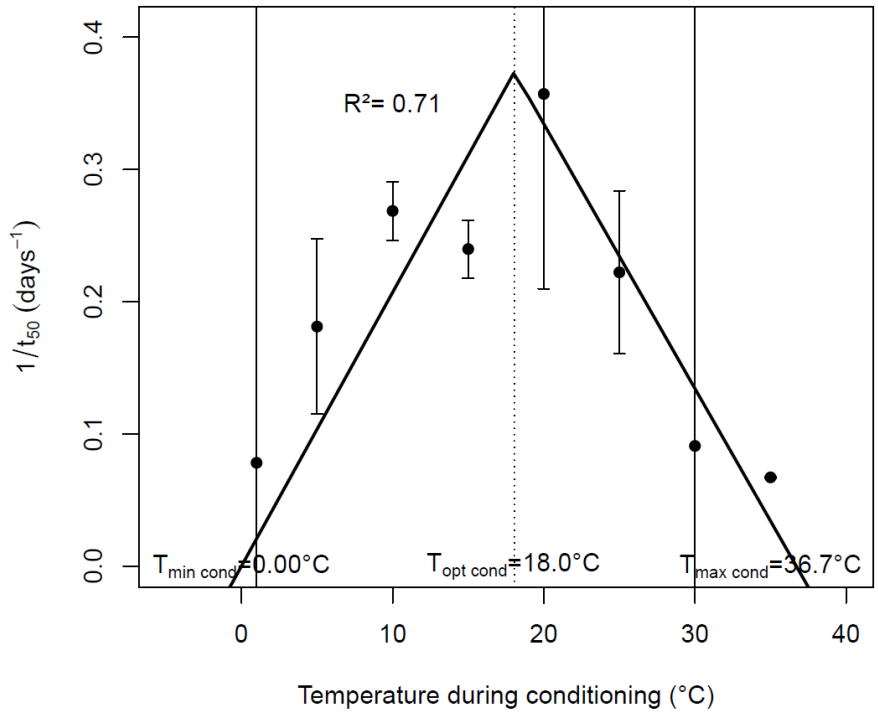

Figure S 15: Inverse of time to reach 50% of the final germination rate ($1/t_{50}$, in days^{-1}) in branched broomrape seeds as a function of temperature during conditioning. Germination rate was measured after 10 to 20 days after stimulation with GR24 (synthetic stimulant) at 1 mg.L^{-1} at 20 °C (optimal GR24 concentration and temperature for broomrape germination). The thick line represents the model fitted to the data. Vertical bars represent standard errors. $T_{min\ cond}$, $T_{opt\ cond}$ and $T_{max\ cond}$ are the minimum, optimum and maximum temperatures for conditioning to be efficient (i.e. to make seeds sensitive to germination stimulants) estimated from the model. Data from (Gibot-Leclerc *et al.*, 2004).

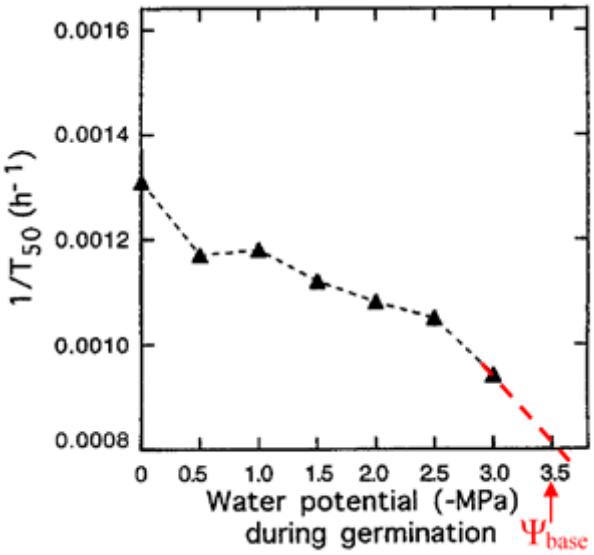

Figure S 16: Estimation of base water potential for germination of branched broomrape from extrapolation on a figure from Gibot-Leclerc *et al.*(2004) (the red dotted line was added to the original figure).

A.3.3. Representing stimulation of broomrape germination around roots

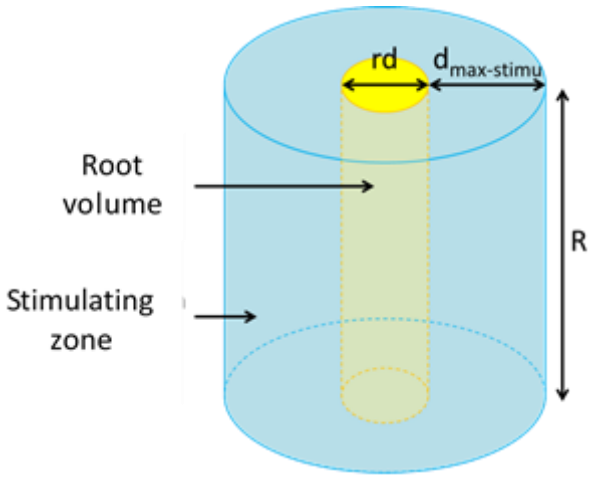

Figure S 17: Illustration of the « stimulating zone » where broomrape seeds perceive germination stimulants of root exudates. rd = root diameter, $d_{max-stimu}$ = maximum distance from the root for seeds to perceive germination stimulants, R = root length.

A.3.4. Merging consecutive germination flushes

A. Same proportion of germinated seeds

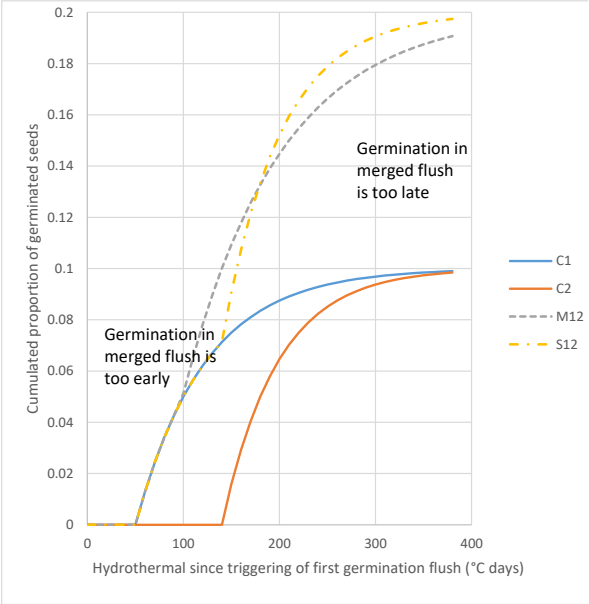

B. More stimulated seeds in second flush

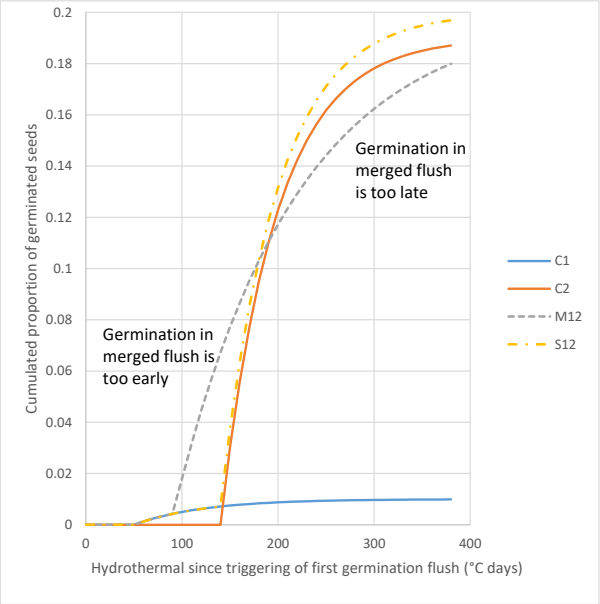

C. More stimulated seeds in first flush

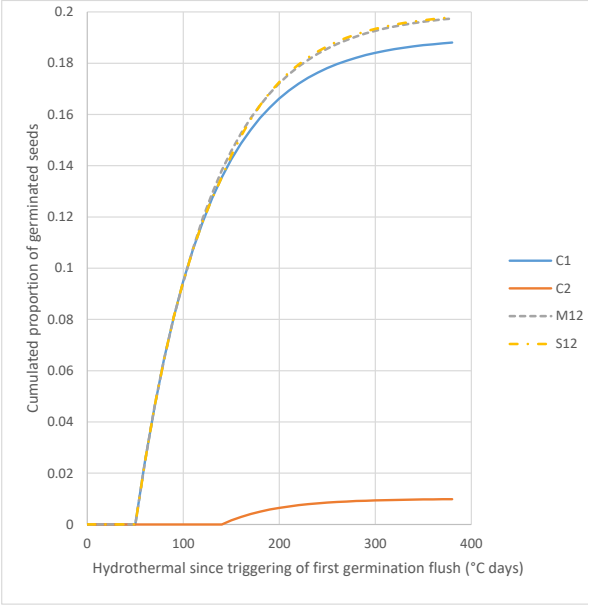

D. Second flush much later

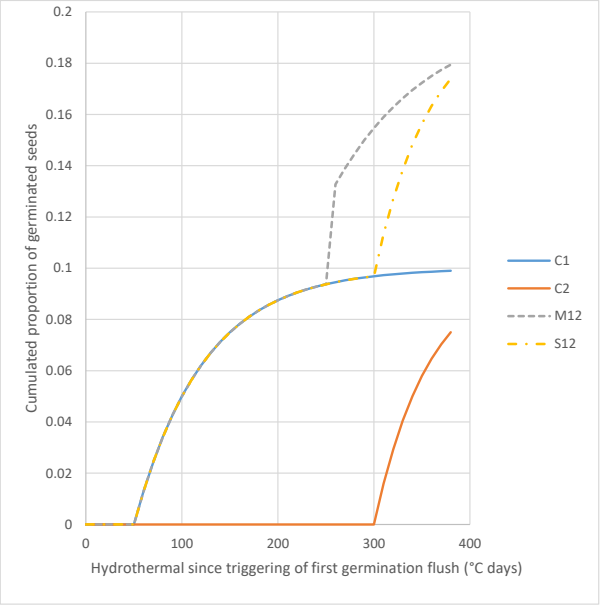

Figure S 18: Various examples of merged simultaneous kinetics of germination with different proportions of germinated seeds (A, B and C) and different durations (A and D) between both flushes. C1 = first kinetics, C2 = second kinetics starting as C1 is still running, S12 = sum of both kinetics, M12 = approximation after kinetics parameters have been reestimated to merge both kinetics.

A.3.5. Date of broomrape fructification

In Gibot-Leclerc (Gibot-Leclerc, 2004), thermal time accumulated between oilseed rape emergence and broomrape fructification (TT) is calculated with the following equation :

(1) $TT = \sum_{d=0}^{n}(Tmoy_d - T_{base})$,
with n the number of days between oilseed rape emergence and broomrape fructification, $Tmoy_d$ the mean temperature on day d and T_{base} the base temperature.

Rearranging (1), we get:

(2) $TT = \sum_{d=0}^{n} Tmoy_d - n \cdot T_{base}$

With T_{base} = 0°C, it gives:

(3) $TT(T_{base} = 0°C) = \sum_{d=0}^{n} Tmoy_d$

According to Gibot-Leclerc (Gibot-Leclerc, 2004), $TT(T_{base} = 0°C)$ = 3074 °C.j and n = 273j. From the later, we can deduce the thermal time in base 5°C (base temperature for broomrape germination):

(4) $TT(T_{base} = 5°C) = \sum_{d=0}^{n} Tmoy_d - n \cdot T_{base}$
$= TT(T_{base} = 0°C) - n \cdot T_{base}$
$= 3074 - 273 \cdot 5 = 1709$

A.3.6. Analysis of simulation results

A.3.6.1. Broomrape seed bank in each cropping system after 30 years

Table S 41: Distribution of broomrape seed banks (seeds·m^{-2}) in each cropping system after 30 years of simulation under infestation with broomrape (A) and with both broomrape and weeds (B). Cropping systems 1 to 5 refer to 1: reference system, 2: diversified rotation, 3: delayed sowing, 4: no plough and 5: no-till.

A. In simulations with broomrape only

Cropping system	1	2	3	4	5
Minimum	139845	4352	32571	58358	154242
1st quartile	216365	18439	78757	188123	209600
Median	361961	99135	81949	374022	322170
Mean	407305	145378	85373	362941	391414
3rd quartile	600681	261272	90844	511375	589667
Maximum	762340	400375	164268	690694	766264

B. In simulations with broomrape in interactions with weeds

Cropping system	1	2	3	4	5
Minimum	108425	828.9	687.3	69535	10943
1st quartile	118605	84814.5	951.2	82472	22566
Median	229974	140447.0	1871.9	181998	31982
Mean	237399	146864.3	6223.6	254780	44963
3rd quartile	328804	211505.1	4643.8	363314	58045
Maximum	447065	303334.1	31007.4	788545	125915

A.3.6.2. Broomrape germinations induced throughout the year

A. In simulations with broomrape only

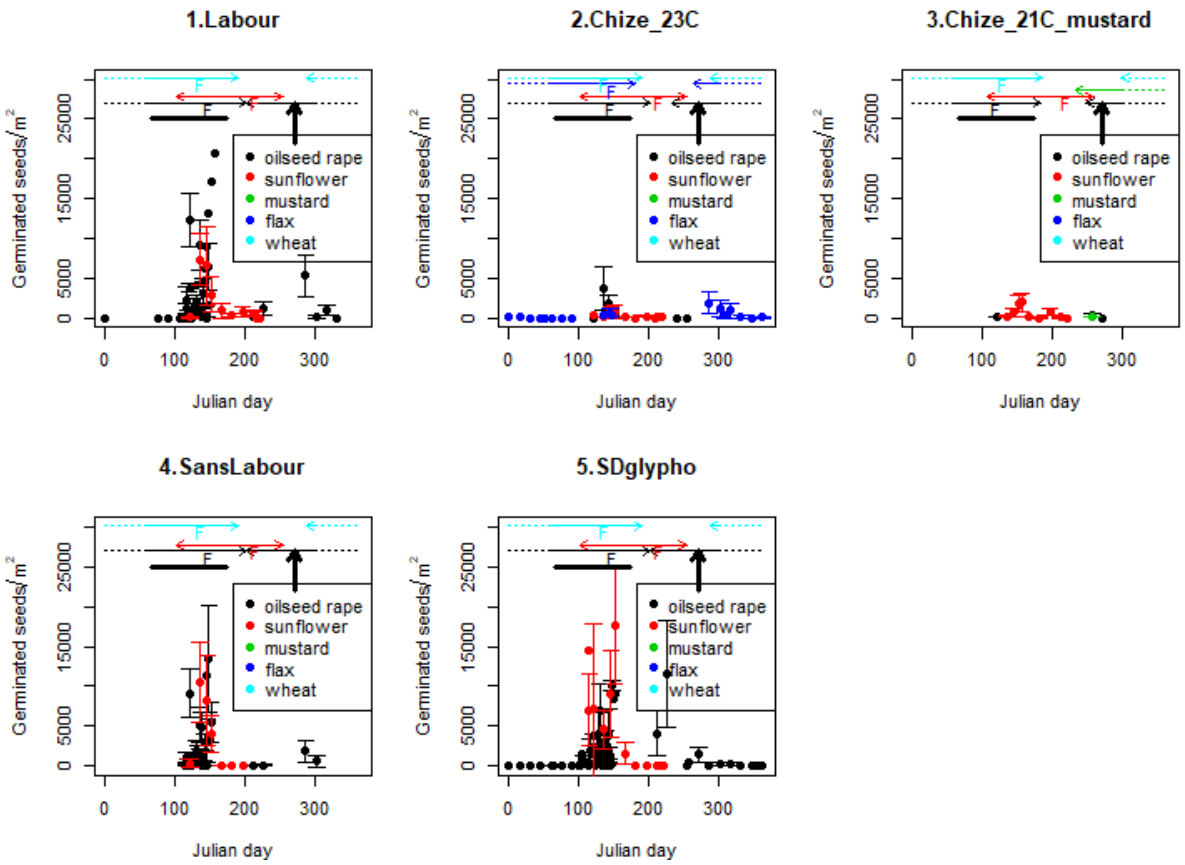

Figure S 19: Broomrape germinations induced by crops throughout the year in weed-free simulations. Each dot represents the mean number of germinated seeds per day averaged over 30 years and 10 weather repetitions. Each colour represents the growing season of a crop (from harvest of the previous crop to harvest). Vertical bars represent standard deviations. Horizontal arrows show durations from sowing to harvest of each crop. The horizontal thick line shows the period of high dormancy in broomrape seeds in PHERASYS.2. F indicate mean dates of crop flowering onset. The vertical thick arrow shows the estimated date when the maximum number of broomrape germinations were induced in an oilseed rape field sown in August 28th in the study of Gibot-Leclerc et al. (2012).

B. In simulations with broomrape in interactions with weeds

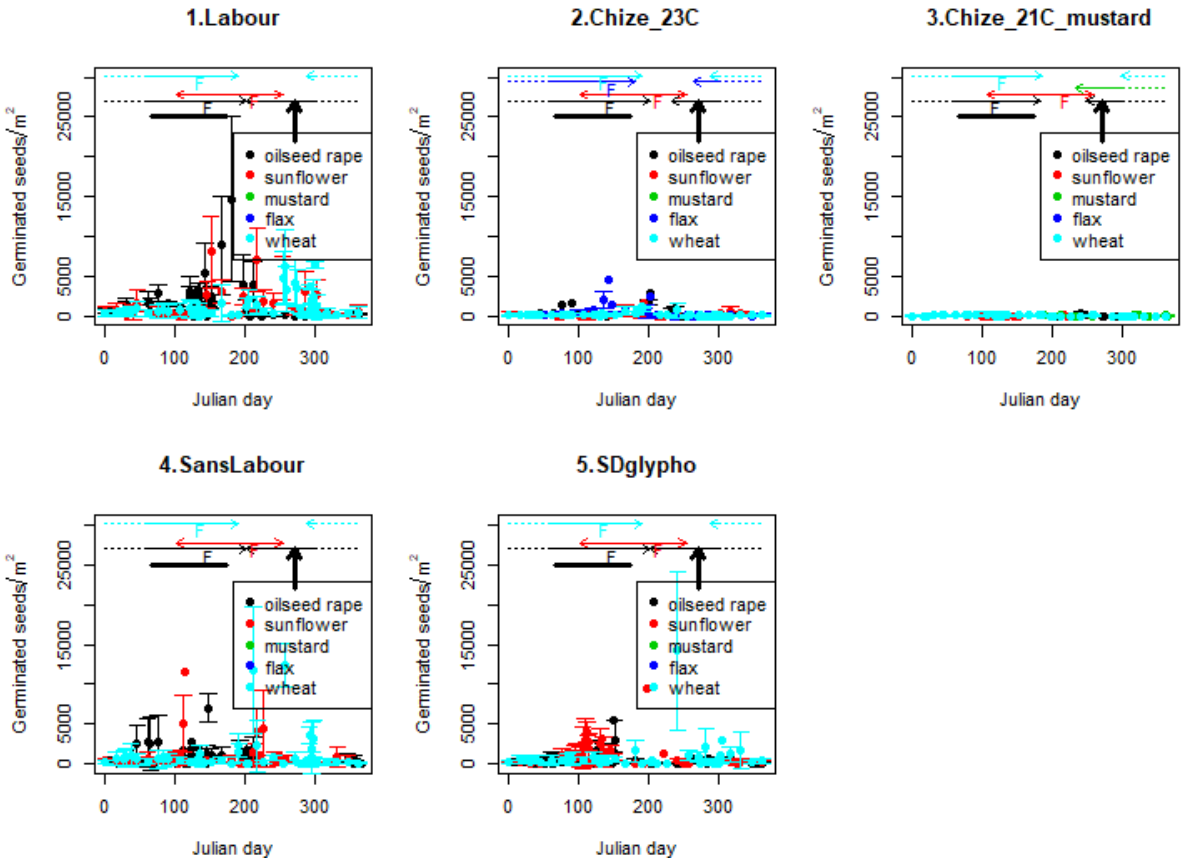

Figure S 20: Broomrape germinations induced by crops and weeds throughout the year in simulations. Each dot represents the mean number of germinated seeds per day averaged over 30 years and 10 weather repetitions. Each colour represents the growing season of a crop (from harvest of the previous crop to harvest). Vertical bars represent standard deviations. Horizontal arrows show durations from sowing to harvest of each crop. The horizontal thick line shows the period of high dormancy in broomrape seeds in PHERASYS.2. F indicate mean dates of crop flowering onset. The vertical thick arrow shows the estimated date when the maximum number of broomrape germinations were induced in an oilseed rape field sown in August 28th in the study of Gibot-Leclerc et al. (2012).

A.3.6.3. Occurrence of broomrapes at maturity throughout the year

A. In simulations with broomrape only

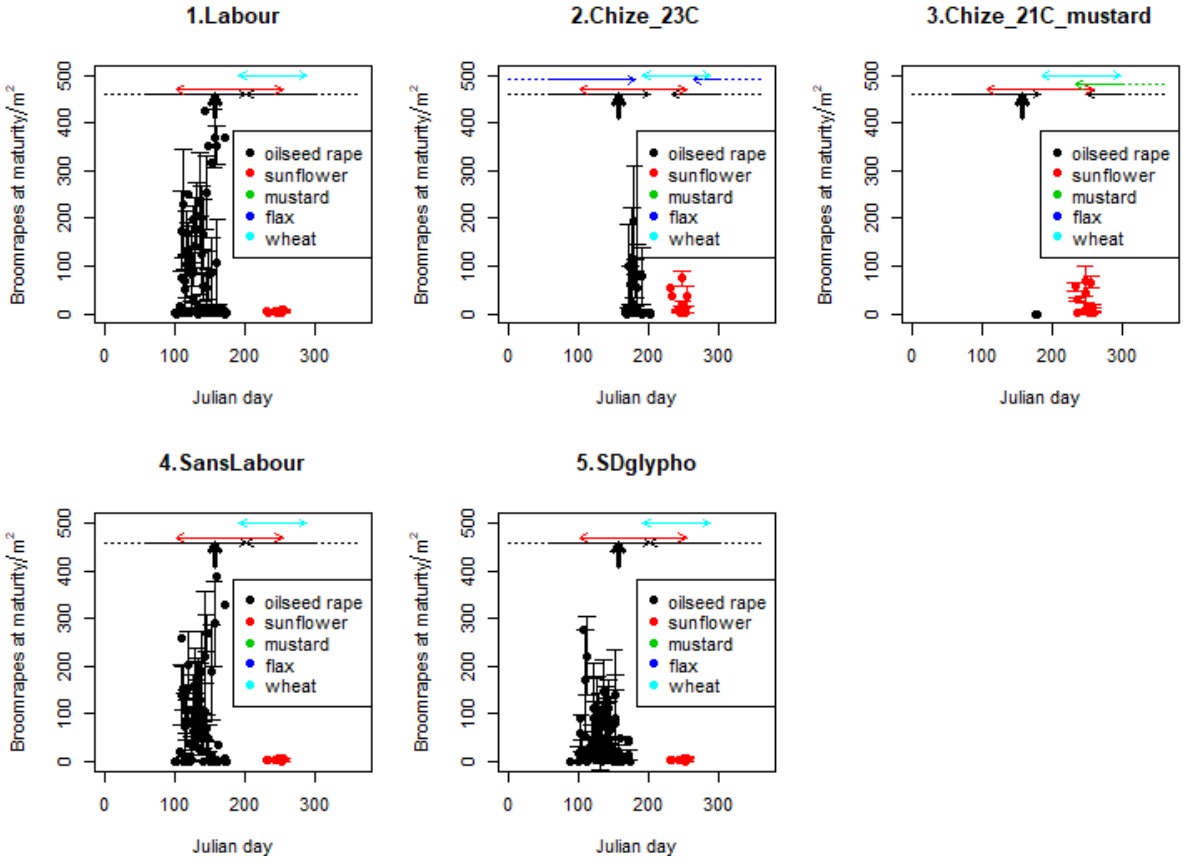

Figure S 21: Number of broomrapes reaching maturity on crops throughout the year in weed-free simulations. Each dot represents the mean number of mature broomrape per day averaged over 30 years and 10 weather repetitions. Each colour represents the growing season of a crop (from harvest of the previous crop to harvest). Vertical bars represent standard deviations. Horizontal arrows show durations from sowing to harvest of each crop. The vertical thick arrow shows the estimated date when broomrapes start fructifying in an oilseed rape field sown in August 28th in the study of Gibot-Leclerc et al. (2012).

B. In simulations with broomrape in interactions with weeds

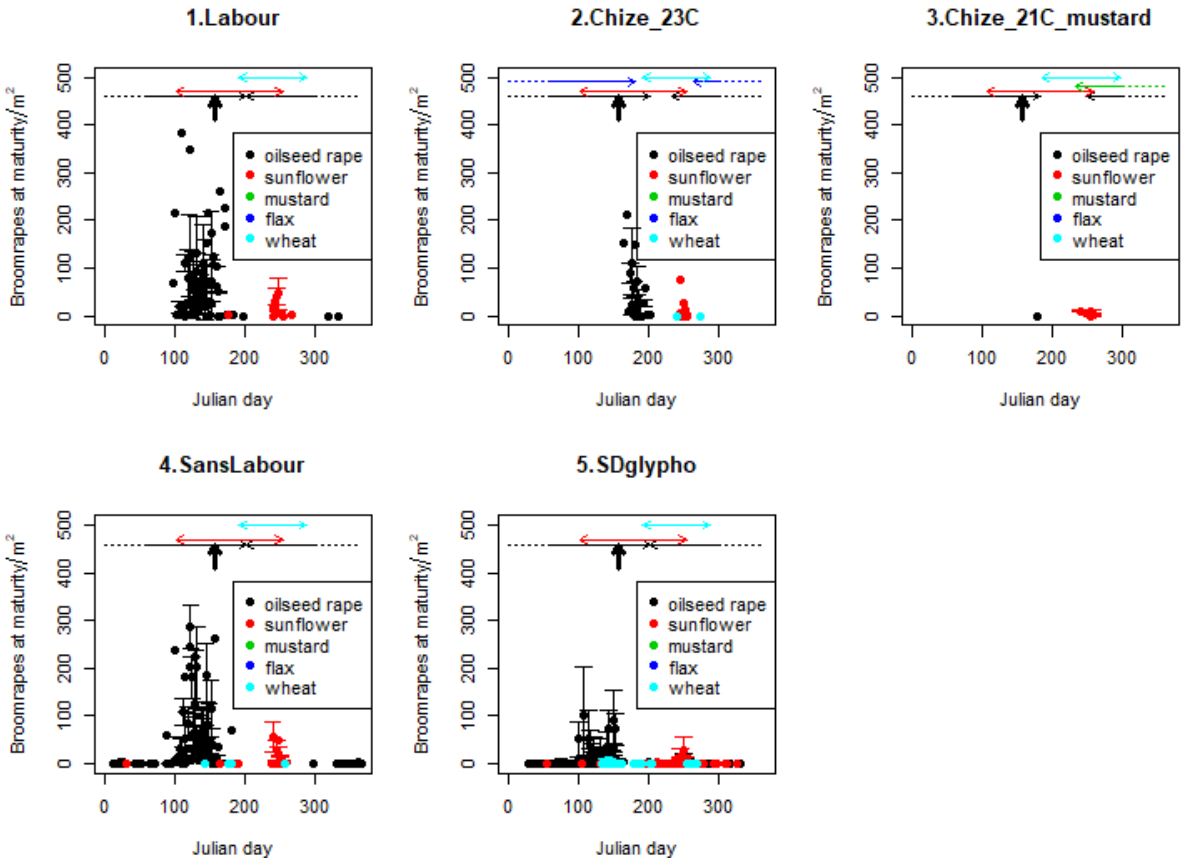

Figure S 22: Number of broomrapes reaching maturity on crops and weeds throughout the year in simulations. Each dot represents the mean number of mature broomrape per day averaged over 30 years and 10 weather repetitions. Each colour represents the growing season of a crop (from harvest of the previous crop to harvest). Vertical bars represent standard deviations. Horizontal arrows show durations from sowing to harvest of each crop. The vertical thick arrow shows the estimated date when broomrapes start fructifying in an oilseed rape field sown in August 28th in the study Gibot-Leclerc et al. (2012).

A.3.6.4. Drivers of crop yield losses due to broomrape and/or weeds

Table S 42: Analysis of variance table of the linear model fitting the annual yield loss due to broomrape and/or weeds as a function of type of infestation (i.e. with weeds and/or broomrape), cropping system, crop, year and weather repetition (see section 4.2.3.5).

	Sum of squares	Df	F values	Pr(>F)
Type of infestation	13.5	1	11.6561	0.0006469
Cropping system	785.0	4	169.3152	<0.0001
Crop	1626.7	3	467.8284	<0.0001
Weather repetition	79.7	9	7.6419	<0.0001
Year	133.0	1	114.7943	<0.0001
Type of infestation × cropping system	321.6	8	34.6796	<0.0001
Type of infestation × crop	158.8	4	34.2439	<0.0001
Residuals	4251.3	3668		
Adjusted R-squared	0.5352			

A.3.6.5. Yield losses due to broomrape in the reference cropping system (1) in weed-free fields

Table S 43: Distribution of yield losses due to broomrape in the reference cropping system (in percentage of energy lost in $MJ \cdot ha \cdot MJ^{-1} \cdot ha^{-1}$)

	Oilseed rape	Sunflower
Minimum	-21.9	34.1
1st quartile	-0.771	42.4
Median	3.32	46.5
Mean	15.9	45.5
3rd quartile	30.6	48.7
Maximum	71.2	56.9

ÉCOLE DOCTORALE
Environnements - Santé
Bourgogne | Franche-Comté

Titre : Modélisation des effets des systèmes de culture sur la dynamique de la plante parasite orobanche rameuse en interaction avec les adventices

Mots clés : modèle mécaniste, plante parasite, système de culture, gestion des adventices, *Phelipanche ramosa*, agroécologie

Résumé : Limiter l'usage de pesticides en agriculture est un enjeu crucial qui requiert de développer des méthodes plus durables, exploitant les techniques culturales non chimiques et les régulations biologiques, selon les principes de l'agroécologie. L'orobanche rameuse (*Phelipanche ramosa* (L.) Pomel) est une plante parasite des racines des cultures qui cause des pertes de rendement considérables dans le monde entier. Sa gestion est complexe car elle requiert de combiner plusieurs techniques culturales et elle doit intégrer la gestion des adventices non-parasites que l'orobanche est également capable de parasiter. L'objectif de cette thèse était de synthétiser les connaissances sur la dynamique de l'orobanche rameuse dans les agroécosystèmes et de les agréger dans un modèle mécaniste afin d'identifier des stratégies de gestion efficaces par simulation. Nous avons synthétisé les connaissances disponibles dans la littérature et acquis les connaissances manquantes par expérimentation (ex : mortalité et dormance des semences d'orobanche) afin de modéliser le cycle de vie complet de l'orobanche. Afin de prédire les effets des systèmes de culture (succession culturale, itinéraires techniques) sur la dynamique de l'orobanche et des adventices en interaction, nous avons couplé notre modèle orobanche à deux modèles existants : un modèle des effets des systèmes de culture sur la dynamique des adventices et un modèle de croissance racinaire (siège de l'infection). Les simulations réalisées ont permis d'identifier des combinaisons de techniques prometteuses pour gérer à la fois l'orobanche et les adventices, et montrent la possibilité de régulation de l'orobanche via les adventices.

Title : Modelling cropping system effects on branched broomrape dynamics in interaction with weeds

Keywords : mechanistic model, parasitic plant, cropping system, weed management, *Phelipanche ramosa*, agroecology

Abstract: Reducing pesticide use is a major challenge in agriculture and involves developing more sustainable methods that rely on non-chemical cropping techniques and biological regulations according to agroecological principles. Branched broomrape (*Phelipanche ramosa* (L.) Pomel) is a root parasitic plant which infects crops and causes dramatic yield losses worldwide. Managing broomrape is complex because it requires combining several cropping techniques whithin a global weed management strategy because broomrape is also able to infect non-parasitic weeds. The aim of this thesis was to stynthetize knowledge on branched broomrape dynamics in agroecosystems and to aggregate it within a mechanistic model in order to identify efficient management strategies from simulations. We synthetized knowledge from the literature, and acquired missing knowledge by setting up expriments (eg. mortality and dormancy of broomrape seeds) in order to model the complette life-cycle of branched broomrape. In order to predict the effects of cropping systems (crop succession and management plans) on broomrape dynamics and weeds in interaction, we connected our broomrape model to two existing models : a model of the effects of cropping systems on weed dynamics and a root growth model (roots being the infection site). The simulations allowed to identify promising combinations of techniques to control both broomrape and weeds, and revealed that weeds may regulate broomrape.